Unique Cellular, Physiological, and Metabolic Adaptations to the Euendolithic Lifestyle in a Boring Cyanobacterium

By

Brandon Scott Guida

A Dissertation Presented in Partial Fulfillment
of the Requirements for the Degree
Doctor of Philosophy

Approved April 2016 by the
Graduate Supervisory Committee:

Ferran Garcia-Pichel, Chair
Douglas Chandler
Robert Roberson
Scott Bingham

ARIZONA STATE UNIVERSITY

May 2016

ABSTRACT

Euendolithic cyanobacteria have the remarkable ability to actively excavate and grow within certain minerals. Their activity leads to increased erosion of marine and terrestrial carbonates, negatively affecting coral reef and bivalve ecology. Despite their environmental relevance, the boring mechanism has remained elusive and paradoxical, in that cyanobacteria alkalinize their surroundings, typically leading to carbonate precipitation, not dissolution. Thus, euendoliths must rely on unique adaptations to bore. Recent work using the filamentous model euendolith *Mastigocoleus testarum* strain *BC008* indicated that excavation relied on transcellular calcium transport mediated by P-type ATPases, but the phenomenon remained unclear. Here I present evidence that excavation in *M. testarum* involves an unprecedented set of adaptations. Long-range calcium transport is achieved through the coordinated pumping of multiple cells, orchestrated by the localization of calcium ATPases in a repeating annular pattern, positioned at a single cell pole, adjacent to each cell septum along the filament. Additionally, specialized chlorotic cells that I named calcicytes, differentiate and accumulate calcium at concentrations more than 500 fold those of canonical cells, likely allowing for fast calcium flow at non-toxic concentrations through undifferentiated cells. I also show, using ^{13}C stable isotope tracers and NanoSIMS imaging, that endolithic *M. testarum* derives most of its carbon from the mineral carbonates it dissolves, the first autotroph ever shown to fix mineral carbon, confirming the existence of a direct link between oxidized solid carbon pools and reduced organic pools in the biosphere. Finally, using genomic and transcriptomic approaches, I analyze gene expression searching for additional adaptations related to the endolithic lifestyle. A large and diverse set of genes

(24% of 6917 genes) were significantly differentially regulated while boring, including several master regulators and genes expectedly needed under this condition (such as transport, nutrient scavenging, oxidative stress, and calcium-binding protein genes). However, I also discovered the up-regulation of several puzzling gene sets involved in alternative carbon fixation pathways, anaerobic metabolism, and some related to photosynthesis and respiration. This transcriptomic data provides us with several new, readily testable hypotheses regarding adaptations to the endolithic lifestyle. In all, my data clearly show that boring organisms show extraordinarily interesting adaptations.

ACKNOWLEDGMENTS

First and foremost, I'd like to thank Dr. Ferran Garcia-Pichel, for taking a chance on me, someone he didn't know at the time, who happened to be good friends with a guy really interested in boring. You have taught me so much about science, how to think about it, and its nuances, in what feels like (to me anyway) such a short but sweet time. I thank you for the ability to present my findings abroad and to experience environmental field work, something I would have never been able to do prior to joining your lab. Thank you for your incredible writing tutelage. I look forward to future collaborations with you and your future students.

I want to thank my wonderful parents for putting up with such an annoyingly inquisitive son. Thank you both for your patience even through all those times you came home and one of your appliances was dismantled. Thank you for buying me that encyclopedia set when I was 12, even though we had no money, it was my Google before Google. Thank you for your understanding even after all my home chemistry experiments. Thank you for instilling such a reverence for academic achievement. I couldn't have asked for two more loving or supporting parents. Thank you for making me the scientist and man I am today, Thank you! Even though I don't say it enough, I love you both!

Thank you Erin, for all your love and support during my journey through graduate school, I will always cherish this time together. I'm so excited to start our new chapters together, I love you!

To any and all I've not the time nor space to mention, thank you for your support, assistance, and guidance, it was invaluable!

TABLE OF CONTENTS

Page

LIST OF TABLES vi

LIST OF FIGURES vii

CHAPTER

INTRODUCTION 1

Of Cyanobacteria and Rocks 1

Global Carbon and Microbes 5

The Mechanistics of the Euendolithic Lifestyle 7

The Problem with Living Inside of a Rock 9

Specific Research Aims 12

Figures 14

1 EXTREME CELLULAR ADAPTATIONS AND CELL DIFFERENTIATION REQUIRED BY A CYANOBACTERIUM FOR CARBONATE EXCAVATION 17

Abstract 18

Introduction 19

Results & Discussion 21

Conclusions 26

Materials and Methods 29

Acknowledgements 34

Figures 35

2 USE OF MINERAL CARBONATE FOR AUTOTROPHY AMONG EUENDOLITHIC CYANOBACTERIA 45

Abstract 46

CHAPTER Page

Introduction 47

Results & Discussion 49

Conclusions 58

Materials and Methods 59

Acknowledgements 66

Figures 67

3 DRAFT GENOME ASSEMBLY OF THE FILAMENTOUS EUENDOLITHIC (TRUE BORING) CYANOBACTERIUM MASTIGOCOLEUS TESTARUM STRAIN BC008. 78

Abstract 79

Introduction 79

Materials, Methods, & Results 80

4 PHYSIOLOGICAL AND METABOLIC PLASTICITY PLAYS A CENTRAL ROLE IN THE EUENDOLITHIC LIFESTYLE 82

Abstract 83

Introduction 84

Results & Discussion 87

Conclusions 111

Materials and Methods 113

Figures 117

CONCLUDING REMARKS 133

REFERENCES 135

APPENDIX

A Transcriptomic Expression Data for ALL Genes 153

LIST OF TABLES

Table		Page
1.	Global Carbon Pools	15
2.	Fluorophore Usage Parameters	44
3.	DIC ^{13}C Isotopic Composition of Enclosed Cultures	73
4.	Multivariate ANOVA of Biomass Fraction Yields	76
5.	Interaction of Culture Conditions on Biomass Yields	77
6.	RNA-Seq Library Statistics	117
7.	Gene Functional Group Expression Statistics	121
8.	Upregulated Putative RTX Calcium Binding Proteins	132

LIST OF FIGURES

Figure		Page
1.	Ancient Fossilized Filamentous Microorganism	14
2.	Previous Boring Model	16
3.	Mechanically Damaged Trichomes “Bleeding”	35
4.	P-type Calcium ATPase Localization	36
5.	Intracellular Calcium Analysis	37
6.	Intracellular Ratiometric pH Measurements	38
7.	Relative P-type ATPase Expression	39
8.	Fluo-5F AM Control Images	40
9.	Intracellular Calcium Quantification Replicate	41
10.	BODIPY Image Controls	42
11.	Updated Carbonate Excavation Model	43
12.	Visual Comparison of Biomass Fractions	67
13.	Biomass Fraction Yields	67
14.	*in vitro* ^{13}C Compositions of *M. testarum*	69
15.	*in situ* ^{13}C Compositions of Isla de Mona Samples	70
16.	Endolithic ^{13}C Spike-in NanoSIMS Analysis	71
17.	Depth Profile of ^{13}C Tracer Assimilation	72
18.	Image of Prototypical Euendolithic Radial Colony	74
19.	Calcite Penetration Depth Comparison	75
20.	RNA-Seq Expression Statistics	118
21.	Expression Statistics and Global Expression Heatmap	119

Figure Page

22. Heatmap of Significantly Differentially Regulated (SDR) Genes 120

23. Heatmap of SDR Transport Genes..... 122

24. Heatmap of SDR Carbon Metabolism Genes..... 123

25. Phylogenetic Tree of CODH (*cutLM*)..... 124

26. Phylogenetic Tree of CODH (*cutS*) 125

27. Operon Structure of CODH Locus..... 126

28. WLP Map..... 127

29. General RTX Operon and Protein Architecture. 128

30. Heatmap of SDR Photosynthetic Genes. 129

31. Heatmap of SDR Oxidative Phosphorylation Genes..... 130

32. Phylogenetic Tree of Na^+ ATPase (*atpD*)..... 131

INTRODUCTION

Of Cyanobacteria and Rocks

A single group of microorganisms is responsible for the establishment and maintenance of the current state of Earth's biosphere. Cyanobacteria play crucial roles in oxygen generation and in carbon sequestration. They represent one of the oldest bacterial linages for which we have direct, reliable, fossil evidence (Fig. 1. from Schopf, 1993), some dating back to the paleoarchean period (~3.4 GYr)[1, 2]. It is known that the early atmosphere was oxygen poor, suggesting most microbial life at the time was anaerobic and relied on either anoxygenic photolithotrophic or chemolithotrophic metabolic pathways[3, 4]. Toward the very end of the Archean period isotopic evidence shows a large increase in the concentration of molecular oxygen in Earth's atmosphere, termed the great oxidation event (GOE)[5]. The event seems to coincide with the global dispersion of a novel microbial metabolic pathway, oxygenic photosynthesis[6]. Indeed, stromatolite fossils suggest that circa 2.45 Ga the carbon fixation pathways utilized by most autotrophs today had already evolved[7]. Spontaneous atmospheric oxygenation most likely would not have occurred and evidence is beginning to accumulate suggesting that the oxygen was being produced in small pockets, slowly providing oxygen "whiffs" which gradually oxidized the surroundings and eventually the planet[5, 8, 9]. Thus, oxygenic photosynthesis most likely significantly predates the GOE. It was the early ancestors to modern cyanobacteria that "figured out" how to harness the untapped (at that time) energy in an almost inexhaustible substrate, water. The oxygen generating portion (photosystem II) of this metabolic pathway has since percolated down through every domain of life except archaea[10]. The GOE is probably the most significant

biogeochemical phenomena ultimately leading to the current state of biology on Earth. On that point alone one should argue that cyanobacteria are the most important group of organisms ever to exist whom directly contributed and continue to contribute to the current state of biology on Earth.

Currently, cyanobacteria have been found in almost every ecological niche (which receives some type of light) on the planet and display an enormous amount of metabolic diversity[11, 12]. They play a primary role in oxygen production, carbon sequestration (CO_2), nitrogen fixation, and as primary biomass producers supporting most of the planet's food webs. Their metabolic diversity is only rivaled by their morphological diversity. They can be unicellular, such as *Synechocystis or Prochlorococcus* and they can be filamentous multicellular organisms, capable of terminal cellular differentiation, such as *Mastigocoleus* or *Fischerella.* The evolution of oxygenic photosynthesis is thought to have occurred in an early lineage of anoxygenic phototrophs in response to increases in UV radiation and/or the inability to secure enough reducing power[13]. Oxygenic photosynthesis coupled to the Calvin-Benson-Bassham (reductive pentose phosphate pathway) cycle is the predominant way in which cyanobacteria use the energy harvested from light-dependent redox reactions, securing electrons via splitting water, to "fix" inorganic carbon (CO_2) into cellular biomass. This pathway relies heavily on a single enzyme complex known as ribulose 1,5-bisphosphate carboxylase/oxygenase (RuBisCO). The overall importance of this enzyme and its central role in the global carbon cycle is exemplified by the fact that it is the most prevalent enzyme on the planet[14]. RuBisCO is an oxygen sensitive enzyme and catalysis of CO_2 reduction is rather slow but it shows a positive response to pCO_2 concentrations[15]. One way cyanobacteria

get around this limitation is by increasing the pCO_2 concentration directly adjacent to the RuBisCO complex by packaging it into a microcompartment. This microcompartment is known as a carboxysome and homologous structures are found throughout the cyanobacterial lineage[16]. Though most cyanobacteria are obligate oxygenic photoautotrophs some strains retain the ability to switch to anoxygenic phototrophy or even grow under heterotrophic, mixotrophic, and anaerobic fermentative conditions[17-20]. The metabolic plasticity of cyanobacteria stems both from their antiquity and the level of horizontal gene transfer found to permeate their evolutionary history. Horizontal transfer has been observed to occur within every gene functional category both at the intra- and interphylum levels[21].

Cyanobacterial adaptability allows survival almost anywhere, from Antarctic lakes[22] to the acidic hot springs of Yellowstone National Park[23]. Perhaps one of the least studied and least understood habitats on the planet, where cyanobacteria also dominate, is the lithic environment. There are several ways in which a microbe can colonize a rock such as attachment to its surface as an epilith or by colonizing the interior as one of three types of endoliths. Endolithic colonization can occur inside a preformed crack or crevice (chasmoendolithic microbe), within natural pore spaces or those created by other organism (cryptoendoliths) or by actively excavating its own space (euendolith). Observations of euendolithic (true-boring) cyanobacteria have been described in the literature dating back to the late 1800's[24-26]. Cyanobacterial members, spanning multiple genera, which have been observed to be true-boring include *Mastigocoleus*[24], *Cyanosaccus*[27], *Hormathonema*[28], *Solentia*[29], *and Kyrtuthrix*[30] among others. Euendolithic cyanobacteria are known to primarily excavate into calcareous and

calcophosphatic mineral substrates, such as calcite, limestone, dolostones, bone, and shell[31]. The endolithic domain can extend centimeters into a substrate, however, cyanobacteria are phototrophs so typically dominate the photic zone, above 1 cm[32]. Exposed carbonate surfaces are quickly colonized[33] and microboring can significantly affect the erosion rates of geologic[34], biogenic[27, 35] and man-made[36] mineral surfaces as well as be significant pests to the aquaculture industry[37]. Microborers are not always destructive however, as members of stromatolite communities, they often promote sand grain cementation increasing the overall stability of the microbial assemblage[29, 38].

Despite their global significance and prevalence, cyanobacteria have been relatively understudied, with only a few genuses (*Synechococcus*, *Prochlorococcus, Synechocystis, Trichodesmium,* and *Nostoc*) adequately studied at both the genetic and physiological level. In fact, according to NCBI (in Feb, 2016) there were 4958 bacterial genomes annotated as complete in the public database. Of those, only 91 were cyanobacteria, and of those, > 50% (47) represent sequences of several type strains of only 5 unique genuses. Thus, at the genus level, unique cyanobacterial genome sequences represent less than 1% of the total publically available, completely sequenced, bacterial genomes in NCBI. This is probably a slight underestimate due to genome completeness annotation errors, completed genomes deposited in non-NCBI databases, and currently ongoing sequenced projects, but the number of completed, public, cyanobacterial genomes is certainly not greater than 5% of the total. This highlights our overall lack in understanding of the true genetic and metabolic diversity contained in the cyanobacteria phylum. Current advances in next generation high-throughput sequencing technology (NGS) has allowed researchers to probe the nature of environmental adaptation in some

cyanobacteria at the complete gene expression level[39-41]. No genomic or transcriptomic studies have been conducted on a euendolithic model system in an attempt to elucidate any specialized adaptations allowing these unique organisms to live in such a specialized niche.

Global Carbon and Microbes:

The global carbon cycle is the most important biogeochemical process on Earth. It plays a role in many important planetary events such as regulating global atmospheric temperature, ocean acidification, and primary productivity. Atmospheric levels of the three primary carbon based greenhouse gases CO, CO_2, and CH_4 play major roles in determining the overall global climate. Levels of these gases are regulated by a deceivingly simple looking, yet complex input/output system; the amount of carbon that gets assimilated vs how much carbon gets released. Assimilation can occur in three primary ways: oceanic absorption, the burying of organics in soil, and by photoautotrophic carbon fixation. There are many ways carbon can be released as well, such as volcanic eruptions, chemical weather of carbon containing rocks, organismal respiration, and the burning of fossil fuels[42]. The latter receiving a lot of attention due to its perceptible effects on our current climate state. Fossil fuels represent carbon which was buried and locked away, essentially removed from the greenhouse cycle for eons, until humans figured out it could be used as fuel. Aside from fossil fuel burial, lithification and subsequent burial, as one of the many forms of a carbonate mineral, is the primary mode of long-term carbon storage and accounts for some 80% of the world's sequestered carbon[42] (Table 1. from Falkowski *et al*, 2000). A runaway greenhouse effect can be prevented if net carbon emission stays close to total carbon sequestered. At

present time, it is estimated that upwards of 40% of all anthropogenic carbon emissions remain in the atmosphere thus exceeding the current sequestration ability of the carbon cycle and is responsible for the observed annual increases in atmospheric pCO_2 concentrations since the industrial revolution[43]. It is imperative then, that we attempt to quantify any and all potential carbon sinks and sources to get a more accurate representation of the global carbon budget.

Microorganisms contribute to both sides of the carbon cycle. Terrestrial microbes, primarily soil bacteria, decompose and respire soil organic material back to the atmosphere. Anaerobic methanogens residing in the anoxic zones of lake and marine sediments contribute about 30% of the global methane emissions[44]. An additional 20% of methane emissions come from microorganisms in the guts of ruminants, including agricultural livestock[45]. The global carbon monoxide cycle is less understood, however we know that there has been a steady increase in atmospheric concentration by about 1% per year, probably due to increases by anthropocentric emission[46]. Certain types of anaerobic autotrophic microorganisms have the capacity to non-photosynthetically fix CO and CO_2, but their contributions as global carbon sinks are unknown[47]. The most important microbial carbon sink comes from photosynthetic microbes such as cyanobacteria. Marine cyanobacteria (*Prochlorococcus* and *Synechococcus*) alone account for most of the oceans primary productivity, which represents about half of the global primary productivity[48, 49]. Typically, cyanobacteria are not thought to liberate much carbon into the environment as they are autotrophic. However, we know euendolithic cyanobacteria live inside and, basically, dissolve carbonate minerals which represent a large portion of the lithosphere reservoir of "buried" carbon. The current

estimated global surface area of exposed carbonate is approximately 1.77 X10^7 km^2, which is 13% of the total exposed land area on Earth[50]. It has been suggested that all exposed carbonate, which receives at least some light, will be colonized by euendoliths[51]. As these organisms displace the mineral they bore, they must be fixing the carbonate, releasing it, or both. In any of those scenarios euendoliths are unlocking previously locked up inorganic carbon, implying these microbes represent a potential direct link between geological and biological carbon pools.

The Mechanistics of the Euendolithic Lifestyle

Euendoliths typically bore in environments (marine) which are both slightly alkaline (pH 8.2) and supersaturated with respect to carbonate minerals making dissolution thermodynamically unfavorable, thus cells must expend energy to bore[52]. Several plausible theories explaining this phenomenon have been proposed. As calcium carbonate is relatively soft and easily dissolved in the presence of a weak acid, the most parsimonious theory involves the secretion of acid by the boring organism, which would allow penetration and growth into the substrate[51]. However, cyanobacteria are photoautotrophs, who, by the very nature of their metabolism alkalinize their immediate surroundings thermodynamically favoring carbonate precipitation not dissolution, simple localized acidification would be impractical for cyanobacteria. Others suggested that perhaps a temporal or spatial separation of photosynthesis and respiration may allow the generation of sufficient acid quantities either during the night or from specialized boring cells which switch off photosynthesis[52]. The utilization of acid as the primary driver of substrate dissolution, while plausible, is not physiologically sustainable. Cyanobacteria do not survive low pH environments well[53, 54] and the number of carboxylic acid moieties

that must be created during carbon fixation is stoichiometrically equivalent to the moles of CO_2 fixed and protons already utilized[52]. This method of dissolution would require most of the organism's fixed carbon to be used for acid generation.

The most thermodynamically favorable theory suggested that removal of the metal ion from the interstitial space (that between the membrane of the organism and the surface of the mineral) could alter the mineral saturation enough to shift the equilibrium, following Le Châtelier's principle, towards dissolution. Indeed, recent work using the model filamentous euendolith *Mastigocoleus testarum* strain BC008 has confirmed that calcium mobilization is the central process driving carbonate dissolution and may represent a fairly widespread mechanism[55, 56]. The current boring model suggests that calcium ions are taken up at the apical cells (inside the chip) of boring filaments and transported, intracellularly, toward the distal ends of the filaments (external to the chip). Once the Ca^{2+}reaches the distal ends it is extruded into the media by ATP-dependent active pumping facilitated by the action of a P-type calcium ATPase. The model was built upon data obtained from bulk culture analysis focusing on calcium extrusion by a population of cells (Fig. 2. taken from Garcia-Pichel, Ramirez-Reinat, & Gao, 2010). While this method was sufficient to invalidate several suggested theories concerning dissolution mechanistics and conclusively show that calcium was actively transported to the mineral surface by the cyanobacterium it still left many important questions unanswered. How do filaments actually transport the calcium? Is it pumped intracellularly or into the periplasm to diffuse up and out? Where are these pumps located, at every cell or just at the external extruding tip? Do all filaments bore simultaneously? How does the organism deal with extreme intracellular calcium

concentrations? What is the fate of the released carbonate anion, is it fixed or does it diffuse away? Are there large physiological and metabolic shifts required to live within a mineral matrix? All questions I needed answers to.

The problem with living inside a rock

If we look closer at the extant endolithic habitat we find fairly extreme conditions. In natural marine settings euendolithic communities are inhabited by several microborers simultaneously which can include fungi and phototrophic eukaryotic algae[57]. Penetration of the mineral substrate by these organisms often occurs to depths of a centimeter or more, depending on light availability[32]. Epilithic growth is often observed forming a biofilm on the surface of endolithic communities. A consequence of boring into calcareous substrates and extruding calcium ions at the mineral surface is a boundary layer supersaturated with calcium which can lead to the formation of a reprecipitated calcite (micrite) rind[58]. A surface biofilm combined with the cementation effect of the micrite as well as the depth to which these euendolithic organisms can penetrate suggests diffusive access to external nutrients may be limited. These communities have many of the same characteristics of well-studied phototrophic microbial biofilms, such as intertidal microbial mats, and should be considered lithic biofilms[32, 59, 60]. Additionally, it has been shown that lower layers of marine biofilms can be diffusively cut off from the external environment[61, 62]. This limitation works in both directions, CO_2 cannot get in, but waste products cannot get out either. This would be an especially precarious situation for any organism whose primary metabolic waste product is oxygen, such is the case for cyanobacteria. Thus, any euendolithic organism must either have remarkable antioxidant properties or be able to limit its O_2 production. The transport and acquisition of many

other, equally important solutes, would also be an issue. The long range transport and exchange of phosphate, nitrogen, iron, sulfur, water, sodium, potassium, hydrogen and magnesium, to name a few, would need to be greatly facilitated. Compared to living in the open ocean, as a planktonic organism, with direct diffusive access to almost everything you need, the endolithic lifestyle seems a poor choice.

So why then would any organism want to bore into and live within a rock? There have been several theories put forth to try and answer this question. We have considerable evidence which suggests that euendolithic organisms already existed between 2.7 and 1.5 Ga[2, 63-65]. The environmental conditions leading to the evolution of this trait unknown. We can, however, make some assumptions based on the little we do know about the Earth at that time. Evidence suggests cyanobacteria predate the GOE; if correct, they must also predate the formation of Earth's ozone layer. Ultraviolet radiation levels at that time would have been much higher than they are now, and would have included the much more damaging UVC component. The ability to live beneath the surface of a mineral would greatly reduce exposure to UV radiation, and if that mineral is, at least partially translucent or photoconductive (such as calcite), photosynthetic rates would be relatively unimpeded. Currently, endolithic microbial communities provide an important food source for various benthic grazers which consume the organisms as they grow out of, or on top of, the rocks[66] and living beneath the surface provides protection from predation. However, euendolithic cyanobacteria predate the evolution of eukaryotic grazers by almost a billion years. Nevertheless, grazers do create a present-day selection pressure to remain euendolithic. Another possibility is temperature or osmotic regulation. There is considerable debate as to what the Earth's early climate was actually like but

there is speculation that Precambrian oceans were hot and salty[67]. Which is supported by the fact that most extant cyanobacteria are heat and salt tolerant. Perhaps a few millimeters below the rocks surface it was a few degrees cooler or endolithic organisms could better regulate their internal osmotic balance by limiting exposure to hypersaline waters. The final theory I'd like to propose is my own, observation of extant marine biofilms, including epi-and endolithic communities, which suggests limited diffusive access to nutrients (including CO_2) towards the lower reaches of the biofilm. Any photoautotrophic organisms in those lower layers, cut off from C_i sources, would need to find an alternative source of inorganic carbon (C_i) to fix. If this early organism was an anoxygenic phototroph which used sulfide as an electron donor, sulfuric acid would have been a metabolic by product. Should that biofilm have formed on a carbonate mineral surface, by virtue of the buried organism's own metabolism, it would liberate all the C_i it needed. This theory can explain the potential evolution and need for the retention of the euendolithic trait but it does not explain the presence of this trait in an oxygenic cyanobacterium which is not known to secrete acidic metabolic byproducts but instead bores based on calcium mobilization.

It is interesting to speculate that perhaps epi- or endolithic anaerobic organisms were actually the first group of microbes to evolve. There is a report suggesting that several reactions of central importance to the reverse Krebs cycle, an ancient type of carbon fixation found in many anaerobes, including anoxygenic phototrophs, can be catalyzed solely at a mineral surface[68, 69]. There is speculation that the protocyanobacterial ancestor evolved from an anaerobic phototroph-like organism[11]. Perhaps oxygenic photosynthesis evolved as reduced electron donors such as ferrous iron

and sulfide became scarce within endolithic microbial communities which could have forced the utilization of water as an electron donor[70, 71]. As these newly evolved "water splitters" created oxygen, the concentrations within these lithic biofilms would have become high, creating the so-called, "oxygen oasis", forcing all members of these communities to essentially adapt or die. There is evidence suggesting that marine biofilms were among the first oxic environments on Earth[72, 73].

Specific Aims

The primary goals of this dissertation are to further our understanding of the euendolithic boring mechanism and to elucidate specific adaptations allowing these unique organisms to survive in such a specialized niche. This work is divided into four primary chapters with Chapter 1 and a sub-section of Chapter 3 already published. In Chapter 1, I address several physiological aspects of calcium transport which remain unresolved such as the cellular arrangement of the P-type ATPases thought to play a central role in calcium transport as well as the intracellular nature of the transport itself. Methodological approaches utilized to this end include confocal fluorescence microscopy using intracellular calcium fluorophores, ratiometric pH probes, fluorescently labeled ATPase probes, and fluorescent membrane binding agents. This chapter presents data highlighting the level of cellular complexity and coordination which is required to efficiently and actively excavate calcium carbonate substrates within our model euendolithic organism, *Mastigocoleus testarum* strain BCOO8.

In an effort to validate a portion of the proposed boring model and to support an additional theory underlying the potential evolution of euendolithic organisms, Chapter 2 focuses on the fate of the liberated inorganic carbon which is released during mineral

dissolution. There I use several geochemical techniques including natural ^{13}C stable isotope analysis as well as ^{13}C spike-in tracer analysis combined with NanoSIMS imaging. The data presented in this chapter will describe the intimate relationship between the mineral and the euendolith. I also attempt to show the potential universality of this relationship by similarly analyzing natural endolithic communities.

As no genomic information is available for any known euendolith a prerequisite to any type of comprehensive gene expression analysis is the characterization of an organism's genome. Chapters 3 and 4 are the "omics" chapters and there I present data related to both the genomic and transcriptomic structure of our model euendolith. Genome sequencing revealed a complex genomic architecture comprised of one of the largest sequenced prokaryotic genomes. In an attempt to uncover euendolithic specific adaptations, I completed a comparative transcriptomic study of both euendolithic and planktonically grown *Mastigocoleus*.

The association of microbes and rocks is perhaps the oldest biological and geological relationship known. However, the exact nature of these associations are relatively unknown. It is my wish that this research will provide some novel insight into this ancient global rapport and that my data will generate new and testable hypotheses for the next generation of "boring" scientists.

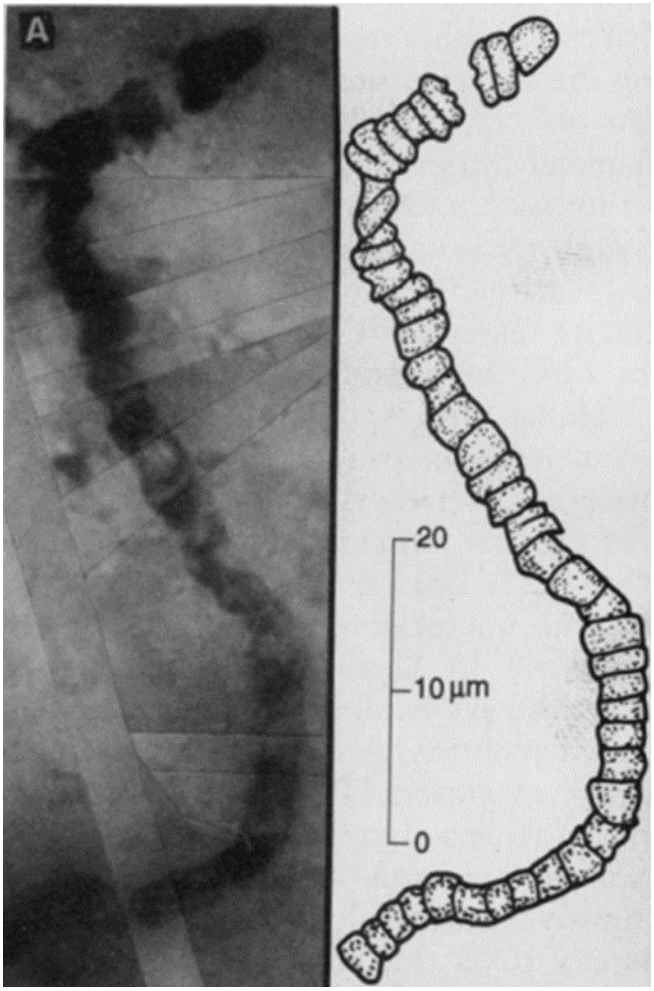


Fig. 1. - A selection of Fig. 4 (Panel A) taken from Schopf, 1993, illustrating fossilized evidence (left) along with an interpretive drawing (right) found in the Apex chert formation (~3.6 Ga) in Australia of a filamentous organism bearing a striking resemblance to extant filamentous cyanobacteria. This evidence suggest an early evolution for cyanobacteria.

Pools	Quantity (Gt)
Atmosphere	720
Oceans	38,400
Total inorganic	37,400
Surface layer	670
Deep layer	36,730
Total organic	1,000
Lithosphere	
Sedimentary carbonates	>60,000,000
Kerogens	15,000,000
Terrestrial biosphere (total)	2,000
Living biomass	600–1,000
Dead biomass	1,200
Aquatic biosphere	1–2
Fossil fuels	4,130
Coal	3,510
Oil	230
Gas	140
Other (peat)	250

Table 1. - Table 1 taken from Falkowski *et al.* 2000, showing the relative amounts of carbon in each of Earth's predicted carbon pools.

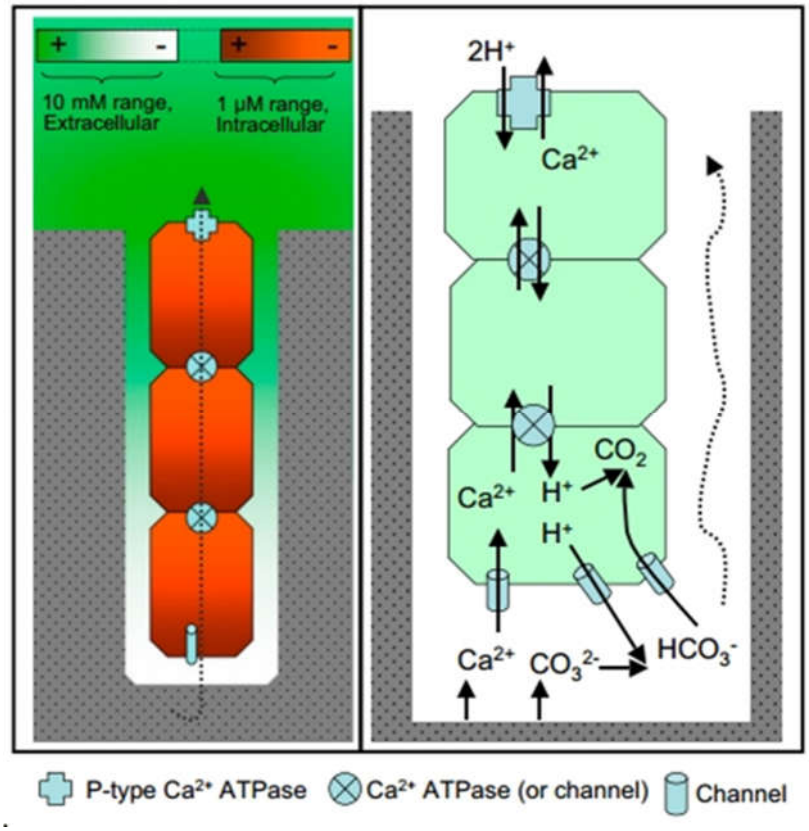


Fig. 2. - Figure 7 taken from Garcia-Pichel, Ramirez-Reinat, & Gao, 2010, depicting the working model of calcium carbonate dissolution based on bulk calcium efflux measurements during incubation with various selective inhibitors.

CHAPTER 1

EXTREME CELLULAR ADAPTATIONS AND CELL DIFFERENTIATION REQUIRED BY A CYANOBACTERIUM FOR CARBONATE EXCAVATION

ABSTRACT

Some cyanobacteria, known as euendoliths, excavate and grow into calcium carbonates, their activity leading to significant marine and terrestrial carbonate erosion, and to deleterious effects on coral reef and bivalve ecology. Despite their environmental relevance, the mechanisms by which they can bore have remained elusive and paradoxical, in that, as oxygenic phototrophs, cyanobacteria tend to alkalinize their surroundings, which will encourage carbonate precipitation, not dissolution. Therefore, they must rely on unique adaptations to bore. Studies with the filamentous euendolith, *Mastigocoleus testarum*, indicated that excavation requires both cellular energy and transcellular calcium transport, mediated by P-type ATPases, but the cellular basis for this phenomenon remains obscure. We present evidence that excavation in *M. testarum* involves two unique cellular adaptations. Long-range calcium transport is based on active pumping at multiple cells along boring filaments, orchestrated by the preferential localization of calcium ATPases at one cell pole, in a ring pattern, facing the cross-walls, and by repeating this placement and polarity, a pattern that breaks at branching and apical cells. Additionally, *M. testarum* differentiates specialized cells we call calcicytes. They accumulate calcium at concentrations more than 500 fold those found in other cyanobacteria, concomitantly and drastically lowering photosynthetic pigments, and enduring severe cytoplasmatic alkalinization. Calcicytes occur commonly, but not exclusively, in apical parts of the filaments distal to the excavation front. We suggest that calcicytes allow for fast calcium flow at low, non-toxic concentrations through undifferentiated cells by providing buffering storage for excess calcium before final excretion to the outside medium.

INTRODUCTION

Cyanobacteria that actively bore into carbonaceous substrates (also known as euendoliths) are a functional class of microbes that contribute to the erosion of marine[34,35] and terrestrial[36] carbonates, both mineral and biogenic. These organisms can impact coral reef ecosystems, and constitute a commercially significant pest to bivalve farms[35, 74]. Carbonate excavation rates of euendolith communities may increase with elevated oceanic pCO_2, as is the case with boring sponges[75, 76]. Despite their global environmental impact, and their potential sensitivity to global climate change, the physiological and cellular mechanisms behind photoautotroph-mediated carbonate dissolution has remained largely elusive[52]. Cyanobacteria, like other autotrophs, alkalinize their local microenvironment by virtue of their carbon fixation activity, typically facilitating carbonate precipitation (Garcia-Pichel et al, 2004), not dissolution. In the case of marine euendoliths, seawater is supersaturated with respect to calcite and aragonite, making carbonate dissolution thermodynamically unfavorable. Both types of constraints render the process of boring quite paradoxical[51, 52].

In our laboratory, we have recently developed a conceptual model of the physiology of cyanobacterial carbonate excavation based on experiments carried out with the model filamentous euendolith, *Mastigocoleus testarum* strain BC008[56]. Like many filamentous cyanobacteria, this strain is a true multicellular microbe: it displays complex morphological plasticity, which includes cell differentiation of lateral heterocysts dedicated to nitrogen fixation, motile multi-celled hormogonia for dispersal, true branching of the main thallus, and the ability to alter filament morphology during boring into solid substrates[55]. In the current model[56], calcium ions are preferentially imported by

passive diffusion into apical cells that are proximal to the boring front, this lowers the Ca^{2+} concentration, in the interstitial microenvironment between this apical cell's surface and the solid mineral, below the solubility product of the corresponding mineral, thus shifting equilibrium there towards dissolution. This allows the organism to selectively dissolve the substrate directly adjacent to the apical tips of boring filaments, and to grow into that space. Intracellular calcium (Ca^{2+}_i) then moves cell to cell from the boring front toward the mineral surface where it is actively pumped out into the liquid medium by distal apical cells. Extruded excess Ca^{2+} can either diffuse away or, in some cases, repricipitate into a micrite rind[77, 78]. Boring continues into the solid substrate until the organism reaches its limit of light intensity for growth.

The model called for the agency of P-type calcium ATPases in the transport process, but did not address if the pumps are predominantly located on the distal cells, where extrusion to the medium occurs, or if they are also located between cells, thus participating in the cell-to-cell transport of Ca^{2+}. The model also assumed that protons constitute the counter-ions exchanged for calcium to maintain charge. The concentrations of Ca^{2+}_i attained during transport, of paramount importance for cell physiology given the ion's toxicity in most cellular systems, including cyanobacteria[79, 80], remain unknown, but there is a potential that a borer's cells might experience prolonged, very high Ca^{2+}_i concentrations[56]. The experimental evidence in support of the current model was obtained using selective inhibitors, and an extracellular calcium fluorophore to study Ca^{2+} dynamics during boring. While this method was appropriate to assess bulk Ca^{2+} transport, it did not address intracellular processes directly. In this contribution, we intended to assess Ca^{2+} transport and related processes in *Mastigocoleus testarum*, by

extending experimentation to the intracellular domain, during both boring and planktonic growth.

RESULTS AND DISCUSSION

Vectorial Transfilamentous Calcium Transport

If transport were driven exclusively by distal apical pumps, then severing a filament midway should not result in leakage of calcium at the breakpoint, given that the extracellular concentration in seawater medium (10 mM) is much higher than physiologically plausible[80]. However, if pumps existed along the entire filament, they would remain active, and localized regions of calcium super-saturation in the medium would be observed adjacent to filament breakpoints, just as it is seen close to the apical cells that extrude Ca^{2+} to the outside medium[56]. Mechanical severing of boring filaments at various filament locations after making them accessible by cleaving the mineral substrate along the direction of excavation, did indeed result in substantial and localized increases in Ca^{2+} in regions directly adjacent to damaged filaments (Fig. 3 - B; White arrowheads), as measured with extracellular Ca^{2+} dyes. In order to continually "bleed" Ca^{2+}, as observed, a back pressure of calcium must have existed. This pressure can only be supplied by continuous active pumping of an adjacent cell into the severed cell (or the space around the severed cell). Thus, Ca^{2+} pumping occurs along the length of each boring filament using many active pumps located in more than one cell within each filament, clearly invalidating the notion that transcellular pumping is driven by a "negative pressure" established at the distal apical cells.

P-type Calcium ATPase Localization

The inhibition of calcium extrusion in BC008 by P-type calcium ATPase-binding antagonists, such as thapsigargin[56, 81] had revealed their agency in the process of calcium extrusion during boring. In an attempt to localize the exact sites of activity of these enzymes, we used fluorescently labeled thapsigargin (BDTH), which has been shown to bind specifically to eukaryotic P-type calcium ATPases[82, 83]. Controls using only the fluorophore (BODIPY-Fl, with no thapsigargin) showed some non-specific binding to the extracellular sheath, but no particular binding patterns, and no membrane colocalization (Fig. 8 - B). A control with thapsigargin alone showed no fluorescence in the appropriate channel. *Mastigocoleus testarum* strain BC008 stained with BDTH displayed homogenous membrane staining, but significantly higher signal was observed close to the cell septal region (Fig. 4 - A). 3D reconstructions of the optical sections show that the regions of increased staining manifest as an annulus adjacent to the septal area (Fig. 4 - B). Importantly, only one of the two septal sides in a given cell showed preferential staining, and the polarity of the annuli tended to be repetitive along neighboring cells. Separate experiments using membrane-specific dies showed that our current technique allows us to resolve both sides of the septa (Fig. 10 - A). This clearly suggests a sequential, vectorial transport in a single, coherent direction along the filament. This coordinated polar pattern seems to break down at filament branches, or at certain regions of adjacent cells containing very low photopigment autofluorescence (PSAF), in which signals are intense all around the membrane (Fig. 4 - A, asterisk). In some of these special regions one can indeed see two zones of intense BDTH staining at opposite sides of the same septum. Boring filaments that had been disinterred from the calcite matrix

showed indistinguishable patterns of binding to those seen in mineral-free filaments. However, the intensity of BDTH signal in boring biomass was significantly higher (six times; $p < 0.03$, t-test), indicating an increased presence of the transporters in membranes of boring cells (Fig. 7). This corroborates previous findings at the gene expression level[56]. As P-Type ATPases extrude calcium, they antiport protons[84] and are likely to alter pH locally if found in sufficient concentration. We used a ratiometric pH sensitive fluorophore to monitor intracellular variations in pH that may denote their activity and preferred location. In agreement with the localization observed by direct staining, we could observe clear periplasmic alkalization adjacent to septal annular regions (Fig. 6 - C). Together, these observations support the central role P-type calcium ATPases in the excavation process indicating the presence of a vectorial arrangement of these pumps in vegetative cells that drives transcellular transport.

Intracellular Calcium Dynamics

Cyanobacteria show a very tight regulation of Ca^{2+}_i levels, typically in the low nanomolar range[80, 85, 86], but Ca^{2+} pumping in euendoliths could potentially create transient or even continued intracellular hyper-accumulation[56]. We used several approaches to probe Ca^{2+}_i in strain BC008. In our initial studies we used the extracellular indicator calcium green 5-N (CG5N), noticing that after prolonged incubation it could penetrate filaments of BC008. Using CG5N with transversally cracked calcite chips containing intact filaments (Fig. 5 - E), Ca^{2+}_i accumulation was clearly observed in cells corresponding to apical distal tips as they extended into the liquid medium. But some groups of cells inside the chip did also show such accumulation. Interestingly, these high-calcium cells, which we call calcicytes, presented visibly less photosynthetic pigment

(judged by their low PSAF signal) than cells with low $Ca^{2+}_{i.}$ This diagnostic inverse PSAF to calcium signal of calcicytes was not exclusive of apical distal areas, but also found in specific stretches along filaments, in individual cells or, more often than not, in a group of adjacent cells. Similar results were obtained using the intracellular Ca^{2+} reporter dye Fluo-5F AM both in cultures that had been grown outside the solid (Figs. 5 - A, 9), and those boring inside of calcite chips (Fig. 8 - B). To determine if this marked cellular heterogeneity in Ca^{2+}_{i} was an unusual trait specific to BC008, or common to cyanobacteria at large, we extended our analyses to two common but not endolithic laboratory strains of filamentous cyanobacteria, *Nostoc punctiforme* 29133 and *Microcoleus vaginatus PCC 9802.* The latter two showed very low Ca^{2+}_{I} signal compared to that obtained in strain BC008, and very small cell-to-cell variations in Ca^{2+}_{i} (Fig. 5 - B and C). *Mastigocoleus testarum* BC008 clearly shows a high degree of cellular heterogeneity of both Ca^{2+}_{i} content and photosynthetic pigment complement. A quantitative analysis of the average volumetric calcium and PSAF intensities in cells of BC008 shows the presence of two distinct cell populations. One encompasses cells with PSAF and calcium similar to *Microcoleus* or *Nostoc* (Fig. 5 - D). The second population, which typically includes cells close to the tips of filaments (Fig. 5-D, colored squares), have high Ca^{2+}_{i} signals; in cells from this population there is a linear inverse relationship between Ca^{2+}_{i} and photopigment, indicative of progressive spatial separation between photosynthesis and Ca^{2+}_{i} hyperaccumulation. It can be logically postulated that high Ca^{2+}_{i} may interfere with photosynthesis, and that there is a causal relationship in this correlation. We would like to note that hyperaccumulating cells are clearly not dead nor moribund: intracellular dyes are only fluorescent in the presence of active cellular

esterases[87, 88], and all cells contained intact DNA (as determined by DAPI staining, not shown), which speak for the integrity of the cell membrane. Thus, the most parsimonious explanation for these findings are that cells in distal apical (and some intercalary) regions may be differentiating into specialized calcium Ca^{2+}_i holding cells, or calcicytes.

The levels of Ca^{2+}_i observed in calcicytes are unprecedented. Average Ca^{2+}_i signals in *M. testarum* (including cells with low and high calcium content) were 6 fold higher than those in *Nostoc* and 3 fold higher than those in *Microcoleus* under identical imaging and staining conditions. Maximal Ca^{2+}_i could reach 22 and 6 fold higher, respectively (Fig. 5- D). While we could not quantitate Ca^{2+}_i in BC008 directly, the resting Ca^{2+}_i concentration in *Anabaena* is around 200 nM[78]. Assuming this level to be typical for filamentous cyanobacteria, then some calcicytes of non-boring BC008 biomass accumulated 4-5 μM Ca^{2+}_i and boring calcicytes upwards of 100 μM, approximately 500 fold the resting levels seen in canonical *Nostoc* cells.

Intracellular pH heterogeneity

Assessing intracellular pH (pH_i) in BC008 was imperative to establish a direct connection between transport of calcium in normal cells, its accumulation in calcicytes, and the mechanism of known calcium ATPases[84]. While homeostatic regulation of pH_i in cyanobacteria is not completely understood, they do not tolerate large drops in external pH[53, 54] and those studied keep circumneutral pH_i, even under alkaline external conditions[89, 90]. We used a ratiometric pH_i indicator (BCECF-AM) to interrogate relative pH_i variability in BC008, and could indeed document clear alkalinization within many of the cells containing low PSAF, including distal apical cell groups (Fig. 6), indicating that they, in fact, correspond to calcicytes, and consistent with the predicted alkalinizing

effect of a calcium/proton antiport. Although our attempts to directly calibrate the pH_i data in *BC008* were unsuccessful, comparisons with absolute calibration curves carried out in *Nostoc punctiforme* were used as a reference. In non-boring cultures we could detect alkalinization ($\Delta pH = 1$) in cells fitting the low PSAF diagnostic for calcicytes, including apical cell groups (Fig. 6 - A and B, arrows). Surprisingly, in these cultures, vegetative cell pH was kept slightly acidic. In boring cultures, cellular variations in pH were much larger ($\Delta pH = 3$), calcicytes reaching pH above 9.5 (upper limit for reliable measurements). In excavating filaments, cells of acidic pH were closer to the boring front (Fig. 6 - C and D), in agreement with an overall directional counter-transport of protons. The magnitude of such pH_i variations is consistent with those seen in $Ca^{2+}{}_i$. Calcicytes thus sustain severe alkalization of the cytoplasm. Incidentally, given that the fluorescent yield of most calcium fluorophores is strongly quenched by increasing pH[56], a second corollary of a calcicyte's high alkalinity, is that the levels of $Ca^{2+}{}_i$ we inferred for them are likely underestimated.

CONCLUSION

Our results shed light on the cellular basis of microbial carbonate excavation. Together, they point to a sophisticated mechanism that involves two types of unique cellular adaptations: marked, coordinated, cell polarity in calcium transport within normal cells, and the differentiation of a specialized cell type, the calcicyte, which accumulates large concentrations of $Ca^{2+}{}_i$ and sustains significant alkalization of the cytoplasm, likely to the detriment to their photosynthetic capacity. We cannot ascertain, at this time, whether high $Ca^{2+}{}_i$ or pH_i simply impedes photosynthesis, leading to degradation of photosynthetic pigmentation or if there is a morphogenetic regulatory

mechanism at play. We postulate that this euendolithic cyanobacterium maintains Ca^{2+}_i levels low and pH_i circumneutral (maybe slightly acidic under boring conditions) in most cells, even in the face of high transport fluxes, by concentrating excesses in a few calcicytes, that serve as "capacitors" or depots for the long range transport of Ca^{2+} between mineral and outside medium. Calcicytes are located at crucial points in the flow or, typically, at the distal apical areas, in preparation for final excretion. If a calcicyte's phototrophic capacity is fully impeded, it must rely on resources imported from vegetative cells for energy and fixed carbon. The cellular basis of calcium transport seems to rely on a biased distribution in the localization of P-type calcium ATPases, across the filaments, which preferentially pump into the periplasm at one side of the cell. For this to work, one has to postulate the presence of calcium channels for passive diffusion into the next cell; we do not have evidence of this yet. Such a distribution, with ATPases at one side of the cell and channels at the other, if repetitive, could easily account for vectorial transport while maintaining intracellular concentrations low. Direct cell-to-cell transport is less likely as it would have to cross large spaces that span 2 cell membranes and one peptidoglycan rich periplasm (The septum is between 30 and 40 nm thick and the outer membrane does not extend into the septal region, Fig. 10 - A and C). A direct transport would fail to explain the localized pH excursions seen in Fig. 6 - C.

Some aspects beyond the presence of calcium channels remain to be studied in any detail, particularly how the initial mineral calcium enters the cell past the cell envelope (through the sheath, across two membranes, and the periplasm) at the apical cells in the boring front, and how they are fully extruded at the apical cells. As far as we know, such transcellular, vectorial calcium transport is unique to euendolithic

cyanobacteria and represents a novel physiological adaptation in these organisms. It is clear that pH_i dynamics are complex in this organism and directly linked to calcium traffic, presumably in the opposite direction of calcium, toward the boring front. This would facilitate crystal dissolution by allowing the continued conversion of carbonate anions to bicarbonate and CO_2, which could be used as a carbon source in autotrophy within the crystal matrix. Potentially, Na^+ may directly or indirectly adjuvate the proton counter-transport by neutralizing any charge imbalance. Each filament would then be made up of repeating units of polar cells, with one side allowing calcium entry (boring side) and the other mediating calcium release (and subsequent proton entry) (Fig. 11.). This model is particularly appealing as it may also explain the ability of single cells[36] to bore, given that such a single cell could not penetrate the mineral without some type of calcium transport polarity.

That the evidence for traits necessary for boring, such as the polar localization of calcium transporters (through thapsigargin staining), calcicyte differentiation, and marked Ca^{2+}_i / pH_i heterogeneity among cells, was not only observed in boring cultures, but also in mineral free filaments, indicates that the boring capacity is constitutive, always on, in *M. testarum*. The differences found between the two growth modes were only in intensity. This likely reflects the fact that these organisms are found exclusively in the boring form in natural settings, so that there is no fitness value in a hard-wired induction. It may be that the only mineral-free form of this organism in nature is that of hormogonia during dispersal. We note here that, in agreement with this view, *Mastigocoleus testarum* strain BC008 cultured without carbonate easily loses its ability to bore. In any event, the sophistication of true multicellular differentiation and division of labor in a single

prokaryotic organism is remarkable. The differentiation of calcicytes, comes in addition to heterocyst formation, true branching, coordinated changes in trichome width, and formation of motile hormogonia for dispersal, all present in BC008[81]. Because we have a rather significant fossil record of euendolithic cyanobacteria dating back 1.5 Ga[64] one can infer that such true multicellular (i.e. beyond morphological)[91] adaptations in cyanobacteria are quite ancient as well.

MATERIALS AND METHODS

Cultures and Growth conditions

Mineral-free cultures of *Mastigocoleus testarum* strain BC008 used for experimentation were grown in standard, vented-cap, tissue culture flasks containing 15 mL PES-30 medium, which consists of 30 g of Instant Ocean® ,10 mM HEPES, and 10 mL of a PES nutrient solution stock[92], per liter of distilled water adjusted to a pH of 8.1. Cultures were incubated on a slowly rocking platform using a 16 hour light/ 8 hour dark diel illumination cycle, at a light intensity of 22 μmol photon m-2 s-1. Boring cultures were obtained by adding ethanol-sterilized calcite chips (blocky calcite, Ward's Scientific) of small size (< 5 mm3) to mineral-free cultures, until the chips were colonized. Cultures of *Nostoc punctiforme* ATCC 21933 and *Microcoleus vaginatus strain PCC 9802,* used for comparisons, were obtained from stocks grown in liquid BG11^{O} medium and Jaworski's Medium[93], respectively.

Confocal microscopy and image analyses

All LASER scanning confocal fluorescence microscopy (LSCM) was performed on either a Leica SP2 or on a Leica SP5 confocal microscope. Images were obtained at a

minimum of 1024X1024 resolution (unless specifically noted) with a minimum line average of 2 and a scan rate maximum of 400 MHz.

Specimen Preparation

All mineral-free samples were imaged live, on glass slides under coverslips, with sealed seams, using a 20X or 63X oil immersion objective. Samples of mineral-boring cyanobacteria were observed *in situ* while placed in 65 X 25 mm dishes containing 10 ml of PES-30 medium and using a 20X or 40X dipping objective.

Fluorescent microscopy and indicators

Fluorescence emission was measured using different excitation wavelengths as needed. Excitation was done sequentially to prevent autofluorescence bleed-through into different fluorophore channels. The "red channel" of emission in all images represents the natural photosynthetic pigment autofluorescence (PSAF) signal and was obtained using an excitation of 561 nm and collected between 660 and 700 nm. The following commercial (Molecular Probes, Eugene, OR, USA) indicators were used: Calcium Green-5N (CG5N), Fluo-5F AM, FM4-64Fx, and BCECF-AM. Hydrophilic indicator stock solutions were prepared at 1 mM concentrations in 10 mM Tris-HCL buffer at pH 7.5 and all hydrophobic stocks were prepared (1 mM) in anhydrous DMSO. BODIPY FL-Thapsigargin (BDTH) and BODIPY-FL were also purchased from Molecular Probes and resuspended in anhydrous DMSO at stock concentrations of 2 mM. Acetoxy-methyl ester dyes are cleaved by active esterases in viable cells which releases the respective fluorophore [94]. See Table 2 for usage parameters.

Image analysis

All image analyses were done using the MBF 64-bit distribution of the image analysis software ImageJ[95]. For each emission channel we acquired individual Z stacks of images. Each channel stack was background normalized by setting the lower pixel intensity value to that which was observed in stacks obtained from appropriate unstained controls using identical imaging conditions. Linear contrast optimization was done on a case-by-case basis and applied equally to all stacks analyzed simultaneously. As needed, normalized images in a stack were then summed, merged, and projected into a single image. To assess relative concentration of analytes, regions of interest were manually circumscribed around cells of interest in a summed stack, and the average value of the area was divided by the cell's thickness yielding a value with units RFU/μm3. The spectral characteristics of the lipid membrane binding dye used (FM4-64FX) overlap with the endogenous pigmentation (PSAF) emission of BC008, thus to visualize the outer lipid membranes, the PSAF channel was used to create a binary mask. This mask was then used to remove PSAF signal from the FM4-64FX channel leaving behind only pixels which correspond to emission from dye bound to the outer cellular envelope. To compare the total amount of BODIPY-thapsigargin binding between boring and mineral-free biomass, we processed the image stacks as previously described and measured the total pixel average (measurement of all image pixels) BDTH signal intensity for the normalized, summed, projected stacks by the average total PSAF signal intensity to account for differences in biomass between each image series to obtain a ratio of BDTH signal to PSAF.

Calcium imaging

CG5N is canonically used as an extracellular dye in eukaryotic cell biology[96], however, we observed that extended incubation time (≥1hr) of *M. testarum* strain BC008 in CG5N resulted in intracellular CG5N signal. Actively excavated mineral chip fragments were placed in 10mL of PES-30 with 1μM CG5N and incubated for at least 1 h under standard culture conditions prior to imaging. In an effort to validate the observed intracellular CG5N signal we choose to use a second calcium fluorophore with a lower K_d value than CG5N , Fluo5F-AM (2.3 μM as opposed to 5 mM), which is typically used as an intracellular calcium indicator. This dye also enabled interspecies comparisons, since CG5N did not seem to penetrate other cyanobacteria. Mineral-free biomass or single chips containing actively boring biomass were placed in 1.5 mL microcentrifuge tubes and rinsed with fresh PES-30 two times. Cultures were then resuspended in 300μL of fresh medium containing 25μM Fluo5F-AM (50μM for boring cultures). The cells were incubated for at least 1 hour at room temperature then washed twice in fresh media. LSCM and image analysis were done as previously stated

P-type Calcium ATPase localization

Thapsigargin is a pharmaceutical found to inhibit P-type calcium ATPases[83] that is also a potent antagonist to the enzymes responsible for calcium transport and excretion during carbonate boring in *M. testarum* strain BC008 as well as in other euendolithic cyanobacteria in nature[56, 81]. In an effort to determine the cellular localization of these P-type calcium ATPases responsible for Ca2+ transport during excavation, we used a fluorescently labeled analog of thapsigargin (BODPIY-FL, BDTH) which retains its binding specificity to the transporters *in vivo* in animal systems[97]. For this, mineral-free

biomass was placed in 1.5 mL microcentrifuge tube, rinsed with fresh PES-30 twice and incubated in 300μL of fresh medium containing 20μM BDTH for 3 hours at room temperature in the dark. Samples were then spun and washed twice with fresh media before imaging, as described above. Controls were run using the fluorescent carrier alone (DMSO), thapsigargin alone (no BODIPY) and BODIPY-FL alone (no thapsigargin). Boring biomass was disinterred from the carbonate substrate following the published protocol [56]. Lightly bored calcite chips with the external biomass lightly brushed free were pre-chilled on ice in 1.5 mL microcentrifuge tubes containing 300uL of PES-30 media for 30 minutes. These chips were then subjected to EDTA disinterment, but without continual brushing, as soon as boring "beds" of filaments became loose, the entire bed was transferred using sterile fine tipped forceps to a 1.5 mL microcentrifuge tube containing chilled fresh PES-30 medium. Beds were gently washed twice without centrifugation and resuspended in PES-30 containing 20μM BD-TH and incubated for 3 h, at room temperature, in the dark. Samples were carefully washed twice without centrifugation and fresh medium was added before imaging.

BCECF-AM Ratiometric imaging

In order to assess intracellular pH we used the ratiometric intracellular pH indicator 2', 7'- Bis - (2 - Carboxyethyl) - 5 - (and - 6) - Carboxyfluorescein Acetoxymethyl Ester (BCECF-AM). This indicator has a pH independent (isobestic) excitation point (~445nm) and a pH dependent excitation point (488-496 nm). The closest LASER excitation wavelength to the isobestic point in our LSCM was 458 nm, which, while not optimal was sufficient to detect changes with significance. We attempted to create a pH calibration curve using nigericin and valinomycin in order to

obtain absolute pH values, however the ionophores showed little effect over a large range of tested concentrations in *M. testarum*. However, were able to obtain a good standard curve using *Nostoc punctiforme* ATCC 21933, which closely followed an exponential regression between pH 6 and 9.5. Prior to loading *Nostoc* with dye cells were incubated in $BG11^{o}$ containing 10mM EDTA, spun, washed, and resuspended in fresh $BG11^{o}$ containing 25 μM BCECF-AM and incubated for 30 m at room temperature in the dark. These cells were then transferred into the various pH-calibrated buffers containing 50 μM nigericin and 5 μM valinomycin and imaged after a 30 minute incubation. Intracellular BCECF values were determined by isolating only pixels contributing to intracellular signal by utilizing image masking. Masking was done similarly to *Corvini et al*, however image thresholding was done using Li's iterative algorithm for minimum cross entropy thresholding which is integrated into imageJ[98, 99]. Each channel stack was multiplied by the masks and then the projected (summed projections) 496 nm image was divided by the 458 nm channel in imageJ (pixel by pixel) to obtain a 32-bit ratiometric image. This final image represents the relative intracellular pH values for the experiment. Each cell was assigned as a region of interest and average cellular ratio values were plotted against respective pH values. The resulting regression curve was used to approximate the intracellular pH in *Mastigocoleus.*

ACKNOWLEDGEMENTS

We would like to thank Dr. Page Baluch for her valuable expertise and advice with the confocal microscopy experiments. This work was primarily supported by the National Science Foundation grant #1224939, "Intracellular metal pumping in microbial excavation by microbes" from the LT Geochemistry and Geobiology Program.

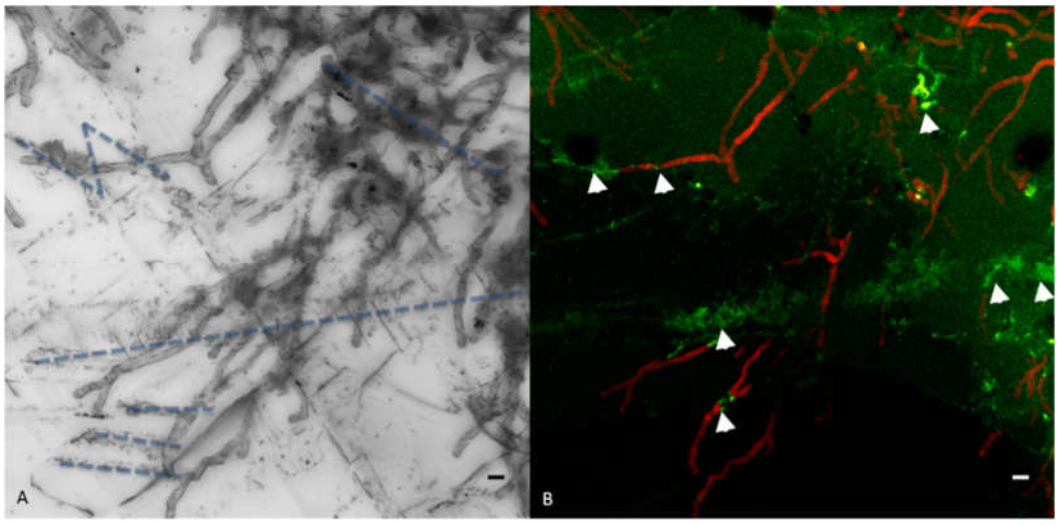


Fig. 3. Calcium pumping occurs along boring trichomes. Infested calcite chips were cleaved at a plane orthogonal to the surface to expose boring filaments lengthwise along the newly exposed face, which was then scraped with a needle, incubated with a calcium sensitive dye and imaged. A) Transmitted light image showing boring filaments within the chip on the cleavage plane. The original surface was to the upper right, boring proceeding towards the bottom left. Dashed lines denote scouring lines. B) Confocal imaging of the same area, where photosynthetic pigment autofluorescence is red and calcium reporter dye is green. Arrowheads point to localized supersaturation in extracellular calcium. When cells were bleach-killed, there was no significant calcium release. Scale bar is 10 μm.



Fig. 4. Cellular localization of P-Type calcium ATPases by thapsigargin targeting. A) Most cells present strong preferential labeling (green) at one side of the septum (white arrowhead), the polarity maintained from cell to cell. Special cells (asterisks) show a generalized, strong labeling appearing on both sides of adjacent septa. Scales are 10 µm. B) 3D reconstructions reveal that the preferential membrane label forms an annulus facing the periphery of the septal region. Controls using unconjugated fluorophore (Fig. S4-B) or thapsigargin alone showed no membrane binding. C) Ratiometric pH image showing increased pH at septal periplasmatic regions facing the ATPase annuli. Absolute calibrations were carried out using *Nostoc* cultures.

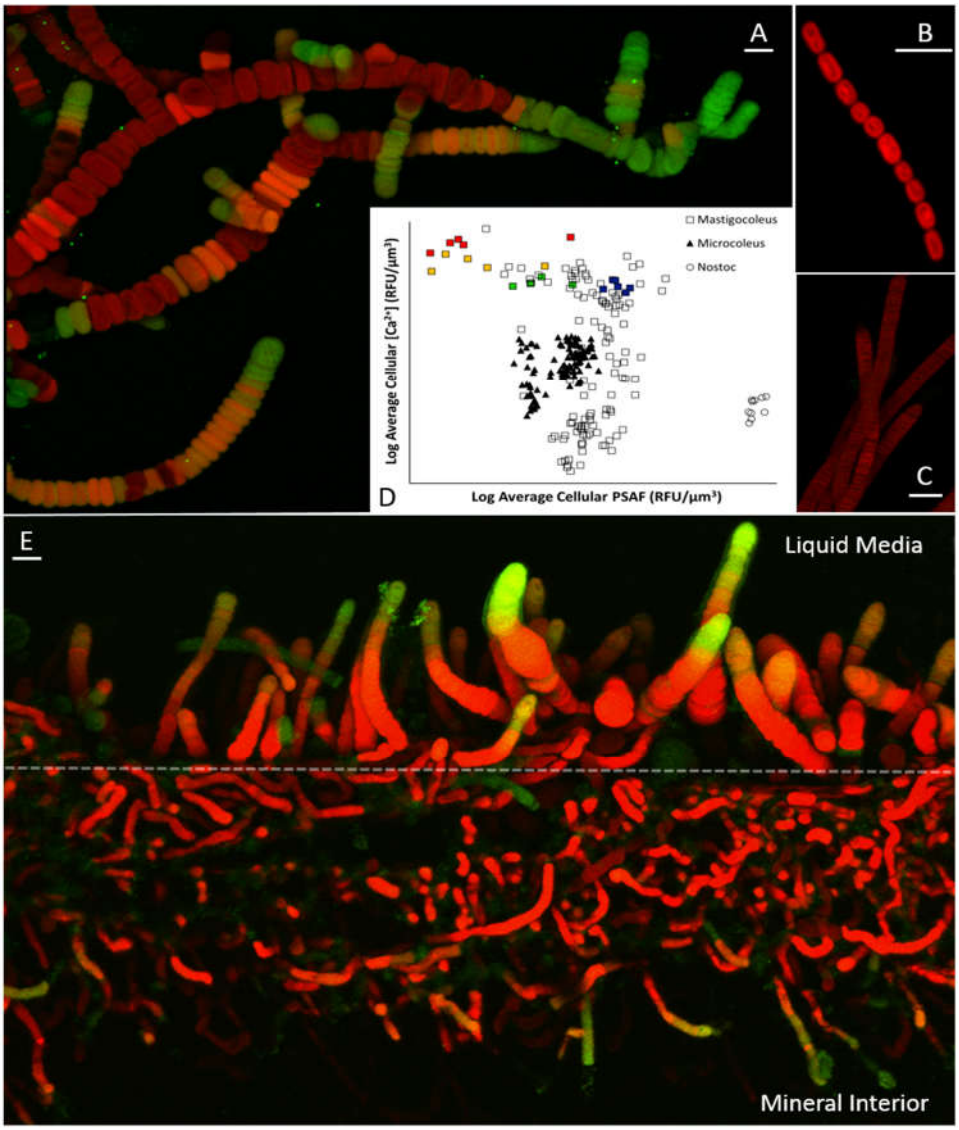


Fig. 5. Cellular heterogeneity in calcium concentration. Confocal projection images of photosynthetic pigment autofluorescence (red) and Ca^{2+}_i reporter fluorescence (Fluo-5F-AM , green) in mineral-free cultures of BC008 (A), *Nostoc punctiforme* ATCC 21933 (B), and *M. vaginatus* PCC 9802 (C). (D) Quantitation of Ca^{2+}_i in cells of BC008 (n=138), *Nostoc* (n=10), and *Microcoleus* (n=113) plotted against their photosynthetic pigment content. Colored squares denote apical cell groups (BC008 only). (E) Confocal projection as in (A) of a calcite chip infested by BC008, split orthogonal to the surface to reveal a cross-section of the boring bed. The dashed line represents the interface between the medium (above) and the solid (below). Scale bar is 10 µm.

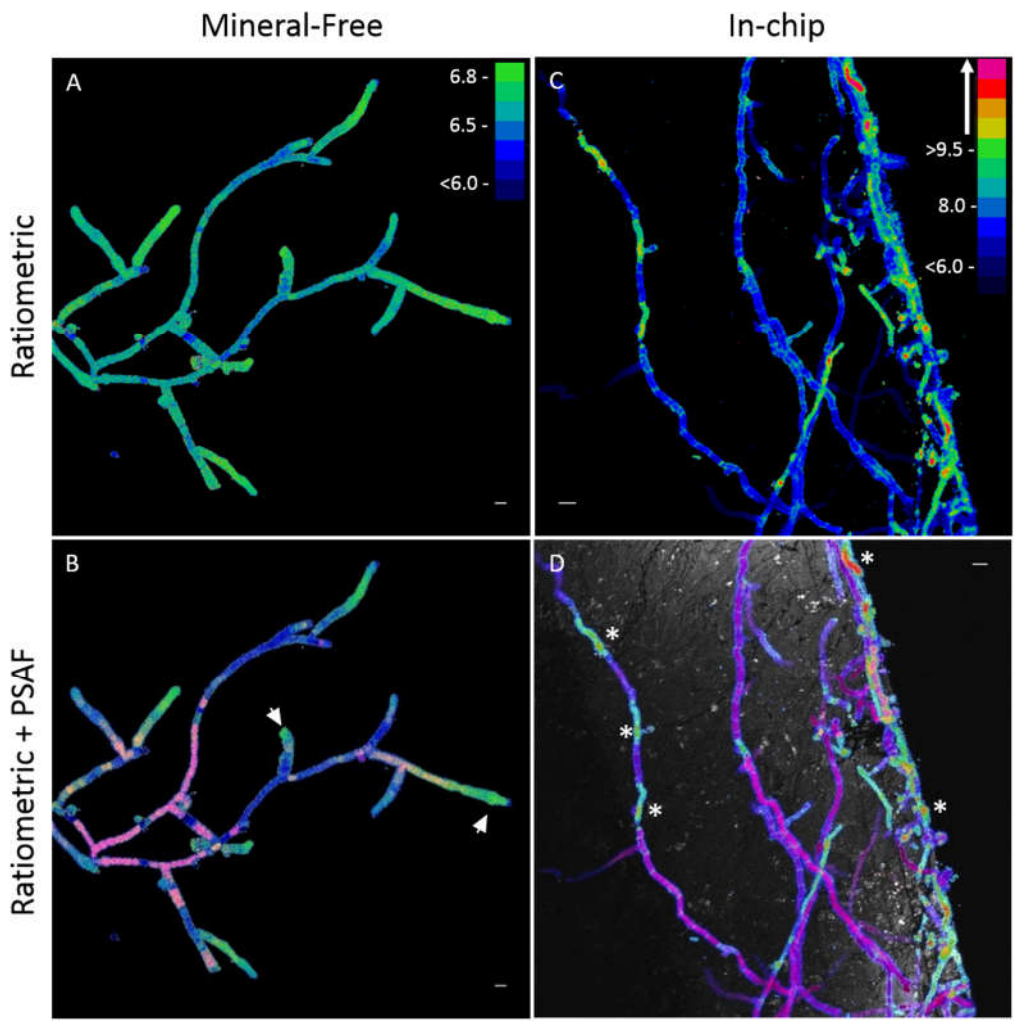


Fig. 6. Ratiometric confocal assessment of intracellular pH. Panels A and B depict mineral-free cultures, where arrowheads point to apical filament regions (calcicytes). Panels C and D depict boring, in-chip filaments, (asterisks mark calcicytes). Scale bars are 10 μm. pHi calibrations were based on Nostoc cells

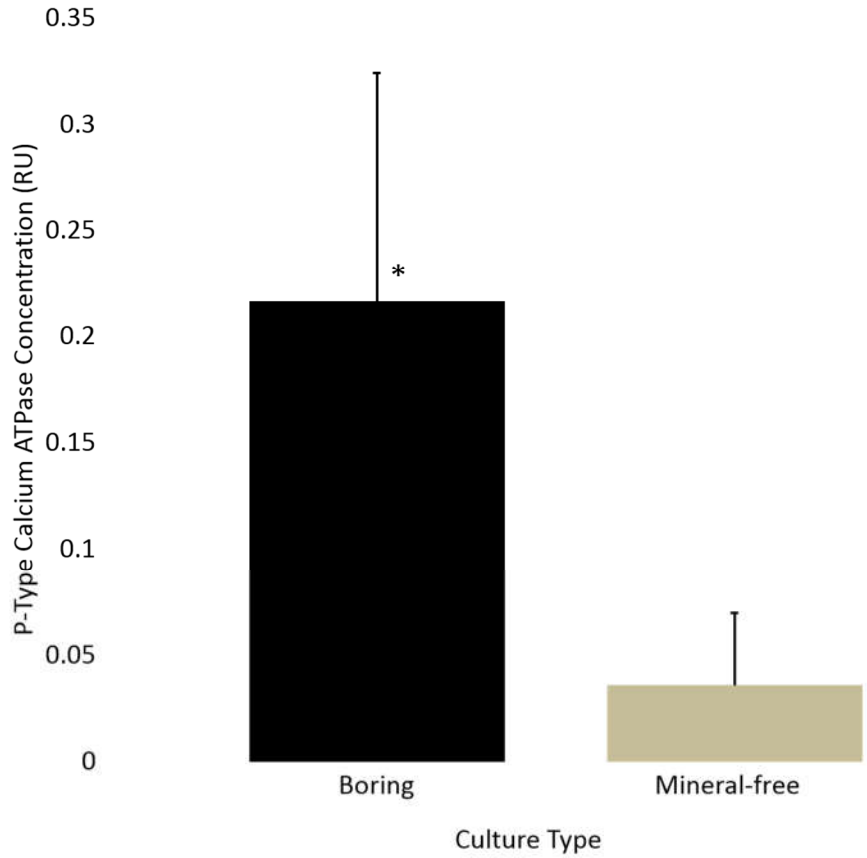


Fig. 7. Differential concentration of septal P-type Calcium ATPases as a function of growth mode. This was gauged as the ratio of bound BDTH signal to PSAF signal (a proxy for Chl a) obtained from background corrected summed Z projections of 6 independently obtained image stacks (3 boring and 3 mineral-free) under the same imaging conditions (Boring biomass was disinterred from the mineral before staining). The ratio was then corrected by the cellular content of Chlorophyll a typical of each growth mode, determined separately, as a ratio to protein content. The concentration of septal P-type Calcium ATPases, was significantly higher in boring cells ($p<0.03$). RU is relative units

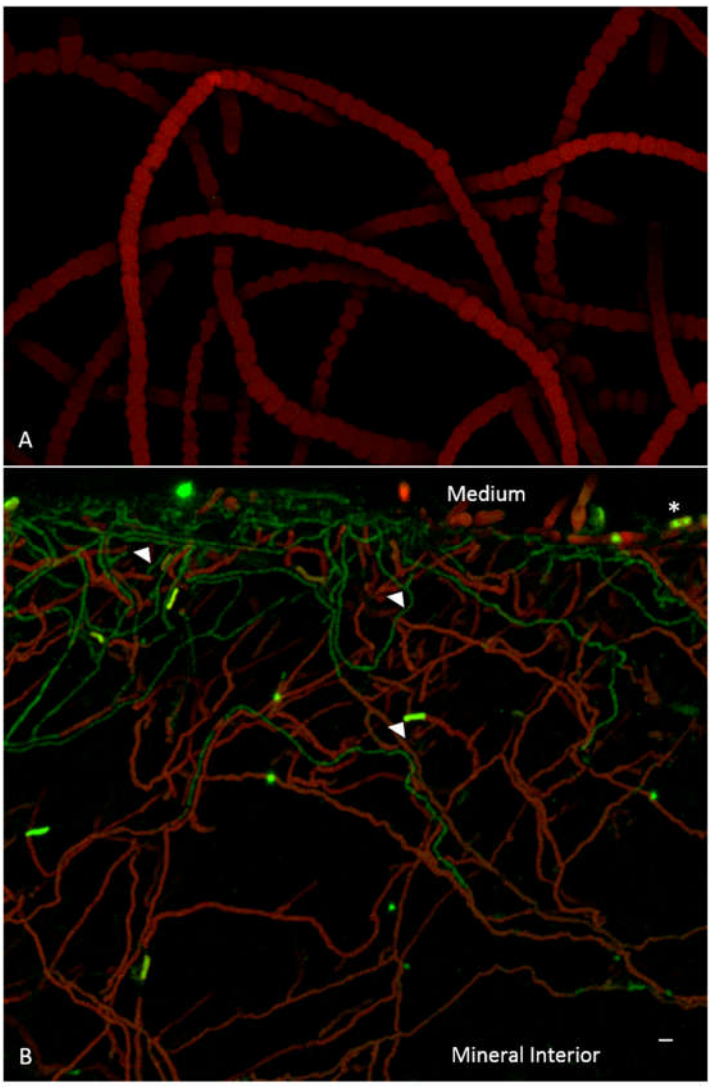


Fig. 8. Intracellular Calcium Control Images
Confocal images (summed stacks) of Fluo-5F (Green) and PSAF (Red) signal in a typical mineral-free culture with no dye but with dye carrier, DMSO as control (A) and a freshly cleaved infested chip showing a cross-section of the newly exposed boring bed which was incubated in 50 μM Fluo-5F AM (B). Long stretches of calcicytes and newly exposed apical boring tips (white arrowheads) can be seen intermixed with non-accumulating photosynthetic filaments as well as an external protruding filament showing high calcium signal (white asterisk). Scale bar equals 10 μm.

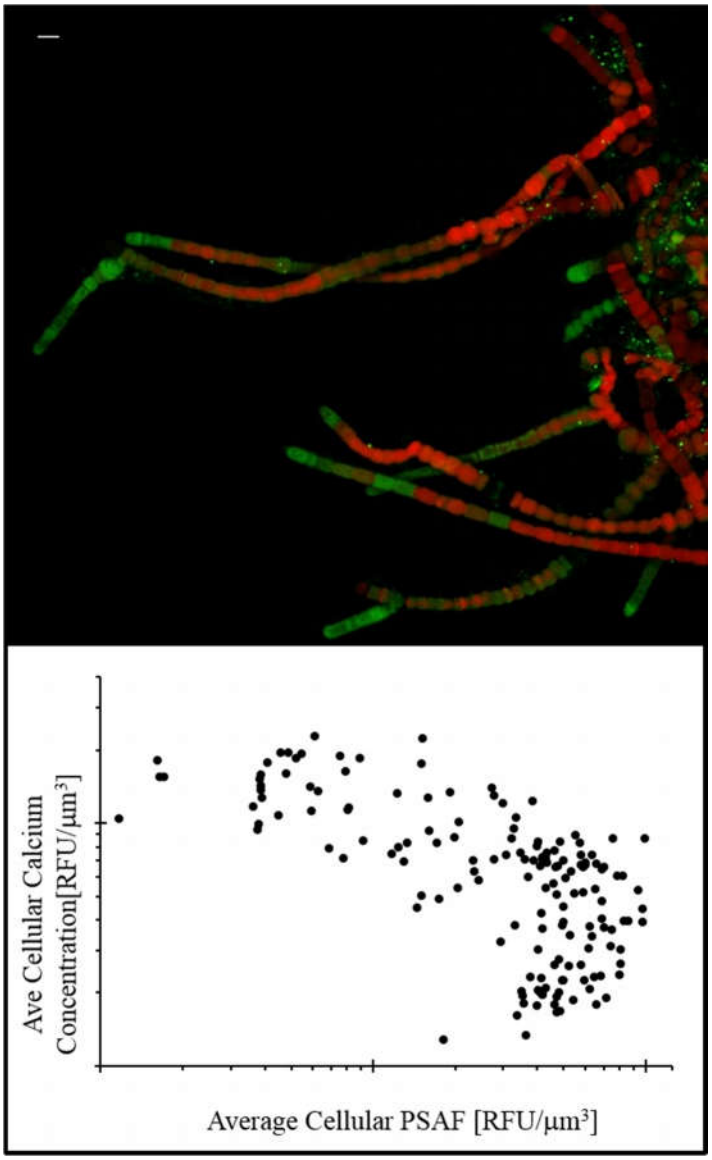


Fig. 9. Mineral-free *M. testarum* BC008 incubated in Fluo-5F illustrating reproducibility of observed Ca^{2+}_{i} patterns. The graph shows a quantitation of individual cellular volumetric calcium concentration vs photosystem autofluorescence. The biomass shows similarly diverging cellular populations as those in Fig. 5. Scale bar represents 10 µm.

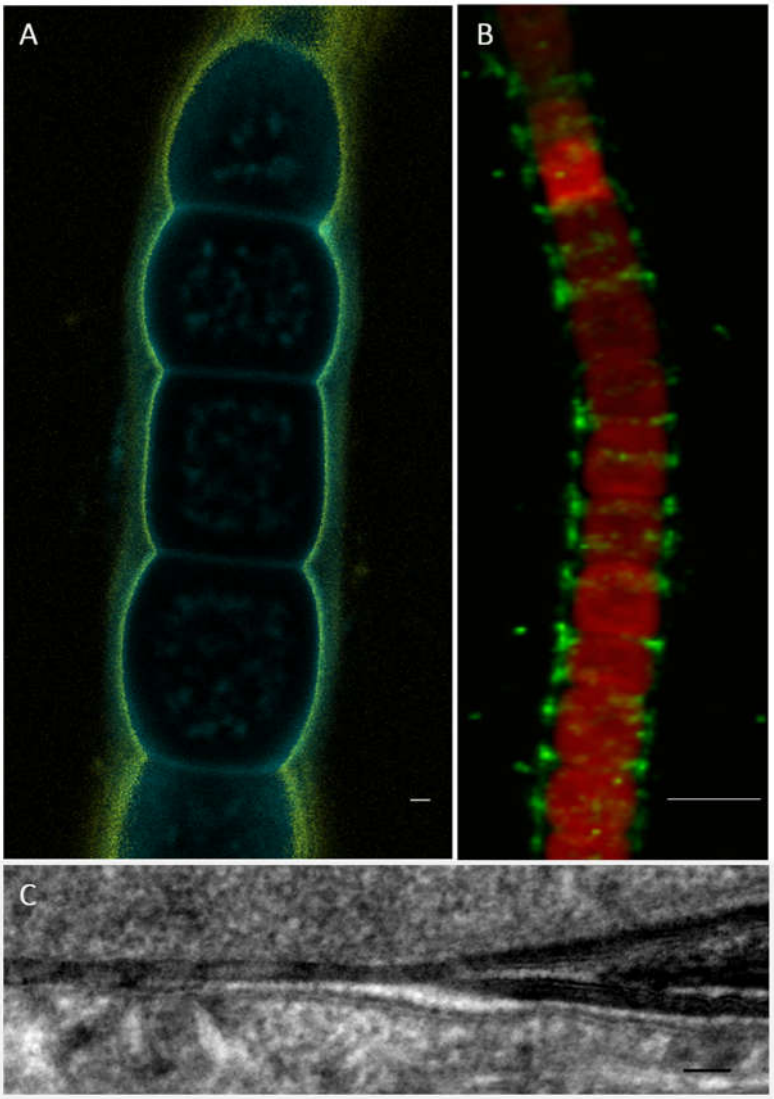


Fig. 10. General organization of the cellular envelope of *M. testarum* BC008. A) Localization of the continuous outer membrane (yellow/green channel, stained with FM4-64FX). This image represents a single optical equatorial slice in a mineral-free grown filament. Blue fluorescence is due to DAPI staining of DNA. The cell septae (as well as the sheath) are autofluorescent, allowing us to easily discern both sides of the cell cross-wall, showing that our technique can resolve membrane staining at either side of the septum. Scale bar is 1 μm. B) The BODIPY-FL moiety alone does not show localization to the membrane but diffusely to the sheath region as indicated by the large distance from the intracellular PSAF signal (white arrowhead). Scale bar is 10 μm. C) TEM image of a cell septum from a typical mineral-free BC008 filament showing a septal thickness of 35 to 45 nm. Scale bar is 50 nm.

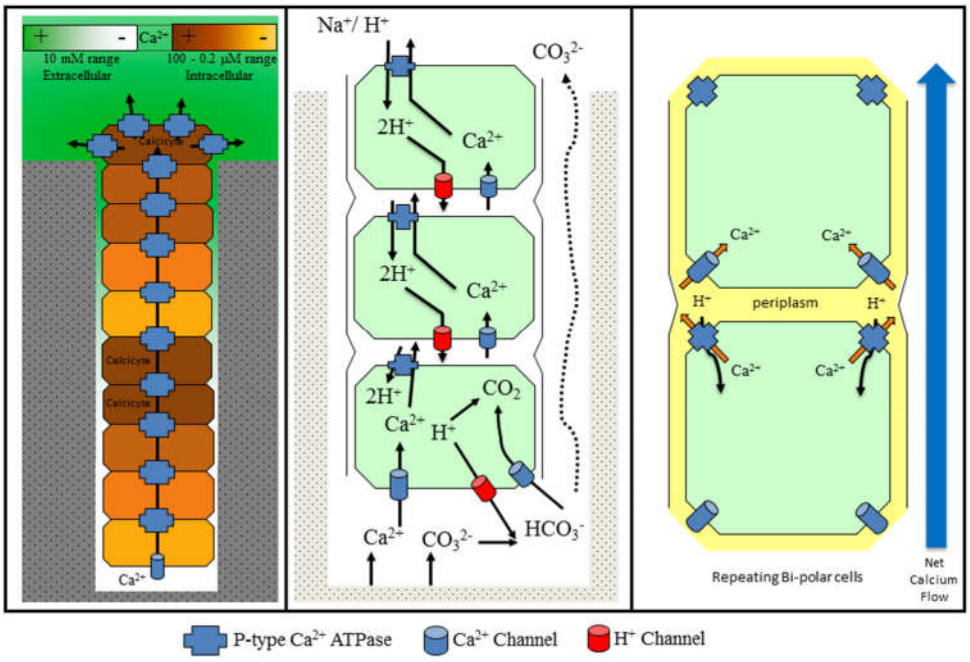


Fig. 11. The left panel shows holistic calcium ion localization during boring with relative calcium concentrations within each compartment indicated. Calcicytes would allow a higher proportion of cells to remain photosynthetically active by controlling intrafilamentous calcium flow. The center panel illustrates the inferred distributions of transport proteins and the potential fates of the calcite dissolution products. The right panel depicts the proposed calcium transport unit within the trichome of euendolithic cyanobacteria (both filamentous and pseudofilamentous) which consists of repeating individual bi-polar cells. One pole is specialized for calcium uptake and the opposite for calcium extrusion.

Table 2. Fluorophore information

Indicator	Detection of	Excitation (nm)	Emission (nm)	[Final] (μm)
CG5N	Extracellular free Ca2+	488	530-540	1
Fluo-5F-AM	Intracellular free Ca2+	496	510-530	25[a],50[b]
BCECF-AM	Intracellular pH	458/488	525-535	25
BD-TH	P-type Calcium ATPases	496	505-515	20
BODIPY-FL	N/A	496	505-515	20
FM4-64Fx	Lipid Membranes	561	720-740	20

a - for mineral-free cultures, b - for boring cultures

CHAPTER 2

USE OF MINERAL CARBONATE FOR AUTOTROPHY AMONG EUENDOLITHIC CYANOBACTERIA

ABSTRACT

Autotrophic organisms reduce and assimilate inorganic, oxidized carbon into biomass, which they obtain from one of two sources: the dissolved pool in the hydrosphere and the gaseous pool in the atmosphere. In spite of its large size, the lithospheric pool of solid carbonates is not known to be a source for autotrophy. However, in a recently proposed physiological model to explain the mechanisms by which euendolithic cyanobacteria can bore their way into carbonate substrates, it was suggested that, as a side effect of mineral dissolution, these photoautotrophs can assimilate and reduce liberated carbonate anions into biomass, and thus become independent of dissolved inorganic carbon pools for growth. We have used stable carbon isotope analyses combined with NanoSIMS small scale imaging of euendoliths to test this. In the laboratory, the model euendolith *Mastigocoleus testarum* BC008, derived most of its carbon from mineral sources when grown as an endolith (but not when grown in mineral free cultures) liberating excess mineral-derived inorganic carbon into the medium. It preferred endolithic growth over planktonic growth, when grown under limitation in dissolved inorganic carbon, but not when dissolved sources were present in abundance. Similar evidence for a mineral source in autotrophy could be obtained from natural abundance isotopic signatures present in endolithic microbial communities from tropical limestone and dolomitic intertidal substrates. Our experiments thus confirm the existence of a direct geomicrobial link between oxidized solid carbon pools and reduced organic carbon through the photoautotrophy of euendoliths, the global relevance of which, given the geographical extent and abundance of carbonate outcrops is likely worth assessing.

INTRODUCTION

The biological reduction of inorganic to organic forms of carbon, known as carbon fixation, is arguably the most important biogeochemical transformation on the planet, bridging the gap between the geological and biological realms, sustaining all global biomass. Organisms that can fix inorganic carbon (C_i) are known as autotrophs, while heterotrophs oxidize organic carbon back to an inorganic form. Oxidized C_i is found in three distinct pools: the atmospheric pool, largely as gaseous CO_2, the aquatic pool, in the form of three dissolved carbonaceous species (CO_2, HCO_3^-, and CO_3^{2-}), and the solid pool found in the lithosphere (as metal carbonates). All three C_i pools are directly linked through several different abiotic processes [100], but only the C_i from the dissolved and gaseous pools, is a known substrate for autotrophs[101, 102], whereas that from solid carbonates is not.

Only organisms living in close proximity to carbonates, could, in principle, have evolved an ability to utilize such vast C_i pool. At more than 6.0×10^7 Gta[42] lithospheric carbonates represent, by far, the largest reservoir of C_i in the global carbon cycle, which could represent a practically inexhaustible source for fixation. Euendolithic, or true-boring, cyanobacteria are widespread photoautotrophs that thrive in intimate contact with carbonate substrates[57]. Through their carbonate dissolving activity, they significantly contribute to the bioerosion of marine and terrestrial carbonate substrates composed of calcite[34], aragonite[35]and dolomite[103]. In natural euendolithic communities, these organisms can penetrate hundreds of microns under the substrate surface[32], and typically the outermost cells are immediately beneath a biofilm (epilithic or benthic growth) or layer of reprecipitated micrite[58]. The distance from the outside, as well as the presence of

such micrite or epilithic barriers may limit the rates of diffusive supply of external, dissolved C_i to euendoliths within the boring bed. In fact, it has been previously shown that marine phototrophic biofilms can easily become CO_2 limited[61, 62], and endolithic communities are but a special case of organomineral phototrophic biofilms[59].

Our recent studies, using the euendolithic cyanobacterium *Mastigocoleus testarum* strain BC008, have served as a foundation to studies on the physiological mechanisms of carbonate boring, which presents a geochemically paradoxical process[52]. The current model for boring suggests that carbonate dissolution occurs via removal of Ca^{2+} from the boring front, followed by transcellular transport and extrusion at the substrate surface[56, 104]. During this process, protons are counter-transported towards the boring front, an action that likely results in the localized formation of bicarbonate and CO_2 as carbonate ions are released during mineral dissolution. This process would theoretically allow for direct fixation, by the excavating organism, of the liberated carbonate. The endolithic cells at the boring front, are precisely the areas of endolithic cyanobacterial thalli that sustain the most active growth. Thus, the hypothesis that euendolithic cyanobacteria may be fixing the C_i they release during excavation of their own habitat is an attractive one, because, on one hand, it neatly completes the geomicrobial action on the substrate, and, on the other, it helps explain how they could obtain a competitive advantage over epilithic biofilms under dissolved C_i limitation.

In order to determine potential sources for autotrophic carbon fixation, $^{13}C/^{12}C$ ratiometric analyses are usually employed[105]. While, due to the inherent isotopic fractionation of biological systems, biomass shows significant depletions of the ^{13}C isotope with respect to that of the source used, the signature of the Ci sources can

typically be still traced[106, 107]. Because carbonates are heterogeneous in their C isotope abundance and usually have $\delta^{13}C$ values quite distinct from that of in seawater[108] dissolved C_i , one can principally pursue this avenue to determine C sources in euendoliths, both in model systems *in vitro,* as well as in nature. Here we studied both types of euendolithic systems in search of evidence to support the use of mineral sources of C_i in endolithic autotrophy, and to probe the role that external C_i limitation may play in this process. Our study provides direct evidence for both.

RESULTS AND DISCUSSION

Impact of dissolved inorganic C limitation on growth mode and yield

Our model euendolith, *M. testarum* strain BC008, has the ability to grow in three distinct modes[81]: in a non-boring mode (producing planktonic biomass), in boring mode, excavating carbonate substrates (producing endolithic biomass), and extending out of a bored substrate into the liquid medium, yet remaining attached to the substrate (producing benthic biomass). We reasoned that if strain BC008 has the ability to fix inorganic carbon liberated during the boring process, then cultures subject to prolonged dissolved C_i limitation should show higher yields of endolithic biomass relative to cultures with no imposed external carbon limitation. We tested this hypothesis directly, using cultures grown for 4 months in hermetically sealed (limited) culture vessels compared with controls grown open to the atmosphere, in which dissolved C_i was not limiting. Cultures were inoculated using either planktonic biomass or with seeded chips containing incipient endolithic biomass, to assess the "choice" to initiate boring under limitation vs. the "choice" to leave the mineral substrate without limitation. Each treatment and inoculation type consisted of triplicate, independent cultures, for a total of

12 trials. All cultures contained equivalent calcite surface area utilizable for endolithic and benthic growth. C budgets ran *post-hoc* (see below) demonstrate that the closed cultures were indeed under dissolved C_i limitation.

Visual comparisons of the calcite chips after incubation showed marked differences in growth patterns between limited and non-limited treatments: chips in open cultures showed much less endolithic infestation, and more benthic biomass growth (Fig. 12. A and B). Post-incubation observations of the planktonic biomass from limited cultures revealed symptoms of physiological stress, in the form of pigment bleaching, but planktonic biomass from open, non-limited cultures appeared normal (Fig. 12. C and D). In closed cultures, endolithic and benthic biomass remained unbleached (Fig. 12. B). We observed an expected differential increase in medium pH (likely due to removal of CO_2 by fixation) in the closed cultures (average final pH = 10.0 ± 0.2 vs. 8.6 ± 0.1 in open cultures). Because cyanobacteria are known to be alkali-tolerant[109, 110], the observed bleaching of the planktonic biomass is unlikely to be attributable to a direct pH effect. Additionally, an increase in photooxidative damage induced by increased $p0_2$ in the closed cultures may also have contributed to this bleaching, however we did not observe such bleaching in benthic or endolithic biomass. Thus, we must conclude that it was the combination of planktonic growth and C_i limitation that lead to culture bleaching, speaking for a direct effect of C starvation. In cultures inoculated with planktonic biomass and grown under limitation, initiation of boring was observed sooner (3 weeks) than in non-limited cultures (some 5 weeks).

At the end of the growth period, the endolithic biomass penetrated into the substrate significantly deeper under C_i limitation than without limitation (Fig. 19).

Expectedly, non-limited cultures produced an average total yield 60% higher than limited cultures (8.45 ± 1.19 vs. 5.12 ± 0.83 mg, dry weight). Planktonic and endolithic inoculation yielded roughly equal amounts of biomass (6.99 ± 1.57 vs. 6.63 ± 2.56 mg). The total amount of available C_i ($CO_{2(g)}$ and dissolved C_i, excluding mineral carbonates) in closed cultures was 1.05 mg, which could principally account for only some 2.6 mg of dry biomass in any one closed culture, a yield that was exceeded in all. The only additional source of carbon in the system was that within the chip, confirming that our limited system was, in fact, under dissolved C_i limitation.

A complete comparison of biomass yields for each inoculum type and limitation mode is in Fig. 13 (statistical analysis can be seen in Tables. 4 & 5). The highest yields ($p<0.01$) of planktonic biomass were obtained from non-limited cultures inoculated with planktonic biomass, as would be expected (Fig. 13). The highest yield in endolithic biomass was obtained in cultures limited by dissolved C_i and inoculated with endolithic biomass ($p<0.05$). In general, limited cultures consistently produced slightly higher yields of endolithic biomass (Fig. 13.). Incidentally, the highest benthic biomass yields were attained from non-limited cultures that were inoculated with endolithic biomass ($p<0.01$), suggesting that under these conditions it was preferable for *M. testarum* to grow out of the chip rather than deeper into it, as it is also obvious from Fig. 12 - A. Both the inoculum type and the limitation of C_i significantly ($p<0.1$) influenced the overall yield of each biomass mode (Table. 4). A different way to look at this dataset is by computing the relative partition of biomass into different growth modes (Fig. 13 - insert). Under C_i limited conditions, a larger proportion of the total yield corresponded to endolithic biomass. It is apparent that under dissolved C_i limitation, *M. testarum* preferentially grew

as an endolith, producing much more internal biomass than observed in the non-limited systems. The data suggests that *M. testarum* strain BC008 will preferentially fix C_i from the most easily obtainable source (dissolved C_i when no limitations are imposed), switching when the easiest source runs low. However, endolithic biomass growth was observed regardless of treatment demonstrating that C_i limitation alone is not a prerequisite for mineral infestation. Our experimental observations demonstrate that C_i limitation strongly influences the propensity of existing endolithic biomass to remain boring as well as for planktonic biomass to initiate boring.

Isotopic signatures for autotrophic C source

M. testarum cultures

We reasoned that if *M. testarum* strain BC008 fixed mineral carbon, the isotopic signature of the mineral source would be detectable in its biomass. Figure 14 shows natural $\delta^{13}C$ values of biomass C from each growth mode (endolithic, benthic and planktonic) obtained in long-term cultures, as well as that of the two potential sources, as measured by isotope ratio mass spectrometry (EA-IRMS). The mean $\delta^{13}C$ for each type were all significantly different from each other ($p < 0.06$). Planktonic biomass showed an average $\delta^{13}C$ value of -22.5 ± 1.1‰, within the range typical for most planktonic marine cyanobacteria[111]. The average $\delta^{13}C$ value of dissolved C_i in our medium was -4.2 ± 0.5‰, and that of our solid calcite substrate was 1.4 ± 0.1‰. Therefore, if biological fractionation were not affected by mode of growth, and if the source of all carbon in endolithic biomass was mineral C, one would expect that the signature of endolithic biomass should be some 5.6‰ more positive than of planktonic biomass. Indeed, $\delta^{13}C$ of endolithic biomass was much more positive than that of planktonic biomass, and the

difference (-22.5 ± 1.1‰ - 13.7 ± 2.0‰ = 8.8 ± 3.1‰) is consistent with that hypothesis. In fact, the only enriched source of ^{13}C available, which could have contributed to isotopically heavier biomass, is the calcite chip. If the sole source of C_i for endolithic biomass was truly external, dissolved C_i, one would expected only a small differential increase in endolithic $\delta^{13}C$ due to diffusive fractionation between the inside (^{13}C rich) and outside (^{13}C poor) of the chip, albeit, at this time and distance scale, the effects would most likely have been small (< 0.5‰)[112].

Benthic biomass, still attached to the mineral but exposed to the liquid medium, gave an intermediate average $\delta^{13}C$ value of -19.5 ± 1.4‰, (Fig. 14), indicating that this type of biomass may be incorporating carbon originating from both sources, either by directly fixing C_i from internal and external pools or exchanging organic photosynthate with endolithic biomass while fixing external C_i. In either scenario, *M. testarum* biomass just outside of the solid substrate is, at least partly, utilizing carbon derived from the mineral. This has interesting ecological implications, in that endolithic communities are also important food sources for benthic grazers[33, 66], which primarily feed on benthic biomass. In this way, it is possible that the mineral isotopic signature may very well propagate throughout the food web, beyond the euendolithic realm.

Natural endolithic communities

Our results with the laboratory model system, if generalizable to much more diverse communities, would allow us to predict that euendolithic microbial communities may bear a carbon isotope signature aligned closer to that of its mineral substrate than to that of the surrounding water or atmosphere. To test this we analyzed the $\delta^{13}C$ of endolithic biomass (as well as their respective non-colonized rock substrate) in

environmental samples of endolithic communities collected around the intertidal area of Isla de Mona, PR. We selected sample areas primarily composed of one of two main minerals, calcite or dolomite, which show very different $\delta^{13}C$ values. The average mineral $\delta^{13}C$ values for our calcite-dominated mineral samples was -6.2 ± 1.1‰, whereas dolomite-rich samples had more much more positive values (2.6 ± 0.8‰); each were quite apart from local seawater dissolved C_i (-0.1‰). The $\delta^{13}C$ of endolithic biomass in any given sample was significantly more negative than any of those potential sources, as one would expect in the presence of biological fractionation, but it was not invariant, as would have been expected if they all had one common C source such as seawater dissolved C_i. In fact, $\delta^{13}C$ of the endolithic biomass was a direct and linear function (Fig. 15. linear regression, $R^2 = 0.88$) of the $\delta^{13}C$ of the carbonate substrate, consistent with the notion that the bulk of the organic C stems from the lithospheric pool and reflects its variability. The apparent average fractionation effect in this data set, $\Delta\delta^{13}C$, in the assumption that all of the organic carbon stems from the mineral carbonate pool would be 9.58 ± 1.93‰, even though a small effect of source was also detected in the fractionation effect, it was a weak direct function of the substrate $\delta^{13}C$ (linear regression of $\Delta\delta^{13}C$ vs. $\delta^{13}C$, $R^2 = 0.62$; not shown) so that for example endoliths in calcite rocks, already quite depleted in ^{13}C, had a significantly weaker fractionation than those on dolomite samples (8.31 ± 1.26 vs. 11.20 ± 1.23 ‰; ANOVA $p < 0.01$). Thus, our dataset is consistent with our *Mastigocoleus* culture experiments, and with our hypothesis that the main C source for these communities are the local carbonates. While these samples contain entire endolithic communities (with a large diversity of microbial members, not just

euendolithic cyanobacteria), all biomass in it presumably originates from photoautotrophic primary carbon fixation, and thus will directly reflect the dominant carbon source.

Tracer incubations using NanoSIMS analysis

To further assess the potential sources of C_i for fixation, particularly its relative proportion, we chose a high resolution tracer approach within our model system, NanoSIMS. We incubated *Mastigocoleus* in closed cultures with highly ^{13}C enriched ($\delta^{13}C$ = 5479 ‰) dissolved C_i to follow directly the incorporation of this tracer vs. that of the mineral source ($\delta^{13}C$ =1.4 ‰) into the biomass within the euendolithic boring bed. The cultures were incubated for one month, starting with very lightly bored inocula, so that the virtual totality of the biomass grew in the presence of the external tracer. Control cultures incubated with tracer but no calcite chips, where the only source of C_i is the dissolved tracer, growing planktonically, expectedly yielded cells heavily enriched in ^{13}C ($\delta^{13}C$ = 4271 ± 579 ‰). A cross-sectional visual depiction of $\delta^{13}C$ in cells from a boring bed is presented in Fig. 16. This conspicuously shows a decrease in biomass $\delta^{13}C$ with increasing boring bed depth, a quantitation of which is presented in Figure 17. Cells just outside of the solid chip surface (benthic) showed the clearest signal of fixation of external C_i tracer, with a $\delta^{13}C$ that, by comparison with the planktonic controls, denotes that some 13% of their organic C originated in the dissolved pool. Endolithic cells close to the chip surface still showed some of this signal (around 6 % of biomass traceable to dissolved pool C), but the signature of external C_i faded quickly with depth, so that below 15 µm, $\delta^{13}C$ become indistinguishable from that of the mineral itself (or that or control cultures grown without tracer). This directly shows that most endolithic biomass below

the surficial layer has no measurable contribution from external C_i. Interestingly, in our protocol, and in order to purge all non-incorporated $H^{13}CO_3^-$ from the biomass and internal chip cavities prior to resin embedding, the culture was incubated in non-tracer medium, open to the atmosphere, for the last 4 days. We observe evidence of new apical growth, fixing the now isotopically light dissolved C_i, in the outermost cells at the apical tips of the benthic filaments (depth of -18 μm, Fig. 17), which began to approach control $^{13}C/^{12}C$ values. This fact, and the fact that the external and internal signals are maintained in a steep gradient over distances less than 50 micrometers (less than 10 cells apart in a filament), clearly indicate that the exchange of organic C between cells is slow at best, and not sufficient to dilute signal. It also implies that, in this experiment (and in those shown in Fig. 14), the "mixed source" signature found in benthic biomass may have to do more with excess mineral C_i being liberated into the medium by boring activity, than with internally transported organic C. In this scenario, such excess mineral carbon would become mixed with external C_i at the boundary layer close to the mineral, and be incorporated by benthic cells as a "mixed" source. We investigate this point in the next paragraph.

Excess C_i release by boring organisms

On a volumetric basis, replacing pure calcite with standard microbial mass, results in an excess of C. Calcite is 12% C by weight, and biomass, not so different, varies between 8 and 10%, but biomass is about 2.5 times less dense than pure calcite. Thus, roughly, there should be a 2 C excess release per C fixed in biomass during boring. We tested this effect in tracer experiments, by measuring dilutions in the dissolved C_i pool $\delta^{13}C$ signals (Table 3). After 1 month of incubation, controls containing neither inoculum

nor chips remained close to initial levels (initial $\delta^{13}C$ = 5479‰, final $\delta^{13}C$ = 5073‰) indicating that there were some but small, leaks in the vessels during this time. Control vials with only sterile mineral chips but no inoculum were no different ($\delta^{13}C$ = 5054‰) than the empty control, indicating that little if any C exchange between the chips and the medium had occurred during the incubation. A culture containing a boring inoculum, and showing abundant endolithic growth showed a final medium $\delta^{13}C$ value of only 1778.2 ± 3.7‰, indicating significant dilution (to 35% of initial tracer) with a lighter source. A culture with only a planktonic inoculum and no mineral to bore, showed only a minimal dilution, probably due to respired organic C from the inoculum itself (final C_i $\delta^{13}C$ of 4089.3 ± 6.7‰.). Thus, a significant dilution with light carbon, which could only come from the mineral, occurred only in the presence of actively boring biomass within a mineral substrate, which is consistent with our initial hypothesis. These data align well with the notion that significant excess C_i is released during the boring process, a result also consistent with the pattern in natural abundance $\delta^{13}C$ of the planktonic, benthic, and endolithic *M. testarum* biomass (Fig. 14.). This has, of course, ecological implications in that the release of mineral-derived C can subsequently be fixed by epilithic or benthic biomass. It is thus feasible that excess C_i liberated by euendolithic biomass during carbonate mineral excavation could suffice to sustain epilithic photosynthetic biomass. In this way, and through grazing by benthic herbivores, like chitons or mollusks, the influence (and isotopic signature) of mineral C_i sources may extend beyond the lithic environment itself. This excess C also likely contributes to the precipitation of micritic rinds typical in bored carbonate rocks[58, 113] and perhaps also to that of the cements

produced by euendoliths that serve to lithify microbialites[114]. Our prediction is that such authigenic minerals will also carry the original $\delta^{13}C$ of the original carbonate rock.

CONCLUSIONS

This study strongly supports the hypothesis that euendolithic communities of cyanobacteria, and in particular of the cultivated model organism *Mastigocoleus testarum* strain BC008, can photoautotrophically fix C_i derived from carbonate minerals liberated during active mineral excavation. We also showed that under dissolved C_i limitation, euendoliths display a preference for euendolithic over benthic or planktonic growth mode. It is interesting to speculate that one evolutionary advantage of boring cyanobacteria may have come about as a means to circumvent dissolved inorganic carbon limitation in benthic microenvironments. Moreover, our data indicates that euendolithic carbonate dissolution may supplement dissolved C_i pools in the vicinity of outcrops with excess carbon liberated during mineral excavation, and that the isotopic signature of the mineral substrate could potentially be carried up through the trophic levels.

Because the surface extent of global carbonate outcrops is large, some 2×10^7 km^2 [50], and because rates of phototrophic endolithic (marine) productivity within carbonate outcrops can be significant, upward of 10^6 g C km^{-2} d^{-1} [33], we expect the global contributions of mineral-source autotrophy to be noteworthy and should not be discounted. At present time, we do not know the global extent of photoautotrophic euendolithic infestation within exposed carbonate but expect it to be high. Detailed surveys of biomass and productivity should be carried out to gauge this rigorously.

MATERIALS AND METHODS

Field Samples

Marine coastal endolithic communities were sampled from Isla de Mona (18.0867° N, 67.8894° W), a small, predominantly carbonate (Mona Dolomite and Lirio Limestone) island located 40 miles West of Puerto Rico [115]. Samples were obtained from six separate localities along the shore, collected within the boring notch of the intertidal zone. Rock samples containing endolithic biomass, verified *post hoc* using a digital field microscope, were broken from large boulders and rock walls using a standard geological hammer. Samples were allowed to dry and then shipped to the laboratory.

Cultivation

Cultures of *the* euendolith *Mastigocoleus testarum* strain BC008 were grown in standard, vented-cap, tissue culture flasks containing 15 mL of filter (0.22μm) sterilized IMR[116] medium (modified with double the vitamin concentration). Cultures were incubated on a slowly rocking platform illuminated with a 16 hour light / 8 hour dark diel cycle, at a light intensity of 22 μmol photon m^{-2} s^{-1} from white fluorescent tubes. Boring cultures were obtained by adding ethanol-sterilized calcite chips (obtained from commercial blocky calcite, Ward's Scientific) of small size (< 150 mm^2 surface area) to mineral-free liquid cultures, until the chips were colonized. Cultures used for stable isotope analysis were incubated for an average period of 6 months.

Dissolved C_i limitation culture experiments

Calcite chip fragments used in these experiments were chosen so as to provide equivalent surface area for colonization (141 ± 4 mm^2). We used 2 types of biomass as inoculum: mineral-free biomass (or "planktonic") and biomass grown inside of calcite

chips (or "endolithic"). Planktonic inoculum was obtained from cultures containing actively bored chips by harvesting biomass not associated with the mineral, which was re-suspended in fresh medium. The inoculum was homogenized by repeated passage through a 24 gauge sterile needle attached to a 3 ml syringe. Seed chips used for boring inoculum were obtained by incubating size-selected chips, without shaking, in 35 X 10 mm tissue culture plates, sealed with Parafilm™, containing 3 ml of homogenized inoculum (obtained as explained above). Initiation of chip infestation was then monitored by optical microscopy, and as soon as radial boring colonies (Fig. 18) were evident (about 3 weeks), chips containing between 15-20 radial colonies were collected, lightly brushed with sterile toothbrushes in sterile media and used as boring inoculum for the experiments. Triplicate independent cultures were grown for each type of inoculum (endolithic and planktonic), and under each of 2 conditions: open or closed to the atmosphere, so as to achieve differential C_i limitation. All cultures were set up in 150 ml borosilicate glass serum bottles containing 50 ml of medium with an initial gas headspace of 100 ml. Inoculum consisted of either 100 µl of the planktonic homogenate together with 3 size-selected sterile naïve chips, or three seed chips. Cultures open to the atmosphere were not sealed but capped with sterile cotton-packed gauze. Closed cultures were hermetically sealed with aluminum and Teflon crimp caps. Headspace in sealed bottles was flushed with N_2. Sterile, degassed Milli-Q™ water was added to open cultures, as needed, to keep volume at 50 ml, and make up for evaporative loss. Cultures were incubated for 4 months. Upon completion, planktonic biomass was collected from each bottle, rinsed 3 times in degassed Milli-Q™ water, pelleted, and dried at 60°C for 72 hours. Chips were removed from the culture vessel and gently rinsed with degassed

sterile Milli-Q™ water in petri dishes, then brushed lightly with sterile toothbrushes to remove and harvest attached (but not endolithic) biomass (i.e "benthic" biomass). Calcite chips were then placed in a 15 mL falcon tube and dissolved with 5 mL 1N HCl to liberate endolithic biomass. After dissolution, tubes were spun, the supernatant discarded and the pelleted biomass rinsed with degassed sterile Milli-Q™ water then pelleted again. Endolithic biomass was then dried as described above. All dry biomass yields were determined gravimetrically. In order to gauge the depth of penetration in euendolithic growth, one chip from each culture was cracked into segments and the maximal penetration depth of the visible boring bed on the freshly opened faced was recorded using the stage micrometer of a stereomicroscope, with measurements on 6 surfaces (n=6).

Stable Isotope Analysis of Biomass Carbon

Organic C and its isotopic composition were measured by continuous flow isotope ratio mass spectrometry (CF-IRMS) in biomass samples from either field or cultures, after carbonate dissolution in acid as explained above, using a Costech Elemental Analyzer, Thermo Conflo III, and Thermo Delta plus Advantage mass spectrometers. Biomass samples were encased in analytical tin capsules, combusted at 1020°C in a reactor packed with chromium oxide and silvered cobaltous oxide, with flash combustion occurred on injection of a pulse of oxygen at the time of sample drop. Under these conditions, the tin capsule ignites, raising the sample temperature to 1800°C. Combustion products were sent into a copper reduction reactor, where incomplete combustion products (NOx, CO, etc.) were reduced and excess O_2 is removed. Water is then chemically scrubbed from the helium. The final product gas (CO_2) was separated on

a 3-meter Porapak-Q packed gas chromatography column. Sample analysis was interspersed with replicates of 3 different laboratory standards to ensure instrument precision. These laboratory standards had been previously calibrated against NIST Standard Reference Materials (USGS40 and USGS41). The long-term standard deviation was 0.2 ‰ for ^{13}C. All final $\delta^{13}C/^{12}C$ values are expressed in permil (‰), calculated using Eq. 1, where values are expressed relative to the international standard V-PDB (Vienna PeeDee Belemnite).

$$^{13}\delta C_{PDB}\,(‰) = 1000\,((R_x/R_{PDB}) - 1) \quad [1]$$

Where:

$R_x = {}^{13}C/^{12}C$ ratio of sample

$R_{PDB} = {}^{13}C/^{12}C$ ratio of PeeDee Belemnite (0.0112372)

Stable Isotope Analysis of inorganic Carbon

The $\delta^{13}C$ content of all inorganic carbon (mineral and dissolved inorganic carbon) was determined after conversion to CO_2 through acidification by addition of excess phosphoric acid in Helium-flushed hermetically-sealed vials, and incubation at 60°C in a multiprep heating block. All sample inorganic carbon ends up in the headspace where the CO_2 $\delta^{13}C$ is equivalent to that of the carbonate or dissolved C_i. CO_2 from the headspace was sampled using a Thermo GasBench, and $\delta^{13}C$ values obtained in an interfaced MAT 253 mass spectrometer

NanoSIMS imaging experiments:

Incubation

Two small (3 X 2 X 2 mm) calcite chips where incubated for one month with planktonic biomass to initiate light infestation (less than 5% of the surface area infested),

then collected, brushed with sterile toothbrushes, and rinsed in sterile media two times, to remove "benthic" outgrowth, and then incubated again for 5 days to allow broken filaments to self-repair. One chip was then placed in a 5 ml hermetically sealed vial containing 4.5 mL of ^{13}C-enriched IMR medium (5479‰) and the other in another vial containing non-enriched medium. Two sets of two cultures were concurrently incubated as controls: the first set contained no inoculum, one vial with a chip and one vial without, the second set contained a planktonic inoculum with no chips, one in enriched medium and the other in non-enriched medium. Cultures were incubated under standard conditions for 31 days, after which headspace gas and liquid medium aliquots were analyzed by isotope ratio mass spectroscopy (IRMS) as described above. Additionally, each chip (or planktonic biomass in the case of the control cultures) was removed, rinsed twice in degassed sterile Milli-Q™ water, then twice in sterile medium. To ensure purging of all unfixed, heavy dissolved C_i, prior to further processing, *all* cultures were further incubated in regular, non-enriched medium for an additional four days, including a medium change on the second day.

Sample preparation

Chips were collected, rinsed with sterile medium, then with degassed sterile Milli-Q™ water and subjected to an acetone dehydration series (15%, 25%, 50%, 75%, and 100%), then completely embedded in Spurr's resin[117] stepwise (10%, 25%, 75%, 100%), and polymerized under vacuum at 61°C for 72 hours. A single side of an embedded chip was exposed using a razor blade, and the calcite dissolved by 5N HCl treatment. The resulting void space was then backfilled, under vacuum, with Spurr's resin and polymerized as before. Blocks were then trimmed to reveal the boring beds, which were

then cut with a diamond knife in cross section for NanoSIMS imaging analysis. Cut blocks were mounted in a single, custom made, 1-inch aluminum SIMS holder and coated with platinum using a Technics sputter coater. Control planktonic biomass was rinsed three times in degassed sterile Milli-Q™ water to remove salt and then deposited on a silicon wafer and dried at 60° C for 72 hours.

NanoSIMS Isotopic Depth Profile

The block surfaces containing the boring bed biomass embedded in resin were mapped isotopically with a NanoSIMS 50L. The position of the filaments was determined with the secondary electron image and the $^{12}C^{14}N^-$ ion image. The $^{12}C^{14}N^-$ ion image, owing to higher count rates, defines cell morphology better, sufficient to distinguish a clear boundary between cell wall and extracellular sheath of the cyanobacteria, which the ^{12}C image alone failed to achieve. A Cs^+ ion beam of 1−2pA with a ~50nm probe diameter was used to sputter the sample surface while secondary ions of $^{12}C^-$, $^{13}C^-$ and $^{12}C^{14}N^-$ were collected simultaneously using electron multipliers. Close isobaric interference by $^{12}C^1H$, ^{13}C, $^{12}C^{14}N$, and $^{13}C_2$ were completely separated by using a high mass resolution (Cameca MRP > 8000). Before collecting the secondary ions, the sample surface was bombarded at high primary beam currents (200pA) for about 10 minutes to achieve a steady-state secondary ion yield and remove any surface contamination. Images were acquired at a resolution of 256 × 256 pixels while rastering the beam over an area of 15 × 15 μm or 20 × 20 μm, with a dwell time of 4 ms per pixel. The entire imaging sequence was performed by moving the stage from the outer part to the inner part of the original chip, thus collecting a depth profile through the boring bed.

Carbon isotope ratios were determined from $^{12}C^-$ and $^{13}C^-$ counts recorded, with corrections for electron-multiplier dead-time of 44 ns. The ion images were corrected for image drift and the $^{13}C/^{12}C$ ratios extracted by drawing regions of interest around each visible cell carefully excluding the extracellular sheath layer using WinImage. No corrections due to Quasi Simultaneous Arrival [118] (<10‰) were done given the magnitude of the enrichments in the labelled samples (up to 1000‰) and the internal analytical precision (~50‰) typical for these measurements. A control culture grown in non-enriched medium was identically measured, and used to bracket between enriched sample measurements. The $^{13}C/^{12}C$ ratios of labelled cells were normalized to background $\delta^{13}C$ values obtained by measuring the embedding Spurr's resin. The $^{13}C/^{12}C$ ratios were then scaled to the Vienna PeeDee Belemnite standard (Eq. 1). The $\delta^{13}C$ uncertainties finally shown include the 1σ random Poisson component and second component due to the scatter obtained while doing reproducibility measurements on unlabeled cells.

Statistics

To test significant differences of biomass fraction yields between differing dissolved C_i limitation treatments, multivariate analysis of variation (ANOVA) was used. Post-hoc comparisons among dissolved C_i treatment and inoculation schemes was done by means of Tukey's HSD for each dissolved C_i and inoculum level. One-way ANOVA analysis was ran for the comparisons of biomass fraction isotopic content. Statistical analyses were performed using IBM SPSS Statistics version 21 software.

ACKNOWLEDGMENTS

We would like to thank Stephen Romaniello and Natalya Zolotova of the ASU Keck Lab for Environmental Biogeochemistry for their assistance with the gas bench and EA-IRMS analysis. Thank you to Peter Williams (NSF ARRA Award #0960334) for his NanoSIMS expertise as well. Maitrayee Bose would like to thank the SIMS facility grant (NSF EAR-1352996) for instrument support. Experimental work was primarily supported by the NSF grant #1224939, "Intracellular metal pumping in microbial excavation by microbes" from the LT Geochemistry and Geobiology Program.

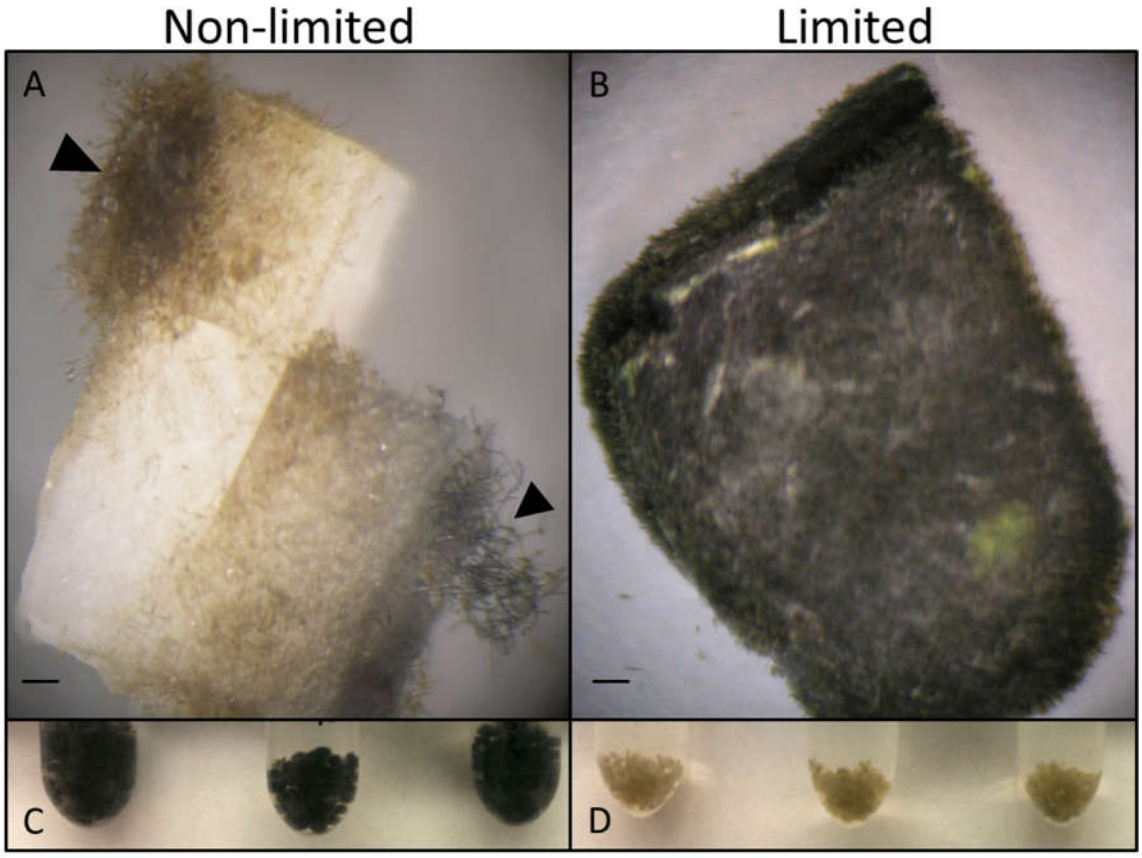


Fig. 12. – Effects of dissolved inorganic C limitation on the appearance of *M. testarum* BC008 cultured biomass. A and B (scale bars = 0.5 mm) show calcite chips with endolithic and benthic biomass growth. C and D show harvested planktonic biomass (not associated with calcite), were each tube comes from an independent culture replicate. Growth under dissolved inorganic C limitation produced virtually complete endolithic surface infestation of the calcite chip, and short benthic outgrowth (B), but little planktonic biomass, which showed signs bleaching (D). Growth without limitation resulted in asymptomatic, abundant planktonic growth (C), but more restricted endolithic yield (A).

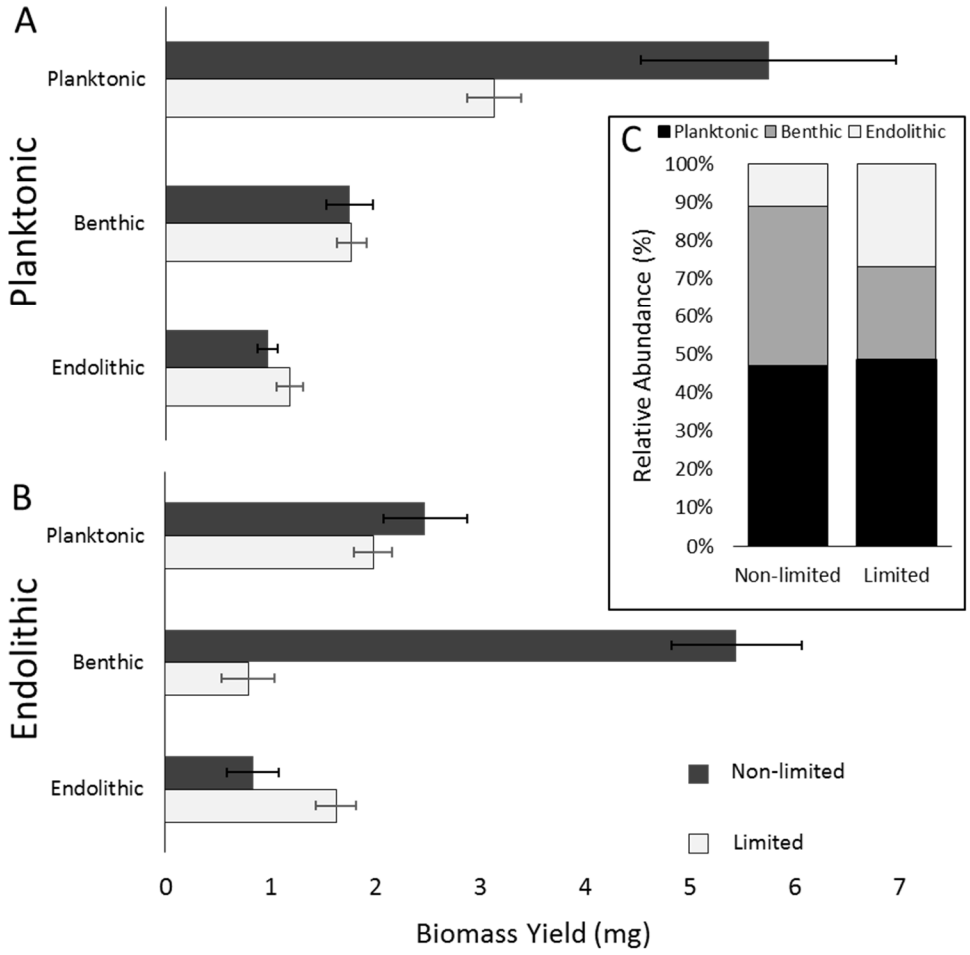


Fig. 13. Biomass yield of each growth mode of *M. testarum* strain BC008 obtained under differential dissolved inorganic C limitation, displayed as a function of initial inoculum type (A and B). The insert (C) shows average total relative biomass distributions among mode type according to carbon limitation treatment.

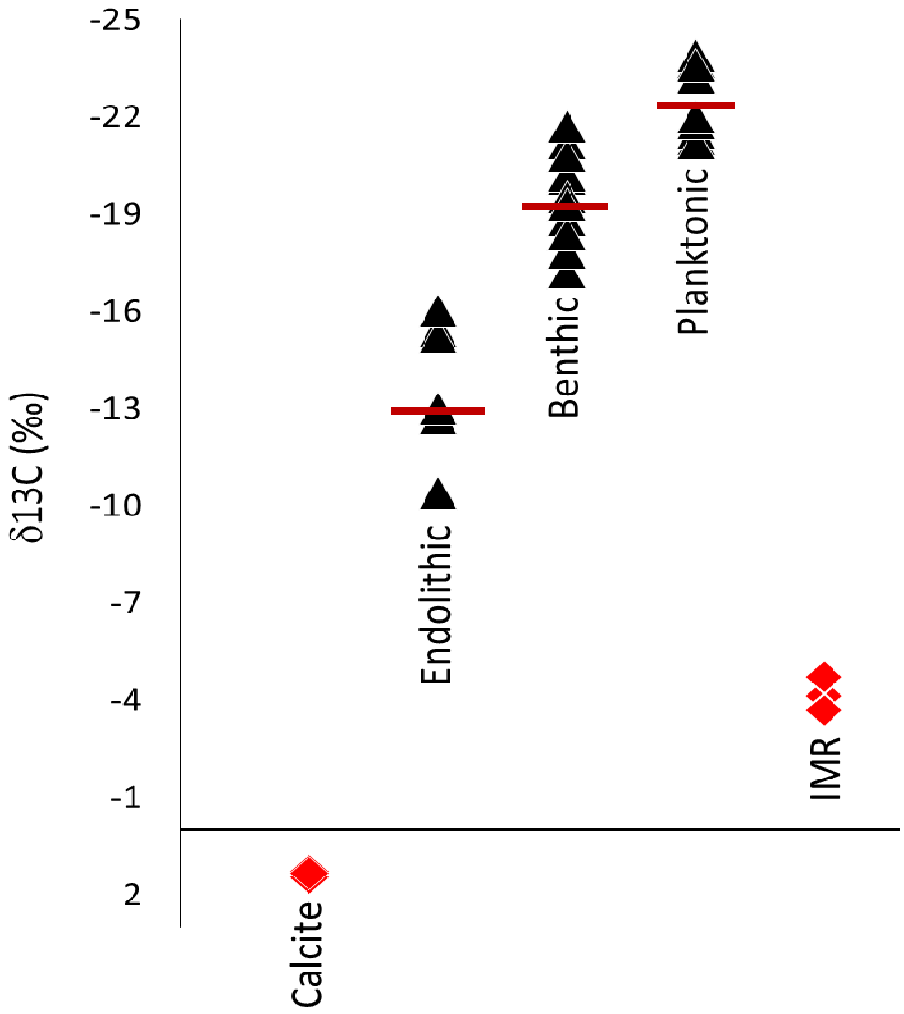


Fig. 14. Differential δ ^{13}C in endolithic, benthic and planktonic biomass of *M. testarum* strain BC008. Red bars indicate means of at least 5 independent cultures. All means were significantly different (ANOVA, $p<0.06$) from one another. The δ ^{13}C of potential sources of C (dissolved inorganic C in the medium and mineral carbonate in calcite chips) are shown for reference (red closed diamonds).

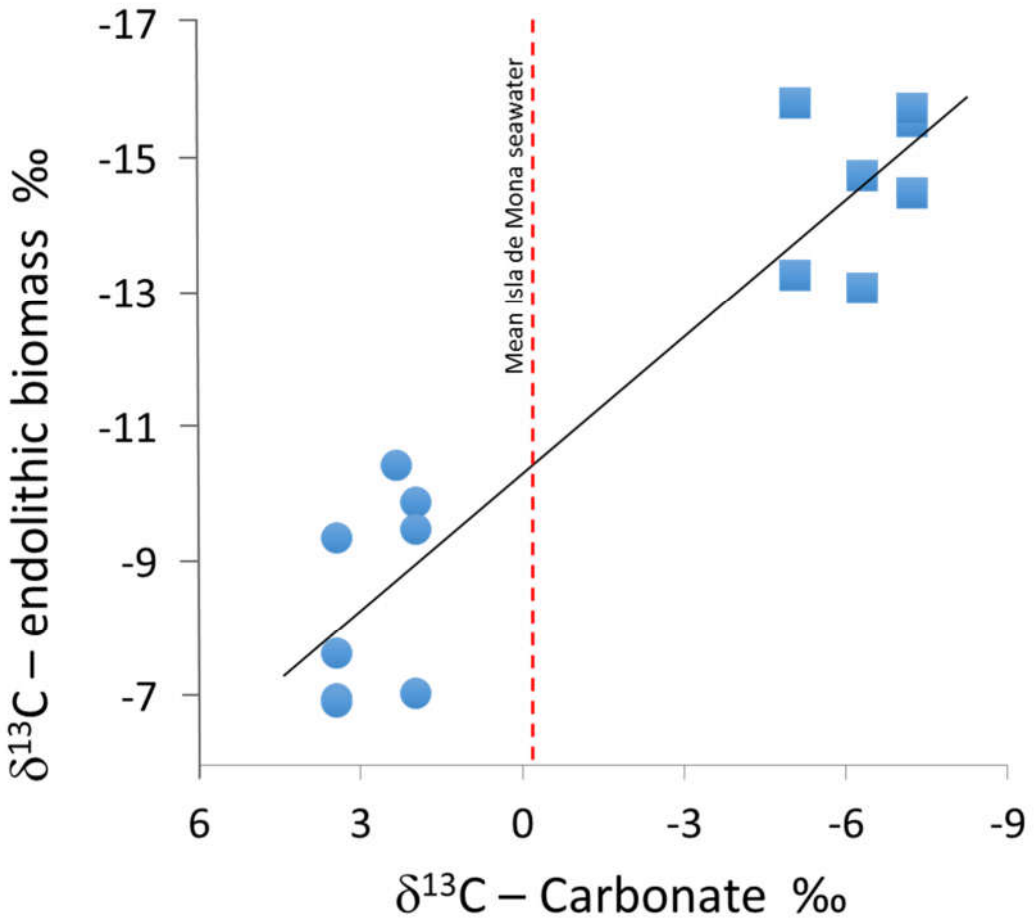


Fig. 15. Differential δ ^{13}C of organic endolithic biomass in a set of six intertidal sites on Isla de Mona, PR. Triplicates of biomass were analyzed in all but one sample, where infestation was low. Endolithic biomasses were significantly depleted in ^{13}C relative to any potential sources, both mineral and seawater, but endolithic δ ^{13}C showed a direct linear function of local mineral carbonate δ ^{13}C. Vertical dotted line indicates the mean value (n=3, SD = 0.005‰) for the δ ^{13}C dissolved inorganic C in local seawater.

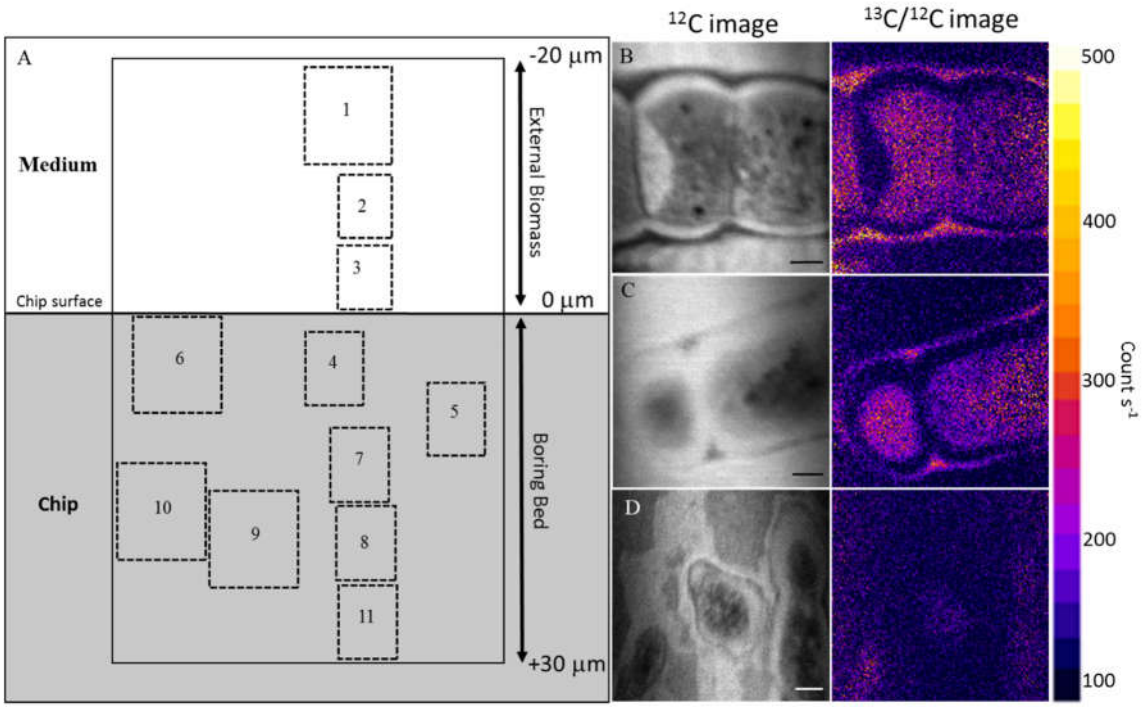


Fig. 16. NanoSIMS–visualized isotopic composition of organic C of *M. testarum* BC008 within an active boring bed, and grown in ^{13}C enriched medium. (A) Map, to scale, of the regions or interest (ROI) analyzed, with exemplary images shown in B, C, D and with ratiometric quantitation plotted in Fig 6. (B) Images of cell filaments in ROI 2. (C) Images of filaments in ROI 3. (D) Images of filaments in ROI 10. ^{13}C enrichments are conspicuous in ROI 2 and 3, but not in ROI 10. Scale bars are 2 microns.

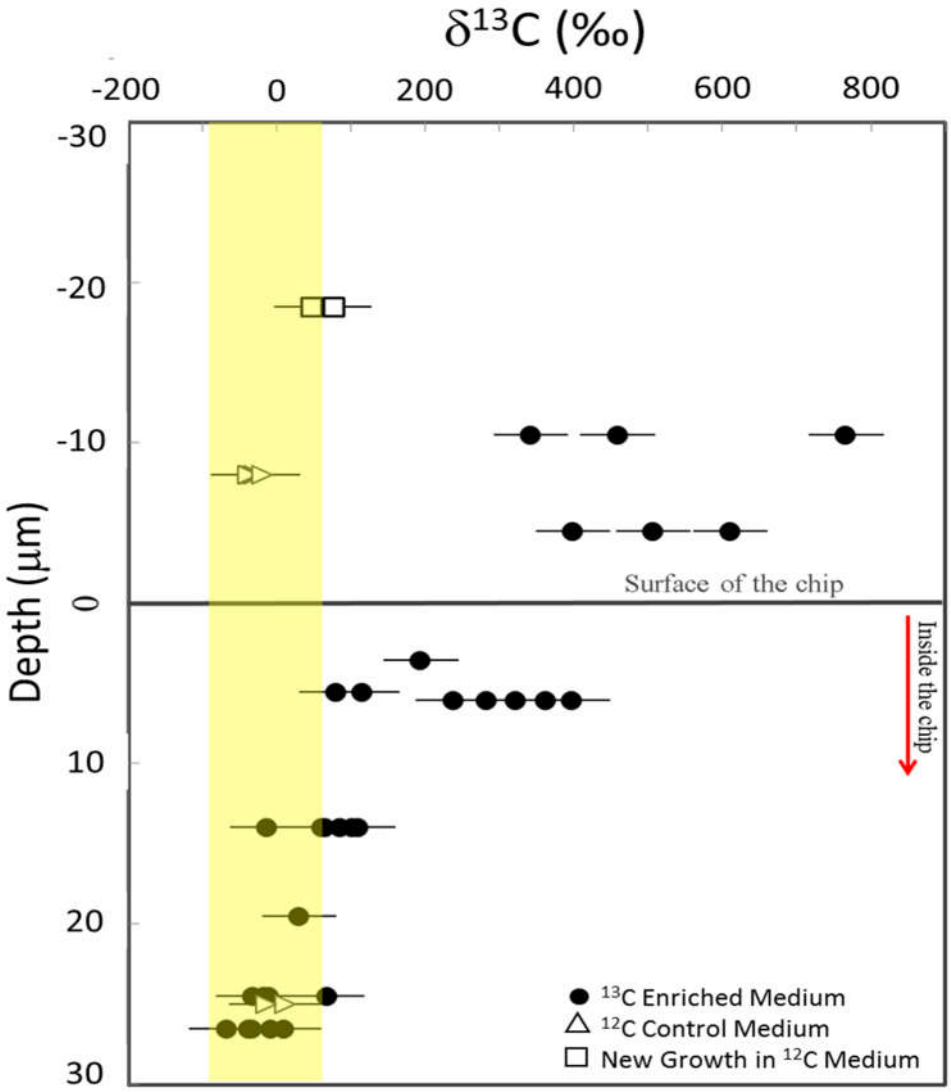


Fig. 17. Long-term incorporation of tracer, dissolved $H^{13}CO_3^-$, into *M. testarum* BC008 cells, according to their position in a boring bed (solid circles). Also included are controls cells grown in medium without tracer (triangles), as well as cells grown after removal of the tracer (squares). The dataset was obtained through $\delta^{13}C$ NanoSIMS imaging of organic cellular C (see Fig. 5). The yellow highlighted box represents $\delta^{13}C$ values which are indistinguishable from background using this technique.

Table 3. Dissolved Inorganic Carbon $\delta^{13}C$ after 1 month incubation in cultures with initial $\delta^{13}C$ = 5479 ‰

Inoculum	Calcite chips	$\delta^{13}C$ (‰)	SD*
None	No	5072.8	4.9
None	Yes	5053.9	28.4
Boring	**Yes**	**1778.2**	**3.7**
Planktonic	No	4089.3	6.7

* Standard deviations are derived from instrumental technical replication of each gas injection.

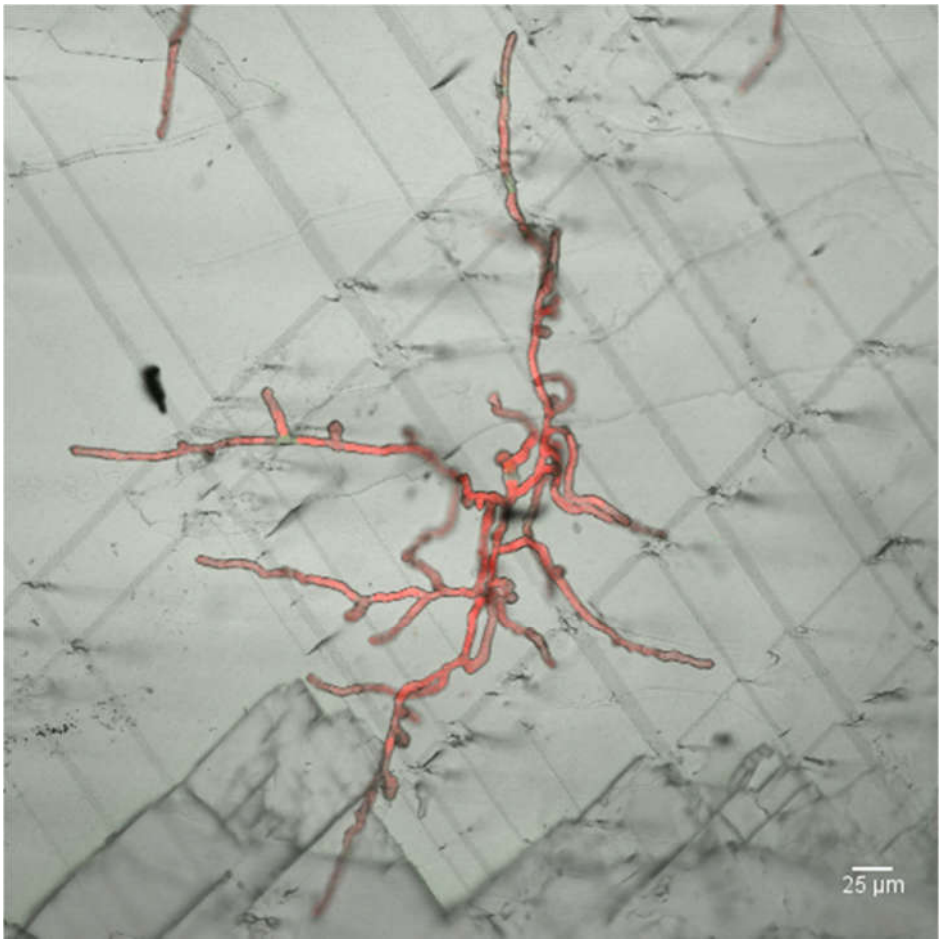


Fig. 18. A single boring radial colony of *M. testarum* grown inside of a crystalline calcite chip after a 3 weeks of inoculation with sheared planktonic biomass. Colonies such as this one constituted the basis for the 'endolithic inoculum' used in the experiments. Photomicrograph is an overlay of a (gray scale) differential interference contrast image, with a confocal fluorescent image (red) based on photopigment autofluorescence (excitation at 561 nm, emission at 660-700 nm) all taken on a Leica SP5 LASER Confocal Microscope.

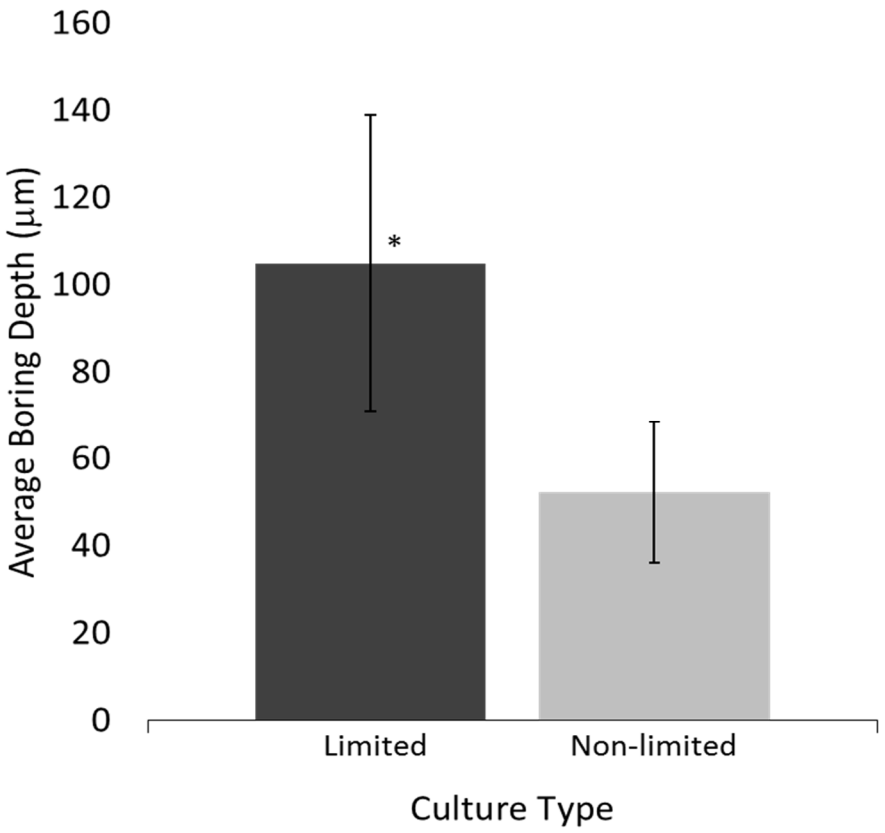


Fig. 19. Maximal boring bed penetration depth within chips grown under C_i limited and non-limited cultures after a 4-month incubation (n=6). All chips were from cultures started with endolithic inoculum. Means were significantly different ($p<0.01$, ANOVA).

Table. 4 - Multivariate ANOVA - Tukey HSD Post-HOC Analysis of Biomass fraction dry weight.

DV	Mode (I)	Mode(J)	$\bar{x}$ Difference (I-J)	Std. Error	Sig.	Lower Bound (95%)
Planktonic	B-L	B-NL	17.167	2.631	0.001	8.742
		P-L	-6.400	2.631	0.148	-14.825
		P-NL	-23.467	2.631	0.000	-31.892
	B-NL	B-L	-17.167	2.631	0.001	-25.592
		P-L	-23.567	2.631	0.000	-31.992
		P-NL	-40.633	2.631	0.000	-49.058
	P-L	B-L	6.400	2.631	0.148	-2.025
		B-NL	23.567	2.631	0.000	15.142
		P-NL	-17.067	2.631	0.001	-25.492
	P-NL	B-L	23.467	2.631	0.000	-51.082
		B-NL	40.633	2.631	0.000	-18.649
		P-L	17.067	2.631	0.001	-9.715
Benthic	B-L	B-NL	-43.833	2.263	0.000	-51.082
		P-L	-11.400	2.263	0.004	-18.649
		P-NL	-2.467	2.263	0.705	-9.715
	B-NL	B-L	43.833	2.263	0.000	36.855
		P-L	32.433	2.263	0.000	25.185
		P-NL	41.367	2.263	0.000	34.118
	P-L	B-L	11.400	2.263	0.004	4.152
		B-NL	-32.433	2.263	0.000	-39.682
		P-NL	8.933	2.263	0.018	1.685
	P-NL	B-L	2.467	2.263	0.705	-4.782
		B-NL	-41.367	2.263	0.000	-48.615
		P-L	-8.933	2.263	0.018	-16.182
Endolithic	B-L	B-NL	26.667	2.560	0.000	18.468
		P-L	17.800	2.560	0.001	96.011
		P-NL	25.933	2.560	0.000	17.734
	B-NL	B-L	-26.667	2.560	0.000	-34.866
		P-L	-8.867	2.560	0.035	-17.066
		P-NL	-0.733	2.560	0.991	-8.932
	P-L	B-L	-17.800	2.560	0.001	-25.999
		B-NL	8.867	2.560	0.035	0.668
		P-NL	8.133	2.560	0.052	-0.066
	P-NL	B-L	-25.933	2.560	0.000	-34.132
		B-NL	0.733	2.560	0.991	-7.466
		P-L	-8.133	2.560	0.052	-16.332

B=Boring Inoculum, P = Planktonic Inoculm, L = C_i Limited, NL = Not C_i Limited.

Non-significant interactions highlighted in gray.

Table 5. - Linear multivariate interaction analysis of inoculum type and carbon limitation system on observed changes in biomass mode yields

		Type III Sum of Squares	df	Mean Square	F	Sig.
Corrected Model	Planktonic	22.399[a]	3	7.466	18.350	0.001
	Benthic	38.617[b]	3	12.872	99.467	0.000
	Endolithic	1.129[c]	3	0.376	12.514	0.002
Intercept	Planktonic	126.692	1	126.692	311.372	0.000
	Benthic	69.336	1	69.336	535.767	0.000
	Endolithic	15.364	1	15.364	510.751	0.000
Inoculum	Planktonic	12.503	1	12.503	30.729	0.001
	Benthic	6.113	1	6.113	47.238	0.000
	Endolithic	0.124	1	0.124	4.110	0.077
System	Planktonic	6.827	1	6.827	16.778	0.003
	Benthic	16.112	1	16.112	124.502	0.000
	Endolithic	0.741	1	0.741	24.635	0.001
Inoculum * System	Planktonic	3.069	1	3.069	7.544	0.025
	Benthic	16.392	1	16.392	126.660	0.000
	Endolithic	0.265	1	0.265	8.797	0.018
Error	Planktonic	3.255	8	0.407		
	Benthic	1.035	8	0.129		
	Endolithic	0.241	8	0.030		
Total	Planktonic	152.346	12			
	Benthic	108.989	12			
	Endolithic	16.733	12			
Corrected Total	Planktonic	25.654	11			
	Benthic	39.653	11			
	Endolithic	1.370	11			

a. R Squared = .873 (Adjusted R Squared = .826)

b. R Squared = .974 (Adjusted R Squared = .964)

c. R Squared = .824 (Adjusted R Squared = .758)

CHAPTER 3

DRAFT GENOME ASSEMBLY OF THE FILAMENTOUS EUENDOLITHIC (TRUE BORING) CYANOBACTERIUM *MASTIGOCOLEUS TESTARUM* STRAIN BC008.

ABSTRACT

Mastigocoleus testarum strain BC008, a euendolith useful to study carbonate excavation and bioerosion, is an environmentally relevant, morphologically and developmentally complex cyanobacterium. We present an accurate draft assembly of its genome, among the largest in bacteria, consisting of 172 contigs spanning 12,700,239 bp with 9,131 annotated genes, and 37.3 GC%.

INTRODUCTION

Some microorganisms, known as euendoliths, have the remarkable capacity to excavate and grow into solid mineral phases, most typically carbonate minerals, often in the face of imposing physiological hurdles[52, 56]. Cyanobacterial euendoliths are ubiquitous constituents of exposed carbonate outcrops, terrestrial and aquatic. In the marine environment they can represent important primary producers in carbonate-dominated systems[33]. Euendolithic cyanobacteria play several significant roles in the dissolution of coral skeletons[35], and the erosion of coastal and terrestrial carbonate outcrops[34, 119]. Their activity also impacts the viability of natural and farmed bivalve populations[74]. Despite their ecological importance, no genomic information is available for any euendolith other than 16S rRNA and other taxonomic marker gene sequences[58, 81] and some Calcium P-type ATPase sequences[56].

Mastigocoleous testarum is a filamentous, true-branching, heterocystous, morphologically and developmentally complex, cyanobacterial species, first described as a euendolith in 1886[24]. It is an important pioneer in endolithic marine communities[120], and a pest for bivalve fisheries[121]. A type strain, BC008, originally isolated from a shell fragment[58], represents the only working physiological model organism for the study of

cyanobacterial euendoliths and microbial bioerosion[56]. While we have gained important insights into the mechanistic underpinning of carbonate dissolution using BC008, we are hampered by a lack of genetic information on this organism. This would enable comparative genomics, transcriptomics, and perhaps even the development of a genetic manipulation system and advances in its management in aquaculture.

MATERIALS, METHODS, AND RESULTS

M. testarum strain BC008 was grown as a unicyanobacterial, but not axenic, culture, in PES-30 medium[92] under a 16/8 h light/dark diel cycle at room temperature. Genomic DNA was isolated as previously described[55] and two separate Illumina MiSEQ paired-end (PE) libraries were created. One, 2X150 (lib1), was generated by the Joint Genome Institute and another, 2X300 (lib2), by the Translational Genomics Institute. The libraries revealed the presence of three distinct, divergent 16S rRNA sequences. In addition to the dominant16S ribosomal sequence for *M. testarum*, the cultures contained 2 contaminants, one in the *Rhizobiales* and one related to *Hyphomonas* (99.7% identity). The genomic dataset was thus treated as a metagenome. After quality filtering, both libraries combined contained over 7.2 Gbp of sequence. Each library underwent independent assembly using the iMETAMOS[122] pipeline of METAMOS[123]. The best assembly was used for each library and the resultant contigs were assembled together using Geneious[124]. Because both contaminants had a high GC content genome (>50%), all contigs above that mark were removed. Contigs longer than 3 kbp were scaffolded using SSPACE[125], resulting in a final draft assembly of 172 scaffolds (>5 kbp, N50:145,830; Mean Length: 65,170) representing 12,700,239 bp of genomic DNA with an average GC% of 37.3, which is among the largest bacterial genome reported. Gene

prediction and annotation was done using the NCBI prokaryotic genome annotation pipeline[126] resulting in 9,131 genes, 73 tRNA loci, and 6 rRNA loci (two complete rRNA operons). Secondary metabolite gene cluster prediction was done using the antiSMASH server[127] and resulted in 22 predicted gene clusters indicating the potential biosynthesis of shinorine, nostopeptolide, hectochlorin, and staurosporine among others.

Nucleotide Accession Number:

This Whole Genome Shotgun project has been deposited at DDBJ/EMBL/GenBank under the accession LMTZ00000000. The version described in this paper is version LMTZ01000000.

Funding Information:

This work was primarily supported by NSF grant 1224939, "Intracellular metal pumping in microbial excavation by microbes"

CHAPTER 4

PHYSIOLOGICAL AND METABOLIC PLASTICITY PLAYS A CENTRAL ROLE IN THE EUENDOLITHIC LIFESTYLE

ABSTRACT

The endolithic niche represents an ancient habitat comprised of a variety of organisms spanning many taxa. A small subset of those organisms are known as euendoliths and can actively penetrate and live confined within their mineral substrates. A species of filamentous euendolithic cyanobacteria has been shown to excavate into calcium carbonate minerals using a novel calcium pumping mechanism and to simultaneously fix the mineral derived carbonate liberated during the dissolution process. The elucidation of this phenomena also highlights the fact that endolithic biomass is diffusively limited from external inorganic carbon sources. Thus, the survival of an oxygenic photoautotroph under these conditions must involve a set of niche-specific traits. In an effort to uncover these euendolithic-specific metabolic or physiological adaptions we conducted a transcriptomic analyses comparing gene expression profiles from cultures of *Mastigocoleus testarum* strain BC008 grown as either endolithic or planktonic biomass. Results indicate the euendolithic lifestyle requires a larger and more diverse set of expressed genes than does planktonic. Indicative of diffusive limitation, genes involved in the transport of various ions, water, carbon compounds and other secondary metabolites were highly upregulated. Unexpectedly, genes involved in the mitigation of oxidative stress were strongly depressed as were genes involved in photosystem II (PSII). Transcriptional profiles of respirative genes further support a decrease in oxygen production. In accordance with the overall downregulation of photosynthesis, the Calvin cycle is also repressed suggesting a switch to an alternative anoxygenic carbon fixation pathway. Validation of our results can only come through

functional biochemical analysis however these data imply that the euendolithic lifestyle may require a vastly different array of metabolic capabilities than planktonic growth.

INTRODUCTION

The lithic habitat, areas directly adjacent to or within rocks, represents one of most ancient and ubiquitous microbial niches on the planet. Fossil evidence supporting the presence of microbes living inside of rock substrata goes back to somewhere between 1.2 - 2.7 Ga[2, 63-65]. The exact nature of these organisms remains unknown. This mineral/microbe interaction provides a critical interface between the geological and biological realms whereby many microbes can liberate nutrients locked away in the mineral matrix thus linking several global nutrient cycles[128]. Microbes living in close association with rocks are very diverse and can be heterotrophic or autotrophic[59, 129]. Their lithic association can be rather loose, with no regard for mineral type, such is the case of surface (epilithic) colonization which occurs on almost any exposed rock surface. A closer association can be achieved when microorganisms colonize the rock interior (endolithic microbes) by finding a preexisting crack or crevice (chasmoendolithic microbes) or within preexisting pore spaces or vacated cavities (cryptoendolithic microbes) formed through the action of another organism[57]. The most specific and intimate association is achieved by actively boring into the mineral substrate: microorganisms that can do this are called euendoliths[57]. In most surface exposed endolithic communities the upper few millimeters, to about a centimeter, are predominately colonized by phototrophs, as their penetration depth is light dependent[57]. The mineral excavation ability of microbes seems to be largely limited to carbonate and phosphate based minerals[56, 130, 131], though reports claim to show evidence of microboring

in silicate minerals[132, 133] despite the lack of observations of extant microbes boring *in situ* on silicate minerals. Carbonate euendoliths play significant roles in the erosion of both biogenic carbonate formations and man-made carbonate structures, as well as in the biogeochemical carbon cycle by recycling calcified material[34-36, 51].

The relevance of endolithic microbe-mineral interactions extends to the potential for increasing our understanding of the origins of life on primordial planets such as Earth[134, 135]. The environmental pressures ultimately leading to the evolution of the endolithic way of life are unknown. Several have been suggested, ranging from protection from exposure to UV radiation, desiccation, temperature fluctuations, predators, as well as the exclusion of local competitors for space and nutrients, or combination thereof[52, 136]. The idea of an oxygenic photoautotrophs as a microborer was originally thought to be somewhat of a thermodynamic paradox due to the propensity of photosynthesis to promote carbonate precipitation not dissolution[51, 52]. In recent years, the picture emerging with regard to the mechanistic nature of carbonate excavation by cyanobacteria is becoming less of a conundrum[56, 104]. Several studies aimed at elucidating the physiological means behind carbonate excavation using the model euendolithic cyanobacterium *Mastigocoleus testarum* strain BC008 show it utilizes a novel calcium pumping mechanism to actively bore into the mineral substrate as well as possesses the ability to tolerate large intracellular calcium concentrations mediated by special differentiated cells[55, 56, 104].

One experimental approach, not yet performed, which would give an understanding of the mechanisms operating in endolithic microorganisms, is transcriptomics. One can surmise that many genetic and biochemical nuances are

required to live encased in crystalline solids. Certain metabolic adaptations must be involved for survival in an environment relatively cut off from external resources. Endolithic communities have been likened to biofilms and marine biofilms have been shown to become diffusively limited with depth[61, 62]. Euendolithic cyanobacteria can bore to depths of several millimeters or more, thus diffusive access to external environmental resources may be a problem[57]. It has been shown (Chapter 2, this work), that the carbonate liberated during the dissolution process is actually fixed into biomass by euendolithic cyanobacteria, thus solving a potential limitation to growth if sources of inorganic carbon had to come from the external pools. This would not be the case for endoliths boring on phosphates or other non-carbonates. Another potentially problematic area is gas exchange. *Mastigocoleus*, as all oxygenic photoautotrophs, produces oxygen during photosynthesis, but this could quickly become toxic if excess gas accumulates, being surrounded by a solid, diffusively impenetrable barrier. Equally important may be the lack of oxygen availability for respiration at night. The availability of nutrients may be an additional problem to contend with in the endolithic habitat. There have been no reports suggesting that calcium carbonate minerals contain usable amounts of N, P, or Fe although Mg and Mn are common[137, 138]. Additional adaptations will likely be required to sustain the calcium-transport based mechanism for boring. While it has been shown that *M. testarum* strain BC008 differentiates specialized cells (calcicytes) to aid in regulating intracellular calcium flow through filaments, maintaining the concentrations relatively low in most cells, many endolithic vegetative cells still endure high intracellular concentrations, greater than 4 μM; which are toxic in most other organisms[80, 104, 139].But in the end, the true nature of the endolithic environment is relatively unknown and no one

has yet probed, at the transcriptomic level, the underlying gene expression changes associated with adaptation to this specialize niche.

With the recent publication (2016) of the *BC008* genome, comparative "omic" analyses are now possible to probe those underpinnings[140]. Using this genomic data as a reference we present here a comprehensive transcriptomic analysis comparing *in vitro* expression differences of endolithic relative to planktonic growth. This type of expression analysis is requisite for building any type of metabolic model which can help us understand how this organism, and euendoliths in general, can survive and grow trapped within a mineral substrate. A caveat to keep in mind in this case, however, is that community transcriptomic approaches are most commonly not cell-specific, and *Mastigoleus testarum* shows an unusually large capacity for cell differentiation, multicellularity, and morphogenesis[55]. We also know that cell differentiation and morphogenetic variations are indeed a part of the boring mechanism[104]. It is possible then, that some gene regulatory responses that are restricted to particular cell types or even in cells at varying depths within the boring bed, may remain buried in the overall signal.

RESULTS AND DISCUSSION

In an effort to characterize the endolithic living environment we utilized the model euendolithic organism *M. testarum* strain BC008 and conducted a comparative transcriptomic analysis of free-living planktonic biomass and strictly endolithic biomass. Each set of cultures were grown in the same volume of IMR medium, using the same light intensity, illumination diel cycle, and temperature, so as to isolate as much as possible the endolithic vs. mineral-free (planktonic) lifestyle as the main response

variable. Using Illumina technology, we obtained 4, high quality sequence libraries (two for the endolithic growth mode and two for the planktonic growth mode), which were aligned against the most updated draft of the BC008 genome, containing 6917 annotated protein coding regions. A generic description of library reads is available in Table 6 and a full list of genes with read count data can be seen in appendix 1. In the following we present an analysis of either general trends or of salient findings that bring some insights to the process.

General differential transcriptomic trends

Endolithic libraries had 7.8 and 23.3 million uniquely mapped reads while planktonic libraries attained 65.8 and 124.9 million uniquely mapped reads, equating to a genomic coverage range of 125 to 6131 fold. A total of 3291 genes (~48% of the total CDS) were significantly (p-value less than 0.1) differentially expressed with an absolute $\log_2$ fold-change of 1.5 (a $\log_2$ fold-change of 1.5 means that a gene was expressed at least $2^{1.5} = 3$ more times in one condition than in the other; as a convention we use positive values of $\log_2$ fold to signify that the gene was relatively overexpressed under endolithic conditions). All fold changes reported will be Log_2 fold changes. Genes expressed at very low levels, essentially off, with a NME of < 200 reads, were not further analyzed.

A larger number of genes (805) were expressed above our conventional threshold of NME >200 during endolithic growth, but more genes (289) were expressed intensely (NME >15000) during planktonic growth (Fig. 20). It appears that under endolithic growth, a more diverse set of genes are expressed but at lower levels compared to growth outside of the mineral. A simple reading of this could be that endolithic growth is a more

complex environment to deal with physiologically. With almost half of the predicted coding sequences, in strain BC008, being significantly differentially regulated, there is no doubt that the euendolithic lifestyle requires a vastly different metabolic scheme than planktonic growth. Of the genes that were effectively off (NME <200) during planktonic growth, 627 were turned on (NME > 200) during endolithic growth. Those appear of particular interest for further investigation.

It is also noteworthy that within the set of genes that presented a strong up-regulation during boring (log_2 fold-change larger than 5), 68% were annotated as hypothetical proteins, a much higher proportion of hypothetical than in the BC008 genome annotation overall (48%). This suggests that the responses to a boring lifestyle draws heavily on unique or unknown mechanisms, and adds a level of relativity to the sense of completeness that one can achieve from these types of studies. By necessity, when moving to a more qualitative functional analysis of transcriptomic patterns, genes annotated as hypothetical were excluded bringing the total number of genes analyzed to 1638, or roughly 24% of the genome.

Reassuringly, a similarity analyses comparing complete transcriptomic profiles of all four cultures (two boring replicates and two non-boring replicates) clearly showed that libraries were most similar to their corresponding replicate (Fig. 21), as would be expected, and that larger differences were found between conditions. From this bulk comparison, it is also evident that several large groups of genes are differentially regulated between the two conditions. Interestingly, genes upregulated during endolithic growth are evenly distributed through all expression levels whereas the genes upregulated during planktonic growth are skewed towards those that are more highly expressed genes

(Fig. 20 -A). This could be interpreted as a reflection that the endolithic lifestyle encompasses a more complex set of adaptations, than that of growth in liquid.

Genes were assigned to one of 27 functional groups, which are outlined in Table 7. The number of upregulated (UR) and downregulated (DR) genes within each category was quantified, as was the UR/DR ratio for each functional group. Overall, only 40% of the functional groups displayed a depression in gene expression (UR/DR < 1) when boring, whereas 60% of the functional groups were upregulated. This again speaks for endolithic growth requiring more complex responses. Of the 1638 significantly differentially regulated genes (Fig. 22.), 81 were highly upregulated (> = 5 fold UP) and 38 were highly downregulated (<= 5 fold DR). The most upregulated functional group was that of non-ABC type transport systems and the most downregulated functional group was that of ribosome construction, which showed downregulation of all of its genes during boring. This likely reflects the well-known fact that endolithic growth rates are much slower than those of planktonic growth.

Higher order regulation

M. testarum strain BC008 has 17 annotated sigma factors in its genome, ten of which were significantly downregulated during boring, 5 showing no significant differences, and 2 being significantly upregulated. These 2 sigma factors were essentially off during planktonic growth with NME < 30. One, a *sigF* ortholog (BC008_02369), was upregulated almost 6 fold, and its orthologs are induced under starvation or nutrient limitation in *Mycobacterium*[141], and orchestrate processes of sporulation in *Bacillus*[142]. The role of *sigF* in cyanobacteria is relatively unknown, but it has been shown to play roles in adaptation to ionic stress, type-4 secretion assembly, motility, and phototaxis[143].

The second (BC008_06847, 3.5 fold), is a member of the general sigma-70 family (of which BC008 has 8 orthologs). The depression of most general sigma factor expression and UR of putative alternative sigma factors indicates a general repression of core metabolic systems and potentially the activation of stress related systems[144].

Several highly expressed (NME > 15000) metabolic pathway regulators are downregulated during boring. Including a homolog of the positive regulator *cmpR* (3.5 fold, BC008_02932) which regulates genes involved in CO_2 uptake[145], a homolog of the negative regulator *perR* (3.4 fold, BC008_02684) which regulates oxidative stress mitigation[146], and a homolog of the posttranslational positive regulator *ycf53* (5.6 fold, BC008_03995), which plays a role in chlorophyll biosynthesis[147]. Several genes annotated as global regulators were upregulated, but these tended to fall in the classes of genes expressed at low to medium intensity (NME between 500 and 5000), such as orthologs of the positive regulator *afsR* (4.4 fold, BC008_01403), the repressor *betI* (4.5 fold, BC008_04646) and the positive regulator *dctB* (4 fold, BC008_06028) which regulate genes involved in secondary-metabolite production, internal osmolite production, and dicarboxylate carbohydrate import respectively[148-150]. The downregulation of the *perR* repressor suggests that the oxidative stress levels inside the mineral are elevated as we predicted they would be. An increased level of oxidative damage may require increased levels of synthesis of chlorophyll to replace photodamaged molecules as well. The significance of the changes in other regulators is less obvious. It is not clear why more secondary metabolites and less osmolites would be needed while boring, or why endolithic biomass may be importing/exporting C4-dicarboxylic acids such as fumarate and succinate.

Transport Systems

Gauging inputs and outputs can provide an assessment of the overall metabolic state of a microorganism. This can be done, indirectly, by observing the number and type of specific transporters activated and inactivated under varying conditions. In our particular case, where the organism lives encased in a diffusionally occluding crystal matrix, the need to efficiently import and export is paramount. This is consistent with the fact that we detected upregulation of 72% of the transport genes (138 of 191) during endolithic growth (Fig. 23). Among these, the level of upregulation was more intense in the non –ABC transporter functional group (UR/DR 3.5 vs 1.9 for the ABC transporters), indicating a preference for upregulation of transport systems not relying on ATP, possibly indicating an more intense need to conserve ATP while boring. Noticeably, seven out of nine highly (>4 fold) upregulated ABC transporters, and all but three non-ABC type transporters were annotated within the "secondary metabolite exporter" functional sub-group. These upregulated genes fall in the moderate to highly expressed categories, with fold changes between 1.7 and 6 fold. The largest group of upregulated gene from this sub-group are annotated as belonging to the RTX and leukotoxin type 1 ATP dependent secretion systems, a large and diverse group of complex transport proteins of unknown function[151]. Their potential role here finds additional evidence in the section on secondary metabolite synthesis below.

Phosphate and reduced iron are often growth limiting micronutrients in marine systems, however, in this system, the liquid medium used (IMR) was supplemented with plentiful supplies of both. Boring in our high-purity calcite chips likely brought about nutrient limitation to our cultures. We note that this may not always be the case when

boring in more mineralogically heterogeneous substrates, such as biogenic carbonates often found in nature. The BC008 genome contains two complete phosphate ABC transport loci, each consisting of the *pstSCAB* (locus 1 = BC008_1772-1775, and locus 2 = BC008_06270-06273) genes and several (>8) annotated orphan *pstS* genes. The orphan *pstS* genes all were downregulated except for two loci, *pstS10* (BC008_02797) and *pstS12* (BC008_04769). Locus 1 is completely downregulated when boring but locus two is highly upregulated (~ 3.3 fold) (Fig. 4 - A). Locus 1 was repressed and locus two activated during boring. This result is unexpected as the known global repressor, *phoU* (BC008_01144) is downregulated almost 3 fold and the *phoB/phoR* (BC008_04908 and BC008_03694) transcriptional activators are upregulated >2 fold each. This regulation pattern aligns to the transcriptional changes we observe for locus 2 but not for locus 1, suggesting an alternative regulatory mechanism for locus 1. These observations would be consistent if locus 1 coded for a high affinity and locus 2 for a low affinity phosphate transport systems.

There are at least 20 iron scavenging systems bioinformatically identified in BC008, most annotated as heme transporters or siderophore transporters. A full 65% of them were upregulated between 2 and 6 fold (Fig. 4 - B) during boring. Down regulated iron transporters fall in the ABC category, again indicating a potential need to conserve ATP. The pattern strongly suggests either iron limitation, or an increased need for iron during endolithic growth. One of the major iron stress indicators is the upregulation of the *isiA* gene (BC008_05554)[152]. The *isiA* gene is downregulated almost 6 fold strongly implying that iron is not limited, in this case, while boring. Additionally, several iron containing oxidoreductases (seen in the functional group “Enzymes”), as well as the

heme biosynthetic pathway are strongly upregulated implying that an increased need for iron is playing a role in the expression pattern we observe.

As would have been predicted by the overexpression of the regulator *dctB* during boring, which regulates the C4-dicarboxyilic acid transport system, BC008 showed elevated expression of the dicarboxylate large periplasmic permease, *dctM* (BC008_01930, 4.8 fold) and it is, most likely, in an operon with the adjacent *dctQ* gene (BC008_01931) which also shows upregulation (1.2 fold) but not significantly (p-value = 0.26) due to its very low level of expression (NME = 116 reads). The *M. testarum* genome also encodes another type of dicarboxylate transporter, the sodium dependent dicarboxylate transporter, *sdcS*, at two separate loci. Both are upregulated (BC008_00154, 2.5 fold and BC008_01181, 1.3 fold). All of this evidence suggest an increase in the production of dicarboxylic acids such as succinate and fumarate, which can be products of fermentative pathways[153, 154] and/or the sharing of reduced carbon compounds among cells within filaments is more important while endolithic.

There are two P-Type calcium ATPases annotated in the BC008 genome but only one is significantly upregulated (BC008_01109) at 2.4 fold, the other remains consistently expressed under both conditions. This is consistent with previous data however only one locus is significantly UR in our hands[56, 104]. Previous expression analysis was performed via qRT-PCR, using a single chip, only showed differential regulation of one locus[56] and not of the same locus we show here. The other report shows an increase in overall Ca^{2+} P-type ATPase protein levels in boring biomass which strengthens our results shown here[104]. This may be due to the lack of biological replication in their experiment as well as the overall robustness of RNA-SEQ. The non-

differentially expressed ATPases may be the primary calcium ATPase with the second upregulated ATPase acting to support the increase calcium traffic seen during active boring. Thus it appears that BC008_01109 is "the" boring ATPase in *Mastigocoleus.*

It has been shown that the boring mechanism employed by BC008 relies heavily on the use of protons for calcium transport but limited proton pools may also require another cation (such as sodium or potassium) to serve as a secondary counter ion[104]. If protons are limiting, endolithic biomass must either reroute proton resources or employ a secondary calcium pumping mechanism. We observed two independent significantly upregulated sodium/proton pumps during boring, *nhaP* and *nhaS3* (Fig. 23 - right). The *nhap* gene (BC008_04846) is upregulated 5 fold and has been shown to be a proton dependent sodium extrusion pump which functions via an antiport mechanism[155]. The *nhaS3* gene has been localized to the thylakoid membrane in *Synechocystis sp.* strain PCC 6803 and shown to pump sodium into the luminal space in the place of a proton[156]. There are also two separate loci encoding homologs of a light-induced sodium dependent proton extrusion pump (*pcxA)* both downregulated about 2 (BC008_04406) and 5 (BC008_05319) fold, respectively, suggesting that during boring, intracellular proton pools are indeed being rerouted. There is a single sodium ABC extrusion system, the *natAB* system, and one of the subunits is downregulated 2 fold, which would makes sense if BC008 is using Na^+ to pump H^+ while conserving ATP to power the calcium ATPases while boring. Thus, we show two systems highly upregulated and two systems downregulated which will effectively fortify cytoplasmic proton pools at the expense of Na^+. Genes putatively involved in increasing membrane permeability to Na^+ are discussed later in the section on secondary metabolite secretion.

The *bicA* bicarbonate transporter is the general inorganic carbon (C_i) uptake pump employed by most cyanobacteria[157, 158]. The number of *bicA* orthologs encoded in a single cyanobacterial genome can vary, *Mastigocoleus testarum* strain BC008 has two annotated *bicA* loci (*bicA1,* BC008_02628 and *bicA2* BC008_03217) sharing 60% amino acid sequence identity to each other. Only one locus shows significant differential expression (downregulated ~ 3 fold) during the boring condition, *bicA1.* This is most likely the primary bicarbonate transporter based on its average expression level compared to the other locus (NME of 5302 reads vs 1330) and on the fact that it *is* differentially regulated. A model for autotrophy in euendoliths (Chapter 2) during carbonate excavation, predicts that C_i surrounding boring filaments to be found in excess with respect to needs; our data supports this contention. The second *bicA* locus has a much lower NME but shows a slight, albeit not significant (p-value = 0.65), increase in expression during boring (0.65 fold) and may be a secondary bicarbonate transporter (lower affinity potentially) or could be transporting something else entirely.

Nitrogen Metabolism

M. testarum strain BC008 is a diazotrophic cyanobacterium with the capability of heterocyst differentiation. Heterocysts can be clearly observed during endolithic growth and we know, from previous observations, that heterocyst pattern formation while boring becomes more regular showing a ratio of heterocysts to vegetative cells lower than that observed during planktonic growth[55]. In agreement with this, the known global heterocyst differentiation factor, *hetR,* is not differentially regulated but still moderately expressed. Yet, the global nitrogen regulator, *ntcA* (BC008_0119), is downregulated 3.4 fold and all associated *nif* genes are also downregulated between 1.6 and 5 fold suggesting that the

majority of the endolithic biomass is not fixing much nitrogen because either requirements are lower (endolithic cells do grow slower) or due to the presence of alternative nitrogen sources[159].

Interestingly, genes involved in the assimilation of nitrogen are highly upregulated (2.3 to 7 fold), the only genes upregulated in this FG actually (Fig. 5.). These genes are orthologs of the *narB* (BC008_06374)*, narK* (BC008_06375)*, nirA* (BC008_06376) and *hcp* (BC008_03519) genes encoding for a nitrate reductase, two nitrate/nitrite transporters, a nitrite reductase, and hydroxylamine reductase respectfully. This seems to indicate to the use of nitrate while boring in our experiment but we cannot pinpoint a source. Nitrate/Nitrite is not a typical component of calcite, meaning all nitrogen should have originated from the medium (which, in our experiments, had no added nitrate or nitrite)

Carbon Metabolism

Cyanobacteria fix C_i primarily through the Calvin cycle. Under carbon limitation they typically upregulate their CO_2 fixation pathways including those involved in carboxysome function[39]. In our case almost all genes annotated as belonging to the Calvin cycle and to the carbon concentrating mechanism in BC008, were downregulated while boring, with the RuBisCo complex (BC008_05475 and 05477) showing a 5 fold reduction (Fig. 24). RuBisCo was highly expressed under liquid medium growth, and still moderately expressed inside the calcite, so these changes do not amount to a complete shut-down. The reduction in expression of some of these genes may simply be due to the fact that growth is slower while boring and that CO_2 and HCO_3^- are not limiting during boring (Chapter 2), thus carbon concentration while boring is not required.

A few genes involved in glycolysis are downregulated such as 2,3-bisphosphoglycerate-independent phosphoglycerate mutase (*gpmI,* BC008_03389, 2 fold), glucose-6-phosphate isomerase (*pgI,* BC008_01437, 2.4 fold), and phosphoglucomutase (*ycjU,* BC008_01111, 2.7 fold) which suggests that glucose may be limiting, which would make sense if the Calvin cycle is repressed. Unexpectedly, however, was that many genes in central carbon metabolism pathways seemed to be upregulated during endolithic growth (Fig. 6). This includes several genes involved in fermentation pathways such as pyruvate kinase (BC008_04354, 5 fold), alcohol dehydrogenase (*adh,* BC008_01722, 2.2 fold) and acetate kinase (BC008_05679, 1.8 fold)[160]. Along with acetate kinase two additional enzymes involved in the functionalization and utilization of pyruvate are also upregulated 1.5 and 3.5 fold resectively, hydroxyacylglutathione hydrolase (BC008_03145) and lactaldehyde dehydrogenase (BC008_04823).

More surprising, perhaps, was that genes involved in the reverse tricarboxylic acid pathway (a carbon fixing pathway typical of anaerobes; RTCAC) were also upregulated. This includes pyruvate kinase (mentioned above as it partakes in fermentation as well), including a putative fumarate reductase (BC008_03790, 6 fold) and succinyl CoA synthase (*sucC,* BC008_01559). An aconitase homolog (*acnB,* BC008_05819) is also upregulated 1.3 fold but presented with a p-value just above the cutoff at 0.17. Aconitase is a key enzyme involved in the TCA, RTCA, and glyoxylate cycles[69]. BC008 contains many but not all of the enzymes central to the RTCAC which are expressed but not differentially regulated such as pyruvate:feredoxin oxidoreductase (*pfoR,* BC008_04880), fumarase (*fumc,* BC008_01162) and citrate synthase (*gltA*,

BC008_00620). As a viable alternative to the Calvin Cycle (which seems to be repressed) the reverse TCA cycle may serve to supplement the necessary fixed carbon under anoxic conditions within the crystal matrix. Typically organisms which utilize the RTCAC use an alternative electron donor such as sulfide, or thiosulfate, which should not be available in this situation but it is possible to route reducing equivalents generated during photosynthesis to the RTCAC[11].

Another set of highly upregulated genes are those encoding a putative carbon monoxide dehydrogenase complex (CODH), *cutLMS*. CODH catalyzes the oxidation of CO to CO_2 (as a source of energy) or the reverse reaction (as a source of C in the Wood-Ljungdahl pathway; WLP), and are central to the metabolism of methanogens, acetogens, and carbon monoxide oxidizers[161]. Phylogenetic analysis of the BC008 CODH subunits reveal significant clustering differences as compared to other cyanobacterial orthologs suggesting functional divergence may have occurred within this gene family (Fig. 25 & 26). The CODH genes lay in a region of the BC008 genome which appears to be mostly upregulated during boring. This region (Fig. 27.) includes a gene involved in molybdopterin assembly, cyclic pyranopterin monophosphate synthase (*moaA,* BC008_3901, UR 6 fold) and a putative CODH maturation factor (*coxF,* BC008_03903, UR 3 fold) and a single NADPH coenzyme F420 dependent oxidoreductase (BC008_03902), which is expressed, but not differentially. The *moaA* gene in this operon is not expressed under endolithic growth but a second ortholog (BC008_05342) is expressed under both conditions but not differentially regulated. Perhaps this gene alters the molybdopterin cofactor for use in the CODH complex. This region appears to code

for an activated CODH which could potentially reduce CO_2 using electrons supplied by reduced coenzyme F420.

The complete WLP typically involves a tungsten formate dehydrogenase and several genes involved in the methylation of tetrahydrofolate. *M. testarum* has an ortholog of the tungsten-selenium formate dehydrogenase, *fdhA* (BC008_01490), which is UR 3.4 fold and also contains two othrologs of the central enzymes involved methyl branch of the WLP, *metH* (BC008_03711) and *folD* (BC008_02891). The *metH* and *folD* genes are not significantly differentially regulated but are both expressed at moderate levels under each condition. BC008 appears to lack any recognizable orthologs to the formate-tetrahydrofolate ligase or the acetyl-CoA synthase bi-functional domain (Fig. 28). The BC008 genome is not complete so it's possible we are simply missing them or that an alternative version of the WLP is present in this usual organism. Along with the previously mentioned unaltered expression of pyruvate:ferredoxin oxidoreductase and the UR of acetate kinase it appears that BC008 may be able to link anaerobic CO_2 assimilation via a Wood-Ljungdhal-like pathway to an incomplete RTCA cycle for the anabolic synthesis of long chain carbon precursors[162].

Some bacteria which use the WLP for C_i fixation, like *Moorea thermoacetica*, have a CODH complexed with an ACS domain (acetyl-CoA synthase) that couples CO_2 reduction, CO methylation, and acetyl-CoA synthesis together with an energy conserving hydrogenase complex (ech)[47, 163, 164]. BC008 does not have the canonical CODH-ACS seen in these anaerobic homoacetogens. However, the BC008 genome does code for an anaerobic NiFe NADPH oxidoreductase (BC008_02290, 6 fold UR) and an anaerobic iron-sulfur oxidoreductase (BC008_02292, 4 fold UR) containing a hybrid cluster

domain similar to what is seen in the ACS subunit of many acetogens. We have no indication these genes function as the ACS subunit of the BC008 CODH but they are upregulated similarly, contain similar domain architecture, and appear to be unique to BC008. Just downstream of this operon are several additional relevant ORF's encoding the components of a coenzyme F420 NiFe hydrogenase (BC008_02295 & 02299, both UR 5 fold) and a putative NADH-quinone oxidoreductase (BC008_02297, UR 7 fold). The fact that these ORF's are adjacent to each other on the genome and co-expressed strongly suggests a functional relation. The hydrogenase genes only show orthologs in two cyanobacterial strains (annotated as sulfite hydrogenases) from *Leptolyngbya boryana* and *Cyanothece sp*. PCC 7425 but show some similarity to the F420 hydrogenases used by methanogenic archaea. These enzymes may serve as the potential NiFe energy conserving hydrogenase similar to what has been shown in *M. thermoacetica*[163].

Carbon monoxide is a toxic molecule, not a common biochemical reaction product; in fact, the bacterial biogenic production of CO is known to occur in only a few instances: methionine regeneration from methylthioadenosine[165], aromatic amino acid metabolism[166], during the oxidation of pyruvate to acetyl-CoA, and during the growth of acetogenic bacteria using the WLP[167]. It seems plausible that, due to the confinement by the mineral matrix, any CO production by either of those reactions could lead to respiratory toxicity. The conversion of CO to CO_2 by the BC008 CODH could simply be a detoxification mechanism.

In summary, carbon metabolic pathways being used by endolithic *M. testarum* appear to be much more complex than simple CO_2 fixation via a RuBisCo driven Calvin

cycle and may involve a combination of several pathways (apparently anaerobic) involved in the regeneration of acetyl-CoA and pyruvate from CO_2 and CO. The necessity to turn off, or down, PSII while boring would prevent the generation of enough reducing equivalents to run any carbon fixation pathway at high rates. However, the utilization of reductant produced via basal photosystem function (reduced ferredoxin) coupled to CO_2 (and CO) reduction by the activated CODH followed by pyruvate synthesis catalyzed by pyruvate:ferredoxin oxidoreductase could be an attractive energetically conserving process to anaerobically fix carbon into biomass[168]. To pinpoint the exact metabolic pathway/s being used during the endolithic lifestyle extensive biochemical and metabolomic studies must be done. These data provide several interesting plausible hypotheses which should be further investigated.

Secondary Metabolite Systems

The secondary metabolite functional group contains enzymes and transport related proteins involved in non-ribosomally mediated peptide biosynthesis (NRP) or proteins related to known cytotoxins containing conserved domains annotated in the secondary metabolite functional class. The BC008 genome contains several NRP enzymes annotated to be responsible for the biosynthesis of gramicidin. The NRP enzyme complexes are large and can be upwards of 4500 amino acids containing multiple catalytic sites (modules). Several of the linear gramicidin peptides have been shown to form membrane channels allowing the passage of monovalent cations[169]. Given that there appears to be increased dependence on sodium/potassium proton antiporters during the endolithic lifestyle; these peptide channels may play a role in allowing sodium or potassium to more easily traverse filaments while boring (potentially via pores in the

outer membrane). The genes encoded by BC008 show some sequence identity (45 - 60%) to other non-ribosomal peptide synthases but given their relatively large size and the high level of sequence divergence within the protein family, assigning specific function based on protein homology alone is practically impossible.

There are 9 separate loci that appear to contain different sets of these genes, of which, a few also contain genes annotated as multi-drug efflux pumps. These may be involved in the transport of NRP secondary metabolites across the cytoplasmic membrane. Three loci in particular stand out as both being relatively highly expressed and significantly differentially regulated under endolithic growth. The (BC008_03589, 03591-03595, almost 40kb) first contains 6 NRP synthase (ORF's in the gramicidin family) enzymes and are highly expressed under both conditions but are downregulated 3-4 fold during boring. The second and third loci (BC008_02240-02242, 02286-02289) combined, contain 7 ORF's which span 48Kb. The second locus is upregulated 2-3 fold while the third is upregulated 4-9 fold with BC008_02240 (a gramicidin synthase subunit) becoming one of the most intensely expressed genes under the endolithic condition (79th highest). The third locus is essentially off during planktonic growth (NME <200), which suggests this locus synthesizes something extremely important to the endolithic lifestyle of this organism.

There is large diverse family of proteins known as the RTX family, typically construed as bacterial exotoxins and are found throughout gram negative bacteria including cyanobacteria[151]. In human pathogens they act as virulence factors inducing cytolysis or apoptosis in eukaryotic cells by forming membrane pores that allow the influx of extracellular free calcium[170, 171]. These proteins typically contain a conserved

hemolysin-like calcium binding domain (COG2931) belonging to the secondary metabolite COG functional group. In BC008 there are 9 upregulated (between 2 to 9 fold) ORF's annotated as containing hemolysin-like calcium binding domains but 4 which stand out the most, BC008_01300, BC008_04180, BC008_04218, and BC008_04361 (henceforth s*cabP, cabP1, cabP2, and mtaP* respectively) (Table. 8). The domain architecture of these genes does not match that of any known RTX hemolysin proteins as they do not contain the prototypical RTX C and N termini (Fig. 29.). They do, however, contain the conserved calcium binding domain, up to 20 of them in a single protein. These four genes where essentially off (NME between 30 and 400) during planktonic growth then activated during boring, so much so that *cabP1* (8 fold UR) became the 4th most highly expressed gene during endolithic growth. The other three were not expressed as highly but were still expressed in the top 2% of all genes. The production of the scabP, cabP1, and cabP2 proteins may serve as soluble calcium chelators aiding the calcicytes and other vegetative cells in the mitigation of Ca^{2+} toxcity, the levels of which are remarkably high during endolithic growth[104]. Interestingly, the *mtaP* protein contains two bacterial C-type lectin domains (CTLD), as well as 13 hemolysin-like calcium binding domains. The CTLD has been shown to have the ability to bind solid surfaces including calcium carbonate[172,173]. This protein does not contain any transmembrane domains but contains a carbohydrate binding domain implying it could be attached to specific carbohydrate residues within the exopolysaccharide sheath or to LPS in the outer membrane.

One additional RTX protein should be discussed, BC008_06405, which contains a conserved domain (TIGR00927) shown to have K^+ dependent bidirectional Na^+/Ca^{2+}

exchange functionality, one Ca^{2+} and K^{+} out, 4 Na^{+} in, pumping in an electrogenic manner[174]. Several conserved domains found in BC008_06405 share homology to other bacterial proteins but the overall domain architecture of this protein is novel, sharing < 76% coverage at < 35% aa identity. This protein could further alleviate Ca^{2+} toxicity and, simultaneously replenish the intracellular Na^{+} pool to help in proton recovery (see section on transporters above). The regulation of these proteins certainly strongly hint to playing significant roles in the endolithic lifestyle and could potentially constitute a major tolerance mechanism allowing survival during such high intracellular calcium observed in boring in BC008. Genes annotated as secreted toxin proteins in human pathogens most likely arose by the duplication and mutation of genes which had previously defined physiological roles. It is interesting to postulate that proteins such as those seen here could be ancestral to what we see in modern human pathogens. Future genetic manipulation of these ORF's could provide more direct evidence as to the mechanism of action of these calcium binding proteins.

Stress Response

As an oxygenic phototroph, *Mastigocoleus testarum* strain BC008 releases excess oxygen as a metabolic byproduct of splitting water. While growing as an endolith is non-porous solids, this oxygen will accumulate inside cells as there is only one escape route, through the borehole, and only diffusional transport available. Any other metabolic by-products will face similar constraints to effective disposal. We see this, and the somewhat associated nutrient limitation discussed above, as one of the predictable stresses associated with the endolithic habitat. Of the 82 genes binned into the stress response functional group, 61 were, however downregulated while boring, and the group

downregulated as a whole. Of the 26 stress response genes in the oxidative stress sub-group, only 5 were upregulated. Four major ROS (reactive oxygen species) detoxification enzymes are actually repressed while boring, the highly expressed peroxiredoxin (*prxU*, or alkyl hydroperoxide reductase, BC008_02138, 6.4 fold) and several superoxide dismutases (*sodB,* BC008_05764, 6 fold, *sodA1,* BC008_06496 and *sodA2*, BC008_06494, both about 2.5 fold). A hybrid catalase-peroxidase gene (katG, BC008_05809) is UR 3 fold. We found 5 downregulated thioredoxin genes and 2 downregulated rubredoxin genes involved in the regulation of the redox state of the cell. Overall, this suggests a general decrease in oxidative stress, which is counterintuitive to what we would expect from an oxygenic phototroph stuck in confined quarters, and it does not match the finding that the *perR* negative regulator was downregulated. The only plausible explanation, short of calling for an absence or reduction of water-splitting is that BC008 has an unknown mechanism for detoxification of ROS.

Photosynthesis

The photosynthesis functional group contains the third highest number (129) of annotated genes in BC008 but with a UR/DR ratio (0.24) constituting the most downregulated functional group. ORF's in this group represent 50% of the top 50 most highly expressed CDS during planktonic growth, compared to only 14% while boring. Both photosystems were highly repressed overall (total transcripts mapped to genes in either PSI or PSII), 20 times for PSI and 70 times for PSII (Fig. 30.). By quantifying the NME value (number of normalized reads) for genes associated with each photosystem (PSII; *psa*, and PSI: *psb* genes) we can get a transcriptomic estimate of their relative importance. During planktonic growth, the $NME_{(psb)}/NME_{(psa)}$ was 0.36, however, this

shifts seven fold, to 2.6 during endolithic growth. Photosystem I seems to attain a greater importance while boring. Given that changes in light intensity between the 2 conditions are minimal, the changes in expression are consistent with an overall decrease in photosynthetic rate (i.e. perhaps because of overall lower growth rates) and an increase in the potential for cycling phosphorylation around PSI to fuel ATP based transport costs.

Interestingly a few photosynthetic genes were upregulated. In the PSI sub-group, four genes, all off during the planktonic growth mode, coding for alternative forms of *psaF* (BC008_04698, 4 fold)*, psaA* (BC008_04712, 5.6 fold)*, psaB* (BC008_04713, 2.3 fold) *and ycf3* (BC008_03612, 4.5 fold) were upregulated. Similarly, a locus, likely a single operon (BC008_04699-04701; also off during planktonic growth) containing three PSII genes was upregulated about 7 fold. It seems to contain alternative forms of the *psbD1, psbB,* and *psbC* subunits of the PSII complex. This cannot be coincidental as each alternate loci is clearly upregulated during boring. In both instances, these alternative genes code for proteins involved in binding the primary chromophore and electron acceptor of each reaction center[175, 176]. These alternative versions of major photosystem subunits may alter the stability, binding affinity, or redox potential of the reaction center complexes under endolithic conditions. The exact nature of these proteins can only be elucidated following mutational analysis, which, in BC008 is currently not possible due to the lack of a genetic manipulation system. In cyanobacteria, similar switches in alternative forms of *psbA* genes are known to modulate PSII redox potentials in response to changing environmental conditions[177, 178].

Consistent with the results of the reaction centers, almost all ORF's encoding for phycobilisome (PBS) antennae pigments or linker polypeptides, except for two, are also

highly downregulated. The two upregulated genes, part of an operon (BC008_04703-04) with the previously mentioned upregulated PSII genes, likely code for alternative forms of an allophycocyanin alpha-B chain and linker polypeptide. All loci encoding proteins of the cytochrome B6F subunit are also downregulated, except a single locus coding for an alternate of the *petB* protein (BC008_06628, 2 fold). Only 5 of the 10 annotated carotenoid biosynthetic are significantly differentially regulated, two involved in zeaxanthin biosynthesis are down about 2 fold each (BC008_04321 and BC009_06761) and three involved in beta-carotene/neurosporene biosynthesis (BC008_00719, BC008_03015, and BC008_06649) are up between 2 and 4 fold. The chlorophyll biosynthetic genes also show complete downregulation between 1.5 and 5 fold, in agreement with this result, we have shown that the chlorophyll A concentration per mg of biomass is about 1.4 times less in endolithic biomass than what is observed in planktonic biomass (Chapter 2). All ferredoxin, plastocyanin, and cytochrome C6 election carriers are downregulated between 2 and 7 fold.

It appears the entire photosynthetic system is downregulated during boring. The reason for this complete downregulation is unknown but could relate to the need to keep oxygen pO_2 low or simply due to a slower growth rate while endolithic. Modulation of photosystem complexes with alternative subunits would most likely not occur if photosynthesis was turned completely off, thus BC008 appears to be altering its photosynthetic apparatuses while endolithic not turning them off.

Respiratory Complexes:

Changes in the F_1F_0-ATPase complex, NADPH-quinone oxidoreductase complex, or the cytochrome C oxidase complex may indicate changes in overall metabolic schemes

in the dark/night. Regulatory changes observed in the genes coding for subunits of these complexes mimic what was observed for the photosynthetic genes. There is an overall reduction of expression within each group of genes associated with each respiratory complex (Fig. 31.). Again, similar to the photosynthetic expression data, there appears to be alternative subunits being expressed under the endolithic growth mode, replacing their counterparts in each respiratory complex. The effects of high intracellular Ca^{2+} concentrations on the respiratory complexes has not been rigorously studied but calcium has been implicated in the regulation of several key respiratory components found in mitochondria[179]. Perhaps these observed alterations play a role in the overall respiratory complex tolerances to calcium.

The cytochrome C oxidase complex appears to be completely modified during endolithic growth as subunit 1 (*ctaD*) is being switched out for an alternative subunit (BC008_03821 for BC008_00489), subunit 2 (which has two orthologs) is downregulated, and subunit 3 (which also has two orthologs) is upregulated 2 fold. A gene encoding the cytochrome bd alternative terminal oxidase (*cydA,* BC008_04720) is upregulated 2 fold which is a cyanide resistant alternative version that typically only functions under low oxygen conditions[180]. This is consistent with our predictions that endolithic cells may become limited by oxygen at night and with the upregulation of fermentative metabolism discussed above. Additionally because cyanide cytochrome toxicity is very similar to CO cytochrome toxicity this may be an adaptation to an increase in intracellular CO levels[181] also supported by an activated CODH (BC008_03893 and 03899-03900) though a potential source of CO is unknown. The

cytochrome C oxidase seems to have been modified but not significantly downregulated suggesting it is still functioning as a terminal oxidase.

The F_1F_O-ATPase and NADPH/NADH complexes all show overall subunit downregulation between 2 and 6 fold. BC008 encodes an additional F_1F_O-ATPase beta subunit ortholog (*atpD,* BC008_06184) which is annotated as being a member of the alternative sodium translocating family of the ATPase complex. This locus is upregulated just above 3 fold, becoming the highest expressed F_1F_O subunit while endolithic. It is unknown if the ATPase complex can simply switch ion pumping preference by swapping out a single subunit, however chimeric Na^+ translocating F_1F_O-ATPases have been constructed that are capable of producing a sodium motive force (NMF)[182, 183]. In light of the expression changes already observed for sodium/proton pumps and the fact that the two types of F_1F_0-ATPases complexes share similar structures, strongly suggest a working Na^+ translocating ATPase in BC008. There are several annotated alternative Na^+ pumping *atpD* orthologs in other cyanobacteria as sequence homology is relatively high (circa 60%). However, those annotated by the NCBI conserved domain database as an alternative ATPase subunit cluster separately from other orthologs in a phylogenic analysis (Fig. 32.). BC008 codes for one alternate and one canonical cyanobacterial *atpD* ortholog. There appears to be some divergent evolution at play as there is evidence implying Na^+ pumping exists in 2 of the three clades of the gene[182, 184-188]. Sodium-dependent ATPase activity has been linked to the Wood-Ljungdhal pathway and has been observed in several anaerobic acetogens including *Acetobacerium woodii*[184].

CONCLUSION

This is the first report detailing transcriptomic changes of a euendolithic cyanobacterium and *M. testarum* strain BC008 is currently the only euendolithic cyanobacterium for which we have genomic information. As such, we have no basis for comparison to gauge the commonality of our observed changes in another euendolithic cyanobacteria and we lack the benefit of any preliminary studies. It is also our belief that the expression changes we observed during endolithic growth may be slightly muted due to several factors. One is the large role that cell differentiation plays in this organism, whereas the analyses here are not cell specific. A second is the fact that there may be, in many genes, diel trends[189] in expression and this was not explicitly studied. And thirdly, there may also be further variability among cells in the filaments that are close to the borehole as opposed to those that are located far into it, close to the boring front. These cells, due to their proximity to the surface and, presumably, easier diffusive access to the external environment may have expression profiles similar to planktonic cells. In spite of these acknowledged limitations, the changes we did observe were significant statistically, and many were also substantial. At least in one case (P-type Ca^{2+} ATPases) our data is concordant with previously published reports[56] (Chapter 1), or observations (*hetR* expression and heterocyst formation) and in many other cases the transcriptome matches logical expectations such as the general down-regulation of central metabolism due to low growth rates, the general up-regulation of transport-related genes, the downregulation of the carbon concentrating mechanisms, and the relevant presence of predicted genes to handle high intracellular calcium content. This was reassuring. But also, in many cases,

the results were unexpected and point to sometimes explainable, sometimes mystifying results that will be useful in guiding focused hypothesis testing in the future.

A few highlights regarding the endolithic lifestyle that one gains from this study include: 1) the general down-regulation of photosynthetic genes, Calvin cycle genes and respiratory complex genes, probably related to decreased growth rate 2) the relative increase in importance of PSI, 3) the substitution by alternatives in many subunits of the respiratory, PS reaction centers, and antenna complexes 3) the unorthodox behavior of the nitrogen assimilation genes, with fixation and nitrate reduction pathways co-expressed, 4) significant, complex and surprising changes in central carbon metabolism, including the likely relevant roles of all or parts of the WLP, RTCAC, and fermentative routes, 5) the presence of a complex orchestration in the handling of mono- and divalent cations within the cells, which involve calcium binding proteins, gramicidin like pores, sodium/proton antiporters, sodium/calcium exchangers, and sodium-based ATPases,

One additional general trend seems to point to the energetic costs of the endolithic lifestyle: *M. testarum* strain BC008 prefers to use ATP-independent transport mechanisms, PSI attains principle relevance, and, potentially, carbon fixation pathways which are energetically much more frugal than the Calvin cycle are turned on[190]. For this, it employs a much more diverse transcriptome than when growing in liquid alone. When living in such a specialized extreme niche, there is much less competition which shifts focus from grow faster to grow smarter for longer, the data presented points to the notion that BC008 adapts a more energetically conservative mode of metabolism while boring. Now the real testing begins.

MATERIALS & METHODS

Culture Growth

Cultures of the euendolith *Mastigocoleus testarum* strain BC008 were grown in standard, vented-cap, tissue culture flasks containing 15 mL of filter (0.22μm) sterilized IMR[116] medium (modified with double the vitamin concentration). Cultures were incubated on a slowly rocking platform illuminated with a 16 hour light / 8 hour dark diel cycle, at a light intensity of 22 μmol photon m^{-2} s^{-1} from white fluorescent tubes. Boring cultures were obtained by adding ethanol-sterilized size selected calcite chips (obtained from commercial blocky calcite, Ward's Scientific).

Experimental Setup

The planktonic fraction from a single boring culture was use to inoculate all cultures used in the experiment. Experimental cultures were incubated for 3 months using the previously described culture conditions. One pair of cultures (non-boring) contained no calcite substrate while another pair (boring), contained three size-selected calcite chips of approximately the same surface area (84 mm^2) each as a substrate for excavation. Post-incubation, each infested chip was removed from the medium, brushed with a sterile toothbrush, rinsed three times in sterile medium and subjected to RNA extraction (see below). RNA harvested from the 3 individual chips from a single culture vessel were pooled to make a single sequencing sample.

RNA Extraction

We were highly interested in expression changes in photosynthetic genes thus to ensure maximal expression and reduce changes in expression due to cyanobacterial diel periodicity, RNA was harvested in the middle of the day portion of the diel cycle. Calcite

chips with endolithic biomass were ground to a course powder with a sterilized RNaseZap® (Sigma) treated agate mortar and pestle after adding 1 mL of TRIzol® (Ambion catalog #15596018), then, transferred to a 2 mL RNAse free Eppendorf tube. The mortar was washed with an additional 500 µL of TRIzol to remove residual powder and added to the Eppendorf. Planktonic biomass was treated similarly but subjected to bead beating instead of grinding. Bead beating was done using three pulses of 30 seconds each interspersed by incubation on ice for 45 seconds. Tubes were vortexed for two, 30 second pulses, then spun at 14K RCF for 5 minutes. The supernatant was removed and split equally between two, new, RNAse free, 2 mL Eppendorf tubes. After adding 200 µL of chloroform to each tube, tubes were mixed well by inversion and spun at 14K RCF for 10 minutes. The aqueous phase was removed from each tube and the corresponding supernatants pooled into a new 2 mL Eppendorf. Any contaminating genomic DNA was removed following the Thermo DNAse I protocol. Equal volume of Phenol/Chloroform/Isoamyl alcohol (25:24:1) was added to the reaction mixture, mixed by inversion, then spun at 14K RCF for 5 minutes. The aqueous phase was moved to a new 2mL Eppendorf and $1/10^{th}$ its volume of 5M RNAse free ammonium acetate was added along with 1 volume of 100% isopropanol. The tube was mixed by inversion and precipitated overnight at -20^{o} C. RNA was pelleted and washed with RNAse free 70% isopropanol twice then dried by vacuum centrifugation. The RNA pellet was resuspended in 30 µL of diethylpyrocarbonate treated molecular water. RNA quantification was done using the Qubit RNA HS kit (Life Technologies Catalog #Q32852) and RNA integrity was measured on the Agilent 2100 Expert bioanalyzer using the prokaryotic total RNA nano-chip (Agilent Catalog # 5067-1511).

RNA-SEQ

cDNA was prepared for each RNA sample using the NuGen Ovation SPIA v2 kit and BioO barcodes were added to each individual library for multiplexing. This was done by the Core Genomics Lab of the Biodesign Institute at Arizona State University. The samples were then pooled and run in a single lane of an Illumina HI-Seq 2000, setup for 2X100bp chemistry, at the Translational Genomics Institute located in Phoenix, Arizona.

Bioinformatics

Sequences were binned according to sample of origin using barcode tags. FastQ files for each RNA-SEQ library were analyzed using the FastQC software and subsequently filtered for quality and adaptor contamination using the Trimmomatic software suite[191]. Processed RNA reads were then mapped to the most current *Mastigocoleus testarum* strain BC008 genome using Bowtie2 (maximum allowable gaps = 2, 99% identity to allow a read match) through the Geneious Bioinformatics GUI ver 8.1.4[124, 192]. Differential gene expression analysis was carried out using DeSEQ2[193]. The Normalized Mean Expression (NME) is the average DeSEQ2 normalized expression value of a gene across all replicates.

Gene Functional Classification

Functional classification of differentially expressed genes was carried out by comparing the automatically generated coding sequence (CDS) annotations obtained from PROKKA with the functional groups assigned by KEGG and GO[194]. A manual PHI-BLAST search was done for any protein with conflicting annotations and putative functional groups were manually assigned based on the top BLAST hits (E value <= 1e-150) and conserved domain content of each protein sequence. 68 significantly

differentially expressed genes which were annotated by PROKKA as hypothetical were able to be assigned to a putative functional group based upon KEGG, GO, and manual BLAST secondary annotation.

Table 6. RNA-SEQ Sample Library Statistics

Sample	Reads mapped to BC008 genome	% reads mapped to rRNA	Unique Reads mapped within a gene	Ave base coverage
B1	67320089	65	23317621	893X
B2	18632609	58	7817213	126X
P1	70424437	6	65866180	2956X
P2	148222600	16	124990662	6131X

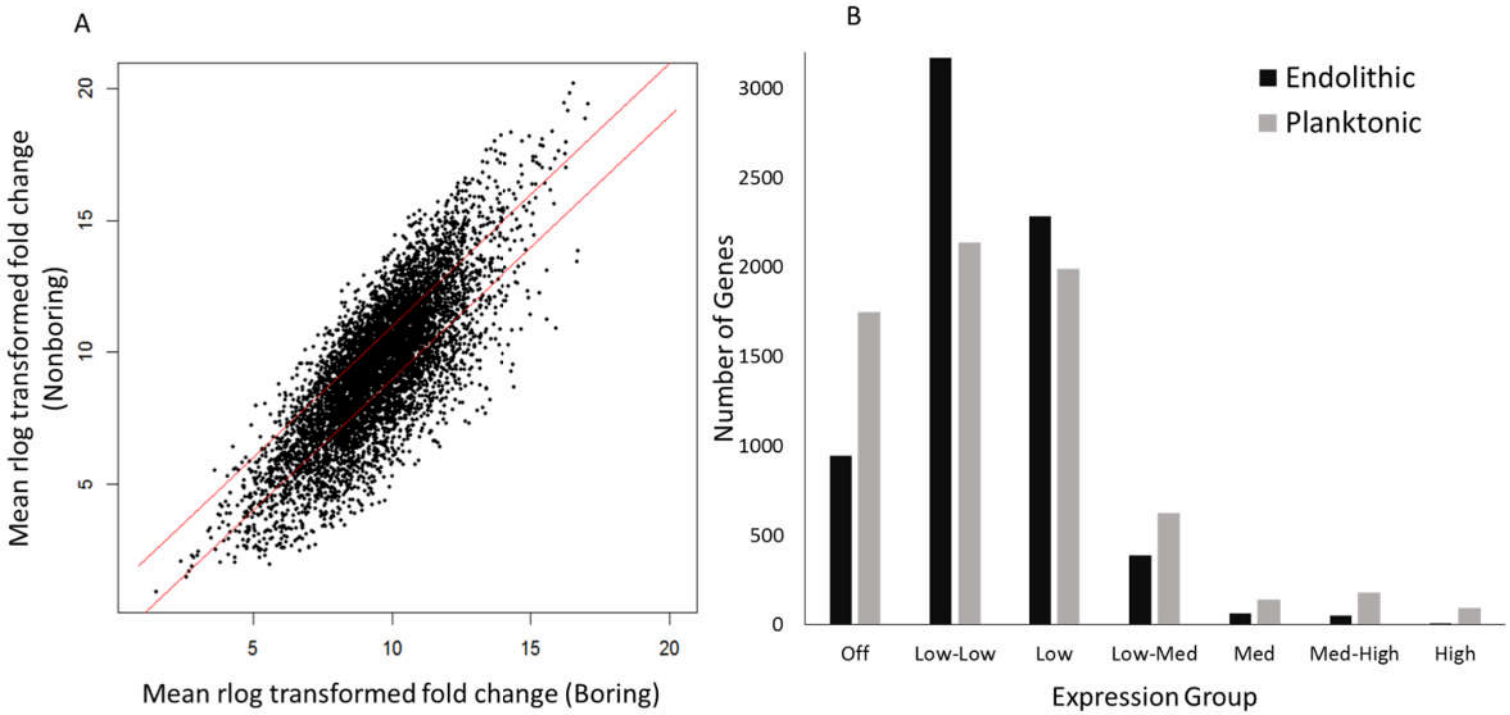


Fig. 20. A) The average (of the condition replicates) rlog transformed fold change for each gene relative to both conditions. Genes outside the red lines show $\log_2$ fold change > 1.5. Many of the most highly expressed genes during planktonic growth are highly repressed and genes that were off or lowly expressed were turned on during endolithic growth. B) A categorical breakdown of the number of genes expressed by average normalized expression levels for each condition were off = <200, low-low = 200-999, Low = 1000-4999, Low-Med = 5000-14999, Med = 15000-24999, Med-High = 25000-74999, and High is >=75000.

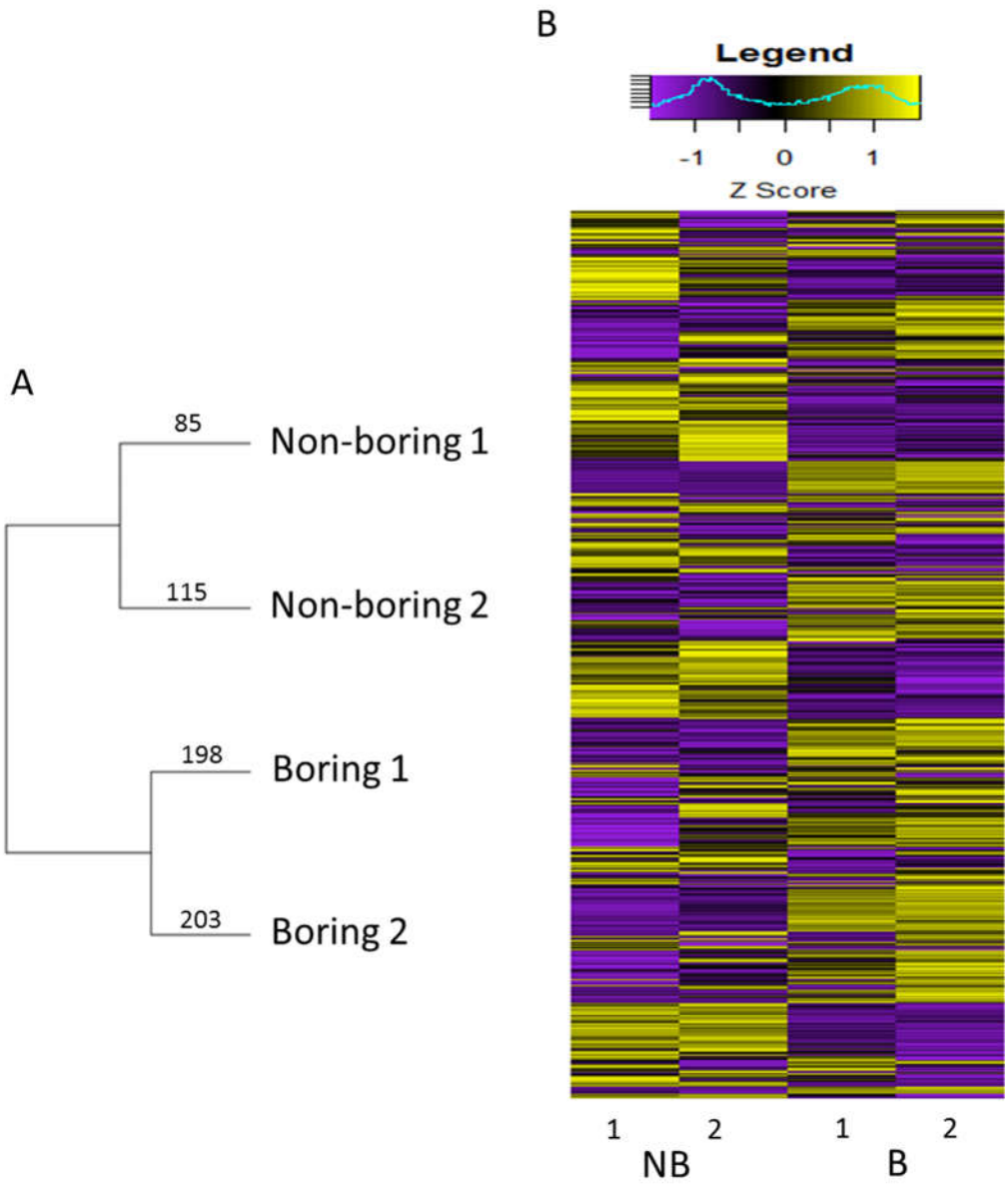


Fig. 21. A) Hierarchical clustering of the Euclidian distances (indicated above each sample branch) calculated for each sample replicate indicating the gene expression pattern in each sample is most similar to its replicate. B) Z-scores for normalized rlog transformed fold change values for All 6917 genes in each culture replicate. Groups of genes of similarly expressed can be observed in each set of condition replicates. NB is non-boring and B is boring.

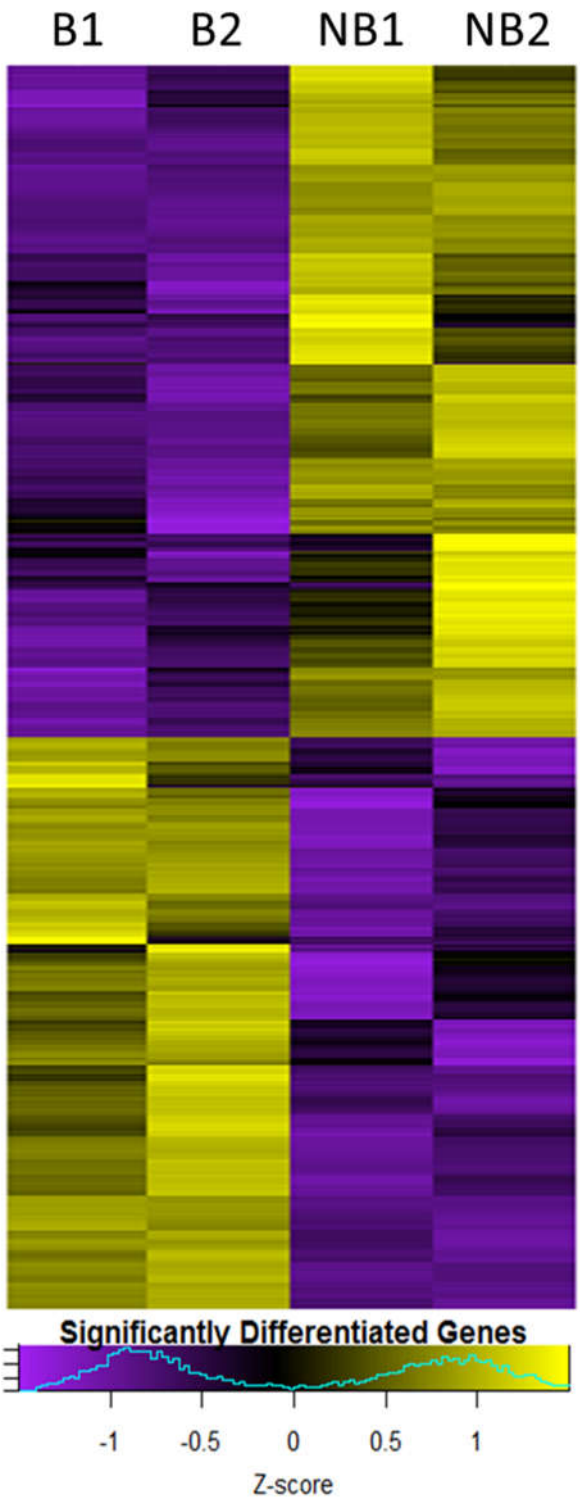


Fig. 22. Z-scores for normalized rlog transformed fold change values for genes in each culture replicate which are significantly differentially regulated genes (1638) with a normalized mean expression value > 200 reads, an absolute $\log_2$ fold change >= 1.5, and a p-value <= 0.10.

Table 7. Gene Functional Group Expression Statistics

Functional Groups (FG)			Gene Expression			
Name	Number of Genes in FG	% of Total (6917) Genes	Number of Upregulated (UR) Genes	Number of Downregulated (DR) Genes	$R_{UR/DR}$	Expression Weighted Ratio[1]
Xenobiotics degradation and metabolism	5	0.31	3	2	**1.5**	0.323
Unknown Function	99	6.04	61	38	**1.61**	0.720
Transporters	103	6.29	81	22	**3.68**	1.183
Sulfur Metabolism	3	0.18	1	2	**0.5**	0.021
Stress Response	81	4.95	20	61	**0.33**	0.040
Signal Transduction	147	8.97	69	78	**0.88**	0.215
Secretion Systems	17	1.04	12	5	**2.4**	1.870
Ribosome Construction	41	2.50	0	41	**N/A**	N/A
Photosynthesis	129	7.88	25	104	**0.24**	0.004
Nucleotide Metabolism	37	2.26	15	22	**0.68**	0.331
Nucleic Acid Maintenance	128	7.81	48	80	**0.6**	0.128
Secondary Metabolite Biosynthesis	53	3.24	38	15	**2.53**	0.174
Nitrogen Metabolism	21	1.28	3	18	**0.17**	0.009
Biosynthesis of Terpenoids	3	0.18	0	3	**N/A**	N/A
Metabolism of other amino acids	2	0.12	1	1	**1**	0.189
Lipid Metabolism	43	2.63	26	17	**1.53**	0.210
Enzymes	181	11.05	88	93	**0.95**	0.411
Energy Metabolism	46	2.81	13	33	**0.39**	0.056
Defense	21	1.28	15	6	**2.5**	2.518
Cofactor and Vitamin Biosynthesis	72	4.40	33	39	**0.85**	0.362
Cellular Processes	24	1.47	4	20	**0.2**	0.017
Cell Envelope	96	5.86	47	49	**0.96**	0.203
Carbon Metabolism	28	1.71	15	13	**1.15**	0.497
Carbon Fixation	32	1.95	9	23	**0.39**	0.018
Carbohydrate Metabolism	52	3.17	28	24	**1.17**	0.213
Amino Acid Biosynthesis	84	5.13	37	47	**0.79**	0.190
ABC Transporters	90	5.49	59	31	**1.9**	0.460

[1] Expression Weighted Ratio is the $R_{UR/DR}$ * ratio of the average NME of the UR genes in the FG to the average NME of the DR genes.

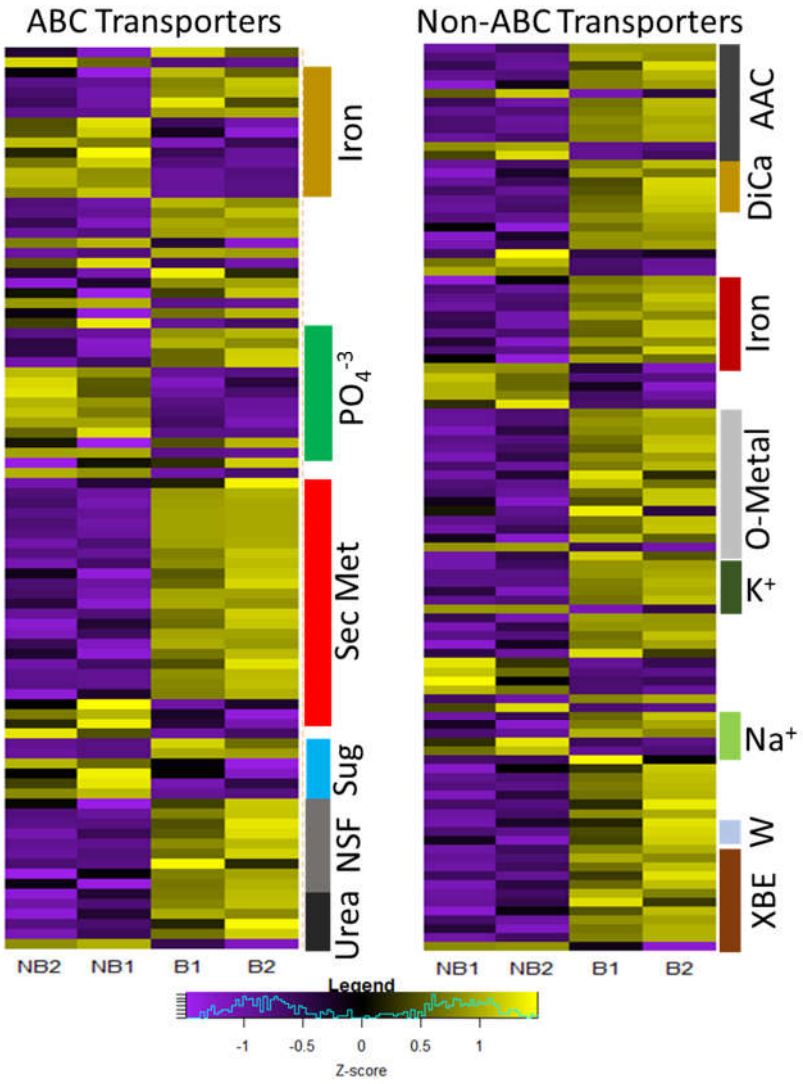


Fig 23. Z-scores for normalized rlog transformed fold change values for genes in each culture replicate which fall into the ABC transporter and Non-ABC Transporter functional groups. Important Sub-Groups are denoted by the colored boxes. Abbreviations: Sec Met = Secondary Metabolites, Sug = Miscellaneous Sugars, NSF = Non-Specific Transport Function, AAC = Amino Acid and Carbohydrate Transport, DiCA = Dicarboxylic Acid Transporters, O-Metal = Other Metal Transporters, W = water porins, XBE = Xenobiotic Export

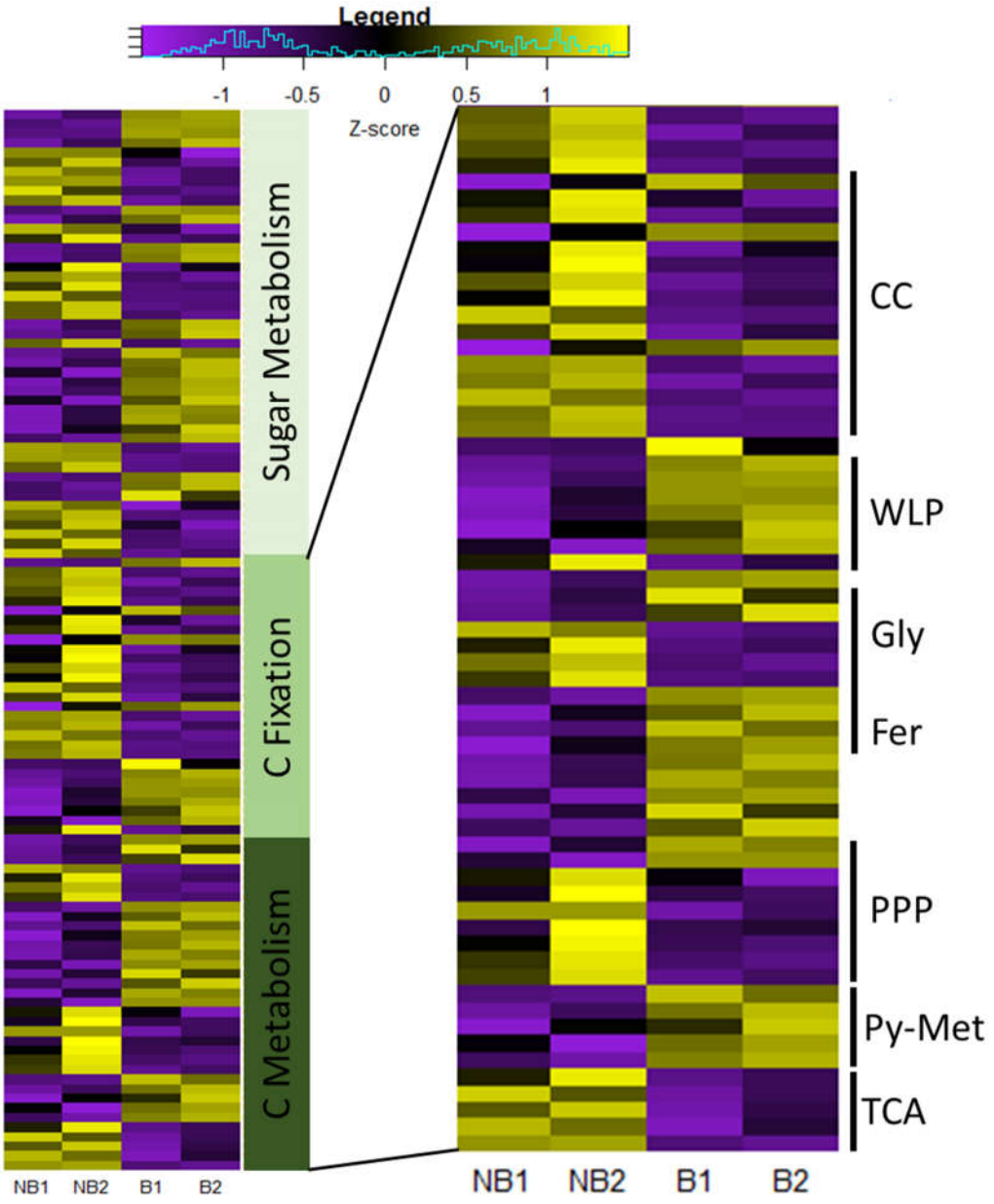


Fig 24. Z-scores for normalized rlog transformed fold change values for genes in each culture replicate which fall into the Carbohydrate Metabolism, Carbon Fixation, and Carbon Metabolism functional Groups. Right) Blow-up of the Carbon Fixation and Carbon Metabolism functional group heatmap illustrating expression of genes within each sub-group. Abbreviations: CC = Calvin Cycle, WLP = Wood-Ljungdhal Pathway, Gly = Glycolysis, Fer = Fermentation, PPP = Pentose Phosphate Pathway, Py-Met = Pyruvate Metabolism, TCA = Tricarboxylic Cycle, B = Boring Culture, NB = Non-boring Culture.

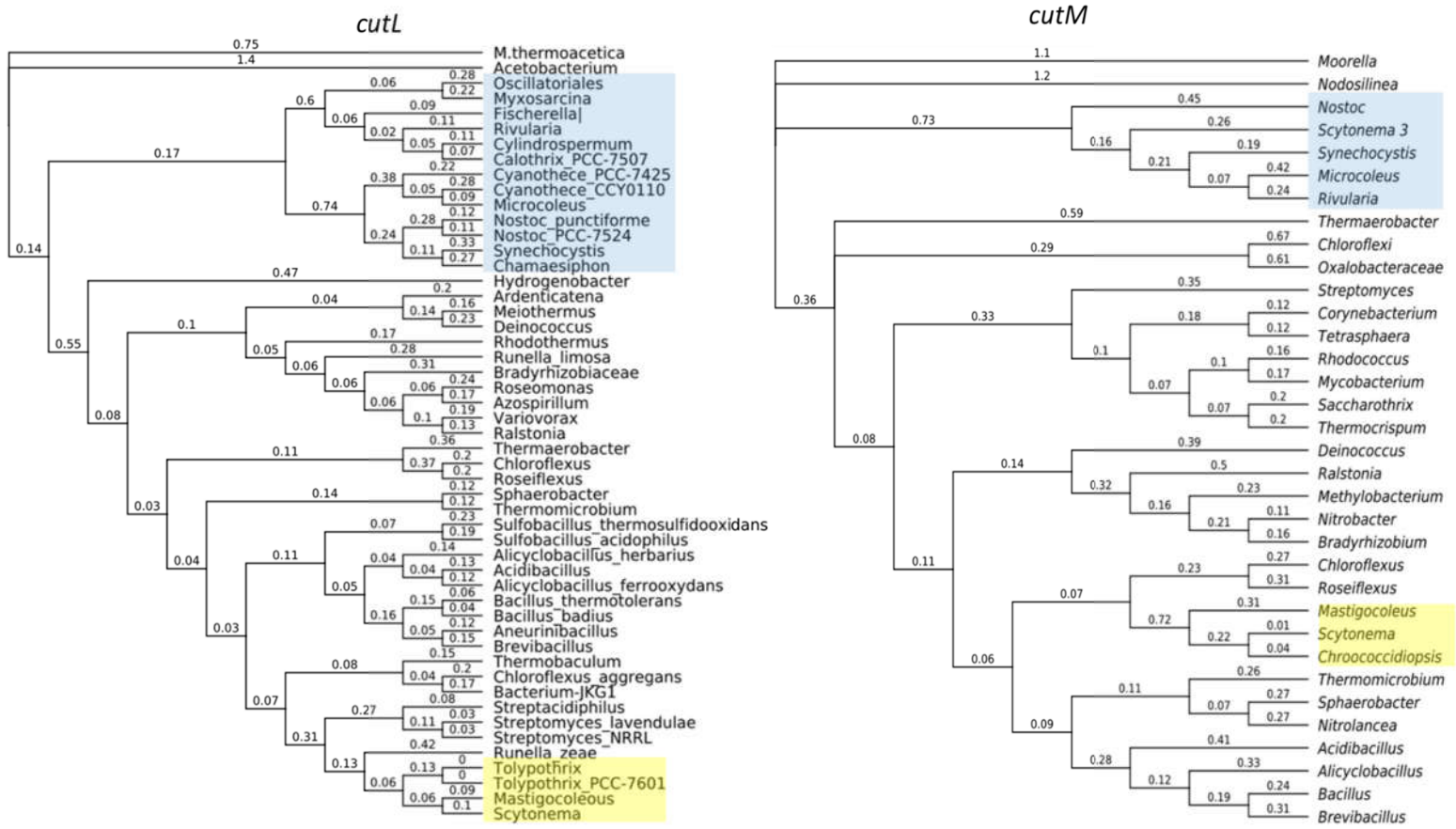


Fig. 25. Maximum Likelihood phylogeny of the large and medium subunits of the putative carbon monoxide dehydrogenase found in an operon in the *M. testarum* strain BC008 genome. These trees were rooted using the orthologous sequences from *Moorella thermoacetica,* an acetogen which employs an ancient carbon fixation pathway known as the reductive acetyl-CoA pathway. The BC008 subunits cluster with just a few select cyanobacteria (yellow) but are more closely related to proteins found in several anaerobic photoheterotrophs such as strains of *Chloroflexus* and *Roseifelxus*. Most cyanobacterial orthologs of these two proteins cluster together and form a deeply rooted branch indicating an ancient divergence for this group. Branch labels indicate relative substitutions per site.

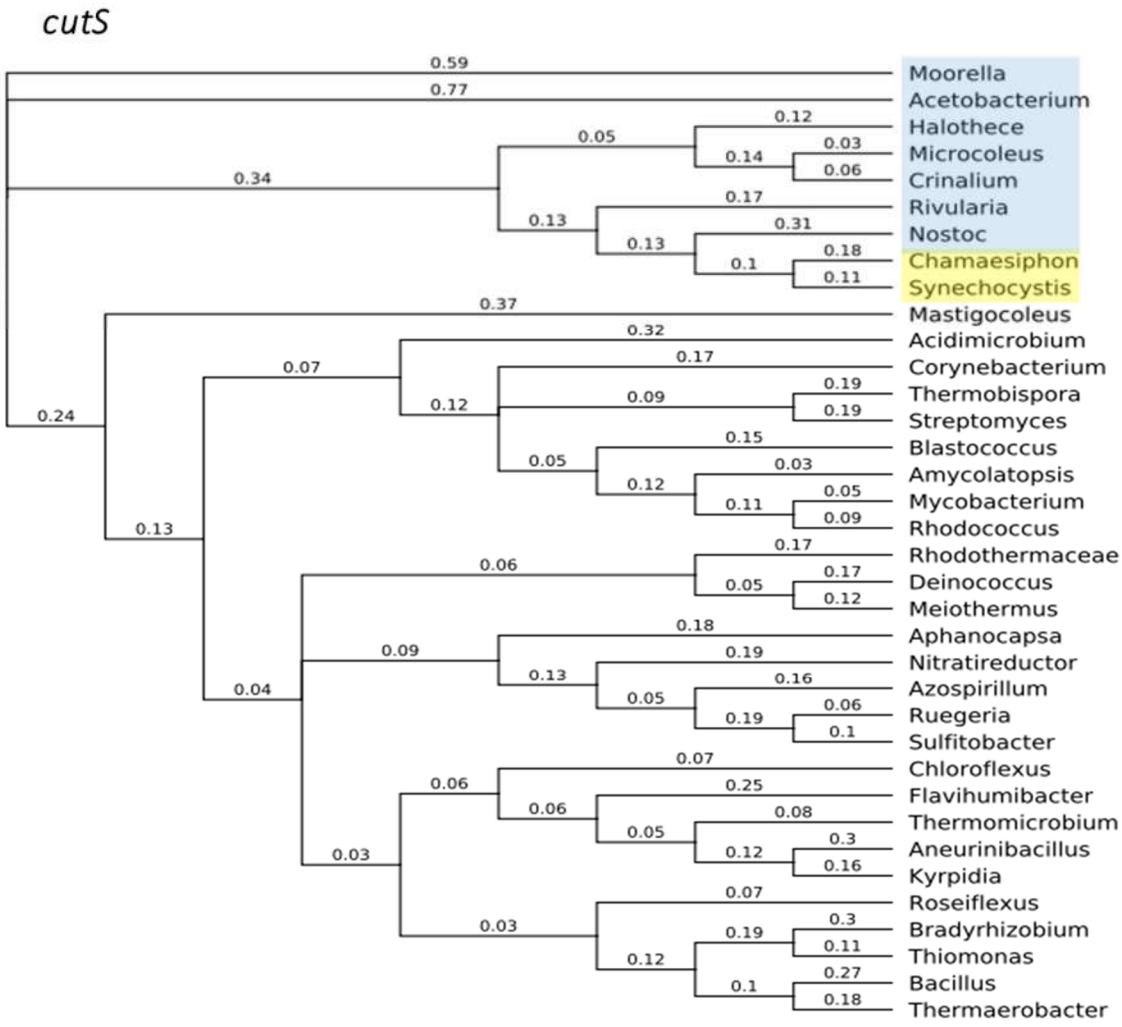


Fig. 26. Maximum Likelihood phylogeny of the orphan small subunit of the putative carbon monoxide dehydrogenase found in the *M. testarum* strain BC008 genome. This tree was rooted using the ortholog sequence from *Moorella thermoacetica,* an acetogen which employs an ancient carbon fixation pathway known as the reductive acetyl-CoA pathway. The BC008 subunit (yellow) appear to represent a very ancient protein acquired by *Mastigocoleus* just after the cyanobacterial split which is ancestral to that seen in the proteobacterial lineage. The orthologs seen in cyanobacteria again cluster together to form a deeply rooted branch indicating the ancient divergence for this protein. Branch labels indicate relative substitutions per site.

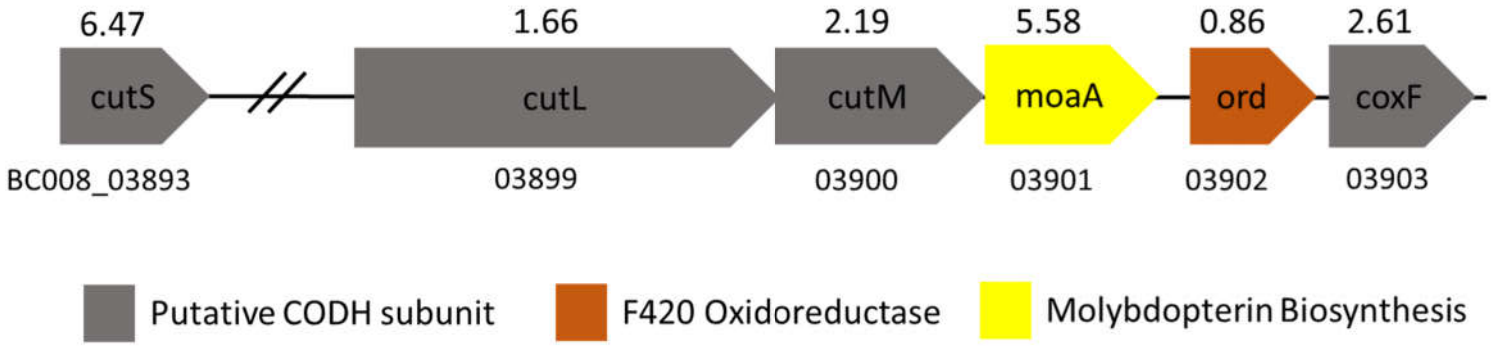


Fig. 27. Structure of local genomic region containing the putative CODH ORF's. Fold change values and locus ID's are listed above and below each ORF respectively. Abbreviation: ord = oxidoreductase

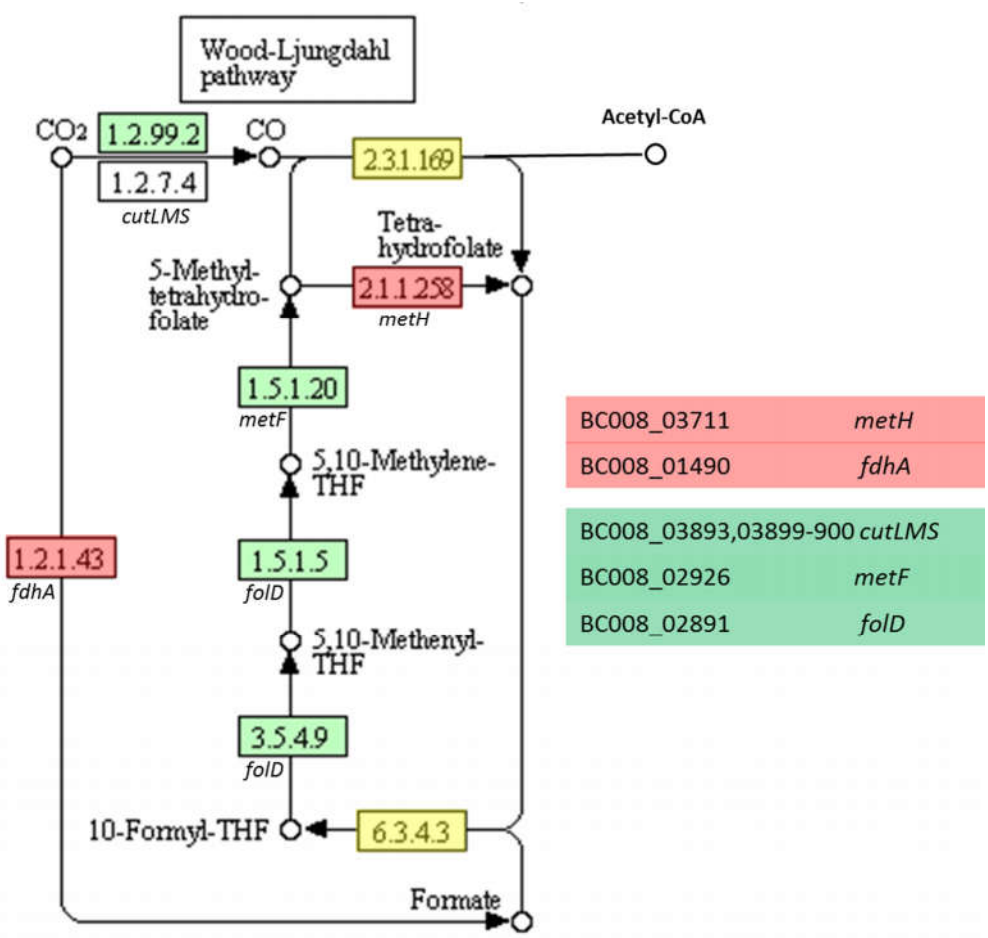


Fig. 28. Wood-Ljungdhal Pathway of carbon fixation. Genes which were auto-annotated via the KAAS KEGG pipeline are highlighted in green, manually annotated orthologs are highlighted in red, and genes with no apparent ortholog in BC008 are highlighted in yellow. Genomic locus identification numbers are indicated to the right for all BC008 orthologs.

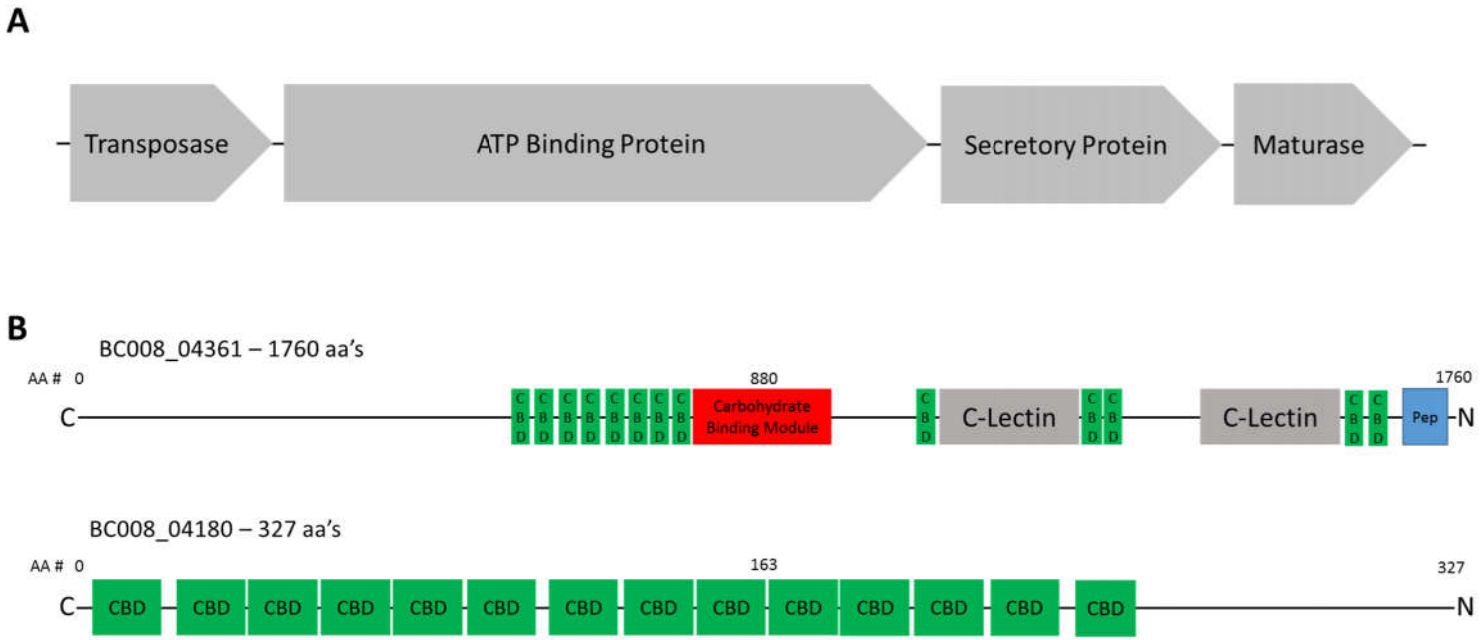


Fig. 29. A) General operon structure of the seven annotated RTX secretion operons. Three loci have this exact layout, three do not have the transposase and one has neither the transposase or the maturase. B) General conserved domain architecture of two M. testarum RTX related calcium binding toxins. BC008_04361 contains two CLECT_VCBS domains (cd03603) known to bind many different surfaces, including $CaCO_3$, a single carbohydrate domain, as well as 13 haemolysin-like calcium binding domains (CBD, pfam00353) with 5 distributed among the other domains and the remaining concentrated towards the C terminus. BC008_04180 only contains 13 haemolysin-like calcium binding domains concentrated in one located shifted toward the carboxy terminus.

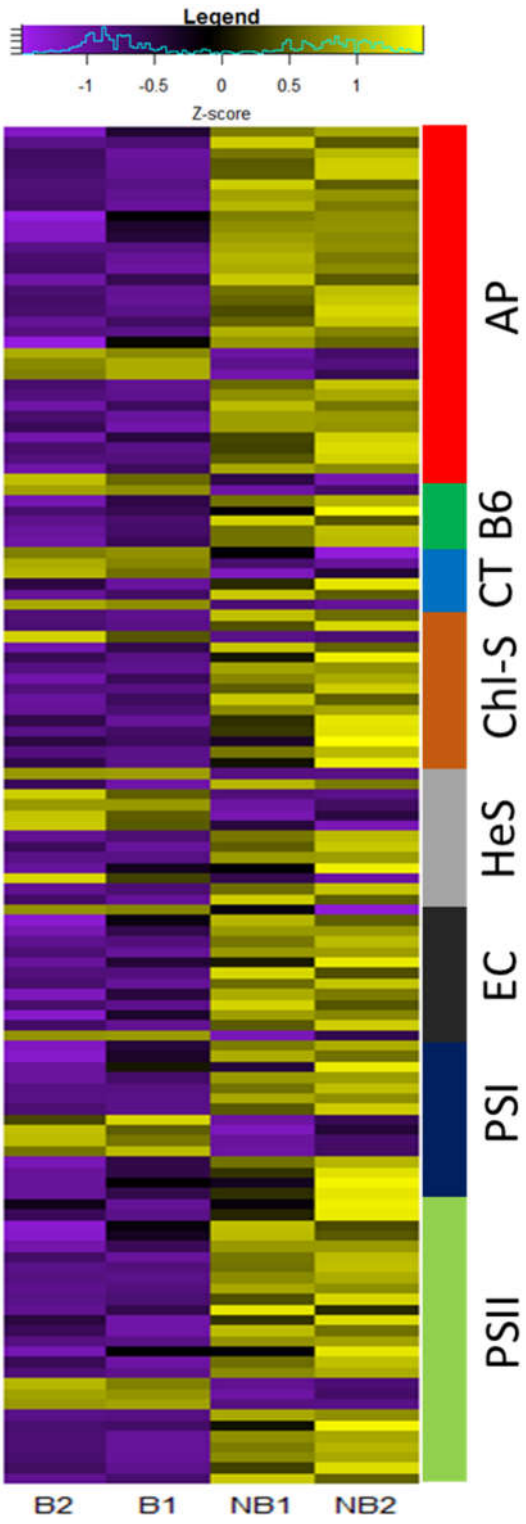


Fig. 30. Z-scores for normalized rlog transformed fold change values for genes in each culture replicate which fall into the Photosynthesis functional group. Important Sub-Groups are denoted by the colored boxes. Sub-group Abbreviations: AP = Antenna Proteins, B6 = Cytochrome B6F Complex, CT = Carotenoid Biosynthesis, Chl-S = Chlorophyll Biosynthesis, HeS = Heme Ring Synthesis, EC = Photosynthesis Electron Carriers, PSI = Photosystem I proteins, PSII = Photosystem II Proteins

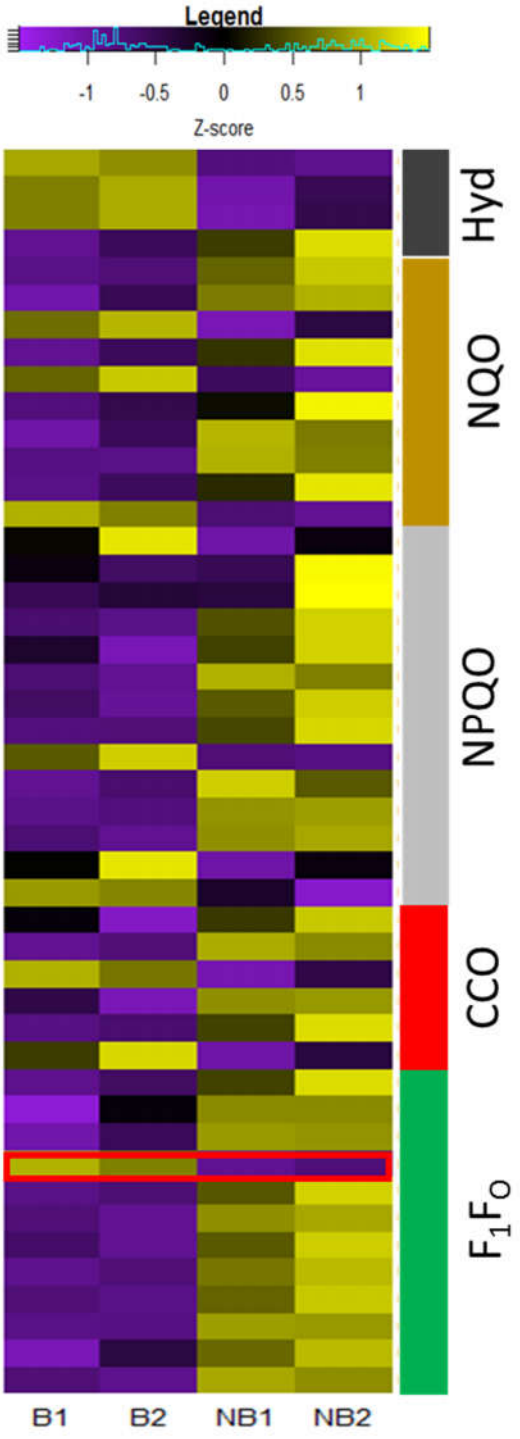


Fig. 31. Z-scores for normalized rlog transformed fold change values for genes in each culture replicate which fall into the Oxidative Phosphorylation functional group. Important Sub-Groups are denoted by the colored boxes. Sodium Specific Alternative ATPase subunit boxed in red. Sub-Group Abbreviations: Hyd = Hydrogenases, NQO = NADH Quinone Oxidoreductase, NPQO = NADPH Quinone Oxidoreductase, CCO – Cytochrome C Oxidase Complex, F_1F_O = F_1F_O – ATPase Complex.

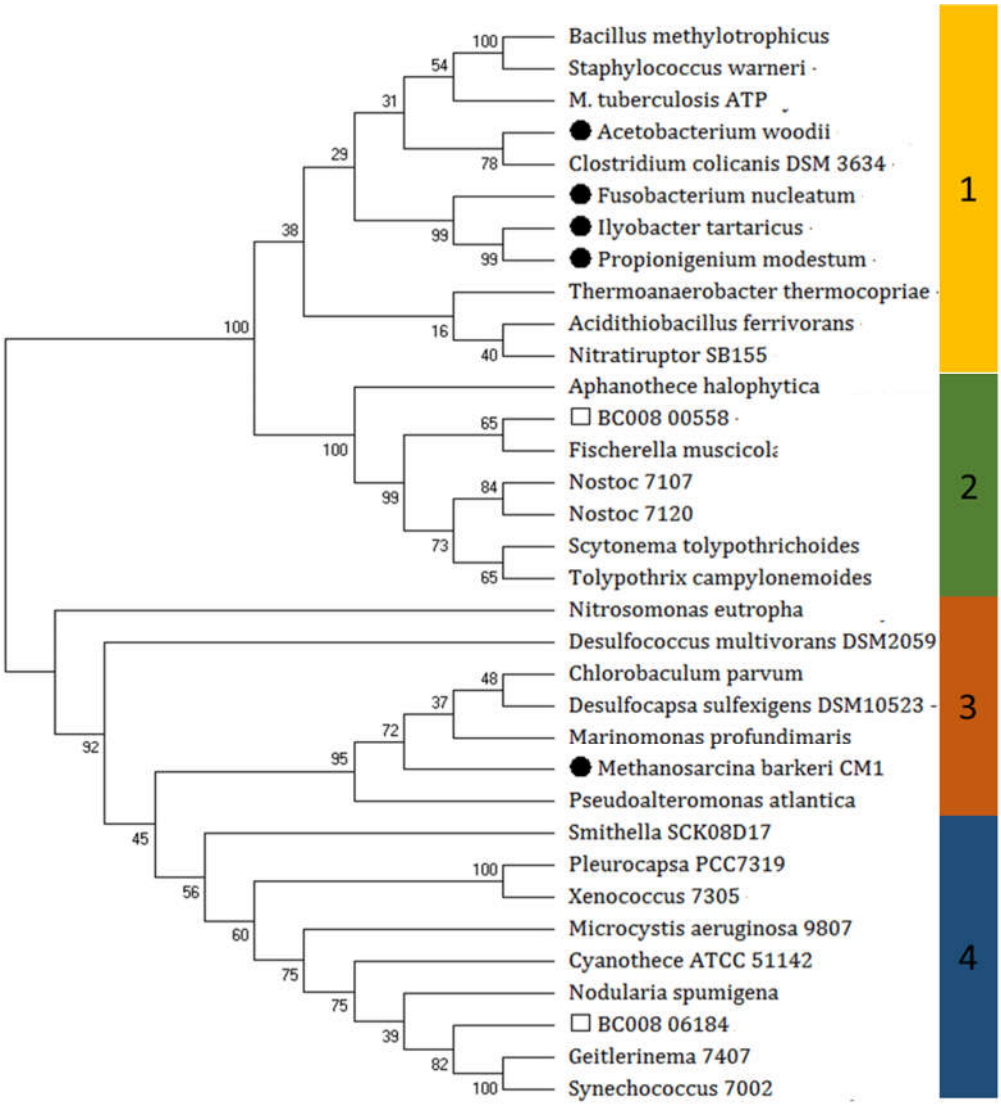


Fig. 32. Maximum Likelihood Phylogenetic Analysis of the *atpD* gene. Sequences belonging to clade 1 are not annotated as alternative F_1F_O-ATPase subunits however there is evidence for sodium translocation for a few members of this clade (solid circles) to which acetogenic organisms belong. Clade 2 represents canonical H^+ translocating subunits found in most cyanobacteria. Sequences clustering in clade 3 belong primarily to anaerobic bacteria, photosynthetic green sulfur bacteria and archaea (for which there is evidence of sodium translocation, closed circle). Clade 4 contains sequences only found in a small percentage of cyanobacteria, typically as an additional subunit. Sequences belonging to clades 3 and 4 are annotated by the NCBI conserved domain database as being alternative F_1F_O- ATPase subunits. *Mastigocoleus testarum* strain BC008 contains a subunit belong to both clade 2 and 4 (open square).

Table 8. RTX-like Calcium Binding Proteins Highly Upregulated During Endolithic Growth

Genome Locus Tag	Endolithic NME[1]	Planktonic NME[1]	Log_2-Fold Change	Size (AA)	Number of CBD*	Refined Annotation
BC008_01300	18309.06	30.36	8.96	83	3	RTX - Calcium binding protein
BC008_04218	36470.24	118.21	8.02	675	18	RTX - Calcium binding Protein
BC008_04180	111296.16	383.63	7.92	327	13	RTX - Cytoplasmic Calcium Binding protein
BC008_01180	31767.25	481.28	5.84	479	20	RTX - Calcium binding Protein
BC008_06405	45510.51	798.91	5.60	1817	16	RTX - Calcium binding K dependent Na/Ca exchanger
BC008_04361	7614.23	168.55	5.31	1760	13	RTX - Calcium binding - surface binding
BC008_00776	53025.59	1429.76	4.97	2273	14	RTX - Calcium binding Protein Carbohydrate binding
BC008_04451	9621.87	1136.55	2.99	714	5	RTX - Calcium binding - PQQ motiff
BC008_01570	9505.80	2284.01	1.98	748	7	RTX- Calcium binding with haem binding peroxidase

[1]Normalized Mean Expression, * Haemolysin type Calcium Binding Domain

CONCLUDING REMARKS

The work presented in this thesis significantly advances our knowledge of the euendolithic environment in several key ways. Firstly, the data presented in chapter 1 solidifies our working understanding of the euendolithic excavation mechanism by providing direct evidence of vectorial calcium transport mediated by specific sub-cellular organization of pumping components. Furthermore, the detection of a novel cellular morphotype (calcicyte) in the model euendolith *M. testaurm* strain BC008 adds to the already complex differentiation ability of this organism and illustrates the overall importance of cellular differentiation to the euendolithic excavation mechanism. Secondly, chapter 2 unequivocally shows the fate of the newly liberated mineral derived inorganic carbon generated during the boring process which is either fixed by boring biomass or released to the surrounding microenvironment. The ecological impacts of this process on both ancient and extant benthic ecosystems may be more significant than previously realized as the isotopic signature of excavated minerals may propagate through food webs dependent on endolithic primary producers. This action may cause significant deviations in the expected isotopic signatures of heterotrophic biomass thought to rely on primary producers fixing solely atmospheric derived dissolved inorganic carbon. Lastly, the final two chapters of this work (3 and 4) present the first genomic and transcriptomic data analysis of a known euendolithic organism respectively. Comparative transcriptomic analysis between planktonic and endolithic biomass of strain BC008 reveal the overall difficulties associated with the euendolithic lifestyle. Along

with data generated in chapter 2, gene expression analysis suggests endolithic biomass is extremely diffusively limited and the transport of essential micronutrients appears to be a limiting factor to growth. Data presented in chapter 4 also indicates that the metabolic and carbon fixation pathways employed by cyanobacterial euendoliths may be markedly different than the canonical pathways known to function in most planktonic cyanobacteria. Several novel genes were also identified which may play central roles in the transport of cations (including calcium), as well as in the mitigation of intracellular calcium cytotoxicity expected from the large intracellular calcium concentrations observed in BC008.

While this thesis answers many pressing questions associated with the euendolithic lifestyle many more remain. The evolutionary event leading to the euendolithic trait is unknown, however, as previously discussed, several theories have been put forth, to which this work adds the hypothesis that inorganic carbon limitation spurred the first proto-euendoliths to begin excavating calcareous mineral substrates. We still do not know how *Mastigocoleus* can survive such large intracellular calcium fluxes; however, the discovery of a novel set of calcium binding proteins may shed light on this mystery. It was my hope to significantly contribute to the holistic understanding of the euendolithic lifestyle, and through the contributions discussed in this document, I feel that I have.

REFERENCES:

1) Schopf, J. W. in *Paleobiology of the Archean* (eds Schopf, J. W. & Klein, C.) 25-39 (Cambridge University Press, Cambridge, 1992).

2) Schopf, J. W. Microfossils of the Early Archean Apex chert : new evidence of the antiquity of life. *Science*, 640-646 (1993).

3) Castresana, J. & Saraste, M. Evolution of energetic metabolism—the respiration-early hypothesis. *Trends in Biochemical Science*, 443-448 (1995).

4) Pereira, M. M., Santana, M. & Teixeira, M. A novel scenario for the evolution of haem-copper oxygen reductases. *Biochim. Biophys. Acta* **1505**, 185-208 (2001).

5) Bekker, A. *et al*. Dating the rise of atmospheric oxygen. . *Nature*, 117-120 (2004).

6) Sessions, A. L., Doughty, D. M., Welander, P. V., Summons, R. E. & Newman, D. K. The continuing puzzle of the great oxidation event. *Current Biology*, R567-R574 (2009).

7) Allwood, A. & Anderson, M. 3.45 billion year old stromatolite reef of Western Australia: a rich, large-scale record of early biota, strategies and habitats. *Orig Life Evol Biosph*, 188-189 (2009).

8) Anbar, A. D. *et al*. A Whiff of Oxygen Before the Great Oxidation Event? *Science* **317**, 1903 1906 (2007).

9) Lyons, T. The rise of oxygen in Earth's early ocean and atmosphere. *Nature (London)* **506**, 307 (2014).

10) Blankenship, R. E. Early Evolution of Photosynthesis. *Plant Physiol.* **154**, 434-438 (2010).

11) Tang, K. H., Tang, Y. J. & Blankenship, R. E. Carbon metabolic pathways in phototrophic bacteria and their broader evolutionary implications. *Front. Microbiol.* **2**, 165 (2011).

12) Beck, C., Knoop, H., Axmann, I. M. & Steuer, R. The diversity of cyanobacterial metabolism: genome analysis of multiple phototrophic microorganisms. *BMC Genomics* **13**, 56-2164-13-56 (2012).

13) Mulkidjanian, A. Y. *et al*. The cyanobacterial genome core and the origin of photosynthesis. *Proc. Natl. Acad. Sci. U. S. A.* **103**, 13126-13131 (2006).

14) Dhingra, A., Portis, A. R. J. & Daniell, H. Enhanced translation of a chloroplast-expressed RbcS gene restores small subunit levels and photosynthesis in nuclear RbcS antisense plants. *Proceedings of the National Academy of Sciences* **101**, 6315-6320 (2004).

15) Ellis, R. J. Biochemistry: Tackling unintelligent design. *Nature* **463**, 164-165 (2010).

16) Kerfeld, C. A., Heinhorst, S. & Cannon, G. C. Bacterial Microcompartments. *Annual Review of Microbiology* **64**, 391-408 (2010).

17) Oren, A. & Padan, E. Induction of anaerobic, photoautotrophic growth in the cyanobacterium *Oscillatoria limnetica*. *J. Bacteriol.* **133**, 558-563 (1978).

18) Padan, E. Facultative Anoxygenic Photosynthesis in Cyanobacteria. *Annual Review of Plant Physiology* **30**, 27 40 (1979).

19) Anderson, S. L. & McIntosh, L. Light-activated heterotrophic growth of the cyanobacterium *Synechocystis* sp. strain PCC 6803: a blue-light-requiring process. *J. Bacteriol.* **173**, 2761-2767 (1991).

20) Stal, L. J. & Moezelaar, R. Fermentation in cyanobacteria. *FEMS Microbiol. Rev.* **21**, 179-211 (2006).

21) Zhaxybayeva, O. Phylogenetic analyses of cyanobacterial genomes: Quantification of horizontal gene transfer events. *Genome Res.* **16**, 1099 1108 (2006).

22) Singh, S. M. & Elster Chapter 16, J. Algae and Cyanobacteria in Extreme Environments; Cyanobacteria in Antarctic Lake Environments. **11**, 303 320 (2007).

23) Miller, S. R. & Castenholz, R. W. Evolution of Thermotolerance in Hot Spring Cyanobacteria of the Genus *Synechococcus*. *Appl. Environ. Microbiol.* **66**, 4222 4229 (2000).

24) Lagerheim, G. Note sur le Mastigocoleus, nouveau genre des algues marines de l' ordre des Phycochromacées. *Notarisia* **1**, 65-69 (1886).

25) Thuret, G. Essai de classification des Nostochinees. *Annales des Sciencies Natureles*, 375-379 (1875).

26) Bornet, E. & Flahault, C. Note sur deux nouveaux genres d' algues perforantes. *Journal de Botanique*, 162-163 (1888).

27) Pantazidou, A., Louvrou, I. & Economou-Amilli, A. Euendolithic shell-boring cyanobacteria and chlorophytes from the saline lagoon Ahivadolimni on Milos Island, Greece. *Eur. J. Phycol.* **41**, 189-200 (2006).

28) Budd, D. A. & Perkin, R. D. Bathymetric Zonation and Paleoecological Significance of Microborings in Puerto Rican Shelf and Slope Sediments. *Journal of Sedimentary Research* **50**, 881-903 (1980).

29) Macintyre, I. G., Prufert-Bebout, L. & Reid, R. P. The role of endolithic cyanobacteria in the formation of lithified laminae in Bahamian stromatolites. *Sedimentology* **47**, 915 921 (2000).

30) Golubic, S. Boring Behavior of marine blue-green algae *Mastigocoleus testarum* Lagerheim and *Kyrtuthrix dalmatica* Ercegovia 21, as a taxonomic character. *Swiss Journal of Hydrology* **35**, 157-161 (1973).

31) Campbell, S. E. in *Biomineralization and Biological Metal Accumulation* (ed P. Westbroek, E. W. d. J.) 99-104 (Reidel Publishing, Boston, 1983).

32) Pohl, W. & Schneider, J. Impact of endolithic biofilms on carbonate rock surfaces. *Geological Society, London, Special Publications* **205**, 177-194 (2002).

33) Tribollet, A., Langdon, C., Golubic, S. & Atkinson, M. Endolithic microflora are major primary producers in dead carbonate substrates of Hawaiin coral reefs. *J. Phycol.* **42**, 292-303 (2006).

34) Trudgill, S. T., Smart, P. L., Friederich, H. & Crabtree, R. W. Bioerosion of intertidal limestone, Co. Clare, Eire — 1: *Paracentrotus lividus*. *Mar. Geol.* **74**, 85-98 (1987).

35) Tribollet, A. Dissolution of dead corals by euendolithic microorgansims across the northern Great Barrier Reef (Australia). *Microbial Ecology* **55**, 569-580 (2008).

36) Golubic, S., Pietrini, A. M. & Ricci, S. Euendolithic activity of the cyanobacterium *Chroococcus lithophilus Erc.* In biodeterioration of the Pyramid of Caius Cestius, Rome, Italy. *Int. Biodeterior. Biodegrad.* **100**, 7-16 (2015).

37) Kaehler, S. Incidence and distribution of phototrophic shell-degrading endoliths of the brown mussel *Perna perna*. *Mar. Biol.* **135**, 505 514 (1999).

38) Golubic, S. & Campbell, S. E. in *Biogenically Formed Aragonite Concretions in Marine Rivularia* (ed Monty, C.) 209-229 (Springer, Berlin, 1981).

39) Ludwig, M. & Bryant, D. A. Acclimation of the Global Transcriptome of the Cyanobacterium *Synechococcus* sp. Strain PCC 7002 to Nutrient Limitations and Different Nitrogen Sources. *Front. Microbiol.* **3**, 145 (2012).

40) Kopf, M. *et al*. Comparative Analysis of the Primary Transcriptome of *Synechocystis* sp.PCC 6803. *DNA Research*, 1-12 (2014).

41) Voigt, K. *et al*. Comparative transcriptomics of two environmentally relevant cyanobacteria reveals unexpected transcriptome diversity. *ISME J.* **8**, 2056-2068 (2014).

42) Falkowski, P. *et al*. The Global Carbon Cycle: A Test of Our Knowledge of Earth as a System. *Science* **290**, 291-296 (2000).

43) Knorr, W. Is the airborne fraction of anthropogenic CO_2 emissions increasing? *Geophys. Res. Lett.* **36** (2009).

44) Laanbroek, H. J. Methane emission from natural wetlands: interplay between emergent macrophytes and soil microbial processes. A mini-review. *Ann. Bot.* **105**, 141-153 (2010).

45) Buddle, B. M. *et al*. Strategies to reduce methane emissions from farmed ruminants grazing on pasture. *Vet. J.* **188**, 11-17 (2011).

46) Khalil, M. A. K. & Rasmussen, R. A. The global cycle of carbon monoxide: Trends and mass balance. *Chemosphere* **20**, 227-242 (1990).

47) Ragsdale, S. W. & Pierce, E. Acetogenesis and the Wood-Ljungdahl pathway of CO(2) fixation. *Biochim. Biophys. Acta* **1784**, 1873-1898 (2008).

48) Field, C. B. Primary Production of the Biosphere: Integrating Terrestrial and Oceanic Components. *Science* **281**, 237 240 (1998).

49) Flombaum, P. *et al*. Present and future global distributions of the marine Cyanobacteria *Prochlorococcu*s and *Synechococcus*. *Proc. Natl. Acad. Sci. U. S. A.* **110**, 9824-9829 (2013).

50) Ford, D. & Williams, P. in *Karst Hydrogeology and Geomorphology* (John Wiley & Sons Ltd, West Sussex, England, 2007).

51) Schneider, J. & Le Campion-Alsumard, T. Construction and destruction of carbonates by marine and freshwater cyanobacteria. *Eur. J. Phycol.* **34**, 417-426 (1999).

52) Garcia-Pichel, F. Plausible mechanisms for the boring on carbonates by microbial phototrophs. *Sediment. Geol.* **185**, 205-213 (2006).

53) Giraldez-Ruiz, N., Mateo, P., Bonilla, I. & Fernandez-Pinas, F. The relationship between intracellular pH, growth characteristics and calcium in the cyanobacterium *Anabaena* sp. strain PCC7120 exposed to low pH. *New Phytol.* **137**, 599-605 (1997).

54) Coleman, J. R. & Colman, B. Inorganic Carbon Accumulation and Photosynthesis in a Blue-green Alga as a Function of External pH. *Plant Physiol.*, 917-921 (1981).

55) Ramírez-Reinat, E. L. & Garcia-Pichel, F. Characterization of a Marine Cyanobacterium that Bores into Carbonates and the Redescription of the Genus *Mastigocoleus*. *J. Phycol.* **48**, 740-749 (2012).

56) Garcia-Pichel, F., Ramirez-Reinat, E. & Gao, Q. Microbial excavation of solid carbonates powered by P-type ATPase-mediated transcellular Ca^{2+} transport. *Proceedings of the National Academy of Sciences* **107**, 21749-21754 (2010).

57) Golubic, S., Friedmann, I. & Schneider, J. The Lithobiontic Ecological Niche, with Special Reference to Microorganisms. *Journal of Sedimentary Research* **51**, 475-478 (1981).

58) Chacón, E., Berrendero, E. & Garcia Pichel, F. Biogeological signatures of microboring cyanobacterial communities in marine carbonates from Cabo Rojo, Puerto Rico. *Sediment. Geol.* **185**, 215-228 (2006).

59) Golubic, S. & Schneider, J. in *Fossil and Recent Biofilms: A Natural History of Life on Earth* (eds Krumbein, W. E., Paterson, D. M. & Zavarzin, G. A.) 249-263 (Springer Netherlands, 2003).

60) Mitra, S., Sana, B. & Mukherjee, J. Ecological roles and biotechnological applications of marine and intertidal microbial biofilms. *Adv. Biochem. Eng. Biotechnol.* **146**, 163-205 (2014).

61) Garcia-Pichel, F., Kühl, M., Nübel, U. & Muyzer, G. Salinity-Dependent Limitation of Photosynthesis and Oxygen Exchange in Microbial Mats. *J. Phycol.* **35**, 227-238 (1999).

62) Staal, M. *et al*. Different carbon isotope fractionation patterns during the development of phototrophic freshwater and marine biofilms. *Biogeosciences* **4**, 613-626 (2007).

63) Awramik, S. M., Schopf, J. W. & Walter, M. R. Filamentous fossil bacteria from the Archean of Western Australia. *Precambrian Res.* **20**, 357 374 (1983).

64) Golubic, S. & Seong-Joo, L. Early cyanobacterial fossil record: preservation, palaeoenvironments and identification. *European Journal of Phycology* **34**, 339-348 (1999).

65) Hoshino, Y. & George, S. C. Cyanobacterial Inhabitation on Archean Rock Surfaces in the Pilbara Craton, Western Australia. *Astrobiology* **15**, 559-574 (2015).

66) Nagarkar, S., Williams, G. A., Subramanian, S. K. & Saha, S. K. Cyanobacteria-dominated biofilms: a high quality food resource for intertidal grazers. *Hydrobiologia* **512**, 89-95 (2004).

67) Knauth, L. P. Temperature and salinity history of the Precambrian ocean: implications for the course of microbial evolution. *Palaeogeogr. , Palaeoclimatol. , Palaeoecol.* **219**, 53 69 (2005).

68) Zhang, X. V. & Martin, S. T. Driving parts of Krebs cycle in reverse through mineral photochemistry. *J. Am. Chem. Soc.* **128**, 16032-16033 (2006).

69) Tang, K. H. & Blankenship, R. E. Both forward and reverse TCA cycles operate in green sulfur bacteria. *J. Biol. Chem.* **285**, 35848-35854 (2010).

70) Frigaard, N. & Dahl, C. Sulfur Metabolism in Phototrophic Sulfur Bacteria. *Advances in Microbial Physiology* **54**, 103-200 (2008).

71) Widdel, F. *et al*. Ferrous iron oxidation by anoxygenic phototrophic bacteria. *Nature* **362**, 834 836 (1993).

72) Riding, R., Fralick, P. & Liang, L. Identification of an Archean marine oxygen oasis. *Precambrian Res.* **251**, 232 237 (2014).

73) Sumner, D. Y., Hawes, I., Mackey, T. J., Jungblut, A. D. & Doran, P. T. Antarctic microbial mats: A modern analog for Archean lacustrine oxygen oases. *Geology* **43**, 887-890 (2015).

74) Kosnik, M., Zardi, G. I., Nicastro, K. R., McQuaid, C. D. & Gektidis, M. Effects of Endolithic Parasitism on Invasive and Indigenous Mussels in a Variable Physical Environment. *PLoS ONE* **4**, e6560 (2009).

75) Tribollet, A., Godinot, C., Atkinson, M. & Langdon, C. Effects of elevated pCO2 on dissolution of coral carbonates by microbial euendoliths. *Global Biogeochem. Cycles* **23**, - GB3008 (2009).

76) Stubler, A. D., Furman, B. T. & Peterson, B. J. Effects of pCO_2 on the interaction between an excavating sponge, *Cliona varians*, and a hermatypic coral, *Porites furcata*. *Mar. Biol.* **161**, 1851-1859 (2014).

77) Bathurst, R. G. C. Boring algae, micrite envelopes and lithification of molluscan biosparites. *Geol. J.* **5**, 15-32 (1966).

78) MARGOLIS, S. & REX, R. W. Endolithic Algae and Micrite Envelope Formation in Bahamian Oölites as Revealed by Scanning Electron Microscopy. *Geological Society of America Bulletin* **82**, 843-852 (1971).

79) Torrecilla, I. A calcium signal is involved in heterocyst differentiation in the cyanobacterium *Anabaena* sp. PCC7120. *Microbiology* **150**, 3731-3739 (2004).

80) Dominguez, D. C. Calcium signaling in bacteria. *Molecular Microbiology* **54**, 291-297 (2004).

81) Ramirez-Reinat, E. L. & Garcia-Pichel, F. Prevalence of Ca^{2+}-ATPase-mediated carbonate dissolution among cyanobacterial euendoliths. *Appl. Environ. Microbiol.* **78**, 7-13 (2012).

82) Vangheluwe, P. *et al*. Ca^{2+} transport ATPase isoforms SERCA2a and SERCA2b are targeted to the same sites in the murine heart. *Cell Calcium* **34**, 457-464 (2003).

83) Lytton, J., Westlin, M. & Hanley, M. R. Thapsigargin inhibits the sarcoplasmic or endoplasmic reticulum Ca-ATPase family of calcium pumps. *J. Biol. Chem.* **266**, 17067-17071 (1991).

84) Kuhlbrandt, W. Biology, Structure and Mechanism of P-Type ATPases. *Nature* **5**, 282-295 (2004).

85) Torrecilla, I. Use of Recombinant Aequorin to Study Calcium Homeostasis and Monitor Calcium Transients in Response to Heat and Cold Shock in Cyanobacteria. *Plant Physiol.* **123**, 161-176 (2000).

86) Leganes, F., Forchhammer, K. & Fernández-Pinas, F. Role of calcium in acclimation of the cyanobacterium *Synechococcus elongatus* PCC 7942 to nitrogen starvation. *Microbiology* **155**, 25-34 (2009).

87) Jochem, F. J. Dark survival strategies in marine phytoplankton assessed by cytometric measurement of metabolic activity with fluorescein diacetate. *Mar. Biol.* **135**, 721-728 (1999).

88) Latour, D., Sabido, O., Salençon, M. & Giraudet, H. Dynamics and metabolic activity of the benthic cyanobacterium *Microcystis aeruginosa* in the Grangent reservoir (France). *Journal of Plankton Research* **26**, 719-726 (2004).

89) Booth, I. R. Regulation of cytoplasmic pH in bacteria. *Microbiol. Rev.* **49**, 359-378 (1985).

90) Kallas, T. & Dahlquist, F. W. Phosphorus-31 nuclear magnetic resonance analysis of internal pH during photosynthesis in the cyanobacterium *Synechococcus*. *Biochemistry (N. Y.)* **20**, 5900-5907 (1981).

91) Schirrmeister, B. E., de Vos, J. M., Antonelli, A. & Bagheri, H. C. Evolution of multicellularity coincided with increased diversification of cyanobacteria and the Great Oxidation Event. *Proceedings of the National Academy of Sciences* **110**, 1791-1796 (2013).

92) Provasoli, L. Media and prospects for the cultivation of marine algae. *Japanese Society of Plant Physiology*, 63-75 (1966).

93) Schlösser, U. G. Sammlung von Algenkulturen. *Berichte der Deutschen Botanischen Gesellschaft* **95**, 181-276 (1982).

94) Diaper, J. P. & Edwards, C. The use of fluorogenic esters to detect viable bacteria by flow cytometry. *J. Appl. Bacteriol.* **77**, 221-228 (1994).

95) Collins, T. ImageJ for microscopy. *BioTechniques* **43**, S25-S30 (2007).

96) Rajdev, S. & Reynolds, I. J. Calcium green-5N, a novel fluorescent probe for monitoring high intracellular free Ca^{2+} concentrations associated with glutamate excitotoxicity in cultured rat brain neurons. *Neuroscience Letters* **162**, 149-152 (1993).

97) Csordas, G. & Hajnoczky, G. Sorting of calcium signals at the junctions of endoplasmic reticulum and mitochondria. *Cell Calcium* **29**, 249-262 (2001).

98) Li, C. & Lee, C. An Iterative Algorithm for Minimum Cross Entropy Thresholding. *Pattern Recognition Letters* **18(8)**, 771-776 (1998).

99) Corvini, P. F. X. *et al*. Intracellular pH determination of pristinamycin-producing *Streptomyces pristinaespiralis* by image analysis. *Microbiology* **146**, 2671-2678 (2000).

100) Ridgwell, A. & Zeebe, R. The role of the global carbonate cycle in the regulation and evolution of the Earth system. *Earth Planet. Sci. Lett.* **234**, 299-315 (2005).

101) Fuchs, G. Alternative Pathways of Carbon Dioxide Fixation: Insights into the Early Evolution of Life. *Annu. Rev. Microbiol.* **65**, 631-658 (2011).

102) Hügler, M. & Sievert, S. M. Beyond the Calvin Cycle: Autotrophic Carbon Fixation in the Ocean. *Annual Review of Marine Science* **3**, 261-289 (2011).

103) Sigler, W. V., Bachofen, R. & Zeyer, J. Molecular characterization of endolithic cyanobacteria inhabiting exposed dolomite in central Switzerland. *Environ. Microbiol.* **5**, 618-627 (2003).

104) Guida, B. & Garcia-Pichel, F. Extreme cellular adaptations and cell differentiation required by a cyanobacterium for carbonate excavation. *Proceedings of the National Academy of Sciences* **In Press,** (2016).

105) Hayes, J. M. Fractionation of Carbon and Hydrogen Isotopes in Biosynthetic Processes. *Reviews in Mineralogy and Geochemistry* **43**, 225-277 (2001).

106) Young, J. D., Shastri, A. A., Stephanopoulos, G. & Morgan, J. A. Mapping photoautotrophic metabolism with isotopically nonstationary (13)C flux analysis. *Metab. Eng.* **13**, 656-665 (2011).

107) Zanden, M. J. V., Casselman, J. M. & Rasmussen, J. B. Stable isotope evidence for the food web consequences of species invasions in lakes. *Nature* **401**, 464 (1999).

108) Cuna, S., Pop, D. & Hosu, A. Carbon and Oxygen Isotope Ratios in Rona Limestone, Romania. *Studia Universitatis Babes-Bolyai, Geologia* **46**, 139-152 (2001).

109) Summerfield, T. C. & Sherman, L. A. Global Transcriptional Response of the Alkali-Tolerant Cyanobacterium *Synechocystis* sp. Strain PCC 6803 to a pH 10 Environment. *Appl. Environ. Microbiol.* **74**, 5276-5284 (2008).

110) Møgelhøj, M., Hansen, P., Henriksen, P. & Lundholm, N. High pH and not allelopathy may be responsible for negative effects of *Nodularia spumigena* on other algae. *Aquat. Microb. Ecol.* **43**, 43-54 (2006).

111) Roeske, C. A. & O'Leary, M. H. Carbon isotope effect on carboxylation of ribulose bisphosphate catalyzed by ribulose bisphosphate carboxylase from *Rhodospirillum rubrum*. *Biochemistry* **24**, 1603-1607 (1985).

112) O'Leary, M. H. Measurement of the isotope fractionation associated with diffusion of carbon dioxide in aqueous solution. *J. Phys. Chem.* **88**, 823-825 (1984).

113) David R. Kobluk, M. J. R. Calcification of Exposed Filaments of Endolithic Algae, Micrite Envelope Formation and Sediment Production. *SEPM Journal of Sedimentary Research* **Vol. 47** (1977).

114) Ian G. MacIntyre. Distribution of Submarine Cements in a Modern Caribbean Fringing Reef, Galeta Point, Panama. *SEPM Journal of Sedimentary Research* **Vol. 47**, 503-516 (1977).

115) González, L.,A, Ruiz, H.,M, Taggart, B.,E, Budd, A.,F & Monell, V. Geology of Isla De Mona, Puerto Rico. *Developments in Sedimentology* **54**, 327-358 (1997).

116) Eppley, R. W., Holmes, R. W. & Strickland, J. D. H. Sinking rates of marine phytoplankton measured with a fluorometer. *J. Exp. Mar. Biol. Ecol.* **1**, 191-208 (1967).

117) Spurr, A. R. A low-viscosity epoxy resin embedding medium for electron microscopy. *J. Ultrastruct. Res.* **26**, 31-43 (1969).

118) Hillion, F., Kilburn.M.R., Hoppe, P., Messenger, S. & Weber, P. K. The effect of QSA on S, C, O and Si isotopic ratio measurements. *Geochimica et Cosmochimica Acta.* **72**, A377 (2008).

119) Shachak, M., Jones, C. G. & Granot, Y. Herbivory in rocks and the weathering of a desert. *Mar.Geol.*, 1098-1099 (1987).

120) Le Campion-Alsumard, T., Golubic, S. & Hutchings, P. Microbial endoliths in skeletons of live and dead corals: *Porites lobata* (Moorea,French Polynesia). *Marine Ecology Progress Series* **117**, 149-157 (1995).

121) Webb, S. C. & Korrûbel, J. L. Shell weakening in marine mytilids attributable to blue-green alga *Mastigocoleus* sp (Nostochopsidaceae). *Journal of Shellfish Research*, 11-17 (1994).

122) Koren, S., Treangen, T. J., Hill, C. M., Pop, M. & Phillippy, A. M. Automated ensemble assembly and validation of microbial genomes. *BMC Bioinformatics* **15**, 126-2105-15-126 (2014).

123) Treangen, T. J. *et al*. MetAMOS: a metagenomic assembly and analysis pipeline for AMOS. *Genome Biol.* **12**, P25 (2011).

124) Kearse, M. *et al*. Geneious Basic: an integrated and extendable desktop software platform for the organization and analysis of sequence data. *Bioinformatics* **28**, 1647-1649 (2012).

125) Boetzer, M. & Pirovano, W. SSPACE-LongRead: scaffolding bacterial draft genomes using long read sequence information. *BMC Bioinformatics* **15**, 211 (2014).

126) Angiuoli, S. V. *et al*. Toward an online repository of Standard Operating Procedures (SOPs) for (meta)genomic annotation. *OMICS* **12**, 137-141 (2008).

127) Medema, M. H. *et al*. antiSMASH: rapid identification, annotation and analysis of secondary metabolite biosynthesis gene clusters in bacterial and fungal genome sequences. *Nucleic Acids Res.* **39**, W339-46 (2011).

128) Akob, D. M. & Küsel, K. Where microorganisms meet rocks in the Earth's Critical Zone. *Biogeosciences* **8**, 3531 3543 (2011).

129) Bartrons, M., Catalan, J. & Casamayor, E. O. High bacterial diversity in epilithic biofilms of oligotrophic mountain lakes. *Microb. Ecol.* **64**, 860-869 (2012).

130) Soudry, D. & Nathan, Y. Microbial infestation: a pathway of fluorine enrichment in bone apatite fragments (Negev phosphorites, Israel). *Sediment. Geol.* **132**, 171 176 (2000).

131) Zhang, X. & Pratt, B. R. Microborings in Early Cambrian phosphatic and phosphatized fossils. *Palaeogeogr. , Palaeoclimatol. , Palaeoecol.* **267**, 185 195 (2008).

132) Walton, A. W. Microtubules in basalt glass from Hawaii Scientific Driling Project #2 phase 1 core and Hilina slope, Hawaii: evidence of the occurrence and behavior of endolithic microorganisms. *Geobiology* **6**, 351-364 (2008).

133) Furnes, H. *et al*. Comparing petrographic signatures of bioalteration in recent to Mesoarchean pillow lavas: Tracing subsurface life in oceanic igneous rocks. *Precambrian Res.* **158**, 156 176 (2007).

134) Martel, J., Young, D., Peng, H., Wu, C. & Young, J. D. Biomimetic Properties of Minerals and the Search for Life in the Martian Meteorite ALH84001. *Annu. Rev. Earth Planet. Sci.* **40**, 167 193 (2012).

135) Wierzchos, J. *et al*. Adaptation strategies of endolithic chlorophototrophs to survive the hyperarid and extreme solar radiation environment of the Atacama Desert. *Front. Microbiol.* **6**, 934 (2015).

136) Cockell, C. S. & Herrera, A. Why are some microorganisms boring? *Trends Microbiol.* **16**, 101-106 (2008).

137) Ionov, D. & Harmer, R. E. Trace element distribution in calcite–dolomite carbonatites from Spitskop: inferences for differentiation of carbonatite magmas and the origin of carbonates in mantle xenoliths. *Earth Planet. Sci. Lett.* **198**, 495 510 (2002).

138) Vander Putten, E., Dehairs, F., André, L. & Baeyens, W. Quantitative in situ microanalysis of minor and trace elements in biogenic calcite using infrared laser ablation – inductively coupled plasma mass spectrometry: a critical evaluation. *Anal. Chim. Acta* **378**, 261-272 (1999).

139) Kass, G. E. & Orrenius, S. Calcium signaling and cytotoxicity. *Environ. Health Perspect.* **107**, 25-35 (1999).

140) Guida, B. S. & Garcia-Pichel, F. Draft Genome Assembly of a Filamentous Euendolithic (True Boring) Cyanobacterium, *Mastigocoleus testarum* Strain BC008. *Genome Announc* **4**, 10.1128/genomeA.01574-15 (2016).

141) Betts, J. C., Lukey, P. T., Robb, L. C., McAdam, R. A. & Duncan, K. Evaluation of a nutrient starvation model of *Mycobacterium tuberculosis* persistence by gene and protein expression profiling. *Mol. Microbiol.* **43**, 717-731 (2002).

142) Min, K. T., Hilditch, C. M., Diederich, B., Errington, J. & Yudkin, M. D. Sigma F, the first compartment-specific transcription factor of *B. subtilis*, is regulated by an anti-sigma factor that is also a protein kinase. *Cell* **74**, 735-742 (1993).

143) Imamura, S. & Asayama, M. Sigma factors for cyanobacterial transcription. *Gene Regul. Syst. Bio* **3**, 65-87 (2009).

144) Paget, M. S. & Helmann, J. D. The sigma70 family of sigma factors. *Genome Biol.* **4**, 203 (2003).

145) Takahashi, Y., Yamaguchi, O. & Omata, T. Roles of CmpR, a LysR family transcriptional regulator, in acclimation of the cyanobacterium *Synechococcus* sp. strain PCC 7942 to low-CO(2) and high-light conditions. *Mol. Microbiol.* **52**, 837-845 (2004).

146) Ricci, S., Janulczyk, R. & Bjorck, L. The regulator PerR is involved in oxidative stress response and iron homeostasis and is necessary for full virulence of Streptococcus pyogenes. *Infect. Immun.* **70**, 4968-4976 (2002).

147) Peter, E., Wallner, T., Wilde, A. & Grimm, B. Comparative functional analysis of two hypothetical chloroplast open reading frames (ycf) involved in chlorophyll biosynthesis from *Synechocystis* sp. PCC6803 and plants. *J. Plant Physiol.* **168**, 1380-1386 (2011).

148) Hong, S. K., Kito, M., Beppu, T. & Horinouchi, S. Phosphorylation of the AfsR product, a global regulatory protein for secondary-metabolite formation in Streptomyces coelicolor A3(2). *J. Bacteriol.* **173**, 2311-2318 (1991).

149) Lamark, T., Rokenes, T. P., McDougall, J. & Strom, A. R. The complex bet promoters of Escherichia coli: regulation by oxygen (ArcA), choline (BetI), and osmotic stress. *J. Bacteriol.* **178**, 1655-1662 (1996).

150) Ronson, C. W., Astwood, P. M., Nixon, B. T. & Ausubel, F. M. Deduced products of C4-dicarboxylate transport regulatory genes of *Rhizobium leguminosarum* are homologous to nitrogen regulatory gene products. *Nucleic Acids Res.* **15**, 7921-7934 (1987).

151) Linhartová, I. *et al*. RTX proteins: a highly diverse family secreted by a common mechanism. *FEMS Microbiol. Rev.* **34**, 1076-1112 (2010).

152) Geiß, U. The iron-regulated isiA gene of *Fischerella muscicola* strain PCC 73103 is linked to a likewise regulated gene encoding a Pcb-like chlorophyll-binding protein. *FEMS Microbiol. Lett.* **197**, 123 129 (2001).

153) Schultz, J. E. & Weaver, P. F. Fermentation and anaerobic respiration by *Rhodospirillum rubrum* and *Rhodopseudomonas capsulata*. *J. Bacteriol.* **149**, 181-190 (1982).

154) Roa Engel, C. A., Straathof, A. J., Zijlmans, T. W., van Gulik, W. M. & van der Wielen, L. A. Fumaric acid production by fermentation. *Appl. Microbiol. Biotechnol.* **78**, 379-389 (2008).

155) Utsugi, J., Inaba, K., Kuroda, T., Tsuda, M. & Tsuchiya, T. Cloning and sequencing of a novel Na+/H+ antiporter gene from *Pseudomonas aeruginosa*. *Biochim. Biophys. Acta* **1398**, 330-334 (1998).

156) Tsunekawa, K. *et al*. Identification and characterization of the $Na^{+/}H^{+}$ antiporter Nhas3 from the thylakoid membrane of *Synechocystis* sp. PCC 6803. *J. Biol. Chem.* **284**, 16513-16521 (2009).

157) Shibata, M. *et al*. Genes essential to sodium-dependent bicarbonate transport in cyanobacteria: function and phylogenetic analysis. *J. Biol. Chem.* **277**, 18658-18664 (2002).

158) Price, G. D. & Howitt, S. M. The cyanobacterial bicarbonate transporter BicA: its physiological role and the implications of structural similarities with human SLC26 transporters. *Biochem. Cell Biol.* **89**, 178-188 (2011).

159) Lindell, D. & Post, A. F. Ecological aspects of ntcA gene expression and its use as an indicator of the nitrogen status of marine *Synechococcus* spp. *Appl. Environ. Microbiol.* **67**, 3340-3349 (2001).

160) Song, H. & Lee, S. Y. Production of succinic acid by bacterial fermentation. *Enzyme and Microbial Technology*, 352-361 (2006).

161) Ferry, J. G. CO dehydrogenase. *Annu. Rev. Microbiol.* **49**, 305-333 (1995).

162) Furdui, C. & Ragsdale, S. W. The role of pyruvate ferredoxin oxidoreductase in pyruvate synthesis during autotrophic growth by the Wood-Ljungdahl pathway. *J. Biol. Chem.* **275**, 28494-28499 (2000).

163) Diender, M., Stams, A. J. M. & Sousa, D. Z. Pathways and Bioenergetics of Anaerobic Carbon Monoxide Fermentation. *Frontiers in Microbiology* **6** (2015).

164) Buckel, W. & Thauer, R. K. Energy conservation via electron bifurcating ferredoxin reduction and proton/Na(+) translocating ferredoxin oxidation. *Biochim. Biophys. Acta* **1827**, 94-113 (2013).

165) Wray, J. W. & Abeles, R. H. The methionine salvage pathway in *Klebsiella pneumoniae* and rat liver. Identification and characterization of two novel dioxygenases. *J. Biol. Chem.* **270**, 3147-3153 (1995).

166) Hino, S. & Tauchi, H. Production of carbon monoxide from aromatic amino acids by *Morganella morganii*. *Arch. Microbiol.* **148**, 167 171 (1987).

167) Menon, S. & Ragsdale, S. W. Evidence that carbon monoxide is an obligatory intermediate in anaerobic acetyl-CoA synthesis. *Biochemistry* **35**, 12119-12125 (1996).

168) Bar-Even, A. Does acetogenesis really require especially low reduction potential? *Biochim. Biophys. Acta* **1827**, 395-400 (2013).

169) Kelkar, D. A. & Chattopadhyay, A. The gramicidin ion channel: A model membrane protein. *Biochimica et Biophysica Acta (BBA) - Biomembranes* **1768**, 2011 2025 (2007).

170) Fiser, R. *et al*. Third activity of *Bordetella* adenylate cyclase (AC) toxin-hemolysin. Membrane translocation of AC domain polypeptide promotes calcium influx into CD11b+ monocytes independently of the catalytic and hemolytic activities. *J. Biol. Chem.* **282**, 2808-2820 (2007).

171) Koschinski, A. *et al*. Why *Escherichia coli* alpha-hemolysin induces calcium oscillations in mammalian cells--the pore is on its own. *FASEB J.* **20**, 973-975 (2006).

172) Drickamer, K. C-type lectin-like domains. *Curr. Opin. Struct. Biol.* **9**, 585 590 (1999).

173) De Reggi, M. Lithostathine, the Presumed Pancreatic Stone Inhibitor, Does Not Interact Specifically with Calcium Carbonate Crystals. *J. Biol. Chem.* **273**, 4967 4971 (1998).

174) Schnetkamp, P. P. The SLC24 Na^+/Ca^{2+}-K^+ exchanger family: vision and beyond. *Pflugers Arch.* **447**, 683-688 (2004).

175) Boehm, M. *et al*. Subunit composition of CP43-less photosystem II complexes of *Synechocystis* sp. PCC 6803: implications for the assembly and repair of photosystem II. *Philos. Trans. R. Soc. Lond. B. Biol. Sci.* **367**, 3444-3454 (2012).

176) Muhlenhoff, U., Haehnel, W., Witt, H. & Herrmann, R. G. Genes encoding eleven subunits of photosystem I from the thermophilic cyanobacterium *Synechococcus* sp. *Gene* **127**, 71-78 (1993).

177) Kos, P. B., Deak, Z., Cheregi, O. & Vass, I. Differential regulation of psbA and psbD gene expression, and the role of the different D1 protein copies in the cyanobacterium *Thermosynechococcus elongatus* BP-1. *Biochim. Biophys. Acta* **1777**, 74-83 (2008).

178) Sander, J. *et al*. Functional characterization and quantification of the alternative PsbA copies in *Thermosynechococcus elongatus* and their role in photoprotection. *J. Biol. Chem.* **285**, 29851-29856 (2010).

179) De Marchi, U., Thevenet, J., Hermant, A., Dioum, E. & Wiederkehr, A. Calcium co-regulates oxidative metabolism and ATP synthase-dependent respiration in pancreatic beta cells. *J. Biol. Chem.* **289**, 9182-9194 (2014).

180) Borisov, V. B., Gennis, R. B., Hemp, J. & Verkhovsky, M. I. The cytochrome bd respiratory oxygen reductases. *Biochim. Biophys. Acta* **1807**, 1398-1413 (2011).

181) Cooper, C. E. & Brown, G. C. The inhibition of mitochondrial cytochrome oxidase by the gases carbon monoxide, nitric oxide, hydrogen cyanide and hydrogen sulfide: chemical mechanism and physiological significance. *J. Bioenerg. Biomembr.* **40**, 533-539 (2008).

182) Matthey, U., Kaim, G. & Dimroth, P. Subunit c from the sodium-ion-translocating F1F0-ATPase of *Propionigenium modestum*--production, purification and properties of the protein in dodecylsulfate solution. *Eur. J. Biochem.* **247**, 820-825 (1997).

183) Kaim, G. & Dimroth, P. Formation of a functionally active sodium-translocating hybrid F1F0 ATPase in *Escherichia coli* by homologous recombination. *Eur. J. Biochem.* **218**, 937-944 (1993).

184) Muller, V., Aufurth, S. & Rahlfs, S. The Na(+) cycle in *Acetobacterium woodii*: identification and characterization of a Na(+) translocating F(1)F(0)-ATPase with a mixed oligomer of 8 and 16 kDa proteolipids. *Biochim. Biophys. Acta* **1505**, 108-120 (2001).

185) Neumann, S., Matthey, U., Kaim, G. & Dimroth, P. Purification and properties of the F1F0 ATPase of *Ilyobacter tartaricus*, a sodium ion pump. *J. Bacteriol.* **180**, 3312-3316 (1998).

186) Dibrova, D. V., Galperin, M. Y. & Mulkidjanian, A. Y. Characterization of the N-ATPase, a distinct, laterally transferred Na^+-translocating form of the bacterial F-type membrane ATPase. *Bioinformatics* **26**, 1473-1476 (2010).

187) Becher, B., Muller, V. & Gottschalk, G. N5-methyl-tetrahydromethanopterin:coenzyme M methyltransferase of *Methanosarcina* strain Go1 is an Na(+)-translocating membrane protein. *J. Bacteriol.* **174**, 7656-7660 (1992).

188) Dutzler, R. *et al*. A New Type of Na+-Driven ATP Synthase Membrane Rotor with a Two-Carboxylate Ion-Coupling Motif. *PLoS Biology* **11**, e1001596 (2013).

189) Shi, T., Ilikchyan, I., Rabouille, S. & Zehr, J. P. Genome-wide analysis of diel gene expression in the unicellular N(2)-fixing cyanobacterium *Crocosphaera watsonii* WH 8501. *ISME J.* **4**, 621-632 (2010).

190) Bar-Even, A., Noor, E. & Milo, R. A survey of carbon fixation pathways through a quantitative lens. *J. Exp. Bot.* **63**, 2325-2342 (2012).

191) Bolger, A. M., Lohse, M. & Usadel, B. Trimmomatic: a flexible trimmer for Illumina sequence data. *Bioinformatics* **30**, 2114-2120 (2014).

192) Langmead, B. & Salzberg, S. L. Fast gapped-read alignment with Bowtie 2. *Nat. Methods* **9**, 357-359 (2012).

193) Love, M., Huber, W. & Anders, S. Moderated estimation of fold change and dispersion for RNA-seq data with DESeq2. *Genome Biology* **15**, 550 (2014).

194) Seemann, T. Prokka: rapid prokaryotic genome annotation. *Bioinformatics* **30**, 2068-2069 (2014).

APPENDIX A

DATA COLLECTED FEBRUARY 2016

All annotated genes, Average Normalized Expression, and Log_2 Fold changes relative to euendolithic growth

Locus Tag	Ave NME	FC	Locus Tag	Ave NME	FC	Locus Tag	Ave NME	FC
BC008_00001	852	-1.7	BC008_02326	1046	0.4	BC008_04646	507	4.6
BC008_00002	799	-1.0	BC008_02327	1422	1.5	BC008_04647	159	2.7
BC008_00003	628	-0.8	BC008_02328	277	0.7	BC008_04648	589	-2.0
BC008_00004	493	-1.6	BC008_02329	1382	0.4	BC008_04649	4303	1.1
BC008_00005	77782	-5.7	BC008_02330	154	2.4	BC008_04650	3941	-1.2
BC008_00006	200	0.2	BC008_02331	218	1.4	BC008_04651	995	1.8
BC008_00007	2001	2.3	BC008_02332	638	-1.0	BC008_04652	1033	0.1
BC008_00008	1967	-0.8	BC008_02333	96	1.7	BC008_04653	1191	-0.5
BC008_00009	1625	-1.1	BC008_02334	624	2.5	BC008_04654	2679	-0.2
BC008_00010	860	0.1	BC008_02335	1928	3.1	BC008_04655	225	2.0
BC008_00011	5673	-3.4	BC008_02336	47066	-5.6	BC008_04656	4436	-0.2
BC008_00012	33	4.2	BC008_02337	2659	2.0	BC008_04657	1049	-0.1
BC008_00013	3565	1.4	BC008_02338	294	-2.3	BC008_04658	1641	-0.1
BC008_00014	3708	-2.5	BC008_02339	10701	0.5	BC008_04659	827	1.4
BC008_00015	2093	3.5	BC008_02340	2182	2.6	BC008_04660	2793	-1.6
BC008_00016	1005	1.2	BC008_02341	823	0.2	BC008_04661	633	-2.3
BC008_00017	12962	-3.3	BC008_02343	18845	-3.3	BC008_04662	4025	3.1
BC008_00018	503	-2.2	BC008_02344	249	1.9	BC008_04663	1331	-0.4
BC008_00019	598	0.6	BC008_02345	590	-1.3	BC008_04664	2569	-3.3
BC008_00020	518	1.1	BC008_02346	5372	-2.1	BC008_04665	2399	-1.7
BC008_00021	104	1.0	BC008_02347	2679	1.8	BC008_04666	2505	-4.7
BC008_00022	2081	-1.0	BC008_02348	2258	1.8	BC008_04667	1529	-2.8
BC008_00023	479	2.3	BC008_02349	652	0.9	BC008_04668	620	0.8
BC008_00024	7648	-2.4	BC008_02350	1009	0.6	BC008_04669	3848	-4.4
BC008_00025	1627	-0.5	BC008_02351	1335	2.3	BC008_04670	40683	-1.0
BC008_00026	230	1.9	BC008_02352	517	2.8	BC008_04671	27325	-3.6
BC008_00027	94	3.0	BC008_02353	687	3.5	BC008_04672	1244	-1.2
BC008_00028	206	0.2	BC008_02354	521	2.8	BC008_04673	1240	0.0
BC008_00029	718	-1.8	BC008_02355	343	-0.5	BC008_04674	1466	2.0
BC008_00030	2062	-1.2	BC008_02356	471	-1.2	BC008_04675	268	6.2
BC008_00031	2773	0.5	BC008_02357	194	-0.4	BC008_04676	105	5.3
BC008_00032	854	4.0	BC008_02358	17586	-3.0	BC008_04677	62	2.3
BC008_00033	2693	4.8	BC008_02359	2616	-1.0	BC008_04678	98	2.3
BC008_00034	1537	4.5	BC008_02360	3154	-0.2	BC008_04679	331	-0.5
BC008_00035	441	0.3	BC008_02361	235	0.9	BC008_04680	559	-0.6
BC008_00036	234	2.9	BC008_02362	1430	-4.2	BC008_04681	410	-2.4

BC008_00037	104	1.1	BC008_02363	739	-2.1	BC008_04682	241	1.6
BC008_00038	201	3.3	BC008_02364	326	-1.7	BC008_04683	48	-1.1
BC008_00039	194	4.2	BC008_02365	1017	-0.3	BC008_04684	5210	2.4
BC008_00040	139	1.4	BC008_02366	828	-0.7	BC008_04685	1023	0.5
BC008_00041	135	3.4	BC008_02367	1630	-2.3	BC008_04686	3437	-0.4
BC008_00042	599	1.7	BC008_02368	3759	-2.7	BC008_04687	192	3.6
BC008_00043	160	1.8	BC008_02369	184	5.6	BC008_04688	300	3.1
BC008_00044	481	1.9	BC008_02370	3917	3.8	BC008_04689	562	-2.2
BC008_00045	244	0.7	BC008_02371	35	1.3	BC008_04690	1400	-2.6
BC008_00046	599	1.4	BC008_02372	210	2.5	BC008_04691	1373	-2.1
BC008_00047	431	2.8	BC008_02373	4076	4.6	BC008_04692	2845	3.1
BC008_00048	385	3.4	BC008_02374	2562	0.5	BC008_04693	206	-0.2
BC008_00049	813	3.0	BC008_02375	6651	0.0	BC008_04694	2319	0.0
BC008_00050	111	4.5	BC008_02376	745	0.1	BC008_04695	1800	4.4
BC008_00051	1268	1.6	BC008_02377	1419	-1.3	BC008_04696	881	-0.5
BC008_00052	306	0.7	BC008_02378	371	0.9	BC008_04697	111	3.2
BC008_00053	75	1.0	BC008_02379	213	0.9	BC008_04698	308	4.1
BC008_00054	990	-0.1	BC008_02380	888	-0.1	BC008_04699	281	7.5
BC008_00055	2253	-2.5	BC008_02381	562	-1.8	BC008_04700	569	7.0
BC008_00056	2127	-1.3	BC008_02382	45	2.6	BC008_04701	234	6.5
BC008_00057	1336	-0.3	BC008_02383	21497	-5.5	BC008_04702	88	3.9
BC008_00058	3305	-1.6	BC008_02384	9976	-5.7	BC008_04703	1152	5.7
BC008_00059	1098	-0.4	BC008_02385	3922	-3.7	BC008_04704	228	2.8
BC008_00060	610	-0.7	BC008_02386	1161	-3.4	BC008_04705	178	5.9
BC008_00061	1170	-1.2	BC008_02387	9621	-3.7	BC008_04706	92	6.7
BC008_00062	790	-1.7	BC008_02388	13728	-3.6	BC008_04707	141	2.5
BC008_00063	3111	-3.7	BC008_02389	720	-2.1	BC008_04708	15912	-3.0
BC008_00064	194	0.7	BC008_02390	280	-0.2	BC008_04709	1762	0.1
BC008_00065	4381	-3.1	BC008_02391	1522	0.8	BC008_04710	523	0.6
BC008_00066	812	0.0	BC008_02392	4406	5.1	BC008_04711	141	4.5
BC008_00067	1183	0.0	BC008_02393	14	-0.2	BC008_04712	957	5.6
BC008_00068	295	-0.4	BC008_02394	4624	4.4	BC008_04713	631	2.3
BC008_00069	10350	-3.3	BC008_02395	298	3.7	BC008_04714	424	-0.8
BC008_00070	741	-1.3	BC008_02396	426	0.0	BC008_04715	233	0.0
BC008_00071	13192	-5.0	BC008_02397	3440	1.1	BC008_04716	262	1.7
BC008_00072	3788	-3.2	BC008_02398	241	-1.2	BC008_04717	1221	7.4
BC008_00073	6346	-0.3	BC008_02399	513	-2.0	BC008_04718	416	0.2
BC008_00074	408	0.9	BC008_02400	1489	-0.8	BC008_04719	397	0.7
BC008_00075	1075	2.5	BC008_02401	105	-1.2	BC008_04720	782	2.0

BC008_00076	67	3.1	BC008_02402	568	2.8	BC008_04721	1208	1.6
BC008_00077	1042	-0.4	BC008_02403	187	-1.1	BC008_04722	204	-1.3
BC008_00078	635	3.9	BC008_02404	2832	-3.4	BC008_04723	2375	-2.5
BC008_00079	576	5.1	BC008_02405	317	0.3	BC008_04725	263	2.4
BC008_00080	920	3.5	BC008_02406	2364	-1.4	BC008_04726	1583	0.7
BC008_00081	1219	-1.9	BC008_02407	1814	-3.2	BC008_04727	625	-0.2
BC008_00082	488	1.4	BC008_02408	1341	0.0	BC008_04728	1413	0.6
BC008_00083	68	-0.3	BC008_02409	358	-0.6	BC008_04729	908	-0.1
BC008_00084	905	-1.4	BC008_02410	320	-0.1	BC008_04730	818	1.8
BC008_00085	1287	-0.8	BC008_02411	109	0.7	BC008_04731	362	1.8
BC008_00086	5429	0.8	BC008_02412	1256	-4.6	BC008_04732	381	0.8
BC008_00087	1719	1.6	BC008_02413	7512	-4.4	BC008_04733	27	3.1
BC008_00088	6466	-0.4	BC008_02414	337	0.5	BC008_04734	4919	0.6
BC008_00089	899	1.3	BC008_02415	1881	0.8	BC008_04735	6107	-1.9
BC008_00090	3693	-1.4	BC008_02416	254	1.0	BC008_04736	58	-1.4
BC008_00091	1094	1.9	BC008_02417	861	0.3	BC008_04737	2228	0.1
BC008_00092	766	0.6	BC008_02418	452	0.0	BC008_04738	1668	1.4
BC008_00093	12172	-0.2	BC008_02419	27922	-2.1	BC008_04739	625	-0.5
BC008_00094	684	-0.8	BC008_02420	1318	1.4	BC008_04740	5886	0.1
BC008_00095	3551	-2.7	BC008_02421	2859	-2.7	BC008_04741	478	-1.8
BC008_00096	5612	0.1	BC008_02422	611	-0.2	BC008_04742	136	3.7
BC008_00097	3526	2.3	BC008_02423	1251	2.3	BC008_04743	38	0.1
BC008_00098	2128	2.6	BC008_02424	4658	-2.4	BC008_04744	24	1.4
BC008_00099	4454	1.1	BC008_02425	674	4.1	BC008_04745	158	1.1
BC008_00100	1576	-1.0	BC008_02427	2978	-1.3	BC008_04746	71	3.3
BC008_00101	3450	-2.3	BC008_02428	1107	0.3	BC008_04747	340	0.9
BC008_00102	502	-0.8	BC008_02429	2758	-1.7	BC008_04748	7786	6.6
BC008_00103	498	-0.7	BC008_02430	428	0.3	BC008_04749	317	-0.7
BC008_00104	886	3.6	BC008_02431	1617	-0.7	BC008_04750	151	1.3
BC008_00105	90	1.1	BC008_02432	1436	-0.3	BC008_04751	3216	2.4
BC008_00106	1928	7.9	BC008_02433	31937	-5.2	BC008_04752	376	0.2
BC008_00107	3091	3.8	BC008_02434	3533	-1.2	BC008_04753	1097	-1.2
BC008_00108	1368	2.0	BC008_02435	2556	-1.3	BC008_04754	457	-0.6
BC008_00109	667	1.7	BC008_02436	1440	-1.5	BC008_04755	1659	1.6
BC008_00110	771	-1.9	BC008_02437	2007	-3.1	BC008_04756	4772	-0.8
BC008_00111	1521	-3.1	BC008_02438	2988	-4.5	BC008_04757	2117	2.4
BC008_00112	14930	-4.9	BC008_02439	592	-0.2	BC008_04758	317	-1.2
BC008_00113	232	5.2	BC008_02440	2722	1.1	BC008_04759	1466	-0.2
BC008_00114	175	3.9	BC008_02441	1195	-0.9	BC008_04760	6507	-2.3

BC008_00115	208	3.4	BC008_02442	177	-0.1	BC008_04761	2348	-1.3
BC008_00116	385	-0.9	BC008_02443	426	-1.5	BC008_04762	610	-4.2
BC008_00117	280	1.9	BC008_02444	1239	-2.1	BC008_04763	2131	-2.7
BC008_00118	2377	1.4	BC008_02445	210	1.7	BC008_04764	947	1.1
BC008_00119	5452	-0.1	BC008_02446	44110	0.8	BC008_04765	45	1.4
BC008_00120	888	-1.0	BC008_02447	4027	0.3	BC008_04766	324	1.4
BC008_00121	1550	-3.7	BC008_02448	882	-1.4	BC008_04767	2737	-3.5
BC008_00122	12346	-0.3	BC008_02449	967	-0.3	BC008_04768	1606	-1.3
BC008_00123	3225	-0.1	BC008_02450	944	0.6	BC008_04769	1587	1.7
BC008_00124	4556	0.1	BC008_02451	725	2.1	BC008_04770	199	0.2
BC008_00125	4370	-2.5	BC008_02452	62	1.4	BC008_04771	1071	-0.3
BC008_00126	515	-4.1	BC008_02453	1077	2.4	BC008_04772	149	-0.3
BC008_00127	14391	-5.0	BC008_02454	645	-2.7	BC008_04773	618	2.3
BC008_00128	1205	-2.2	BC008_02455	319	0.4	BC008_04775	1354	0.3
BC008_00129	1743	-1.4	BC008_02456	2482	0.2	BC008_04776	3727	-0.9
BC008_00130	88	-0.8	BC008_02457	14448	-2.1	BC008_04777	238	1.6
BC008_00131	1381	-2.3	BC008_02458	17012	-2.7	BC008_04778	618	-0.8
BC008_00132	4045	-1.4	BC008_02459	491	-0.8	BC008_04779	1164	-0.6
BC008_00133	703	-0.5	BC008_02460	2251	-2.0	BC008_04780	4768	-0.3
BC008_00134	1354	-2.5	BC008_02461	36367	-4.6	BC008_04781	400	-0.7
BC008_00135	613	-2.4	BC008_02462	3876	-2.1	BC008_04782	788	-0.7
BC008_00136	163	1.7	BC008_02463	4534	-4.1	BC008_04783	618	-1.5
BC008_00137	35	0.6	BC008_02464	20513	-4.2	BC008_04784	1864	-2.5
BC008_00138	658	-1.0	BC008_02465	1366	2.5	BC008_04785	1989	-3.3
BC008_00139	130	-2.5	BC008_02466	89	0.6	BC008_04786	860	-0.5
BC008_00140	321	-0.3	BC008_02467	2009	-0.3	BC008_04787	2626	-2.9
BC008_00141	697	-0.1	BC008_02468	1213	-0.6	BC008_04788	104	-1.2
BC008_00142	451	0.7	BC008_02469	1042	-1.0	BC008_04789	6282	-4.1
BC008_00143	470	-0.5	BC008_02470	123	-2.0	BC008_04790	15994	-3.9
BC008_00144	7105	3.8	BC008_02471	534	1.2	BC008_04791	1801	-0.7
BC008_00145	1454	2.5	BC008_02472	688	-0.2	BC008_04792	1559	-3.4
BC008_00146	289	1.5	BC008_02473	679	0.7	BC008_04793	8248	2.1
BC008_00147	896	3.3	BC008_02474	9138	0.1	BC008_04794	404	0.1
BC008_00148	1777	0.4	BC008_02475	3592	-1.3	BC008_04795	292	0.0
BC008_00149	307	-1.7	BC008_02476	114	1.7	BC008_04796	560	-1.1
BC008_00150	1782	-1.8	BC008_02477	860	-3.8	BC008_04797	652	3.2
BC008_00151	932	-2.6	BC008_02478	532	-0.4	BC008_04798	575	1.4
BC008_00152	1148	1.9	BC008_02479	59	2.2	BC008_04799	7276	-0.7
BC008_00153	1300	-3.4	BC008_02480	707	-1.0	BC008_04800	236	0.3

BC008_00154	557	2.5	BC008_02481	212	1.5	BC008_04801	2732	-1.5
BC008_00155	505	0.3	BC008_02482	1895	-0.4	BC008_04802	804	-0.3
BC008_00156	1854	-0.6	BC008_02483	11729	-5.7	BC008_04803	3313	-2.5
BC008_00157	188	0.2	BC008_02484	386	1.5	BC008_04804	1934	-3.0
BC008_00158	409	2.3	BC008_02485	368	-0.5	BC008_04805	1361	0.0
BC008_00159	612	-0.6	BC008_02486	924	1.8	BC008_04806	1123	0.1
BC008_00160	307	0.1	BC008_02487	509	0.4	BC008_04807	536	-0.2
BC008_00161	3464	-0.3	BC008_02488	606	-0.2	BC008_04808	676	-2.1
BC008_00162	1241	-0.8	BC008_02489	361	0.4	BC008_04809	706	-2.3
BC008_00163	2244	0.0	BC008_02490	781	1.3	BC008_04810	327	0.4
BC008_00164	2080	-0.3	BC008_02491	165	1.5	BC008_04811	556	0.6
BC008_00165	513	0.3	BC008_02492	455	4.1	BC008_04812	707	-1.9
BC008_00166	310	-0.3	BC008_02493	457	-1.0	BC008_04813	259	4.5
BC008_00167	2328	-2.6	BC008_02494	6329	-1.2	BC008_04814	376	2.2
BC008_00168	468	-2.5	BC008_02495	1065	0.3	BC008_04815	1278	-1.5
BC008_00169	307	2.0	BC008_02496	1434	-4.1	BC008_04816	1550	2.1
BC008_00170	203	-0.3	BC008_02497	72	-0.1	BC008_04817	954	-0.5
BC008_00171	3327	-2.5	BC008_02498	2342	-1.1	BC008_04818	1008	-0.2
BC008_00172	1250	-2.5	BC008_02499	2893	-1.9	BC008_04819	1076	-0.7
BC008_00173	1972	-2.3	BC008_02500	6788	-4.3	BC008_04820	17882	-5.8
BC008_00174	1132	-0.4	BC008_02501	8462	-3.9	BC008_04821	1173	-2.0
BC008_00175	963	-0.1	BC008_02502	5283	-4.0	BC008_04822	1025	0.8
BC008_00176	2214	0.8	BC008_02503	339	-2.2	BC008_04823	710	3.2
BC008_00177	4445	-0.8	BC008_02504	378	-1.3	BC008_04824	473	1.4
BC008_00178	89	0.9	BC008_02505	1073	1.6	BC008_04825	880	1.7
BC008_00179	1557	0.1	BC008_02506	5903	-3.7	BC008_04826	2017	0.5
BC008_00180	90	0.1	BC008_02507	319	-3.1	BC008_04827	1181	1.7
BC008_00181	344	-0.6	BC008_02508	1045	-1.4	BC008_04828	7156	-0.3
BC008_00182	2848	-1.0	BC008_02509	1801	1.8	BC008_04829	1987	-0.1
BC008_00183	2456	2.1	BC008_02510	1598	-2.2	BC008_04830	238	0.3
BC008_00184	710	1.6	BC008_02511	403	1.6	BC008_04831	1382	1.1
BC008_00185	1321	-1.9	BC008_02512	2658	-1.9	BC008_04832	15058	2.5
BC008_00186	1900	-0.7	BC008_02513	3799	-2.5	BC008_04833	6213	-2.7
BC008_00187	2190	-2.5	BC008_02514	159	2.2	BC008_04834	3051	-1.1
BC008_00188	1092	-0.3	BC008_02515	1874	3.6	BC008_04835	1074	0.6
BC008_00189	37628	-4.6	BC008_02516	612	0.1	BC008_04836	598	-1.1
BC008_00190	286	1.6	BC008_02517	810	2.6	BC008_04837	354	-0.9
BC008_00191	993	1.8	BC008_02518	2845	1.5	BC008_04838	110	0.0
BC008_00192	1501	-1.1	BC008_02519	495	-1.9	BC008_04839	252	2.0

BC008_00193	28	4.1	BC008_02520	323	-1.6	BC008_04840	3348	0.7
BC008_00194	650	-0.8	BC008_02521	738	2.1	BC008_04841	3387	2.4
BC008_00195	531	2.1	BC008_02522	387	6.0	BC008_04842	429	3.2
BC008_00196	147	3.2	BC008_02523	438	5.5	BC008_04843	466	-0.7
BC008_00197	374	0.8	BC008_02524	42	4.3	BC008_04844	4167	-0.1
BC008_00198	5499	5.9	BC008_02525	20	2.9	BC008_04845	816	0.7
BC008_00199	1291	-0.6	BC008_02526	352	3.3	BC008_04846	2116	5.1
BC008_00200	2676	-4.7	BC008_02527	265	3.0	BC008_04847	771	1.5
BC008_00201	2818	-0.6	BC008_02528	5296	-1.4	BC008_04848	961	1.5
BC008_00202	5695	5.4	BC008_02529	1888	-1.4	BC008_04849	1249	-2.1
BC008_00203	42	1.1	BC008_02530	613	2.5	BC008_04850	1063	-1.9
BC008_00204	244	2.5	BC008_02531	468	-1.4	BC008_04851	273	-0.4
BC008_00205	296	3.0	BC008_02532	38	-0.1	BC008_04852	459	-0.6
BC008_00206	494	-0.1	BC008_02533	1319	5.9	BC008_04853	575	2.7
BC008_00207	169	0.0	BC008_02534	429	0.9	BC008_04854	2333	-0.9
BC008_00208	1141	0.7	BC008_02535	1055	-3.6	BC008_04855	5777	-2.8
BC008_00209	325	-2.2	BC008_02536	1411	-0.7	BC008_04856	1533	-3.2
BC008_00210	2771	0.0	BC008_02537	982	-0.2	BC008_04857	2669	4.8
BC008_00211	721	-1.1	BC008_02538	529	2.3	BC008_04858	259	0.3
BC008_00212	1600	0.7	BC008_02539	879	0.8	BC008_04859	97	0.3
BC008_00213	92	-0.4	BC008_02540	680	0.5	BC008_04860	396	3.9
BC008_00214	1088	0.6	BC008_02541	1837	-0.1	BC008_04861	1483	-1.2
BC008_00215	139	-1.1	BC008_02542	654	-2.8	BC008_04862	12272	-1.9
BC008_00216	737	4.0	BC008_02543	2256	-0.3	BC008_04863	745	-2.0
BC008_00217	2879	5.2	BC008_02544	2450	2.5	BC008_04864	2562	0.3
BC008_00218	197	0.2	BC008_02545	2304	4.5	BC008_04865	62	2.0
BC008_00219	1158	0.8	BC008_02546	1096	2.4	BC008_04866	1178	0.6
BC008_00220	1640	4.4	BC008_02547	150	0.0	BC008_04867	439	0.5
BC008_00221	5655	3.1	BC008_02548	8214	-0.2	BC008_04868	1024	-0.1
BC008_00222	1454	4.6	BC008_02549	4366	2.6	BC008_04869	1054	-1.0
BC008_00223	2535	-3.2	BC008_02550	3314	2.6	BC008_04870	75	4.9
BC008_00224	322	0.6	BC008_02551	2377	2.6	BC008_04871	54	2.8
BC008_00225	2564	1.0	BC008_02552	862	1.0	BC008_04872	930	3.5
BC008_00226	384	0.1	BC008_02553	946	1.5	BC008_04873	368	3.3
BC008_00227	7855	1.5	BC008_02554	2028	1.3	BC008_04874	260	4.0
BC008_00228	1108	0.6	BC008_02555	2110	0.1	BC008_04875	218	5.2
BC008_00229	1002	1.1	BC008_02556	254	-0.4	BC008_04876	185	4.2
BC008_00230	538	-0.3	BC008_02557	1379	0.3	BC008_04877	3503	5.9
BC008_00231	2642	-1.2	BC008_02558	5559	-4.2	BC008_04878	1790	4.4

BC008_00233	1675	-1.1	BC008_02559	202	-4.5	BC008_04879	390	2.0
BC008_00234	31959	-3.7	BC008_02560	354	1.5	BC008_04880	3150	0.0
BC008_00235	7682	-0.8	BC008_02561	350	0.4	BC008_04881	32	3.2
BC008_00236	5119	-3.2	BC008_02562	328	-1.0	BC008_04882	685	3.9
BC008_00237	826	-1.0	BC008_02563	540	-2.2	BC008_04883	150	1.0
BC008_00238	3130	-3.2	BC008_02564	641	-0.3	BC008_04884	173	1.5
BC008_00239	2176	-2.5	BC008_02565	438	0.0	BC008_04885	746	3.0
BC008_00240	11252	-1.9	BC008_02566	230	0.5	BC008_04886	59	0.8
BC008_00241	2620	0.7	BC008_02567	62	0.1	BC008_04887	429	0.6
BC008_00242	516	-2.9	BC008_02568	588	-0.1	BC008_04888	472	0.8
BC008_00243	1352	-0.7	BC008_02569	2001	-1.4	BC008_04889	28	5.7
BC008_00244	1255	-1.2	BC008_02570	6603	-2.1	BC008_04890	340	-0.7
BC008_00245	1415	-3.0	BC008_02571	4365	-4.5	BC008_04891	241	3.6
BC008_00246	3527	1.5	BC008_02572	236	-2.7	BC008_04892	2563	-0.3
BC008_00247	1003	-1.3	BC008_02573	2678	-0.5	BC008_04893	2460	0.8
BC008_00248	203	-1.1	BC008_02574	3263	-2.1	BC008_04894	1075	2.7
BC008_00249	1493	-2.2	BC008_02575	36696	3.5	BC008_04895	877	1.2
BC008_00250	2430	3.3	BC008_02576	3859	-3.1	BC008_04896	556	4.7
BC008_00251	1804	1.8	BC008_02577	160	-0.6	BC008_04897	3944	1.8
BC008_00252	174	-1.3	BC008_02578	1028	-2.4	BC008_04898	832	0.4
BC008_00253	496	-0.1	BC008_02579	1495	-3.9	BC008_04899	562	4.6
BC008_00254	311	2.2	BC008_02580	487	-0.9	BC008_04900	27	1.6
BC008_00255	6527	-1.4	BC008_02581	643	-2.8	BC008_04901	970	3.2
BC008_00256	1863	0.3	BC008_02582	583	-0.2	BC008_04902	65	2.2
BC008_00257	462	-2.1	BC008_02583	5335	-2.6	BC008_04903	174	2.4
BC008_00258	140	0.5	BC008_02584	6684	-3.3	BC008_04904	8605	-0.1
BC008_00259	949	-1.1	BC008_02585	1348	-1.5	BC008_04905	4595	1.1
BC008_00260	7471	-2.5	BC008_02586	1536	-4.8	BC008_04906	707	-1.5
BC008_00261	657	1.4	BC008_02587	1304	3.9	BC008_04907	84	2.7
BC008_00262	1850	0.1	BC008_02588	1165	0.8	BC008_04908	534	2.1
BC008_00263	1729	0.7	BC008_02589	637	-0.2	BC008_04909	1212	-1.0
BC008_00264	1273	2.7	BC008_02590	9474	1.9	BC008_04910	1033	-4.1
BC008_00265	1065	-1.5	BC008_02591	143	3.5	BC008_04911	163	-1.3
BC008_00266	366	-0.8	BC008_02592	96	2.1	BC008_04912	226	2.2
BC008_00267	35787	-3.3	BC008_02593	271	2.4	BC008_04913	13334	5.0
BC008_00268	250	2.3	BC008_02594	130	3.8	BC008_04914	85	0.7
BC008_00269	847	0.6	BC008_02595	109	3.4	BC008_04915	1489	-1.7
BC008_00270	8434	-1.9	BC008_02596	341	5.8	BC008_04916	6798	0.2
BC008_00271	714	2.1	BC008_02597	113	3.8	BC008_04917	212	2.1

BC008_00272	19206	0.3	BC008_02598	2270	-1.4	BC008_04918	364	-1.6
BC008_00273	3132	-2.8	BC008_02599	915	-0.6	BC008_04919	1237	-1.1
BC008_00274	4146	-2.1	BC008_02600	134	0.2	BC008_04920	4188	-2.3
BC008_00275	7465	1.5	BC008_02601	3427	-2.8	BC008_04921	14439	-5.0
BC008_00276	400	0.7	BC008_02602	12007	-4.3	BC008_04922	663	0.1
BC008_00277	1073	0.3	BC008_02603	941	2.3	BC008_04923	1840	0.8
BC008_00278	2457	2.9	BC008_02604	190	0.8	BC008_04924	6217	-3.8
BC008_00279	4548	2.1	BC008_02605	279	0.9	BC008_04925	46752	-0.4
BC008_00280	398	0.5	BC008_02606	2224	-1.2	BC008_04926	6263	0.4
BC008_00281	71	0.0	BC008_02607	166	0.0	BC008_04927	4651	-3.0
BC008_00282	2404	4.3	BC008_02608	2516	-0.4	BC008_04928	2517	-1.1
BC008_00283	88	5.7	BC008_02609	405	0.1	BC008_04929	2469	-0.1
BC008_00284	59	3.8	BC008_02610	248	0.4	BC008_04930	921	1.0
BC008_00285	1351	-0.3	BC008_02611	842	0.5	BC008_04931	44	3.3
BC008_00286	1402	1.4	BC008_02612	1620	0.4	BC008_04932	780	1.3
BC008_00287	1136	2.7	BC008_02613	1417	6.9	BC008_04933	735	1.2
BC008_00289	1018	4.9	BC008_02614	1115	1.9	BC008_04934	151	-0.2
BC008_00290	801	-0.3	BC008_02615	467	0.2	BC008_04935	968	-2.6
BC008_00291	169	-0.6	BC008_02616	621	-0.4	BC008_04936	1507	-2.1
BC008_00292	518	-2.4	BC008_02617	892	0.3	BC008_04937	420	1.4
BC008_00293	829	3.1	BC008_02618	623	0.0	BC008_04938	442	2.0
BC008_00294	20	4.3	BC008_02619	18	2.3	BC008_04939	697	1.2
BC008_00295	677	-0.2	BC008_02620	438	-1.4	BC008_04940	2319	0.7
BC008_00296	869	0.9	BC008_02621	4730	0.4	BC008_04941	1168	-0.9
BC008_00297	11730	1.3	BC008_02622	1179	-0.9	BC008_04942	4638	-2.3
BC008_00300	1438	1.3	BC008_02623	1022	-0.5	BC008_04943	144	1.2
BC008_00301	144	-1.4	BC008_02624	9750	-2.0	BC008_04944	849	-1.7
BC008_00302	516	1.3	BC008_02625	35325	-2.4	BC008_04945	409	0.0
BC008_00303	2093	-3.0	BC008_02626	3440	0.3	BC008_04946	1893	-0.7
BC008_00304	862	0.9	BC008_02627	902	0.3	BC008_04947	2766	-2.1
BC008_00305	199	0.0	BC008_02628	5302	-2.7	BC008_04948	3068	-1.4
BC008_00306	536	-1.3	BC008_02629	2482	3.3	BC008_04949	2143	-1.3
BC008_00307	6043	-2.9	BC008_02630	4132	1.9	BC008_04950	771	-0.3
BC008_00308	6233	-2.8	BC008_02631	3462	0.0	BC008_04951	268	1.9
BC008_00309	1843	-0.9	BC008_02632	2370	-2.3	BC008_04952	623	1.6
BC008_00310	146	-1.8	BC008_02633	2101	2.1	BC008_04953	435	-0.7
BC008_00311	1845	-1.8	BC008_02634	2061	0.1	BC008_04954	22060	1.8
BC008_00312	277	6.4	BC008_02635	2007	-3.5	BC008_04955	978	1.1
BC008_00313	682	2.8	BC008_02636	1183	-1.1	BC008_04956	240	1.6

BC008_00314	158	-0.8	BC008_02637	19642	-3.6	BC008_04957	355	0.7
BC008_00315	753	-2.6	BC008_02638	1815	2.4	BC008_04958	52	0.2
BC008_00316	4211	-2.4	BC008_02639	985	-2.5	BC008_04959	1911	-1.0
BC008_00317	7648	-1.6	BC008_02640	532	2.8	BC008_04960	128	0.1
BC008_00318	256	-1.9	BC008_02641	162	3.2	BC008_04961	376	1.6
BC008_00319	42	2.1	BC008_02642	391	2.3	BC008_04962	374181	-2.1
BC008_00320	994	-1.9	BC008_02643	252	2.5	BC008_04963	989	-1.2
BC008_00321	835	-4.1	BC008_02644	336	1.9	BC008_04964	856	-0.8
BC008_00322	159	-0.5	BC008_02645	143	0.2	BC008_04965	213	1.7
BC008_00323	1920	1.7	BC008_02646	504	-2.0	BC008_04966	51	0.9
BC008_00324	1076	3.3	BC008_02647	1882	-1.2	BC008_04967	636	-0.2
BC008_00325	44	0.7	BC008_02648	4294	1.0	BC008_04968	834	-0.6
BC008_00326	3173	-1.4	BC008_02649	316	-0.4	BC008_04969	639	0.8
BC008_00327	4491	-1.4	BC008_02650	759	1.1	BC008_04970	2390	-1.2
BC008_00328	120	-1.6	BC008_02651	3017	-0.5	BC008_04971	1648	0.4
BC008_00329	7206	-2.5	BC008_02652	3723	-3.1	BC008_04972	205	0.9
BC008_00330	1454	0.3	BC008_02653	281	-0.8	BC008_04973	6618	0.2
BC008_00331	1518	0.6	BC008_02654	1386	-1.2	BC008_04974	24534	1.4
BC008_00332	2598	-0.7	BC008_02655	2210	-2.7	BC008_04975	1684	2.6
BC008_00333	1174	0.8	BC008_02656	2322	0.8	BC008_04976	470	2.9
BC008_00334	377	-2.1	BC008_02657	2920	1.7	BC008_04977	854	0.6
BC008_00336	3687	-3.5	BC008_02658	759	-0.9	BC008_04978	93	0.6
BC008_00337	14685	-3.2	BC008_02659	25055	-3.0	BC008_04979	29663	-4.3
BC008_00338	6591	-3.2	BC008_02660	2903	-1.7	BC008_04980	183026	-2.9
BC008_00339	2316	-1.4	BC008_02661	409	2.2	BC008_04981	942	-0.3
BC008_00340	13844	-3.6	BC008_02662	296	-0.6	BC008_04982	411	-2.2
BC008_00341	1466	-1.6	BC008_02663	922	-0.1	BC008_04983	693	-1.2
BC008_00342	4958	1.3	BC008_02664	1339	0.1	BC008_04984	6158	-2.3
BC008_00343	11878	-3.4	BC008_02665	1340	1.2	BC008_04985	1710	-3.5
BC008_00344	1062	0.1	BC008_02666	660	-0.6	BC008_04986	1535	1.8
BC008_00345	9388	-2.1	BC008_02667	1480	-1.6	BC008_04987	367	-0.8
BC008_00346	11592	-0.7	BC008_02668	821	5.0	BC008_04988	1124	0.1
BC008_00347	5309	-0.9	BC008_02669	886	1.0	BC008_04989	2013	5.3
BC008_00348	8468	-1.4	BC008_02670	2521	-1.9	BC008_04990	839	1.1
BC008_00349	4158	-1.4	BC008_02671	355	1.9	BC008_04991	312	3.9
BC008_00350	6380	-2.2	BC008_02672	165	0.0	BC008_04992	373	2.1
BC008_00351	11216	-5.1	BC008_02673	7359	-4.2	BC008_04993	184	1.0
BC008_00352	14249	-1.8	BC008_02674	3218	0.6	BC008_04994	603	0.2
BC008_00353	797	-0.9	BC008_02675	944	-0.4	BC008_04995	507	2.8

BC008_00354	2932	-3.5	BC008_02676	1175	-1.1	BC008_04996	408	0.2
BC008_00355	1739	3.2	BC008_02677	1118	2.6	BC008_04997	1434	0.7
BC008_00356	978	-0.9	BC008_02678	59	1.0	BC008_04998	274	1.4
BC008_00357	634	0.2	BC008_02679	86	1.8	BC008_04999	516	1.8
BC008_00358	5958	4.3	BC008_02680	1303	0.7	BC008_05000	1982	-0.2
BC008_00359	51	0.3	BC008_02681	962	-1.6	BC008_05001	523	2.3
BC008_00360	197	0.8	BC008_02682	3849	-0.4	BC008_05002	689	2.2
BC008_00361	604	0.9	BC008_02683	72	0.4	BC008_05003	410	1.7
BC008_00362	56	2.8	BC008_02684	40156	-3.4	BC008_05004	379	0.8
BC008_00363	449	0.8	BC008_02685	2212	4.1	BC008_05005	582	1.3
BC008_00364	2289	-2.3	BC008_02686	10145	-2.4	BC008_05006	101	0.9
BC008_00365	621	-1.2	BC008_02687	176	-0.3	BC008_05007	1816	1.0
BC008_00366	11038	-4.8	BC008_02688	421	-1.2	BC008_05008	271	-0.5
BC008_00367	820	-2.7	BC008_02689	7038	-1.4	BC008_05009	6474	0.1
BC008_00368	195	-2.1	BC008_02690	998	-1.2	BC008_05010	552	0.4
BC008_00369	1809	1.6	BC008_02691	253	-0.8	BC008_05011	1140	1.5
BC008_00370	480	1.8	BC008_02692	2223	-2.6	BC008_05012	79	1.4
BC008_00371	807	0.5	BC008_02693	2694	-1.8	BC008_05013	60	-0.2
BC008_00372	292	-3.5	BC008_02694	2749	-1.4	BC008_05014	522	0.2
BC008_00373	2423	-0.1	BC008_02695	1976	-1.9	BC008_05015	910	6.3
BC008_00374	70	-0.2	BC008_02696	1389	-1.2	BC008_05016	201	3.2
BC008_00375	340	-1.9	BC008_02697	678	1.0	BC008_05017	786	5.6
BC008_00376	2821	0.3	BC008_02698	4663	-4.0	BC008_05018	456	4.9
BC008_00377	4585	2.4	BC008_02699	346	-1.3	BC008_05019	771	4.2
BC008_00378	1679	-3.7	BC008_02700	1024	0.3	BC008_05020	496	-0.2
BC008_00379	1056	1.4	BC008_02702	44	1.1	BC008_05021	173	0.0
BC008_00380	2519	1.7	BC008_02703	990	0.7	BC008_05022	864	0.5
BC008_00381	1340	0.9	BC008_02704	248	4.1	BC008_05023	15574	-4.1
BC008_00382	991	-1.4	BC008_02705	591	0.5	BC008_05024	276	2.0
BC008_00383	4343	-1.8	BC008_02706	934	2.0	BC008_05025	101	1.7
BC008_00384	151	-0.6	BC008_02707	101	3.0	BC008_05026	39	3.9
BC008_00385	8163	-1.8	BC008_02708	146	2.7	BC008_05027	105	4.6
BC008_00386	1412	0.1	BC008_02709	602	-1.3	BC008_05028	258	4.2
BC008_00387	342	-1.3	BC008_02710	377	1.4	BC008_05029	61	7.2
BC008_00388	1287	-0.1	BC008_02711	1446	1.0	BC008_05030	90	1.8
BC008_00389	1971	-3.9	BC008_02712	119	-0.6	BC008_05031	59	4.5
BC008_00390	2152	0.6	BC008_02713	1672	-4.5	BC008_05032	46	5.1
BC008_00391	60058	-4.6	BC008_02714	1123	-1.7	BC008_05033	60	5.8
BC008_00392	752	-0.9	BC008_02715	1773	-2.4	BC008_05034	35	5.1

BC008_00393	844	-0.4	BC008_02716	544	0.5	BC008_05035	45	2.0
BC008_00394	48154	-5.0	BC008_02717	1377	0.4	BC008_05036	89	1.6
BC008_00395	25105	-4.7	BC008_02718	1134	1.8	BC008_05037	40	1.9
BC008_00396	7987	-2.1	BC008_02719	2559	-0.8	BC008_05038	55	6.5
BC008_00397	22520	-3.8	BC008_02720	726	0.4	BC008_05039	47	7.6
BC008_00398	65	0.9	BC008_02721	1067	-0.7	BC008_05040	130	9.2
BC008_00399	1151	-2.5	BC008_02722	2354	-1.6	BC008_05041	77	8.2
BC008_00400	38	5.9	BC008_02723	1889	-1.2	BC008_05042	91	7.3
BC008_00401	1188	-0.8	BC008_02724	563	0.0	BC008_05043	233	6.9
BC008_00402	2473	0.0	BC008_02725	555	1.0	BC008_05044	135	6.9
BC008_00403	1161	2.2	BC008_02726	1075	0.5	BC008_05045	876	8.0
BC008_00404	184	0.3	BC008_02727	362	-0.1	BC008_05046	220	7.2
BC008_00405	814	-0.7	BC008_02728	607	-0.4	BC008_05047	472	8.4
BC008_00406	2071	-0.5	BC008_02729	3286	-2.8	BC008_05048	238	8.0
BC008_00407	3627	-2.3	BC008_02730	871	-1.2	BC008_05049	154	4.5
BC008_00408	79	2.2	BC008_02731	6712	2.0	BC008_05050	415	5.0
BC008_00409	231203	-3.0	BC008_02732	557	0.6	BC008_05051	625	8.5
BC008_00410	1996	2.2	BC008_02733	2548	0.9	BC008_05052	418	7.5
BC008_00411	815	-1.1	BC008_02734	2620	-2.6	BC008_05053	337	7.8
BC008_00412	444	-0.7	BC008_02735	1737	-2.3	BC008_05054	41	6.0
BC008_00413	697	1.3	BC008_02736	1555	-2.1	BC008_05055	48	5.2
BC008_00414	393	-0.6	BC008_02737	2925	-4.2	BC008_05056	32	5.6
BC008_00415	2684	-0.4	BC008_02738	982	0.4	BC008_05057	70	6.6
BC008_00416	989	1.1	BC008_02739	1067	-2.4	BC008_05058	44	7.5
BC008_00417	491	1.5	BC008_02740	5202	0.4	BC008_05059	111	8.9
BC008_00418	1038	3.5	BC008_02741	1248	0.5	BC008_05060	149	9.4
BC008_00419	6781	2.9	BC008_02742	434	-1.0	BC008_05061	86	6.9
BC008_00420	752	-2.1	BC008_02743	763	-0.4	BC008_05062	294	8.7
BC008_00421	861	-3.1	BC008_02744	875	0.9	BC008_05063	67	7.4
BC008_00422	237	-0.2	BC008_02745	19353	-4.3	BC008_05064	100	5.7
BC008_00423	10118	3.5	BC008_02746	1198	0.8	BC008_05065	109	6.7
BC008_00424	8055	5.3	BC008_02747	1126	-2.0	BC008_05066	252	6.8
BC008_00425	1794	-0.6	BC008_02748	277	-0.6	BC008_05067	198	7.3
BC008_00426	2816	-1.3	BC008_02749	2229	-2.3	BC008_05068	70	5.4
BC008_00427	674	-0.9	BC008_02750	10122	-1.2	BC008_05069	174	6.8
BC008_00428	2699	1.4	BC008_02751	470	-1.5	BC008_05070	362	4.6
BC008_00429	1140	-1.6	BC008_02752	4375	-0.2	BC008_05071	67	1.1
BC008_00430	627	1.4	BC008_02753	2049	-1.4	BC008_05072	1227	0.5
BC008_00431	139	0.4	BC008_02754	1768	-2.5	BC008_05073	683	1.0

BC008_00432	312	-0.5	BC008_02755	5598	-4.0	BC008_05074	146	4.4
BC008_00433	75	-0.5	BC008_02756	579	-2.1	BC008_05075	809	3.8
BC008_00434	145	-1.7	BC008_02757	1304	1.2	BC008_05076	1041	3.6
BC008_00435	340	-0.2	BC008_02758	1289	-0.7	BC008_05077	100	1.2
BC008_00436	7163	-3.4	BC008_02759	448	-1.2	BC008_05078	1300	-0.5
BC008_00437	224	0.6	BC008_02760	1157	-2.4	BC008_05079	3954	-0.1
BC008_00438	252	2.5	BC008_02761	7166	3.7	BC008_05080	734	1.3
BC008_00439	502	1.4	BC008_02762	383	0.0	BC008_05081	1536	0.8
BC008_00440	973	0.7	BC008_02763	887	2.4	BC008_05082	587	1.0
BC008_00441	492	0.2	BC008_02764	342	-0.5	BC008_05083	2561	2.5
BC008_00442	340	0.4	BC008_02765	124	3.0	BC008_05084	2486	-1.0
BC008_00443	104	0.9	BC008_02766	380	3.7	BC008_05085	844	-0.9
BC008_00445	664	-0.6	BC008_02767	302	2.7	BC008_05086	1338	2.7
BC008_00446	579	0.4	BC008_02768	116	-0.2	BC008_05087	43	1.2
BC008_00447	2289	-1.6	BC008_02769	2130	-1.4	BC008_05088	1393	-2.3
BC008_00448	963	2.0	BC008_02770	2381	4.5	BC008_05089	2500	0.3
BC008_00449	939	2.7	BC008_02771	1105	-1.6	BC008_05090	1051	-1.5
BC008_00450	12267	-3.6	BC008_02772	3544	-1.5	BC008_05091	3258	-2.4
BC008_00451	223	2.8	BC008_02773	2439	-2.0	BC008_05092	2947	3.6
BC008_00452	1428	-2.0	BC008_02774	2243	-2.2	BC008_05093	61	-1.9
BC008_00453	583	0.1	BC008_02775	168	-1.3	BC008_05094	578	1.6
BC008_00454	10050	-0.6	BC008_02776	794	-1.2	BC008_05095	54	2.8
BC008_00455	4759	-1.7	BC008_02777	161	1.5	BC008_05096	854	4.5
BC008_00456	1611	-2.8	BC008_02778	1134	0.0	BC008_05097	1257	0.2
BC008_00457	14524	-2.6	BC008_02779	256	-0.2	BC008_05098	2432	-1.5
BC008_00458	2623	-1.6	BC008_02780	897	-0.5	BC008_05099	398	1.1
BC008_00459	780	-1.0	BC008_02781	262	-0.9	BC008_05100	47	6.2
BC008_00460	7403	1.6	BC008_02782	1762	-1.2	BC008_05101	201	6.6
BC008_00461	47558	-5.6	BC008_02783	205	0.9	BC008_05102	92	1.9
BC008_00462	2265	-0.6	BC008_02784	294	3.3	BC008_05103	1640	-1.8
BC008_00463	982	-2.3	BC008_02785	1287	4.1	BC008_05104	628	-1.2
BC008_00464	700	-0.7	BC008_02786	644	0.5	BC008_05105	410	-1.3
BC008_00465	779	1.3	BC008_02787	1245	0.6	BC008_05106	68	1.8
BC008_00466	777	0.8	BC008_02788	1019	3.8	BC008_05107	196	-0.3
BC008_00467	717	-0.4	BC008_02789	650	1.3	BC008_05108	284	2.0
BC008_00468	498	0.1	BC008_02790	1546	0.2	BC008_05109	409	1.3
BC008_00469	1727	6.3	BC008_02791	1525	0.3	BC008_05110	1714	-0.9
BC008_00470	3280	6.3	BC008_02792	7257	2.5	BC008_05111	546	0.3
BC008_00471	629	0.4	BC008_02793	53439	0.1	BC008_05112	86	1.8

BC008_00472	1720	-0.6	BC008_02794	201	1.8	BC008_05113	132	3.9
BC008_00473	2125	-2.7	BC008_02795	289	2.2	BC008_05114	308	2.0
BC008_00474	33	0.5	BC008_02796	1500	2.1	BC008_05115	114	4.0
BC008_00475	493	-1.0	BC008_02797	1091	3.4	BC008_05116	67	4.4
BC008_00476	2056	-1.4	BC008_02798	288	1.7	BC008_05117	110	1.4
BC008_00477	655	1.2	BC008_02799	3522	2.9	BC008_05118	110	3.7
BC008_00478	207	5.4	BC008_02800	3012	2.3	BC008_05119	672	4.3
BC008_00479	2509	2.1	BC008_02801	4772	-0.8	BC008_05120	474	0.1
BC008_00480	5478	-1.1	BC008_02802	3535	-0.5	BC008_05121	898	3.7
BC008_00481	831	1.4	BC008_02803	3684	3.1	BC008_05122	269	1.7
BC008_00482	1073	-3.3	BC008_02804	2517	-1.2	BC008_05123	604	3.4
BC008_00483	553	-1.1	BC008_02805	206	-0.5	BC008_05124	1235	1.7
BC008_00484	2940	-2.9	BC008_02806	261	-1.8	BC008_05125	917	2.1
BC008_00485	443	-2.3	BC008_02807	733	-3.0	BC008_05126	1021	-0.9
BC008_00486	139	2.1	BC008_02808	856	0.9	BC008_05127	2234	5.5
BC008_00487	272	3.8	BC008_02809	3482	-0.8	BC008_05128	252	2.3
BC008_00488	418	0.9	BC008_02810	633	0.7	BC008_05129	731	-1.2
BC008_00489	4232	4.7	BC008_02811	431	-1.1	BC008_05130	66	-0.9
BC008_00490	1400	1.6	BC008_02812	552	0.4	BC008_05131	338	-1.7
BC008_00491	2369	1.9	BC008_02813	1729	-2.3	BC008_05132	2499	-1.3
BC008_00492	1291	0.5	BC008_02814	359	-2.3	BC008_05133	192	1.4
BC008_00493	6163	-3.0	BC008_02815	1091	0.2	BC008_05134	427	2.3
BC008_00494	1140	0.4	BC008_02816	1757	-3.4	BC008_05135	234	2.3
BC008_00495	552	-1.1	BC008_02817	577	0.0	BC008_05136	922	-1.1
BC008_00496	178	2.2	BC008_02818	1014	2.4	BC008_05137	23319	-4.1
BC008_00497	176	1.4	BC008_02819	3258	-2.0	BC008_05138	176449	-3.4
BC008_00498	443	-0.2	BC008_02820	200	0.3	BC008_05139	35189	-4.0
BC008_00499	529	2.3	BC008_02821	230	-0.4	BC008_05140	2538	-0.5
BC008_00500	179	0.7	BC008_02822	370	0.5	BC008_05141	874	-0.6
BC008_00501	873	-1.0	BC008_02823	489	-0.8	BC008_05142	18435	-2.4
BC008_00502	1786	-0.8	BC008_02824	51	-0.6	BC008_05143	30	3.3
BC008_00503	636	0.2	BC008_02825	313	0.0	BC008_05144	800	-1.6
BC008_00504	81	1.4	BC008_02826	869	-3.2	BC008_05145	3032	2.3
BC008_00505	1527	-1.5	BC008_02827	5063	-0.2	BC008_05146	407	2.2
BC008_00506	1762	-1.8	BC008_02828	3192	-1.8	BC008_05147	113	-0.9
BC008_00507	159	-0.4	BC008_02829	58617	-5.1	BC008_05148	2088	-2.1
BC008_00508	126	-0.3	BC008_02830	395	-2.3	BC008_05149	4354	-2.9
BC008_00509	303	-0.6	BC008_02831	3908	-4.0	BC008_05150	519	-3.4
BC008_00510	1182	0.0	BC008_02832	12073	-4.4	BC008_05151	228	-0.8

BC008_00511	41	2.0	BC008_02833	49311	-4.7	BC008_05152	7481	-4.0
BC008_00512	397	1.3	BC008_02834	59849	-5.2	BC008_05153	9540	-5.0
BC008_00513	10995	-2.9	BC008_02835	4192	-0.1	BC008_05154	3304	-1.6
BC008_00514	1859	-4.1	BC008_02836	3514	-2.5	BC008_05155	2453	-1.5
BC008_00515	1555	-2.4	BC008_02837	127848	-5.7	BC008_05156	782	2.3
BC008_00516	4570	-1.5	BC008_02838	2233	-1.7	BC008_05157	275	1.2
BC008_00517	2193	-2.2	BC008_02839	3574	-2.8	BC008_05158	1537	3.8
BC008_00518	2073	-0.3	BC008_02840	19268	-3.0	BC008_05159	524	2.1
BC008_00519	1516	-2.5	BC008_02841	688	-2.1	BC008_05160	846	4.0
BC008_00520	1401	-1.6	BC008_02842	1438	-2.9	BC008_05161	184	-0.2
BC008_00521	550	0.0	BC008_02843	3605	-1.3	BC008_05162	5234	1.2
BC008_00522	555	0.3	BC008_02844	29765	-2.8	BC008_05163	1801	-2.2
BC008_00523	13400	-3.0	BC008_02845	2882	-2.8	BC008_05164	667	-1.6
BC008_00524	1700	0.0	BC008_02846	7614	-3.2	BC008_05165	201	-0.2
BC008_00525	7363	-3.4	BC008_02848	2138	1.3	BC008_05166	367	-2.3
BC008_00526	19717	-0.2	BC008_02849	371	0.9	BC008_05167	3097	3.2
BC008_00527	3007	-3.6	BC008_02850	1945	-0.9	BC008_05168	255	4.4
BC008_00528	1617	-1.0	BC008_02851	5022	-1.5	BC008_05169	1532	3.9
BC008_00529	517	-0.9	BC008_02852	1770	-0.6	BC008_05170	512	0.1
BC008_00530	809	-2.3	BC008_02853	902	-1.2	BC008_05171	573	-2.7
BC008_00531	497	-0.1	BC008_02854	18083	-5.1	BC008_05172	175	-1.2
BC008_00532	548	-0.5	BC008_02855	80420	-3.7	BC008_05173	775	-0.2
BC008_00533	546	1.8	BC008_02856	1366	-3.5	BC008_05174	12305	-0.4
BC008_00534	1318	0.0	BC008_02857	1184	-1.3	BC008_05175	1988	2.1
BC008_00535	3862	-2.2	BC008_02858	5210	-5.0	BC008_05176	50	4.2
BC008_00536	666	-0.7	BC008_02859	26601	-3.6	BC008_05177	467	4.7
BC008_00537	281	0.3	BC008_02860	10989	-3.1	BC008_05178	430	2.0
BC008_00538	2372	-1.4	BC008_02861	12459	-5.8	BC008_05179	105	1.0
BC008_00539	435	1.9	BC008_02862	274	-0.5	BC008_05180	820	-1.5
BC008_00540	673	-0.3	BC008_02863	1009	0.4	BC008_05181	231	0.7
BC008_00541	14348	-4.1	BC008_02864	1512	-2.9	BC008_05182	550	0.1
BC008_00542	18182	-4.2	BC008_02865	6754	-4.5	BC008_05183	1108	2.3
BC008_00543	3081	-5.3	BC008_02866	1392	-3.4	BC008_05184	309	3.3
BC008_00544	467	-0.3	BC008_02867	4277	-2.5	BC008_05185	41	-0.2
BC008_00545	425	-1.7	BC008_02868	734	0.2	BC008_05186	1383	1.6
BC008_00546	3590	-3.6	BC008_02869	9699	-4.5	BC008_05187	474	-1.2
BC008_00547	7462	-4.1	BC008_02870	770	-1.3	BC008_05188	323	0.8
BC008_00548	2288	-3.1	BC008_02871	4171	-0.5	BC008_05189	10272	-2.0
BC008_00549	258	1.1	BC008_02872	288	0.6	BC008_05190	1103	-1.6

BC008_00550	513	-1.5	BC008_02873	1309	1.1	BC008_05191	1310	-0.1
BC008_00551	5303	-0.8	BC008_02874	2702	0.7	BC008_05192	862	0.9
BC008_00552	537	-0.3	BC008_02875	4298	-4.0	BC008_05193	172	0.4
BC008_00553	633	-2.0	BC008_02876	1287	-0.4	BC008_05194	760	0.6
BC008_00554	1763	0.5	BC008_02877	756	1.1	BC008_05195	8518	-3.3
BC008_00555	1953	-2.5	BC008_02878	280	0.1	BC008_05196	634	-0.3
BC008_00556	1253	0.2	BC008_02879	8473	-0.3	BC008_05197	1813	-1.9
BC008_00557	10304	-4.0	BC008_02880	1026	2.1	BC008_05198	321	-1.8
BC008_00558	27972	-4.6	BC008_02881	502	0.3	BC008_05199	352	1.0
BC008_00559	40652	-4.6	BC008_02882	835	3.6	BC008_05200	401	0.5
BC008_00560	285	0.9	BC008_02883	495	-0.9	BC008_05201	4566	-1.0
BC008_00561	2536	-2.0	BC008_02884	627	1.3	BC008_05202	53	1.8
BC008_00562	450	-1.2	BC008_02885	678	-2.7	BC008_05203	280	1.5
BC008_00563	2662	-3.4	BC008_02886	311	1.9	BC008_05204	479	1.5
BC008_00564	2321	-4.2	BC008_02887	6004	-3.4	BC008_05205	4505	-1.6
BC008_00565	7657	-0.9	BC008_02888	1509	1.2	BC008_05206	1495	-3.2
BC008_00566	2265	-0.1	BC008_02889	600	0.4	BC008_05207	226	-2.2
BC008_00567	462	-0.7	BC008_02890	465	-0.2	BC008_05208	3386	-0.2
BC008_00568	3490	-2.0	BC008_02891	1815	-0.9	BC008_05209	780	0.3
BC008_00569	1319	-0.9	BC008_02892	8423	-3.8	BC008_05210	1288	3.9
BC008_00570	3041	-1.4	BC008_02893	420	-2.0	BC008_05211	672	0.6
BC008_00571	2166	-0.7	BC008_02894	1243	-2.8	BC008_05212	4287	1.9
BC008_00572	1029	-2.8	BC008_02895	914	-2.6	BC008_05213	766	3.3
BC008_00573	8682	-2.2	BC008_02896	2742	-2.5	BC008_05214	232	-0.6
BC008_00574	1076	-1.6	BC008_02897	2320	-3.2	BC008_05215	14	2.7
BC008_00575	5793	-3.5	BC008_02898	1872	1.8	BC008_05216	834	0.7
BC008_00576	2547	-1.1	BC008_02899	1368	-1.4	BC008_05217	98	-0.5
BC008_00577	345	-0.6	BC008_02900	719	-0.7	BC008_05218	1014	-1.7
BC008_00578	710	6.0	BC008_02901	284	-0.4	BC008_05219	1137	-2.2
BC008_00579	8994	2.0	BC008_02902	774	1.0	BC008_05220	265	-2.6
BC008_00580	221	0.9	BC008_02903	405	-0.9	BC008_05221	253	0.5
BC008_00581	39	1.6	BC008_02904	717	4.6	BC008_05222	1536	3.9
BC008_00582	33	0.1	BC008_02905	913	1.8	BC008_05223	417	-1.1
BC008_00583	312	1.5	BC008_02906	124	2.6	BC008_05224	17278	-2.0
BC008_00584	177	0.9	BC008_02907	205	4.5	BC008_05225	714	0.3
BC008_00585	244	0.0	BC008_02908	372	3.6	BC008_05226	189	-0.8
BC008_00586	386	2.7	BC008_02909	4871	1.4	BC008_05227	3756	3.5
BC008_00587	661	-1.8	BC008_02910	204	0.0	BC008_05228	17	1.1
BC008_00588	552	-2.3	BC008_02911	285	3.3	BC008_05229	67	1.4

BC008_00589	41	2.6	BC008_02912	966	-1.7	BC008_05230	79	4.0
BC008_00590	15	2.3	BC008_02913	1281	-2.1	BC008_05231	1412	5.2
BC008_00591	247	2.1	BC008_02914	2070	-3.3	BC008_05232	60	1.2
BC008_00592	2343	-1.7	BC008_02915	10412	-2.4	BC008_05233	827	1.7
BC008_00593	7430	0.0	BC008_02916	1429	-0.6	BC008_05234	505	1.7
BC008_00594	7721	-2.8	BC008_02917	6863	-1.2	BC008_05235	2633	3.6
BC008_00595	95	0.4	BC008_02918	127	2.9	BC008_05236	460	2.7
BC008_00596	2261	-1.0	BC008_02919	895	2.4	BC008_05237	152	1.3
BC008_00597	518	-0.6	BC008_02920	1869	0.2	BC008_05238	201	1.0
BC008_00598	3493	-3.1	BC008_02921	12478	-3.3	BC008_05239	434	1.2
BC008_00599	6470	-4.0	BC008_02922	11393	-2.2	BC008_05240	3747	0.0
BC008_00600	549	0.5	BC008_02923	256	0.9	BC008_05241	4487	-0.9
BC008_00601	362	0.6	BC008_02924	211	-0.8	BC008_05242	10657	-1.6
BC008_00602	453	-1.2	BC008_02925	1415	-0.8	BC008_05243	1806	-1.9
BC008_00603	82735	-2.5	BC008_02926	1381	-3.3	BC008_05244	589	0.6
BC008_00604	2741	-2.9	BC008_02927	883	-1.8	BC008_05245	555	2.4
BC008_00605	696	-1.8	BC008_02928	3123	-1.6	BC008_05246	4533	0.7
BC008_00606	1374	0.4	BC008_02929	756	-1.4	BC008_05247	1060	1.1
BC008_00607	973	1.4	BC008_02930	4795	-1.2	BC008_05248	1411	3.7
BC008_00608	3456	-1.0	BC008_02931	589	0.3	BC008_05249	1210	0.5
BC008_00609	4587	-0.8	BC008_02932	11650	-3.5	BC008_05250	579	-3.8
BC008_00610	423	-2.2	BC008_02933	3187	-3.1	BC008_05251	2111	-0.6
BC008_00611	1362	-2.8	BC008_02934	5793	-1.4	BC008_05252	168	-2.5
BC008_00612	6168	-3.0	BC008_02935	46104	-3.8	BC008_05253	1716	-2.3
BC008_00614	381	-0.4	BC008_02936	808	-2.6	BC008_05254	1447	-0.2
BC008_00615	116	1.3	BC008_02937	2161	-2.8	BC008_05255	3020	-1.5
BC008_00616	552	-0.9	BC008_02938	870	-3.2	BC008_05256	222	-0.7
BC008_00617	8998	-2.3	BC008_02939	2326	1.2	BC008_05257	593	-2.0
BC008_00618	2873	-1.6	BC008_02940	4452	-2.8	BC008_05258	314	0.9
BC008_00619	236	2.1	BC008_02941	7598	-4.2	BC008_05259	232	1.2
BC008_00620	590	-0.7	BC008_02942	2297	-3.2	BC008_05260	131	-0.4
BC008_00621	6709	-3.6	BC008_02943	364	4.4	BC008_05261	1289	0.7
BC008_00622	11388	-4.2	BC008_02944	321	0.4	BC008_05262	384	2.3
BC008_00623	12785	-4.7	BC008_02945	892	2.8	BC008_05263	924	0.2
BC008_00624	1367	-4.4	BC008_02946	827	-0.2	BC008_05264	544	0.1
BC008_00625	1015	1.6	BC008_02947	1473	-1.8	BC008_05265	293	0.2
BC008_00626	3691	2.3	BC008_02948	874	-1.7	BC008_05266	299	0.7
BC008_00627	787	4.4	BC008_02949	1484	-0.8	BC008_05267	1510	-1.8
BC008_00628	1522	1.5	BC008_02950	76464	-4.9	BC008_05268	302	1.4

BC008_00629	11833	0.1	BC008_02951	31421	-6.9	BC008_05269	1583	1.6
BC008_00630	394	2.8	BC008_02952	5511	-4.4	BC008_05270	1366	0.7
BC008_00631	1954	1.9	BC008_02953	3468	-2.8	BC008_05271	2729	-1.5
BC008_00632	2068	1.6	BC008_02954	339	-0.2	BC008_05272	2722	-0.4
BC008_00633	290	0.9	BC008_02955	374	0.5	BC008_05273	32682	4.5
BC008_00634	1210	1.3	BC008_02956	501	1.4	BC008_05274	1396	-3.2
BC008_00635	531	-0.4	BC008_02957	1301	1.3	BC008_05275	1341	1.5
BC008_00636	1840	-0.7	BC008_02958	161	3.1	BC008_05276	921	3.4
BC008_00637	3066	2.9	BC008_02959	265	1.6	BC008_05277	1074	-1.4
BC008_00638	488	-0.2	BC008_02960	70	2.6	BC008_05278	1226	-2.5
BC008_00639	568	-0.2	BC008_02961	444	3.6	BC008_05279	274	1.8
BC008_00640	429	-0.1	BC008_02962	4023	-0.9	BC008_05280	2814	7.0
BC008_00641	1268	-1.9	BC008_02963	348	-0.5	BC008_05281	884	0.3
BC008_00642	1399	-0.9	BC008_02964	398	-0.2	BC008_05282	2727	0.8
BC008_00643	3382	-1.5	BC008_02965	1564	-1.7	BC008_05283	594	1.2
BC008_00644	509	-0.8	BC008_02966	774	-1.1	BC008_05284	1339	-1.2
BC008_00645	931	0.0	BC008_02967	9465	-0.8	BC008_05285	740	-1.1
BC008_00646	995	-1.3	BC008_02968	26152	-3.8	BC008_05286	16982	5.2
BC008_00647	2548	-1.4	BC008_02969	1093	-2.9	BC008_05288	122	1.2
BC008_00648	224	0.3	BC008_02970	1739	-0.3	BC008_05289	1220	0.3
BC008_00649	591	0.4	BC008_02971	12487	-2.3	BC008_05290	1823	-1.1
BC008_00650	779	-1.9	BC008_02972	7618	-5.3	BC008_05291	163	0.1
BC008_00651	424	1.0	BC008_02973	26533	-6.3	BC008_05292	1029	-2.7
BC008_00652	283	-0.4	BC008_02974	415	0.3	BC008_05293	9855	-3.0
BC008_00653	535	1.7	BC008_02975	742	2.8	BC008_05294	821	0.9
BC008_00654	10104	2.9	BC008_02976	566	2.2	BC008_05295	1356	1.8
BC008_00655	369	0.3	BC008_02977	1073	-1.5	BC008_05296	5919	5.1
BC008_00656	821	0.8	BC008_02978	4505	-1.7	BC008_05297	6877	-2.6
BC008_00657	101	1.4	BC008_02979	455	0.9	BC008_05298	759	2.7
BC008_00658	2976	-2.5	BC008_02980	982	0.1	BC008_05299	478	-0.4
BC008_00659	1097	-0.1	BC008_02981	379	-2.1	BC008_05300	12700	-2.9
BC008_00660	741	-0.2	BC008_02982	39577	-5.2	BC008_05301	2933	-1.5
BC008_00661	2037	-0.9	BC008_02983	810	-3.7	BC008_05302	36257	-0.6
BC008_00662	1309	-1.2	BC008_02984	664	1.0	BC008_05303	61	-0.1
BC008_00663	2319	1.1	BC008_02985	116	-1.4	BC008_05304	863	-1.5
BC008_00664	304	0.8	BC008_02986	191	-1.7	BC008_05305	320	1.4
BC008_00665	1391	-1.2	BC008_02987	571	0.6	BC008_05306	666	2.9
BC008_00666	2014	4.9	BC008_02988	539	-1.1	BC008_05307	324	0.1
BC008_00667	5622	2.9	BC008_02989	1543	-2.6	BC008_05308	1217	1.0

BC008_00668	418	1.6	BC008_02990	1057	-1.6	BC008_05309	5918	-6.5
BC008_00669	11024	-0.5	BC008_02991	1800	0.8	BC008_05310	1775	-0.5
BC008_00670	519	1.1	BC008_02992	1688	0.1	BC008_05311	252	-1.1
BC008_00671	5064	2.4	BC008_02993	1398	-0.6	BC008_05312	2435	2.2
BC008_00672	67	2.0	BC008_02994	13433	1.2	BC008_05313	1440	2.2
BC008_00673	133	2.0	BC008_02995	1828	-1.6	BC008_05314	1131	0.1
BC008_00674	107	2.2	BC008_02996	94	-1.1	BC008_05315	20471	-6.6
BC008_00675	2140	-2.2	BC008_02997	932	1.0	BC008_05316	29228	-4.3
BC008_00676	7662	-4.2	BC008_02998	1413	6.7	BC008_05317	6259	-1.4
BC008_00677	36	-0.3	BC008_02999	1219	-2.2	BC008_05318	33295	-5.4
BC008_00678	1072	2.7	BC008_03000	513	0.3	BC008_05319	18790	-4.9
BC008_00679	776	0.0	BC008_03001	83419	4.2	BC008_05320	530	-2.7
BC008_00680	104	-1.1	BC008_03002	4984	3.6	BC008_05321	76	-1.5
BC008_00681	523	1.3	BC008_03003	815	-1.6	BC008_05322	512	-0.9
BC008_00682	1175	-2.6	BC008_03004	1624	-3.5	BC008_05323	984	1.2
BC008_00683	176	1.5	BC008_03005	1859	-2.2	BC008_05324	211	1.4
BC008_00684	1661	-0.3	BC008_03006	9180	-2.1	BC008_05325	1521	3.3
BC008_00685	3510	-0.9	BC008_03007	1339	0.9	BC008_05326	1277	0.6
BC008_00686	1003	-0.1	BC008_03008	629	-0.8	BC008_05327	4407	0.5
BC008_00687	845	-1.3	BC008_03009	3772	2.7	BC008_05328	15790	-1.9
BC008_00688	7491	-1.0	BC008_03010	1684	-0.9	BC008_05329	1516	-0.2
BC008_00689	1915	-0.2	BC008_03011	1636	2.6	BC008_05330	104	-0.7
BC008_00690	60451	-3.5	BC008_03012	6824	-0.2	BC008_05331	601	-0.4
BC008_00691	282090	-4.9	BC008_03013	2302	-0.6	BC008_05332	2237	-1.4
BC008_00692	34957	-4.4	BC008_03014	1006	0.3	BC008_05333	1120	-3.5
BC008_00693	7402	-4.6	BC008_03015	378	3.9	BC008_05334	783	-2.7
BC008_00694	470	-1.1	BC008_03016	296	1.3	BC008_05335	429	0.2
BC008_00695	496	0.7	BC008_03017	2842	5.4	BC008_05336	2146	2.1
BC008_00696	1516	-0.2	BC008_03018	30	1.9	BC008_05337	54	0.8
BC008_00697	12089	-2.9	BC008_03019	4040	5.0	BC008_05338	1495	-0.8
BC008_00698	297	-1.7	BC008_03020	235	1.9	BC008_05339	673	-1.4
BC008_00699	2698	-0.9	BC008_03021	401	-0.9	BC008_05340	4390	-4.4
BC008_00700	622	-0.5	BC008_03022	128	0.8	BC008_05341	1417	-1.8
BC008_00701	561	0.6	BC008_03023	271	-0.7	BC008_05342	1347	0.1
BC008_00702	3068	-0.3	BC008_03024	6052	-4.1	BC008_05343	2423	-0.8
BC008_00703	3463	-3.3	BC008_03025	9405	-3.8	BC008_05344	812	0.8
BC008_00704	2470	-0.1	BC008_03026	224	0.7	BC008_05345	8025	-1.5
BC008_00705	3893	-1.9	BC008_03027	476	2.9	BC008_05346	34691	-3.7
BC008_00706	194	4.1	BC008_03028	64	1.0	BC008_05347	2756	-1.6

BC008_00707	406	0.2	BC008_03029	22965	-2.9	BC008_05348	2784	-2.2
BC008_00708	719	-0.1	BC008_03030	8137	-3.9	BC008_05349	935	-1.8
BC008_00709	268	0.6	BC008_03031	2143	0.0	BC008_05350	726	-1.2
BC008_00710	142	2.6	BC008_03032	66071	-2.1	BC008_05351	335	1.1
BC008_00711	193	1.4	BC008_03033	2660	3.4	BC008_05352	108	0.1
BC008_00712	171	-0.8	BC008_03034	4928	-3.7	BC008_05353	3038	-0.4
BC008_00713	633	-1.5	BC008_03035	743	-0.8	BC008_05354	167	2.5
BC008_00714	1001	1.6	BC008_03036	1206	-1.6	BC008_05355	233	1.3
BC008_00715	3167	-2.0	BC008_03037	2491	-2.6	BC008_05356	981	-1.7
BC008_00716	3115	-1.8	BC008_03038	2076	-0.8	BC008_05357	2054	1.9
BC008_00717	424	-1.1	BC008_03039	507	-2.1	BC008_05358	965	-0.6
BC008_00718	2594	1.6	BC008_03040	880	-1.0	BC008_05359	512	-1.4
BC008_00719	448	4.3	BC008_03041	229	0.3	BC008_05360	1444	-2.8
BC008_00720	52	6.3	BC008_03042	559	-0.6	BC008_05361	804	-1.4
BC008_00721	316	2.3	BC008_03043	216	1.5	BC008_05362	5428	-2.9
BC008_00722	185	2.3	BC008_03044	596	-1.7	BC008_05363	29437	-4.9
BC008_00723	204	2.3	BC008_03045	838	-2.1	BC008_05364	2649	-0.4
BC008_00724	2092	-3.5	BC008_03046	183	-0.3	BC008_05365	567	-0.5
BC008_00725	948	-2.5	BC008_03047	19978	-0.5	BC008_05366	593	-0.3
BC008_00726	472	-1.0	BC008_03048	257	-0.5	BC008_05367	269	0.5
BC008_00727	243	-2.0	BC008_03049	2378	-0.1	BC008_05368	426	0.4
BC008_00728	1632	2.1	BC008_03050	4486	-2.6	BC008_05369	1325	1.6
BC008_00729	504	0.3	BC008_03051	1106	-0.6	BC008_05370	2339	-1.4
BC008_00730	2037	-2.8	BC008_03052	419	1.0	BC008_05371	645	2.1
BC008_00731	1080	2.2	BC008_03053	872	-1.0	BC008_05372	20764	-3.2
BC008_00732	2454	-0.3	BC008_03054	1134	-0.4	BC008_05373	2088	-0.6
BC008_00733	802	0.6	BC008_03055	5751	-2.2	BC008_05374	1364	3.1
BC008_00734	1137	-1.5	BC008_03056	4363	-2.8	BC008_05375	534	2.1
BC008_00735	5507	0.7	BC008_03057	6205	-2.5	BC008_05376	518	0.5
BC008_00736	381	-0.3	BC008_03058	1040	-3.0	BC008_05377	1615	-1.1
BC008_00737	95	0.2	BC008_03059	1207	-2.9	BC008_05378	2636	1.3
BC008_00738	638	2.3	BC008_03060	1086	-1.9	BC008_05379	129	-1.3
BC008_00739	730	3.0	BC008_03061	804	0.9	BC008_05380	597	-0.4
BC008_00740	227	2.8	BC008_03062	486	0.0	BC008_05381	237	0.1
BC008_00741	150	2.2	BC008_03063	159	-1.2	BC008_05382	1580	-1.2
BC008_00742	324	2.0	BC008_03064	961	-2.0	BC008_05383	606	-2.0
BC008_00743	404	4.9	BC008_03065	22866	-5.0	BC008_05384	1076	1.0
BC008_00744	216	-3.9	BC008_03066	534	0.7	BC008_05385	1219	5.3
BC008_00745	368	2.5	BC008_03067	2059	0.2	BC008_05386	112	-0.2

BC008_00746	320	2.8	BC008_03068	376	3.2	BC008_05387	122	0.2
BC008_00747	29	3.9	BC008_03069	4901	-2.3	BC008_05388	93	0.8
BC008_00748	475	1.6	BC008_03070	1399	1.1	BC008_05389	180	0.9
BC008_00749	408	1.0	BC008_03071	1069	-0.3	BC008_05390	581	-0.3
BC008_00750	545	1.8	BC008_03072	235	-1.1	BC008_05391	1432	-1.3
BC008_00751	384	-1.5	BC008_03073	10129	-0.9	BC008_05392	458	-1.3
BC008_00752	230	2.2	BC008_03074	400	-1.2	BC008_05394	6253	-1.6
BC008_00753	429	0.2	BC008_03075	1398	0.0	BC008_05395	5640	-0.2
BC008_00754	88	2.0	BC008_03076	1592	0.9	BC008_05396	339	2.0
BC008_00755	488	1.6	BC008_03077	4317	6.2	BC008_05397	488	-0.5
BC008_00756	2490	6.8	BC008_03078	85	1.2	BC008_05398	15417	-2.0
BC008_00757	488	1.0	BC008_03079	2890	-3.2	BC008_05399	7322	-2.8
BC008_00758	2346	-1.0	BC008_03080	54365	-4.2	BC008_05400	83767	-6.0
BC008_00759	1193	2.1	BC008_03081	237	0.3	BC008_05401	1215	-0.6
BC008_00760	484	-0.4	BC008_03082	200	0.1	BC008_05402	802	-0.7
BC008_00761	1742	-0.9	BC008_03083	808	-0.3	BC008_05403	1672	-0.8
BC008_00762	1013	-0.8	BC008_03084	83	-0.4	BC008_05404	1271	0.3
BC008_00763	5045	-1.0	BC008_03085	11135	-2.8	BC008_05405	3502	-0.4
BC008_00764	318	-2.1	BC008_03086	1852	-1.9	BC008_05406	7354	-2.5
BC008_00765	2011	-2.1	BC008_03087	1360	-0.5	BC008_05407	1267	0.5
BC008_00766	577	-1.5	BC008_03088	9296	0.7	BC008_05408	544	-2.1
BC008_00767	1519	-2.0	BC008_03089	617	-0.7	BC008_05409	334	0.0
BC008_00768	8497	-2.6	BC008_03090	1195	-0.9	BC008_05410	1060	0.8
BC008_00769	24789	-4.4	BC008_03091	481	0.0	BC008_05411	1125	0.0
BC008_00770	758	6.9	BC008_03092	1705	-0.4	BC008_05413	437	3.0
BC008_00771	2600	3.7	BC008_03093	522	-1.4	BC008_05414	283	0.8
BC008_00772	185	-0.3	BC008_03094	583	-1.7	BC008_05415	1708	-1.0
BC008_00773	117	1.4	BC008_03095	329	-0.2	BC008_05416	1485	0.5
BC008_00774	719	-1.3	BC008_03096	469	-0.9	BC008_05417	225	-0.9
BC008_00775	2186	-2.0	BC008_03097	4027	-1.9	BC008_05418	121	0.5
BC008_00776	27228	5.0	BC008_03098	6332	0.0	BC008_05419	1652	2.2
BC008_00777	1351	4.0	BC008_03099	1350	-2.7	BC008_05420	332	-0.3
BC008_00778	1526	0.8	BC008_03100	6178	-0.7	BC008_05421	46356	-1.0
BC008_00779	1620	-0.8	BC008_03101	8069	-4.1	BC008_05422	1983	1.8
BC008_00780	127	1.6	BC008_03102	1093	-1.5	BC008_05423	10335	3.0
BC008_00781	1352	-1.8	BC008_03103	124	1.2	BC008_05424	641	1.9
BC008_00782	865	-0.7	BC008_03104	3581	-2.0	BC008_05425	817	1.9
BC008_00783	1366	2.7	BC008_03105	434	-1.3	BC008_05426	86	-0.5
BC008_00784	166	2.5	BC008_03106	5285	1.3	BC008_05427	329	1.0

BC008_00785	571	-0.2	BC008_03107	1078	-1.2	BC008_05428	206	2.7
BC008_00786	428	-0.1	BC008_03108	900	-0.5	BC008_05429	3466	3.0
BC008_00787	327	1.2	BC008_03109	193	-1.8	BC008_05430	390	0.1
BC008_00788	395	1.5	BC008_03110	13282	-1.8	BC008_05431	738	1.7
BC008_00789	3468	0.0	BC008_03111	46036	-2.5	BC008_05432	83	0.7
BC008_00790	1410	-1.1	BC008_03112	5040	-1.4	BC008_05433	819	1.4
BC008_00791	106	4.8	BC008_03113	1448	-2.5	BC008_05434	534	-0.8
BC008_00792	1093	2.4	BC008_03114	545	-3.2	BC008_05435	21225	-0.3
BC008_00793	136	-0.6	BC008_03115	541	-1.7	BC008_05436	3799	-1.1
BC008_00794	1239	2.6	BC008_03116	598	-2.6	BC008_05437	502	-1.7
BC008_00795	1174	0.0	BC008_03117	1446	-2.8	BC008_05438	754	0.5
BC008_00796	170	-0.4	BC008_03118	2197	-2.0	BC008_05439	4969	-0.4
BC008_00797	493	-0.1	BC008_03119	12976	-4.4	BC008_05440	4355	-1.2
BC008_00798	288	3.9	BC008_03120	3079	-5.5	BC008_05441	374	-0.2
BC008_00799	203	-0.2	BC008_03121	15506	-5.1	BC008_05442	7779	-4.4
BC008_00800	406	-0.4	BC008_03122	2463	-1.7	BC008_05443	406	4.3
BC008_00801	540	-0.7	BC008_03123	88	-0.4	BC008_05444	709	1.1
BC008_00802	308	1.2	BC008_03124	15	0.6	BC008_05445	1276	-0.2
BC008_00803	8870	-2.1	BC008_03125	1305	1.7	BC008_05446	1059	-0.4
BC008_00804	242	3.0	BC008_03126	2803	4.5	BC008_05447	697	2.2
BC008_00805	462	1.5	BC008_03127	325	1.2	BC008_05448	477	1.5
BC008_00806	10849	-4.1	BC008_03128	1060	0.8	BC008_05449	530	1.3
BC008_00807	1208	-2.7	BC008_03129	2115	4.8	BC008_05450	90	2.2
BC008_00808	624	1.5	BC008_03130	736	2.3	BC008_05451	1588	-0.3
BC008_00809	408	2.1	BC008_03131	264	1.1	BC008_05452	1513	-0.6
BC008_00810	1474	-2.2	BC008_03132	769	2.2	BC008_05453	145	0.5
BC008_00811	49	2.1	BC008_03133	348	2.9	BC008_05454	1169	1.1
BC008_00812	183	0.7	BC008_03134	2622	-0.8	BC008_05455	1054	2.3
BC008_00813	141	-0.3	BC008_03135	2368	-0.9	BC008_05456	72	1.6
BC008_00814	1068	-0.4	BC008_03136	3055	-0.8	BC008_05457	1806	-0.8
BC008_00815	348	1.4	BC008_03137	171	1.6	BC008_05458	7	1.8
BC008_00816	1326	4.0	BC008_03138	3790	2.1	BC008_05459	1930	-2.0
BC008_00817	815	-1.6	BC008_03139	445	1.8	BC008_05460	6821	3.6
BC008_00818	3993	3.3	BC008_03140	512	2.4	BC008_05461	515	3.2
BC008_00819	354	4.1	BC008_03141	248	-0.1	BC008_05462	398	0.7
BC008_00820	2161	-0.2	BC008_03142	1258	0.1	BC008_05463	3931	4.0
BC008_00821	2987	-2.2	BC008_03143	304	1.7	BC008_05464	1319	0.7
BC008_00822	2292	0.0	BC008_03144	2427	-1.0	BC008_05465	68	0.4
BC008_00823	3450	-1.8	BC008_03145	701	3.5	BC008_05466	3029	-2.1

BC008_00824	3847	1.2	BC008_03146	856	-0.5	BC008_05467	230	-2.1
BC008_00825	1067	3.5	BC008_03147	323	0.4	BC008_05468	1862	-1.4
BC008_00826	101	0.6	BC008_03148	578	-0.7	BC008_05469	7249	-3.1
BC008_00827	267	0.7	BC008_03149	3096	-0.1	BC008_05470	1053	-2.3
BC008_00828	1775	0.9	BC008_03150	1891	1.3	BC008_05471	513	-1.9
BC008_00829	2814	2.9	BC008_03151	3724	2.2	BC008_05472	1228	0.1
BC008_00830	506	-0.2	BC008_03152	387	1.5	BC008_05473	328	1.1
BC008_00831	231	-0.1	BC008_03153	154	0.7	BC008_05474	1549	2.4
BC008_00832	234	-0.4	BC008_03154	457	2.3	BC008_05475	143422	-5.4
BC008_00833	213	-1.5	BC008_03155	131	0.5	BC008_05476	146351	-5.1
BC008_00834	1009	-1.8	BC008_03156	128	-2.4	BC008_05477	98848	-5.3
BC008_00835	670	-0.6	BC008_03157	163	2.6	BC008_05478	1658	-0.7
BC008_00836	1112	1.9	BC008_03158	831	3.4	BC008_05479	868	-1.1
BC008_00837	414	-0.9	BC008_03159	51	1.7	BC008_05480	2935	1.1
BC008_00838	5421	-2.9	BC008_03160	4150	-0.6	BC008_05481	1207	-2.0
BC008_00839	27	1.4	BC008_03161	1199	0.9	BC008_05482	4209	-1.7
BC008_00840	472	-0.5	BC008_03162	739	-1.1	BC008_05483	7085	0.0
BC008_00841	615	1.9	BC008_03163	77263	-5.3	BC008_05484	6889	2.0
BC008_00842	638	-0.6	BC008_03164	378	-1.7	BC008_05485	361	-1.0
BC008_00843	728	0.3	BC008_03165	408	0.7	BC008_05486	1354	0.1
BC008_00844	271	0.3	BC008_03166	333	-0.5	BC008_05487	899	-1.2
BC008_00845	5101	-2.1	BC008_03167	1367	0.6	BC008_05488	539	-0.5
BC008_00846	536	-2.4	BC008_03168	105	-0.8	BC008_05489	1916	-1.7
BC008_00847	4630	-1.3	BC008_03169	1157	-2.0	BC008_05490	882	0.2
BC008_00848	5492	0.9	BC008_03170	1007	-0.5	BC008_05491	1221	-2.6
BC008_00849	465	1.8	BC008_03171	2770	-1.1	BC008_05492	569	0.1
BC008_00850	1146	1.8	BC008_03172	629	-0.9	BC008_05493	230	1.0
BC008_00851	3202	-1.5	BC008_03173	6631	-3.1	BC008_05494	38	2.2
BC008_00852	39	-3.4	BC008_03174	511	0.4	BC008_05495	477	2.1
BC008_00853	908	-3.4	BC008_03175	791	0.9	BC008_05496	992	0.0
BC008_00854	1211	-1.0	BC008_03176	601	-1.7	BC008_05497	625	-0.2
BC008_00855	4191	-4.1	BC008_03177	1631	-0.6	BC008_05498	199	0.5
BC008_00856	3368	-3.1	BC008_03178	1203	-2.1	BC008_05499	435	-2.6
BC008_00857	305	0.6	BC008_03179	1597	-0.3	BC008_05500	977	-1.9
BC008_00858	29	0.7	BC008_03180	929	-1.1	BC008_05501	3573	-2.2
BC008_00859	1054	-0.9	BC008_03181	3180	-4.0	BC008_05502	989	1.7
BC008_00860	1828	-5.3	BC008_03182	2011	-1.6	BC008_05503	367	-4.1
BC008_00861	867	0.5	BC008_03183	938	-0.2	BC008_05504	2161	1.7
BC008_00862	1812	-2.0	BC008_03184	1029	-0.3	BC008_05505	898	-2.5

BC008_00863	2487	2.8	BC008_03185	1172	-0.2	BC008_05506	3437	-1.0
BC008_00864	3631	-0.6	BC008_03186	2320	-1.9	BC008_05507	1349	1.4
BC008_00865	3415	3.2	BC008_03187	23502	-4.4	BC008_05508	49	1.0
BC008_00866	146	4.1	BC008_03188	3769	-3.3	BC008_05509	1227	1.3
BC008_00867	882	-1.2	BC008_03189	3434	-3.6	BC008_05510	411	-0.1
BC008_00868	1784	-2.4	BC008_03190	619	0.6	BC008_05511	2113	-0.4
BC008_00869	378	-0.9	BC008_03191	368	-1.8	BC008_05512	167	-0.8
BC008_00870	2973	-1.9	BC008_03192	1031	-0.5	BC008_05513	858	2.0
BC008_00871	1657	1.1	BC008_03193	827	-2.4	BC008_05514	899	-0.2
BC008_00872	1155	0.3	BC008_03194	3833	-0.6	BC008_05515	735	1.2
BC008_00873	608	0.5	BC008_03195	595	2.0	BC008_05516	1518	0.0
BC008_00874	327	0.6	BC008_03196	725	1.7	BC008_05517	424	0.8
BC008_00875	125	-0.5	BC008_03197	2008	-3.1	BC008_05518	4997	-2.3
BC008_00876	1132	1.2	BC008_03198	4608	-3.0	BC008_05519	1581	-0.5
BC008_00877	410	-0.6	BC008_03199	23765	-6.2	BC008_05520	11336	-2.6
BC008_00878	1784	0.4	BC008_03200	314	-1.1	BC008_05521	5727	-1.7
BC008_00879	271	0.0	BC008_03201	594	1.7	BC008_05522	3425	-2.2
BC008_00880	485	-1.6	BC008_03202	467	-1.1	BC008_05523	4585	-1.7
BC008_00881	690	-0.2	BC008_03203	520	4.0	BC008_05524	3310	-1.9
BC008_00882	1535	1.7	BC008_03204	177	2.2	BC008_05525	745	1.1
BC008_00883	688	1.7	BC008_03205	654	-1.5	BC008_05526	735	0.6
BC008_00884	1352	1.9	BC008_03206	443	1.4	BC008_05527	300	3.4
BC008_00885	2933	-0.8	BC008_03207	693	-1.5	BC008_05528	376	0.9
BC008_00886	826	2.3	BC008_03208	532	-0.5	BC008_05529	382	-2.1
BC008_00887	2188	-2.1	BC008_03209	1443	-0.6	BC008_05530	771	-1.2
BC008_00888	1339	0.8	BC008_03210	2828	-1.8	BC008_05531	947	2.4
BC008_00889	101	1.2	BC008_03211	55	1.8	BC008_05532	459	0.2
BC008_00890	1203	-1.1	BC008_03212	1866	0.2	BC008_05533	267	-0.2
BC008_00891	4630	-3.5	BC008_03213	5786	0.1	BC008_05534	750	-0.8
BC008_00892	2338	-1.4	BC008_03214	3074	-1.7	BC008_05535	2057	-3.1
BC008_00893	3203	-2.9	BC008_03215	883	-1.9	BC008_05536	219	5.1
BC008_00894	2007	-0.4	BC008_03216	2569	1.6	BC008_05537	443	0.2
BC008_00895	206	-0.4	BC008_03217	1332	0.4	BC008_05538	259	-1.7
BC008_00896	1305	-1.6	BC008_03218	1099	-0.6	BC008_05539	387	1.3
BC008_00897	1258	0.6	BC008_03219	72	0.0	BC008_05540	56	0.6
BC008_00898	587	1.8	BC008_03220	430	-1.5	BC008_05541	22	6.2
BC008_00899	5483	-1.4	BC008_03221	100	-0.1	BC008_05542	3098	8.6
BC008_00900	3584	0.0	BC008_03222	97	-0.3	BC008_05543	2733	7.8
BC008_00901	665	-2.0	BC008_03223	717	-1.5	BC008_05544	3911	1.3

BC008_00902	6876	-1.4	BC008_03224	233	0.4	BC008_05545	1139	-0.1
BC008_00903	131	-0.1	BC008_03225	625	0.8	BC008_05546	5652	-3.9
BC008_00904	1135	-1.7	BC008_03226	497	1.7	BC008_05547	3929	-2.0
BC008_00905	4627	-1.4	BC008_03227	1132	0.1	BC008_05548	93	-1.3
BC008_00906	1493	-4.3	BC008_03228	259	0.7	BC008_05549	884	-0.3
BC008_00907	2453	-3.1	BC008_03229	1706	-0.6	BC008_05550	603	-0.7
BC008_00908	932	-2.8	BC008_03230	2927	1.6	BC008_05551	901	-4.9
BC008_00909	5209	1.7	BC008_03231	2194	-3.0	BC008_05552	6941	-1.2
BC008_00910	171	-0.3	BC008_03232	1367	-0.2	BC008_05553	568	-1.8
BC008_00911	279	-0.6	BC008_03233	522	2.1	BC008_05554	94190	-5.9
BC008_00912	319	-0.2	BC008_03234	1979	3.4	BC008_05555	5967	-3.3
BC008_00913	1123	1.0	BC008_03235	653	-0.1	BC008_05556	4906	-3.8
BC008_00914	998	1.2	BC008_03236	838	1.2	BC008_05557	4160	-1.7
BC008_00915	267	2.1	BC008_03237	946	2.9	BC008_05558	619	-1.3
BC008_00916	1274	-3.4	BC008_03238	836	-2.3	BC008_05559	700	-0.9
BC008_00917	2034	-1.2	BC008_03239	1285	-2.3	BC008_05560	93	1.1
BC008_00918	7175	-3.9	BC008_03240	520	2.9	BC008_05561	201	4.2
BC008_00919	15925	-4.7	BC008_03241	535	2.0	BC008_05562	275	1.0
BC008_00920	6269	-3.8	BC008_03242	191	2.8	BC008_05563	656	-0.2
BC008_00921	3009	-1.9	BC008_03243	1359	2.0	BC008_05564	4990	-1.6
BC008_00922	1955	-2.5	BC008_03244	140	0.4	BC008_05565	951	0.0
BC008_00923	922	-0.1	BC008_03245	232	0.7	BC008_05566	2034	-3.1
BC008_00924	723	-0.5	BC008_03246	275	-0.7	BC008_05567	1024	1.2
BC008_00925	1528	0.3	BC008_03247	3225	-1.4	BC008_05568	238	1.5
BC008_00926	1919	-2.6	BC008_03248	558	2.2	BC008_05569	14064	-1.4
BC008_00927	571	1.8	BC008_03249	674	-2.5	BC008_05570	2175	-1.1
BC008_00928	2270	-1.2	BC008_03250	377	1.5	BC008_05571	172	0.4
BC008_00929	9162	-4.2	BC008_03251	563	-0.7	BC008_05572	1737	-0.2
BC008_00930	6353	-2.8	BC008_03252	1664	2.8	BC008_05573	2259	0.3
BC008_00931	1534	0.6	BC008_03253	135	0.2	BC008_05574	2743	0.0
BC008_00932	2998	-2.0	BC008_03254	272	2.2	BC008_05575	1879	0.3
BC008_00933	2039	0.4	BC008_03255	112	3.3	BC008_05576	4192	0.4
BC008_00934	277	-0.7	BC008_03256	9184	0.1	BC008_05577	221	2.9
BC008_00935	1787	-0.7	BC008_03257	1233	-2.8	BC008_05578	243	0.4
BC008_00936	7447	-3.1	BC008_03258	964	2.6	BC008_05579	4730	-5.0
BC008_00937	2846	-0.4	BC008_03259	541	-1.3	BC008_05580	2035	-3.3
BC008_00938	217	2.1	BC008_03260	348	-2.1	BC008_05581	918	-1.9
BC008_00939	3205	-0.9	BC008_03261	43	0.8	BC008_05582	5203	-0.3
BC008_00940	157	0.8	BC008_03262	1968	-0.3	BC008_05583	929	-1.5

BC008_00941	1137	0.6	BC008_03263	751	0.0	BC008_05584	641	-0.7
BC008_00942	1470	3.1	BC008_03264	317	-0.2	BC008_05585	554	-3.2
BC008_00943	99	0.5	BC008_03265	1387	0.4	BC008_05586	10306	0.5
BC008_00944	203	0.8	BC008_03266	672	2.9	BC008_05587	11829	-1.4
BC008_00945	2901	-1.1	BC008_03267	822	-1.3	BC008_05588	309	1.7
BC008_00946	22	1.9	BC008_03268	575	-0.5	BC008_05589	137	1.1
BC008_00947	4562	-0.1	BC008_03269	2768	-0.2	BC008_05590	173	2.4
BC008_00948	1514	-1.9	BC008_03270	5945	1.6	BC008_05591	963	3.4
BC008_00949	1438	-0.6	BC008_03271	280	1.6	BC008_05592	274	-1.6
BC008_00950	399	-1.8	BC008_03272	389	3.0	BC008_05593	711	1.7
BC008_00951	470	-1.8	BC008_03273	151	0.5	BC008_05594	531	4.8
BC008_00952	484	-1.1	BC008_03274	1117	1.2	BC008_05595	106	0.9
BC008_00953	1595	-0.4	BC008_03275	540	-0.7	BC008_05596	64	3.1
BC008_00954	139	1.8	BC008_03276	3007	-4.5	BC008_05597	663	1.6
BC008_00956	1254	-1.6	BC008_03277	2036	2.6	BC008_05598	177	0.8
BC008_00957	289	-1.2	BC008_03278	246	1.0	BC008_05599	3502	-0.5
BC008_00958	562	-2.6	BC008_03279	317	2.2	BC008_05600	2822	3.5
BC008_00959	5885	-1.5	BC008_03280	2602	-0.2	BC008_05601	7002	3.9
BC008_00960	125	1.7	BC008_03281	486	-0.9	BC008_05602	226	2.3
BC008_00961	315	1.0	BC008_03282	54160	-4.4	BC008_05603	582	5.0
BC008_00962	1056	-0.1	BC008_03283	588	1.8	BC008_05604	115	5.1
BC008_00963	152051	-5.1	BC008_03284	150	2.2	BC008_05605	105	7.2
BC008_00964	1944	1.4	BC008_03285	1279	1.7	BC008_05606	58	4.7
BC008_00965	980	-0.3	BC008_03286	938	1.0	BC008_05607	242	4.8
BC008_00966	1579	0.6	BC008_03287	1683	-1.3	BC008_05608	802	1.4
BC008_00967	894	-2.3	BC008_03288	1073	1.5	BC008_05609	190	-0.2
BC008_00968	287	-0.2	BC008_03289	515	3.7	BC008_05610	2454	4.4
BC008_00969	328	0.2	BC008_03290	288	1.7	BC008_05611	101	0.6
BC008_00970	26	0.4	BC008_03291	1606	2.4	BC008_05612	166	1.7
BC008_00971	320	-0.6	BC008_03292	2108	3.3	BC008_05613	2636	1.0
BC008_00972	793	-0.6	BC008_03293	286	1.6	BC008_05614	215	5.1
BC008_00973	418	0.3	BC008_03294	390	-0.4	BC008_05615	58	3.6
BC008_00974	14399	-3.6	BC008_03295	368	-0.2	BC008_05616	64	1.9
BC008_00975	1652	-1.3	BC008_03296	83	0.0	BC008_05617	1573	-0.9
BC008_00976	2559	-1.8	BC008_03297	319	-3.3	BC008_05618	1370	2.5
BC008_00978	518	-2.3	BC008_03298	352	0.1	BC008_05619	5575	6.3
BC008_00979	265	0.9	BC008_03299	136	2.9	BC008_05620	2991	8.3
BC008_00980	684	0.8	BC008_03300	87	1.8	BC008_05621	453	6.9
BC008_00981	792	1.3	BC008_03301	173	4.0	BC008_05622	1681	7.9

BC008_00982	1263	2.7	BC008_03302	89	4.3	BC008_05623	4697	-1.0
BC008_00983	82	2.6	BC008_03303	70	-0.1	BC008_05624	1161	2.1
BC008_00984	661	3.3	BC008_03304	3279	3.6	BC008_05625	2893	-0.2
BC008_00985	115	-0.3	BC008_03305	301	2.2	BC008_05626	3278	5.4
BC008_00986	918	-0.1	BC008_03306	582	5.1	BC008_05627	257	-0.3
BC008_00987	577	-1.4	BC008_03307	413	0.4	BC008_05628	202	4.8
BC008_00988	147	0.5	BC008_03308	212	-2.1	BC008_05629	1878	-1.6
BC008_00989	9319	-4.4	BC008_03309	281	-0.1	BC008_05630	552	1.7
BC008_00990	4729	2.9	BC008_03310	278	3.4	BC008_05631	13225	0.0
BC008_00991	394	1.3	BC008_03311	227	1.3	BC008_05632	597	1.5
BC008_00992	863	0.6	BC008_03312	724	-0.9	BC008_05633	227	4.5
BC008_00993	400	2.0	BC008_03313	2573	-0.8	BC008_05634	483	-2.0
BC008_00994	4107	-1.5	BC008_03314	4634	-1.8	BC008_05635	1493	-2.8
BC008_00995	1147	-0.1	BC008_03315	1742	-0.3	BC008_05636	3986	-0.8
BC008_00996	1336	-0.5	BC008_03316	697	0.7	BC008_05637	5142	4.0
BC008_00997	831	-1.6	BC008_03317	7403	-3.5	BC008_05638	106	1.1
BC008_00998	1758	0.3	BC008_03318	297805	-6.7	BC008_05639	3249	3.7
BC008_00999	394	1.9	BC008_03319	5101	-3.7	BC008_05640	3530	2.3
BC008_01000	711	0.8	BC008_03320	1690	-3.2	BC008_05641	1410	0.4
BC008_01001	333	0.6	BC008_03321	825	-1.1	BC008_05642	351	-0.4
BC008_01002	791	-0.3	BC008_03322	460	1.3	BC008_05643	890	1.6
BC008_01003	945	-2.4	BC008_03323	737	-3.8	BC008_05644	232	0.5
BC008_01004	210	1.5	BC008_03324	645	-1.8	BC008_05645	1624	0.8
BC008_01005	539	5.0	BC008_03325	757	-0.9	BC008_05646	509	1.9
BC008_01006	1897	-1.1	BC008_03326	1246	0.4	BC008_05647	5747	-2.6
BC008_01007	1642	0.2	BC008_03327	167	6.0	BC008_05648	1885	-2.4
BC008_01008	1336	-1.6	BC008_03328	311	1.3	BC008_05649	703	-0.7
BC008_01009	1944	0.4	BC008_03329	723	1.6	BC008_05650	472	0.8
BC008_01010	871	3.5	BC008_03330	1070	1.1	BC008_05651	809	-0.2
BC008_01011	501	3.3	BC008_03331	1113	5.9	BC008_05652	431	-0.3
BC008_01012	293	0.7	BC008_03332	415	0.9	BC008_05653	1518	-0.2
BC008_01013	562	1.2	BC008_03333	664	1.6	BC008_05654	804	-1.4
BC008_01014	2417	1.1	BC008_03334	597	-0.9	BC008_05655	1650	-1.2
BC008_01015	5507	-0.3	BC008_03335	3034	-2.5	BC008_05656	3512	-1.9
BC008_01016	1035	-1.9	BC008_03336	2495	-0.6	BC008_05657	2898	-0.7
BC008_01017	1148	-0.8	BC008_03337	802	-0.4	BC008_05658	887	-2.6
BC008_01018	2447	-2.6	BC008_03338	252	1.4	BC008_05659	710	-1.3
BC008_01019	1153	-0.9	BC008_03339	23782	-0.5	BC008_05660	3715	-0.4
BC008_01020	2598	-0.8	BC008_03340	60	0.7	BC008_05661	391	1.6

BC008_01021	123	-0.3	BC008_03341	439	0.4	BC008_05662	471	2.3
BC008_01022	4335	-1.0	BC008_03342	106	-0.3	BC008_05663	895	-0.5
BC008_01023	22976	-0.6	BC008_03343	4601	-1.3	BC008_05664	880	4.2
BC008_01024	8035	-1.6	BC008_03344	165	2.4	BC008_05665	183	1.0
BC008_01025	10860	-2.2	BC008_03345	1196	-1.2	BC008_05666	180	1.0
BC008_01026	265104	-3.4	BC008_03346	225	1.0	BC008_05667	481	-0.2
BC008_01027	993228	-5.5	BC008_03347	244	0.5	BC008_05668	142	0.9
BC008_01028	542	-1.5	BC008_03348	311	2.4	BC008_05669	586	-1.2
BC008_01029	930	-0.5	BC008_03349	1488	1.7	BC008_05670	1045	-1.5
BC008_01030	2220	-0.9	BC008_03350	1126	1.7	BC008_05671	1400	0.4
BC008_01031	369	0.4	BC008_03351	68	-0.4	BC008_05672	285	2.6
BC008_01032	1272	0.6	BC008_03352	3486	-2.7	BC008_05673	377	1.8
BC008_01033	276	-1.4	BC008_03353	717	2.5	BC008_05674	455	1.2
BC008_01034	53387	-5.6	BC008_03354	136	1.3	BC008_05675	89	0.8
BC008_01035	3827	-4.1	BC008_03355	433	3.7	BC008_05676	63467	-4.0
BC008_01036	9075	-4.5	BC008_03356	51	-1.5	BC008_05677	13946	-4.4
BC008_01037	1243	-0.8	BC008_03357	575	2.3	BC008_05678	831	0.3
BC008_01038	1226	1.8	BC008_03358	1834	-1.8	BC008_05679	366	1.8
BC008_01039	32	1.0	BC008_03359	3511	-2.8	BC008_05680	122	0.8
BC008_01040	173	2.5	BC008_03360	3201	-2.4	BC008_05681	593	-1.6
BC008_01041	2631	6.9	BC008_03361	2290	-2.2	BC008_05682	453	-1.5
BC008_01042	5833	-3.3	BC008_03362	820	-1.7	BC008_05683	4144	-2.9
BC008_01043	988	0.9	BC008_03363	1381	-0.6	BC008_05684	4930	-3.5
BC008_01044	531	3.5	BC008_03364	4113	-2.7	BC008_05685	3093	-0.9
BC008_01045	1268	2.8	BC008_03365	2092	-2.4	BC008_05686	7460	-0.1
BC008_01046	1629	0.7	BC008_03366	1227	-0.5	BC008_05687	1741	-2.0
BC008_01047	225	0.5	BC008_03367	1206	-1.5	BC008_05688	1015	-2.2
BC008_01048	809	0.8	BC008_03368	1534	-2.3	BC008_05689	70841	-5.8
BC008_01049	1428	1.4	BC008_03369	6491	-2.2	BC008_05690	2864	-1.2
BC008_01050	108	5.2	BC008_03370	2385	-0.9	BC008_05691	1080	-1.0
BC008_01051	124	6.7	BC008_03371	1378	-1.8	BC008_05692	3025	-1.5
BC008_01052	271	2.5	BC008_03372	2661	-3.0	BC008_05693	450	-0.7
BC008_01053	618	4.5	BC008_03373	1942	-2.7	BC008_05694	2705	7.2
BC008_01054	38	1.9	BC008_03374	979	-1.7	BC008_05695	3400	3.8
BC008_01055	38	3.9	BC008_03375	897	-1.2	BC008_05696	1918	0.4
BC008_01056	68	6.1	BC008_03376	2611	-1.6	BC008_05697	2184	4.9
BC008_01057	64	6.6	BC008_03377	871	-0.8	BC008_05698	689	0.7
BC008_01058	73	3.9	BC008_03378	2518	-2.7	BC008_05699	515	-1.5
BC008_01059	221	2.1	BC008_03379	6956	-1.1	BC008_05700	739	1.1

BC008_01060	233	3.0	BC008_03380	3009	-0.6	BC008_05701	2754	-0.6
BC008_01061	156	4.0	BC008_03381	6923	-2.0	BC008_05702	57	-0.9
BC008_01062	70	1.9	BC008_03382	1209	-2.9	BC008_05716	610	0.3
BC008_01063	109	4.1	BC008_03383	1841	-1.6	BC008_05717	130	0.8
BC008_01064	4634	5.8	BC008_03384	8965	-1.7	BC008_05718	216	2.4
BC008_01065	140	1.9	BC008_03385	19262	-4.4	BC008_05719	289	0.5
BC008_01066	67	1.0	BC008_03386	6849	-3.1	BC008_05720	212	5.2
BC008_01067	603	3.2	BC008_03387	4553	-2.3	BC008_05721	18	0.5
BC008_01068	630	1.6	BC008_03388	1297	-0.6	BC008_05722	126	0.3
BC008_01069	1090	-0.6	BC008_03389	1580	-2.0	BC008_05723	41	6.0
BC008_01070	794	5.4	BC008_03390	539	-1.6	BC008_05724	162	5.1
BC008_01071	1130	1.6	BC008_03391	1787	-1.6	BC008_05725	68	1.3
BC008_01072	1464	-0.4	BC008_03392	1065	0.0	BC008_05726	248	2.4
BC008_01073	461	2.1	BC008_03393	1850	-0.9	BC008_05727	340	4.6
BC008_01074	494	0.2	BC008_03394	6574	-1.0	BC008_05728	589	-0.3
BC008_01075	2374	-2.9	BC008_03395	2272	-1.1	BC008_05729	601	-0.1
BC008_01076	51	0.4	BC008_03396	2135	-2.0	BC008_05730	1385	-1.4
BC008_01077	1645	0.5	BC008_03397	6624	-1.6	BC008_05731	1643	1.3
BC008_01079	747	-0.6	BC008_03400	1614	-2.7	BC008_05732	283	-1.8
BC008_01080	3005	-0.3	BC008_03401	3297	-3.1	BC008_05733	345	1.7
BC008_01081	8076	-3.3	BC008_03402	4608	-2.9	BC008_05734	1320	0.3
BC008_01082	500	1.5	BC008_03403	558	-0.7	BC008_05735	4178	-2.7
BC008_01083	1161	2.4	BC008_03404	39	-2.4	BC008_05736	1414	-2.6
BC008_01084	5931	-0.6	BC008_03405	4711	-2.4	BC008_05737	152	-1.9
BC008_01085	298	1.5	BC008_03406	1995	-3.7	BC008_05738	1271	-2.7
BC008_01086	1537	-0.4	BC008_03407	11085	0.3	BC008_05739	29	1.3
BC008_01087	794	-2.0	BC008_03408	2255	-0.9	BC008_05740	31	2.6
BC008_01088	1549	0.4	BC008_03409	2101	-3.9	BC008_05741	370	1.4
BC008_01089	973	-1.5	BC008_03410	1773	-3.2	BC008_05742	1084	3.7
BC008_01090	2267	1.0	BC008_03411	585	-2.3	BC008_05743	815	0.5
BC008_01091	290	-0.6	BC008_03412	9876	-0.9	BC008_05744	1377	-2.6
BC008_01092	358	2.1	BC008_03413	1077	-1.0	BC008_05745	3013	1.2
BC008_01093	339	-0.8	BC008_03414	419	1.2	BC008_05746	302	0.1
BC008_01094	1377	-0.4	BC008_03415	36293	-2.9	BC008_05747	1540	1.6
BC008_01095	928	0.8	BC008_03416	3822	0.3	BC008_05748	1309	-0.4
BC008_01096	12537	0.6	BC008_03417	821	-0.5	BC008_05749	1258	3.4
BC008_01097	379	-0.7	BC008_03418	661	-1.4	BC008_05750	469	1.1
BC008_01098	2086	-0.6	BC008_03419	1176	-0.1	BC008_05751	1090	0.9
BC008_01099	8514	-3.3	BC008_03420	4214	2.7	BC008_05752	276	0.2

BC008_01100	556	2.8	BC008_03421	1188	-1.4	BC008_05753	1104	-0.5
BC008_01101	2618	-1.3	BC008_03422	493	-1.4	BC008_05754	328	0.3
BC008_01102	2629	-0.6	BC008_03423	1033	2.4	BC008_05755	413	0.6
BC008_01103	918	-0.5	BC008_03424	2460	-0.9	BC008_05756	1068	-1.2
BC008_01104	6196	-1.5	BC008_03425	1362	0.6	BC008_05757	104	-0.1
BC008_01105	1289	1.4	BC008_03426	98	0.2	BC008_05758	754	0.8
BC008_01106	2658	0.6	BC008_03427	692	-1.0	BC008_05759	701	-0.6
BC008_01107	2640	0.1	BC008_03428	309	-0.9	BC008_05760	249	1.9
BC008_01108	841	-1.9	BC008_03429	1317	-3.5	BC008_05761	214	2.4
BC008_01109	5356	2.4	BC008_03430	1476	-0.8	BC008_05762	906	-3.0
BC008_01110	2553	0.7	BC008_03431	308	-0.1	BC008_05763	897	-0.3
BC008_01111	4208	-2.7	BC008_03432	729	0.2	BC008_05764	6649	-6.0
BC008_01112	57	0.2	BC008_03433	365	0.6	BC008_05765	4383	-3.2
BC008_01113	1603	0.3	BC008_03434	4697	-1.0	BC008_05766	565	0.7
BC008_01114	5016	0.1	BC008_03435	1597	-3.3	BC008_05767	383	-0.3
BC008_01115	1874	2.0	BC008_03436	1663	-2.0	BC008_05768	533	1.8
BC008_01116	1275	-0.3	BC008_03437	136	-0.1	BC008_05769	3373	-3.6
BC008_01117	1092	0.9	BC008_03438	1906	3.7	BC008_05770	1740	3.0
BC008_01118	403	0.9	BC008_03439	869	-1.3	BC008_05771	1470	-1.3
BC008_01119	8761	-3.3	BC008_03440	500	0.0	BC008_05772	858	-3.3
BC008_01120	1480	-2.4	BC008_03441	390	1.2	BC008_05773	800	2.5
BC008_01121	584	-1.7	BC008_03442	304	0.1	BC008_05774	6313	-3.0
BC008_01122	3243	-3.5	BC008_03443	305	1.1	BC008_05775	4256	3.0
BC008_01123	299	0.6	BC008_03444	205	0.0	BC008_05776	1442	1.6
BC008_01124	133	-0.5	BC008_03445	306	-0.4	BC008_05777	693	3.3
BC008_01125	558	-0.3	BC008_03446	839	0.6	BC008_05778	1156	2.7
BC008_01126	12221	-3.2	BC008_03447	11603	-2.8	BC008_05779	401	3.5
BC008_01127	4443	-1.8	BC008_03448	1877	-3.0	BC008_05780	123	2.0
BC008_01128	3283	-3.0	BC008_03449	1289	-0.5	BC008_05781	503	-0.5
BC008_01129	4431	-1.9	BC008_03450	257	6.2	BC008_05782	2150	-1.1
BC008_01130	2767	-1.4	BC008_03451	879	6.2	BC008_05783	563	-0.2
BC008_01131	2383	-1.9	BC008_03452	721	4.7	BC008_05784	146	1.1
BC008_01132	500	2.3	BC008_03453	201	2.6	BC008_05785	774	-0.8
BC008_01133	343	0.8	BC008_03454	41	-1.0	BC008_05786	1059	-0.3
BC008_01134	3136	-3.4	BC008_03455	407	-1.1	BC008_05787	167	-0.1
BC008_01135	4465	-2.2	BC008_03456	765	-0.7	BC008_05788	1846	0.6
BC008_01136	5059	1.2	BC008_03457	50477	-2.1	BC008_05789	409	-1.1
BC008_01137	875	1.8	BC008_03458	8817	-2.7	BC008_05790	127	-0.1
BC008_01138	174	-0.1	BC008_03459	1135	-0.7	BC008_05791	10638	-2.0

BC008_01139	229	-1.8	BC008_03460	10626	-3.0	BC008_05792	668	1.9
BC008_01140	349	0.5	BC008_03461	457	-0.3	BC008_05793	53	0.5
BC008_01141	13312	-3.4	BC008_03462	1076	-1.0	BC008_05794	723	0.1
BC008_01142	2415	-2.1	BC008_03463	264	2.7	BC008_05795	1471	0.9
BC008_01143	3282	-2.1	BC008_03464	810	2.6	BC008_05796	132	7.0
BC008_01144	6933	-2.6	BC008_03465	801	-1.1	BC008_05797	123	0.0
BC008_01145	1913	0.0	BC008_03466	822	1.1	BC008_05798	1803	2.7
BC008_01146	673	-0.3	BC008_03467	1757	-1.3	BC008_05799	1039	-1.9
BC008_01147	364	1.8	BC008_03468	1182	0.0	BC008_05800	582	-3.7
BC008_01148	452	-0.5	BC008_03469	730	0.3	BC008_05801	1686	-4.1
BC008_01149	453	1.2	BC008_03470	937	0.0	BC008_05802	245	-0.2
BC008_01150	563	-1.3	BC008_03471	4618	-3.7	BC008_05803	790	2.7
BC008_01151	92	0.0	BC008_03472	2262	-0.4	BC008_05804	207	3.7
BC008_01152	1182	0.7	BC008_03473	2578	-1.1	BC008_05805	183	2.5
BC008_01153	1006	0.8	BC008_03474	5032	-0.5	BC008_05806	1151	3.3
BC008_01154	438	2.3	BC008_03475	1154	0.8	BC008_05807	660	-0.6
BC008_01155	1024	-1.7	BC008_03476	466	0.2	BC008_05808	197	1.3
BC008_01156	4850	-0.5	BC008_03477	1077	-0.8	BC008_05809	1340	2.7
BC008_01157	1970	-0.6	BC008_03478	5012	-1.6	BC008_05810	146889	-6.0
BC008_01158	24858	-1.6	BC008_03479	408	-2.5	BC008_05811	228035	-6.6
BC008_01159	1071	-2.1	BC008_03480	110	1.5	BC008_05812	17034	-3.3
BC008_01160	3821	-2.5	BC008_03481	731	0.4	BC008_05813	5046	-2.5
BC008_01161	6299	-0.8	BC008_03482	467	1.7	BC008_05814	1378	-3.5
BC008_01162	1013	-0.1	BC008_03483	36	1.5	BC008_05815	14583	-2.2
BC008_01163	157	0.6	BC008_03484	171	2.9	BC008_05816	1141	-2.6
BC008_01164	1119	1.5	BC008_03485	75	0.7	BC008_05817	3049	-0.7
BC008_01165	214	2.2	BC008_03486	56	1.5	BC008_05818	445	0.9
BC008_01166	452	5.0	BC008_03487	139	3.1	BC008_05819	1056	1.3
BC008_01167	613	0.8	BC008_03488	25	3.3	BC008_05820	155	1.7
BC008_01168	218	3.6	BC008_03489	83	3.4	BC008_05821	396	-0.5
BC008_01169	185	4.6	BC008_03492	69	0.5	BC008_05822	1927	-0.1
BC008_01170	529	3.7	BC008_03493	242	2.1	BC008_05823	1110	0.3
BC008_01171	306	1.6	BC008_03494	238	0.0	BC008_05824	12695	-3.3
BC008_01172	862	4.3	BC008_03495	178	-1.2	BC008_05825	1021	1.4
BC008_01173	220	1.9	BC008_03496	300	3.1	BC008_05826	871	-1.3
BC008_01174	1837	5.2	BC008_03497	327	1.3	BC008_05827	998	-1.1
BC008_01175	541	1.1	BC008_03498	302	1.0	BC008_05828	1445	0.8
BC008_01176	283	1.0	BC008_03499	261	1.8	BC008_05829	1128	1.0
BC008_01177	311	3.5	BC008_03500	699	2.3	BC008_05830	1412	-1.8

BC008_01178	2241	4.7	BC008_03501	309345	-6.2	BC008_05831	254	-0.3
BC008_01179	930	2.8	BC008_03502	674	0.2	BC008_05832	2733	-1.5
BC008_01180	16124	5.8	BC008_03503	520	3.3	BC008_05833	113	0.8
BC008_01181	1752	1.3	BC008_03504	42	4.6	BC008_05834	312	2.6
BC008_01182	2623	2.1	BC008_03505	3628	-1.1	BC008_05835	315	2.7
BC008_01183	303	0.0	BC008_03506	72	5.0	BC008_05836	304	-0.4
BC008_01184	423	2.8	BC008_03507	856	4.0	BC008_05837	1029	1.1
BC008_01185	247	0.7	BC008_03508	3621	4.7	BC008_05838	194	-0.5
BC008_01186	1938	-3.0	BC008_03509	2237	3.0	BC008_05839	580	1.5
BC008_01187	730	-0.6	BC008_03510	233	3.5	BC008_05840	78	0.7
BC008_01188	827	0.6	BC008_03511	130	2.6	BC008_05841	511	-0.3
BC008_01189	454	-0.8	BC008_03512	2228	2.7	BC008_05842	115	3.1
BC008_01190	622	0.8	BC008_03513	1971	5.1	BC008_05843	205	1.3
BC008_01191	339	-0.4	BC008_03514	1205	3.9	BC008_05844	784	0.2
BC008_01192	658	-1.0	BC008_03515	174	0.0	BC008_05845	143	-0.9
BC008_01193	201	-1.6	BC008_03516	1968	5.3	BC008_05846	1013	-2.1
BC008_01194	284	-0.4	BC008_03517	1054	5.7	BC008_05847	1044	-2.6
BC008_01195	211	-1.1	BC008_03518	294	4.8	BC008_05848	1266	0.2
BC008_01196	1489	-2.6	BC008_03519	1219	2.5	BC008_05849	1772	0.2
BC008_01197	3852	-0.3	BC008_03520	187	0.9	BC008_05850	5354	3.9
BC008_01198	641	-0.3	BC008_03521	1836	6.0	BC008_05851	1605	-0.5
BC008_01199	2293	1.0	BC008_03522	289	3.6	BC008_05852	524	3.3
BC008_01200	1069	-1.3	BC008_03523	580	5.7	BC008_05853	112	1.3
BC008_01201	1875	-2.8	BC008_03524	949	5.6	BC008_05854	1111	-2.6
BC008_01202	5332	-2.5	BC008_03525	150	0.0	BC008_05855	1367	-2.4
BC008_01203	9893	-4.3	BC008_03526	222	0.8	BC008_05856	488	-1.7
BC008_01204	49903	-2.8	BC008_03527	57	-1.2	BC008_05857	1265	-1.2
BC008_01205	87	0.2	BC008_03528	755	-0.2	BC008_05858	878	-1.1
BC008_01206	1913	0.6	BC008_03529	471	-0.5	BC008_05859	1277	0.1
BC008_01207	393	-2.2	BC008_03530	241	4.0	BC008_05860	1325	0.0
BC008_01208	30891	-3.6	BC008_03531	174	6.1	BC008_05861	381	0.3
BC008_01209	3343	-0.4	BC008_03532	452	0.3	BC008_05862	720	-1.3
BC008_01210	1979	-0.5	BC008_03533	2332	-2.4	BC008_05863	123	-0.3
BC008_01211	786	-0.9	BC008_03534	164	0.7	BC008_05864	35	1.0
BC008_01212	798	-0.9	BC008_03535	254	-0.5	BC008_05865	1119	4.2
BC008_01213	1959	-1.1	BC008_03536	129	2.2	BC008_05866	228	1.1
BC008_01214	1820	-1.5	BC008_03537	1192	1.6	BC008_05867	3435	5.4
BC008_01215	1289	-2.7	BC008_03538	960	-0.8	BC008_05868	367	4.1
BC008_01216	5056	-4.4	BC008_03539	7166	-3.6	BC008_05869	275	1.3

BC008_01217	806	-1.0	BC008_03540	879	0.7	BC008_05870	227	2.2
BC008_01218	1242	-1.0	BC008_03541	6563	9.2	BC008_05871	135	2.1
BC008_01219	2138	-1.7	BC008_03542	99	-0.7	BC008_05872	218	0.4
BC008_01220	1072	-1.3	BC008_03543	128	-0.2	BC008_05873	140	4.1
BC008_01221	2697	-1.5	BC008_03544	81	2.3	BC008_05874	185	3.5
BC008_01222	1780	-0.7	BC008_03545	109	1.7	BC008_05875	2436	0.6
BC008_01223	1108	-0.8	BC008_03546	61	1.6	BC008_05876	249	0.1
BC008_01224	2184	-2.6	BC008_03547	297	1.1	BC008_05877	356	2.0
BC008_01225	217	0.3	BC008_03548	1462	0.4	BC008_05878	10735	-1.8
BC008_01226	283	2.2	BC008_03549	834	5.5	BC008_05879	710	3.4
BC008_01227	1052	-2.8	BC008_03550	533	6.2	BC008_05880	704	0.2
BC008_01228	2997	-2.6	BC008_03551	240	0.5	BC008_05881	289	3.9
BC008_01229	679	-1.9	BC008_03552	318	1.3	BC008_05882	9	2.8
BC008_01230	2152	-2.1	BC008_03553	162	0.7	BC008_05883	24	4.5
BC008_01231	3004	-2.4	BC008_03554	320	-0.1	BC008_05884	3036	0.8
BC008_01232	10002	-3.0	BC008_03555	770	0.0	BC008_05885	1305	-1.5
BC008_01233	1480	-1.8	BC008_03556	3233	1.4	BC008_05886	79	1.4
BC008_01234	16955	-2.6	BC008_03557	1236	-1.7	BC008_05887	3328	-1.3
BC008_01235	82837	-5.5	BC008_03558	4389	-3.1	BC008_05888	716	2.7
BC008_01236	70431	-5.5	BC008_03559	791	1.1	BC008_05889	168	2.7
BC008_01237	6432	0.8	BC008_03560	519	2.5	BC008_05890	230	4.4
BC008_01238	6174	3.5	BC008_03561	2528	-2.0	BC008_05891	153	5.5
BC008_01239	4769	4.3	BC008_03562	1376	-3.3	BC008_05892	1246	0.0
BC008_01240	2958	-0.2	BC008_03563	25661	-6.1	BC008_05893	119	-0.6
BC008_01241	619	-1.1	BC008_03564	34571	-5.0	BC008_05894	375	3.6
BC008_01242	1299	2.3	BC008_03565	2745	-4.9	BC008_05895	139	3.0
BC008_01243	431	3.5	BC008_03566	7866	-3.9	BC008_05896	151	0.7
BC008_01244	181	5.5	BC008_03567	4767	-3.1	BC008_05897	367	-0.5
BC008_01245	319	-1.5	BC008_03568	3472	-3.6	BC008_05898	134	0.8
BC008_01246	240	-1.2	BC008_03569	17906	-3.9	BC008_05899	3847	-1.5
BC008_01247	250	2.2	BC008_03570	820	-2.2	BC008_05900	973	5.9
BC008_01248	798	-2.4	BC008_03571	323	2.0	BC008_05901	46	4.4
BC008_01249	325	1.7	BC008_03572	429	1.8	BC008_05902	9904	7.4
BC008_01250	564	4.3	BC008_03573	739	5.4	BC008_05903	82	1.8
BC008_01251	722	3.3	BC008_03574	1483	3.3	BC008_05904	88	1.8
BC008_01252	110	1.7	BC008_03575	752	2.1	BC008_05905	9839	7.3
BC008_01253	1715	1.6	BC008_03576	143	0.6	BC008_05906	32	3.8
BC008_01254	263	5.2	BC008_03577	180301	-1.7	BC008_05907	987	5.7
BC008_01255	851	4.9	BC008_03578	2591	-1.9	BC008_05908	247	3.0

BC008_01256	1363	4.9	BC008_03579	8027	-0.8	BC008_05909	306	0.7
BC008_01257	366	0.6	BC008_03580	3048	2.4	BC008_05910	649	0.2
BC008_01258	20882	-5.1	BC008_03581	2964	-2.0	BC008_05911	2231	-1.4
BC008_01259	891	-0.9	BC008_03582	3036	0.1	BC008_05912	724	-0.9
BC008_01260	2300	-2.8	BC008_03583	485	-1.4	BC008_05913	311	2.4
BC008_01261	192	-2.7	BC008_03584	1820	-1.0	BC008_05914	2505	1.4
BC008_01262	271	-2.0	BC008_03585	2578	-4.0	BC008_05915	3622	0.4
BC008_01263	686	1.7	BC008_03586	9298	-4.3	BC008_05916	904	-2.2
BC008_01264	67	-1.6	BC008_03587	45633	-3.8	BC008_05917	929	-2.2
BC008_01265	47	2.2	BC008_03588	12022	-4.2	BC008_05918	5746	-0.9
BC008_01266	2140	0.5	BC008_03589	448833	-4.0	BC008_05919	8432	-2.0
BC008_01267	1348	-3.3	BC008_03590	75624	-4.9	BC008_05920	640	-0.6
BC008_01268	2201	-2.5	BC008_03591	135877	-3.4	BC008_05921	553	-1.8
BC008_01269	3728	3.5	BC008_03592	179955	-3.6	BC008_05922	1111	-1.3
BC008_01270	205	-0.8	BC008_03593	531359	-3.3	BC008_05923	30460	-2.1
BC008_01271	644	-0.7	BC008_03594	82662	-2.9	BC008_05924	377	-1.9
BC008_01272	1180	-1.6	BC008_03595	106568	-3.5	BC008_05925	19340	-3.6
BC008_01273	950	-2.1	BC008_03596	25006	-3.2	BC008_05926	3173	-2.9
BC008_01274	403	-0.6	BC008_03597	10740	-3.1	BC008_05927	14072	-3.5
BC008_01275	1099	-0.3	BC008_03598	5214	-3.0	BC008_05928	35231	-1.1
BC008_01276	2328	-2.3	BC008_03599	5727	-0.5	BC008_05929	7049	-2.4
BC008_01277	639	-1.8	BC008_03600	17645	-3.6	BC008_05930	16713	-2.7
BC008_01278	47390	-0.6	BC008_03601	14262	-4.4	BC008_05931	1977	-1.5
BC008_01279	5583	-0.6	BC008_03602	8292	-2.1	BC008_05932	1879	0.0
BC008_01280	3948	-1.5	BC008_03603	2077	-2.5	BC008_05933	2137	-2.5
BC008_01281	455	-0.8	BC008_03604	1320	0.5	BC008_05934	7744	-3.0
BC008_01282	1894	-2.7	BC008_03605	715	4.5	BC008_05935	7212	-3.7
BC008_01283	2910	0.3	BC008_03606	698	3.7	BC008_05936	1036	0.5
BC008_01284	594	0.5	BC008_03607	3304	5.2	BC008_05937	159	-0.6
BC008_01285	1364	-1.0	BC008_03608	3614	3.6	BC008_05939	622	-0.4
BC008_01286	329	-1.5	BC008_03609	816	-0.8	BC008_05940	1069	-2.7
BC008_01287	603	0.6	BC008_03610	304	1.1	BC008_05941	6785	-2.3
BC008_01288	1041	-0.7	BC008_03611	795	-0.2	BC008_05942	45	-0.8
BC008_01289	379	1.1	BC008_03612	1313	-0.3	BC008_05943	1317	-1.5
BC008_01290	1055	-0.4	BC008_03613	664	2.5	BC008_05944	3173	1.2
BC008_01291	225	4.0	BC008_03614	631	3.7	BC008_05945	2012	1.1
BC008_01292	8507	-1.6	BC008_03615	1292	5.1	BC008_05946	5125	-0.3
BC008_01293	114	2.3	BC008_03616	297	4.2	BC008_05947	24215	-2.2
BC008_01294	2742	2.7	BC008_03617	359	3.4	BC008_05948	725	2.8

BC008_01295	163	0.8	BC008_03618	605	1.2	BC008_05949	6412	-3.3
BC008_01296	8	1.8	BC008_03619	1620	1.3	BC008_05950	3482	-1.1
BC008_01297	707	2.6	BC008_03620	159	0.6	BC008_05951	700	-1.1
BC008_01299	884	1.9	BC008_03621	767	4.5	BC008_05952	1229	2.7
BC008_01300	9170	9.0	BC008_03622	103	2.4	BC008_05953	829	1.4
BC008_01301	3445	-2.8	BC008_03623	4337	1.1	BC008_05954	562	-1.4
BC008_01302	1207	0.7	BC008_03624	619	-0.8	BC008_05955	1614	-1.5
BC008_01303	528	-0.6	BC008_03625	3792	-5.1	BC008_05956	38339	-1.8
BC008_01304	365	-0.8	BC008_03626	420	-1.1	BC008_05957	615	-0.9
BC008_01305	2043	1.9	BC008_03627	296	4.0	BC008_05958	85	3.4
BC008_01306	1675	1.9	BC008_03628	3807	4.7	BC008_05959	1054	1.4
BC008_01307	996	1.4	BC008_03629	1041	-2.0	BC008_05960	1662	-2.4
BC008_01308	558	-2.2	BC008_03630	204	1.2	BC008_05961	1346	-1.5
BC008_01309	943	1.0	BC008_03631	1436	0.9	BC008_05962	645	-0.2
BC008_01310	1074	0.3	BC008_03632	488	4.9	BC008_05963	716	1.4
BC008_01311	315	-0.3	BC008_03633	849	0.2	BC008_05964	1751	-0.3
BC008_01312	666	-1.0	BC008_03634	66	2.8	BC008_05965	764	2.2
BC008_01313	2217	1.4	BC008_03635	66	1.2	BC008_05966	269	3.5
BC008_01314	16742	-2.5	BC008_03636	1641	1.5	BC008_05967	471	1.5
BC008_01315	68045	-0.6	BC008_03637	1063	-1.7	BC008_05968	3670	2.9
BC008_01316	17286	-4.5	BC008_03638	849	0.2	BC008_05969	691	-1.9
BC008_01317	26071	-4.5	BC008_03639	174	0.4	BC008_05970	437	-1.3
BC008_01318	27681	-4.6	BC008_03640	1766	2.1	BC008_05971	1899	-0.7
BC008_01319	376	1.1	BC008_03641	13614	-2.9	BC008_05972	288	4.3
BC008_01320	706	3.9	BC008_03642	1030	-0.7	BC008_05973	974	-2.0
BC008_01321	208	4.4	BC008_03643	113871	-4.5	BC008_05974	1271	5.1
BC008_01322	2011	-1.6	BC008_03644	3539	-0.7	BC008_05975	168	2.1
BC008_01323	1446	0.8	BC008_03645	1837	-0.6	BC008_05976	117	0.5
BC008_01324	912	-0.3	BC008_03646	639	-1.5	BC008_05977	1400	-0.1
BC008_01325	94	0.0	BC008_03647	453	-0.9	BC008_05978	354	-1.3
BC008_01326	477	-0.9	BC008_03648	274	-1.4	BC008_05979	6483	-2.3
BC008_01327	938	-1.9	BC008_03649	31	-0.6	BC008_05980	2045	-3.5
BC008_01328	103	0.6	BC008_03650	128	-0.5	BC008_05981	515	-2.1
BC008_01329	4242	-2.4	BC008_03651	6824	0.5	BC008_05982	1900	-2.0
BC008_01330	1564	3.1	BC008_03652	1487	4.3	BC008_05983	9949	-1.4
BC008_01331	237	1.5	BC008_03653	974	4.0	BC008_05984	859	-1.3
BC008_01332	69	2.8	BC008_03654	1339	-1.7	BC008_05985	1496	-0.1
BC008_01333	138	1.4	BC008_03655	1236	1.8	BC008_05986	1831	-0.2
BC008_01334	3518	-1.0	BC008_03656	947	-1.7	BC008_05987	559	-0.3

BC008_01335	7948	-2.9	BC008_03657	1098	0.2	BC008_05988	136	0.9
BC008_01336	3078	-3.2	BC008_03658	440	0.4	BC008_05989	86	-0.4
BC008_01337	775	2.3	BC008_03659	7646	0.8	BC008_05990	51	0.1
BC008_01338	366	-1.0	BC008_03660	3963	-0.3	BC008_05991	12935	-3.4
BC008_01339	9702	-1.0	BC008_03661	638	-0.8	BC008_05992	1465	-0.4
BC008_01340	3652	3.0	BC008_03662	1776	-0.4	BC008_05993	79	1.9
BC008_01341	1367	-0.4	BC008_03663	12384	3.0	BC008_05994	395	2.9
BC008_01342	3867	-1.1	BC008_03664	1513	-0.8	BC008_05995	2327	-1.3
BC008_01343	2594	-1.1	BC008_03665	1238	3.6	BC008_05996	1273	3.2
BC008_01344	1605	-3.8	BC008_03666	2202	3.3	BC008_05997	1063	-0.1
BC008_01345	2471	0.0	BC008_03667	588	0.8	BC008_05998	1721	-1.5
BC008_01346	7913	-1.4	BC008_03668	1000	-0.4	BC008_05999	5364	-1.3
BC008_01347	475	-2.5	BC008_03669	130	3.0	BC008_06000	44	0.6
BC008_01348	361	-1.1	BC008_03670	129	3.3	BC008_06001	4835	-1.5
BC008_01349	1279	0.6	BC008_03671	335	3.7	BC008_06002	605	0.1
BC008_01350	835	1.4	BC008_03672	275	3.4	BC008_06003	616	0.0
BC008_01351	1834	-0.1	BC008_03673	997	5.1	BC008_06004	1445	-1.2
BC008_01352	233	-0.4	BC008_03674	836	1.5	BC008_06005	1753	2.7
BC008_01353	252	1.8	BC008_03675	212	0.4	BC008_06006	2360	-3.9
BC008_01354	47	1.1	BC008_03676	379	0.3	BC008_06007	31425	-4.4
BC008_01355	358	1.6	BC008_03677	2187	0.0	BC008_06008	242	0.4
BC008_01356	670	-0.5	BC008_03678	496	0.3	BC008_06009	320	4.1
BC008_01358	957	-0.6	BC008_03679	1430	0.4	BC008_06010	176	2.2
BC008_01359	560	-1.4	BC008_03680	1144	0.6	BC008_06011	1986	-1.4
BC008_01360	1873	2.9	BC008_03681	252	2.9	BC008_06012	2499	0.9
BC008_01361	1468	-3.1	BC008_03682	307	0.5	BC008_06013	3704	-1.7
BC008_01362	126631	-5.0	BC008_03683	907	1.1	BC008_06014	1315	-1.6
BC008_01363	945	0.7	BC008_03684	1265	1.1	BC008_06015	580	-0.5
BC008_01364	304	0.4	BC008_03685	2147	-0.1	BC008_06016	197	3.1
BC008_01365	3256	0.1	BC008_03686	1389	-2.2	BC008_06017	122	-0.8
BC008_01366	1810	-1.5	BC008_03687	941	-0.6	BC008_06018	794	-1.1
BC008_01367	525	0.0	BC008_03688	4979	-1.9	BC008_06019	1543	1.1
BC008_01368	21	2.1	BC008_03689	4292	1.0	BC008_06020	148	2.1
BC008_01369	139	0.7	BC008_03690	12751	0.2	BC008_06021	5260	-6.3
BC008_01370	199	0.6	BC008_03691	6414	-2.5	BC008_06022	841	-1.4
BC008_01371	8287	4.7	BC008_03692	5510	-1.9	BC008_06023	130	2.5
BC008_01372	1815	0.5	BC008_03693	31318	-2.4	BC008_06024	486	-1.2
BC008_01373	837	-0.7	BC008_03694	6134	3.3	BC008_06025	3141	2.4
BC008_01374	1495	-2.9	BC008_03695	2270	-1.5	BC008_06026	410	3.2

BC008_01375	2400	-1.7	BC008_03696	1188	-3.3	BC008_06027	906	0.8
BC008_01376	2200	0.1	BC008_03697	958	-0.2	BC008_06028	2422	4.0
BC008_01377	489	2.8	BC008_03698	130	0.4	BC008_06029	2300	-2.5
BC008_01378	261	-0.5	BC008_03699	1462	0.4	BC008_06030	1699	1.9
BC008_01379	2229	3.3	BC008_03700	332	2.2	BC008_06031	1004	1.2
BC008_01380	4901	1.2	BC008_03701	1126	-2.1	BC008_06032	525	1.4
BC008_01381	3918	-4.3	BC008_03702	583	3.0	BC008_06033	513	0.8
BC008_01382	679	-2.7	BC008_03703	812	-0.5	BC008_06034	984	-2.4
BC008_01383	810	-2.3	BC008_03704	2681	1.7	BC008_06035	829	-2.5
BC008_01384	615	-1.1	BC008_03705	1726	-2.8	BC008_06036	248	-1.2
BC008_01385	10507	-1.8	BC008_03706	2151	0.7	BC008_06037	675	0.4
BC008_01386	2463	-0.9	BC008_03707	362	1.7	BC008_06038	358	0.8
BC008_01387	583	5.2	BC008_03708	1716	-0.2	BC008_06039	453	0.2
BC008_01388	320	1.2	BC008_03709	3439	2.2	BC008_06040	12241	0.0
BC008_01389	12930	1.3	BC008_03710	961	-1.7	BC008_06041	583	6.6
BC008_01390	868	-2.3	BC008_03711	3653	1.1	BC008_06042	35	4.9
BC008_01391	703	-1.0	BC008_03712	69	-0.3	BC008_06043	280	1.9
BC008_01392	778	-2.9	BC008_03713	10762	-5.6	BC008_06044	77	2.1
BC008_01393	6415	-2.0	BC008_03714	4870	-5.5	BC008_06045	433	0.3
BC008_01394	3197	-1.3	BC008_03715	363	1.3	BC008_06046	588	-0.6
BC008_01395	949	-3.0	BC008_03716	1985	-0.1	BC008_06047	445	-0.5
BC008_01396	306	-0.4	BC008_03717	740	-0.8	BC008_06048	8631	-4.1
BC008_01397	975	-2.1	BC008_03718	967	0.4	BC008_06049	191	-0.9
BC008_01398	3361	-2.1	BC008_03719	2233	-2.5	BC008_06050	658	-0.5
BC008_01399	2669	-2.1	BC008_03720	3413	-2.6	BC008_06051	66139	-2.4
BC008_01400	21832	-4.6	BC008_03721	2711	-2.3	BC008_06052	198402	-2.1
BC008_01401	2805	-3.4	BC008_03722	1531	-1.5	BC008_06053	31429	-0.8
BC008_01402	1082	-2.0	BC008_03723	444	0.4	BC008_06054	275	0.8
BC008_01403	2353	6.0	BC008_03724	8048	2.4	BC008_06055	2397	0.3
BC008_01404	925	-0.2	BC008_03725	75	-0.1	BC008_06056	6765	-0.7
BC008_01405	693	0.9	BC008_03726	1172	0.8	BC008_06057	2890	-1.2
BC008_01406	1593	0.1	BC008_03727	283	3.5	BC008_06058	2293	-2.3
BC008_01407	573	0.5	BC008_03728	2073	-2.0	BC008_06059	157	0.5
BC008_01408	1213	-0.8	BC008_03729	650	-2.3	BC008_06060	4721	3.3
BC008_01409	1413	1.1	BC008_03730	241	-1.6	BC008_06061	23204	3.8
BC008_01410	1916	0.9	BC008_03731	26401	-3.3	BC008_06062	2934	3.0
BC008_01411	791	-1.6	BC008_03732	374	-1.9	BC008_06063	3255	1.7
BC008_01412	24886	-0.9	BC008_03733	76698	-1.6	BC008_06064	415	-1.1
BC008_01413	975	-0.4	BC008_03734	536	0.5	BC008_06065	1701	1.3

BC008_01414	756	0.0	BC008_03735	219	-0.2	BC008_06066	1038	-0.8
BC008_01415	548	-1.2	BC008_03736	321	0.2	BC008_06067	1101	-1.0
BC008_01416	3922	-1.4	BC008_03737	771	-0.5	BC008_06068	22914	-3.1
BC008_01417	27700	-5.3	BC008_03738	1653	-0.7	BC008_06069	455	-1.1
BC008_01418	92	-1.7	BC008_03739	1067	-1.8	BC008_06070	5067	0.1
BC008_01419	2588	-2.7	BC008_03740	311	1.0	BC008_06071	533	-0.6
BC008_01420	518	-2.3	BC008_03741	199	-0.1	BC008_06072	1102	0.9
BC008_01421	4975	-3.8	BC008_03742	321	-0.3	BC008_06073	1145	0.3
BC008_01422	4058	-1.1	BC008_03743	309	0.0	BC008_06074	7755	-1.6
BC008_01423	3354	-0.9	BC008_03744	882	-0.4	BC008_06075	27691	-6.5
BC008_01424	258	-1.7	BC008_03745	416	1.2	BC008_06076	2073	-1.5
BC008_01425	21	0.4	BC008_03746	2633	1.0	BC008_06077	1105	-1.8
BC008_01426	296	-3.0	BC008_03747	1971	-0.6	BC008_06078	2557	0.0
BC008_01427	3272	-2.4	BC008_03748	429	1.4	BC008_06079	198	-1.1
BC008_01428	2522	-3.0	BC008_03749	1768	-0.7	BC008_06080	1158	-0.4
BC008_01429	405	-0.3	BC008_03750	384	0.3	BC008_06081	700	-0.7
BC008_01430	1422	-3.4	BC008_03751	7264	-0.8	BC008_06082	2504	-0.9
BC008_01431	162	1.0	BC008_03752	3420	2.0	BC008_06083	277	0.0
BC008_01432	3066	-0.6	BC008_03753	246	0.9	BC008_06084	327	-0.1
BC008_01433	1019	-1.7	BC008_03754	2688	-0.8	BC008_06085	4243	2.5
BC008_01434	1753	-0.4	BC008_03755	725	0.2	BC008_06086	2404	0.1
BC008_01435	369	2.8	BC008_03756	8917	-2.4	BC008_06087	1170	0.7
BC008_01436	502	2.5	BC008_03757	3438	-2.0	BC008_06088	476	4.4
BC008_01437	4010	-2.4	BC008_03758	996	-1.9	BC008_06089	213	3.3
BC008_01438	150	-0.8	BC008_03759	2511	-3.7	BC008_06090	310	1.0
BC008_01439	20040	-3.8	BC008_03760	229	4.0	BC008_06091	661	1.8
BC008_01440	18262	-0.7	BC008_03761	844	5.1	BC008_06092	355	0.6
BC008_01441	875	-2.8	BC008_03762	1890	3.7	BC008_06093	166	-0.7
BC008_01442	35881	-1.7	BC008_03763	423	0.2	BC008_06094	175	-0.7
BC008_01443	9652	-2.1	BC008_03764	2411	-2.0	BC008_06095	4471	-1.6
BC008_01444	3385	-2.6	BC008_03765	186	-0.4	BC008_06096	2693	-0.7
BC008_01445	8083	-1.2	BC008_03766	12624	-5.8	BC008_06097	2713	0.3
BC008_01446	3979	-3.2	BC008_03767	1146	2.8	BC008_06098	2747	-2.0
BC008_01447	4023	-2.7	BC008_03768	712	1.9	BC008_06099	9171	-2.3
BC008_01448	881	-0.6	BC008_03769	89	1.9	BC008_06100	4372	-2.2
BC008_01449	10019	0.7	BC008_03770	134	0.4	BC008_06101	4165	-0.4
BC008_01450	400	2.0	BC008_03771	1652	0.5	BC008_06102	525	0.3
BC008_01451	1183	-2.2	BC008_03772	3199	-0.9	BC008_06103	565	-0.2
BC008_01452	298	-1.1	BC008_03773	2219	-2.1	BC008_06104	1418	2.4

BC008_01453	2660	-1.0	BC008_03774	2980	2.4	BC008_06105	9014	-4.5
BC008_01454	1661	0.5	BC008_03775	520	-2.1	BC008_06106	10169	-2.9
BC008_01455	13751	-3.1	BC008_03776	748	3.7	BC008_06107	1157	0.5
BC008_01456	4566	0.4	BC008_03777	2380	4.9	BC008_06108	302	0.9
BC008_01457	392	-0.2	BC008_03778	926	7.3	BC008_06109	672	2.7
BC008_01458	220	-0.6	BC008_03779	54	2.6	BC008_06110	753	2.3
BC008_01459	2688	-1.7	BC008_03780	897	4.5	BC008_06111	1617	0.8
BC008_01460	30984	1.2	BC008_03781	533	4.9	BC008_06112	420	0.8
BC008_01461	362	-0.6	BC008_03782	87	4.8	BC008_06113	2331	-1.1
BC008_01462	384	0.8	BC008_03783	333	4.2	BC008_06114	158	3.6
BC008_01463	379	2.2	BC008_03784	106	2.8	BC008_06115	2330	-2.0
BC008_01464	518	-0.2	BC008_03785	620	3.9	BC008_06116	3469	1.2
BC008_01465	652	-0.9	BC008_03786	192	3.9	BC008_06117	2657	-1.6
BC008_01466	5125	-3.1	BC008_03787	314	4.5	BC008_06118	3195	-3.2
BC008_01467	3337	-2.7	BC008_03788	1267	5.2	BC008_06119	12459	1.0
BC008_01468	836	0.3	BC008_03789	101	5.5	BC008_06120	13398	-4.3
BC008_01469	479	0.8	BC008_03790	557	6.3	BC008_06121	4424	-3.4
BC008_01470	547	0.1	BC008_03791	685	6.4	BC008_06122	111	-0.9
BC008_01471	367	-0.5	BC008_03792	177	5.1	BC008_06123	1405	0.8
BC008_01472	9643	-2.9	BC008_03793	34	1.3	BC008_06124	2250	0.0
BC008_01473	605	-0.2	BC008_03794	1338	5.2	BC008_06125	1646	-4.7
BC008_01474	1055	0.2	BC008_03795	4020	6.7	BC008_06126	666	1.3
BC008_01475	3617	-2.6	BC008_03796	309	4.6	BC008_06127	222	1.2
BC008_01476	2978	-4.3	BC008_03797	437	-0.1	BC008_06128	3704	1.3
BC008_01477	2843	2.6	BC008_03798	683	1.9	BC008_06129	2355	-0.4
BC008_01478	5555	-0.1	BC008_03799	368	-2.7	BC008_06130	2196	-2.9
BC008_01479	6527	-0.9	BC008_03800	9389	4.3	BC008_06131	256	-3.3
BC008_01480	348	-1.8	BC008_03801	13514	5.9	BC008_06132	25242	-5.9
BC008_01481	411	-0.4	BC008_03802	1724	2.2	BC008_06133	897	0.3
BC008_01482	3865	-0.3	BC008_03803	1796	0.7	BC008_06134	2205	-2.7
BC008_01483	30229	-0.3	BC008_03804	2442	-1.1	BC008_06135	1839	-0.2
BC008_01484	17027	-3.6	BC008_03805	2172	0.6	BC008_06136	4598	-1.0
BC008_01485	38859	-2.2	BC008_03806	9998	9.9	BC008_06137	357	0.9
BC008_01486	78098	-1.3	BC008_03807	157	4.6	BC008_06138	945	0.6
BC008_01487	624	-2.4	BC008_03808	219	2.7	BC008_06139	843	1.2
BC008_01488	751	-0.2	BC008_03809	75	0.6	BC008_06140	562	1.9
BC008_01489	1076	0.2	BC008_03810	7692	2.0	BC008_06141	358	0.2
BC008_01490	**781**	**3.4**	BC008_03811	100	2.0	BC008_06142	1012	-1.8
BC008_01491	418	-0.2	BC008_03812	2126	0.7	BC008_06143	4673	2.9

BC008_01492	5440	-0.1	BC008_03813	1330	2.4	BC008_06144	2622	-3.0
BC008_01493	6518	-3.8	BC008_03814	865	0.7	BC008_06145	4008	-1.3
BC008_01494	126	0.1	BC008_03815	1871	-3.0	BC008_06146	275	-1.1
BC008_01495	1038	-1.5	BC008_03816	4174	-4.2	BC008_06147	74	-0.6
BC008_01496	1913	-0.9	BC008_03817	538	-4.2	BC008_06148	419	0.6
BC008_01497	2376	-2.6	BC008_03818	53997	-5.4	BC008_06149	17069	-5.6
BC008_01498	5178	-5.0	BC008_03819	2544	-3.9	BC008_06150	3819	-3.2
BC008_01499	2107	-0.2	BC008_03820	11823	-2.2	BC008_06151	10760	-2.4
BC008_01500	4364	-0.6	BC008_03821	14974	-3.0	BC008_06152	9282	-2.0
BC008_01501	8046	-3.0	BC008_03822	739	-0.9	BC008_06153	987	-0.9
BC008_01502	32268	-1.1	BC008_03823	3655	-3.9	BC008_06154	1614	0.2
BC008_01503	7767	0.7	BC008_03824	9119	-4.6	BC008_06155	547	-1.0
BC008_01504	150	-0.2	BC008_03825	1670	-3.5	BC008_06156	371	2.8
BC008_01505	751	1.6	BC008_03826	598	-0.3	BC008_06157	52	1.7
BC008_01506	1426	-1.8	BC008_03827	1041	2.5	BC008_06158	1697	2.4
BC008_01507	1416	0.1	BC008_03828	288	3.6	BC008_06159	456	2.8
BC008_01508	361	2.2	BC008_03829	200	2.2	BC008_06160	371	8.2
BC008_01509	3639	7.1	BC008_03830	2674	0.7	BC008_06161	440	4.2
BC008_01510	531	1.0	BC008_03831	211	1.8	BC008_06162	51	0.0
BC008_01511	4578	4.3	BC008_03832	1832	-1.4	BC008_06163	1820	-0.8
BC008_01512	8751	0.0	BC008_03833	1345	0.0	BC008_06164	16	2.8
BC008_01513	6733	-4.7	BC008_03834	1972	4.4	BC008_06165	4726	-0.8
BC008_01514	1007	-2.5	BC008_03835	840	2.5	BC008_06166	14943	-2.6
BC008_01515	1175	-0.7	BC008_03836	914	-1.9	BC008_06167	2159	-0.8
BC008_01516	2958	-1.1	BC008_03837	479	-0.8	BC008_06168	102	-0.2
BC008_01517	21770	-3.2	BC008_03838	5021	-1.9	BC008_06169	208	2.0
BC008_01518	1233	0.7	BC008_03839	1749	-0.3	BC008_06170	4142	-1.4
BC008_01519	972	-2.2	BC008_03840	10591	-2.3	BC008_06171	684	0.7
BC008_01520	605	2.3	BC008_03841	3825	-2.9	BC008_06172	367	-0.7
BC008_01521	317	0.5	BC008_03842	7698	-2.2	BC008_06173	239	2.3
BC008_01522	1975	-0.2	BC008_03843	1518	-2.5	BC008_06174	295	-1.1
BC008_01523	85	-1.1	BC008_03844	8106	-4.0	BC008_06175	1057	0.4
BC008_01524	367	2.7	BC008_03845	1370	2.1	BC008_06176	993	0.8
BC008_01525	373	0.9	BC008_03846	1657	3.7	BC008_06177	279	-1.8
BC008_01526	702	2.4	BC008_03847	858	-2.0	BC008_06178	280	-0.5
BC008_01527	70	1.3	BC008_03848	335	-0.7	BC008_06179	220	2.1
BC008_01528	338	-1.7	BC008_03849	1047	3.4	BC008_06180	1117	-1.0
BC008_01529	970	0.3	BC008_03850	753	8.9	BC008_06181	232	1.1
BC008_01530	14474	0.1	BC008_03851	69	5.8	BC008_06182	77	0.2

BC008_01531	29797	-2.0	BC008_03852	43	1.9	BC008_06183	4011	1.3
BC008_01532	15208	1.3	BC008_03853	128	0.9	BC008_06184	3557	3.5
BC008_01533	336	1.7	BC008_03854	736	-0.6	BC008_06185	155	0.0
BC008_01534	471	1.4	BC008_03855	19329	7.6	BC008_06186	2910	2.8
BC008_01535	1570	2.7	BC008_03856	1105	2.7	BC008_06187	85	-1.0
BC008_01536	1214	0.7	BC008_03857	668	4.6	BC008_06188	673	-1.7
BC008_01537	391	0.4	BC008_03858	847	2.7	BC008_06189	897	-0.2
BC008_01538	368	4.4	BC008_03859	1624	0.1	BC008_06190	20352	-5.0
BC008_01539	396	1.4	BC008_03860	1275	-0.2	BC008_06191	1157	-0.8
BC008_01540	560	1.8	BC008_03861	303	1.0	BC008_06192	817	-1.5
BC008_01541	1693	1.8	BC008_03862	299	1.5	BC008_06193	7973	-5.2
BC008_01542	91	1.4	BC008_03863	2882	2.2	BC008_06194	3714	-4.4
BC008_01543	33	1.9	BC008_03864	529	3.7	BC008_06195	1166	3.3
BC008_01544	68	2.4	BC008_03865	204	0.9	BC008_06196	359	1.2
BC008_01545	125	1.9	BC008_03866	1147	-0.7	BC008_06197	253	0.2
BC008_01546	732	1.3	BC008_03867	1502	-0.9	BC008_06198	758	3.0
BC008_01547	222	1.8	BC008_03868	273	0.9	BC008_06199	85	1.3
BC008_01548	162	2.5	BC008_03869	315	3.2	BC008_06200	125	1.7
BC008_01549	130	2.3	BC008_03870	1818	-1.6	BC008_06201	969	-1.1
BC008_01550	859	-0.6	BC008_03871	3510	0.8	BC008_06202	738	4.1
BC008_01551	1141	1.0	BC008_03872	975	-1.6	BC008_06203	649	-0.6
BC008_01552	2146	1.3	BC008_03873	18048	1.5	BC008_06204	31	1.4
BC008_01553	365	-1.0	BC008_03874	1733	-0.2	BC008_06205	382	1.0
BC008_01554	344	0.1	BC008_03875	3055	-1.2	BC008_06206	751	1.2
BC008_01555	417	0.8	BC008_03876	4794	0.9	BC008_06207	245	-1.8
BC008_01556	100	0.2	BC008_03877	513	-0.6	BC008_06208	94	-0.3
BC008_01557	334	0.9	BC008_03878	1309	0.3	BC008_06209	179	0.0
BC008_01558	192	4.2	BC008_03879	458	-1.6	BC008_06210	811	3.4
BC008_01559	5389	2.4	BC008_03880	786	-1.3	BC008_06211	269	0.1
BC008_01560	1474	0.4	BC008_03881	2353	2.5	BC008_06212	413	3.1
BC008_01561	252	0.6	BC008_03882	707	1.6	BC008_06213	2555	-1.0
BC008_01562	548	-0.1	BC008_03883	251	3.0	BC008_06214	3004	0.3
BC008_01563	1680	-1.1	BC008_03884	5452	3.7	BC008_06215	4942	3.3
BC008_01564	8983	0.3	BC008_03885	102	2.6	BC008_06216	958	-0.2
BC008_01565	538	-0.2	BC008_03886	449	5.1	BC008_06217	668	0.3
BC008_01566	2639	-1.0	BC008_03887	301	5.2	BC008_06218	247	1.7
BC008_01567	943	-1.4	BC008_03888	3269	6.6	BC008_06219	537	0.2
BC008_01568	425	-1.3	BC008_03889	160	4.3	BC008_06220	445	1.8
BC008_01569	3766	-2.4	BC008_03890	459	0.4	BC008_06222	1289	4.2

BC008_01570	5895	2.0	BC008_03891	363	2.3	BC008_06223	47	0.1
BC008_01571	750	1.5	BC008_03892	234	3.8	BC008_06224	258	1.8
BC008_01572	525	-1.9	BC008_03893	544	6.5	BC008_06226	694	-2.0
BC008_01573	745	-1.7	BC008_03894	222	3.9	BC008_06227	1088	-2.1
BC008_01574	298	0.9	BC008_03895	199	5.2	BC008_06228	345	1.2
BC008_01575	1884	-3.2	BC008_03896	186	4.7	BC008_06229	2199	-2.0
BC008_01576	18418	-5.0	BC008_03897	113	4.8	BC008_06230	972	-3.7
BC008_01577	742	-0.8	BC008_03898	152	2.9	BC008_06231	1860	-2.0
BC008_01578	1554	-2.3	BC008_03899	1339	1.7	BC008_06232	753	-1.3
BC008_01579	804	-0.7	BC008_03900	241	2.2	BC008_06233	4450	1.1
BC008_01580	5003	-2.6	BC008_03901	339	5.6	BC008_06234	19	0.5
BC008_01581	2553	-0.2	BC008_03902	150	0.9	BC008_06235	890	0.7
BC008_01582	20576	-5.4	BC008_03903	599	2.6	BC008_06236	41	0.3
BC008_01583	205	-0.4	BC008_03904	671	-0.8	BC008_06237	50	4.1
BC008_01584	2404	-1.6	BC008_03905	557	7.2	BC008_06238	30	1.5
BC008_01585	4205	1.5	BC008_03906	834	2.7	BC008_06239	87	2.2
BC008_01586	122	-3.6	BC008_03907	202	-0.9	BC008_06240	116	0.8
BC008_01587	1416	-2.1	BC008_03908	816	-0.3	BC008_06241	12664	-1.1
BC008_01588	1129	-0.9	BC008_03909	6429	-1.6	BC008_06242	1346	-0.8
BC008_01589	156	3.7	BC008_03910	182	0.0	BC008_06243	1327	2.3
BC008_01590	7614	-3.1	BC008_03911	828	-0.3	BC008_06244	737	-1.4
BC008_01591	13240	-2.9	BC008_03912	311	1.4	BC008_06245	890	-0.4
BC008_01592	2281	-1.8	BC008_03913	2600	1.6	BC008_06246	415	-1.4
BC008_01593	1129	0.8	BC008_03914	1072	-1.1	BC008_06247	460	-1.8
BC008_01594	1240	0.1	BC008_03915	3946	1.0	BC008_06248	1149	-0.4
BC008_01595	296	0.1	BC008_03916	1422	3.8	BC008_06249	442	2.0
BC008_01596	1741	-0.4	BC008_03917	2071	-0.3	BC008_06250	4295	0.5
BC008_01597	309	1.1	BC008_03918	5711	0.5	BC008_06251	425	-0.7
BC008_01598	294	0.5	BC008_03919	681	3.2	BC008_06252	892	2.4
BC008_01599	630	-3.1	BC008_03920	72	3.2	BC008_06253	2213	2.6
BC008_01600	2486	-0.2	BC008_03921	1803	-1.4	BC008_06254	263	-0.5
BC008_01601	1003	-0.2	BC008_03922	2871	0.2	BC008_06255	3078	1.6
BC008_01602	1880	3.1	BC008_03923	25953	-1.4	BC008_06256	11252	-5.0
BC008_01603	1163	6.4	BC008_03924	8730	-3.7	BC008_06257	6030	-2.6
BC008_01604	29	-0.9	BC008_03925	2574	-3.9	BC008_06258	800	-0.3
BC008_01605	2386	-1.5	BC008_03926	75983	1.0	BC008_06259	102	1.9
BC008_01606	836	2.6	BC008_03927	939	-0.3	BC008_06260	28	-0.4
BC008_01607	428	5.2	BC008_03928	4499	-0.5	BC008_06261	147	-1.1
BC008_01608	760	-1.3	BC008_03929	303	-0.8	BC008_06262	748	2.0

BC008_01609	769	-1.6	BC008_03930	1113	-1.1	BC008_06263	7596	-3.6
BC008_01610	1380	-1.2	BC008_03931	10136	0.2	BC008_06264	996	-1.3
BC008_01611	261	1.2	BC008_03932	1175	-0.4	BC008_06265	5841	0.4
BC008_01612	255	1.5	BC008_03933	843	1.1	BC008_06266	2283	-0.6
BC008_01613	328	2.4	BC008_03934	1338	-2.2	BC008_06267	2070	2.1
BC008_01614	288	4.8	BC008_03935	31057	-1.1	BC008_06268	11150	0.3
BC008_01615	339	4.2	BC008_03936	777	-1.2	BC008_06269	24487	-0.3
BC008_01616	280	2.2	BC008_03937	1441	-2.2	BC008_06270	150	1.7
BC008_01617	729	-0.4	BC008_03938	255	4.5	BC008_06271	276	3.8
BC008_01618	375	0.3	BC008_03939	1482	0.1	BC008_06272	187	2.8
BC008_01619	2436	0.3	BC008_03940	1022	-1.0	BC008_06273	129	4.9
BC008_01620	2355	0.2	BC008_03941	2620	-0.7	BC008_06274	702	2.9
BC008_01621	866	-0.9	BC008_03942	563	1.0	BC008_06275	135	3.0
BC008_01622	120	1.0	BC008_03943	1187	2.6	BC008_06276	1120	6.7
BC008_01623	693	-1.3	BC008_03944	987	0.4	BC008_06277	567	1.6
BC008_01624	227	0.5	BC008_03945	381	-1.1	BC008_06278	422	1.3
BC008_01625	119	2.6	BC008_03946	1042	1.5	BC008_06279	735	0.5
BC008_01626	2461	-2.5	BC008_03947	1329	0.6	BC008_06280	2710	6.6
BC008_01627	1195	-0.4	BC008_03948	1139	-3.5	BC008_06281	717	0.9
BC008_01628	2109	-2.5	BC008_03949	2773	-0.4	BC008_06282	931	1.9
BC008_01629	4030	-4.2	BC008_03950	1538	-0.9	BC008_06283	537	-1.1
BC008_01630	608	-4.3	BC008_03951	2430	-2.1	BC008_06284	485	-1.3
BC008_01631	6900	-5.3	BC008_03952	897	-0.8	BC008_06285	392	3.4
BC008_01632	695	-2.8	BC008_03953	2269	-1.1	BC008_06286	210	-1.2
BC008_01633	4230	-1.7	BC008_03954	5191	-3.4	BC008_06287	5081	1.9
BC008_01634	3326	-1.2	BC008_03955	3680	-3.3	BC008_06288	3453	0.5
BC008_01635	981	-0.9	BC008_03956	988	-1.1	BC008_06289	803	1.6
BC008_01636	213	2.5	BC008_03957	11889	-4.3	BC008_06290	15298	-2.0
BC008_01637	1726	1.9	BC008_03958	5180	-1.4	BC008_06291	1818	1.5
BC008_01638	693	2.0	BC008_03959	3814	-2.0	BC008_06292	174	0.8
BC008_01639	114	4.1	BC008_03960	5062	-0.7	BC008_06293	8123	-3.6
BC008_01640	186	1.4	BC008_03961	4705	-1.9	BC008_06294	1036	-3.1
BC008_01641	1503	-3.0	BC008_03962	6221	-1.5	BC008_06295	3141	1.1
BC008_01642	477	-0.1	BC008_03963	2837	2.9	BC008_06296	923	3.6
BC008_01643	11308	-1.1	BC008_03964	673	4.7	BC008_06297	571	3.6
BC008_01644	226	-1.0	BC008_03965	242	4.9	BC008_06298	472	0.7
BC008_01645	2497	2.8	BC008_03966	862	0.4	BC008_06299	2738	-3.0
BC008_01646	541	-2.4	BC008_03967	1585	-0.6	BC008_06300	284	2.0
BC008_01647	1561	-2.5	BC008_03968	583	0.8	BC008_06301	1239	0.3

BC008_01648	1129	-0.7	BC008_03969	351	-0.4	BC008_06302	342	-0.4
BC008_01649	1076	0.6	BC008_03970	784	-1.1	BC008_06303	469	2.2
BC008_01650	457	-2.1	BC008_03971	468	-0.6	BC008_06304	87	1.3
BC008_01651	7245	1.0	BC008_03972	1034	-0.3	BC008_06305	796	2.9
BC008_01652	1797	-1.2	BC008_03973	250	0.5	BC008_06306	332	-0.1
BC008_01653	653	-0.2	BC008_03974	3882	-1.8	BC008_06307	103	3.7
BC008_01654	11386	2.1	BC008_03975	213	1.7	BC008_06308	535	-1.2
BC008_01655	290	1.1	BC008_03976	10878	-0.1	BC008_06309	2070	0.4
BC008_01656	364	-1.0	BC008_03977	14040	1.0	BC008_06310	311	0.1
BC008_01657	2051	-1.5	BC008_03978	504	0.1	BC008_06311	778	-1.8
BC008_01658	44	0.6	BC008_03979	1654	1.2	BC008_06312	561	1.7
BC008_01659	3519	-3.6	BC008_03980	2155	-3.0	BC008_06313	773	0.9
BC008_01660	10671	-5.6	BC008_03981	43	0.2	BC008_06314	298	4.1
BC008_01661	506	-0.8	BC008_03982	53363	-0.9	BC008_06315	533	3.7
BC008_01662	963	-0.8	BC008_03983	6242	-3.8	BC008_06316	3451	4.2
BC008_01663	185	0.9	BC008_03984	1055	2.8	BC008_06317	369	2.3
BC008_01664	1095	-1.1	BC008_03985	1556	-0.6	BC008_06318	291	0.7
BC008_01665	1702	0.3	BC008_03986	1301	-1.8	BC008_06319	914	2.3
BC008_01666	2614	-4.3	BC008_03987	513	0.9	BC008_06320	414	-0.1
BC008_01667	973	-0.9	BC008_03988	1307	-0.1	BC008_06321	2667	3.8
BC008_01668	2811	-1.3	BC008_03989	156	-0.4	BC008_06322	487	-0.3
BC008_01669	250	-0.5	BC008_03990	1746	-1.4	BC008_06323	294	1.4
BC008_01670	1069	-0.9	BC008_03991	692	-1.4	BC008_06324	15851	-3.2
BC008_01671	6063	-2.0	BC008_03992	599	0.6	BC008_06325	422	0.3
BC008_01672	452	-0.3	BC008_03993	1900	0.2	BC008_06326	90	3.0
BC008_01673	230	-1.6	BC008_03994	302	1.1	BC008_06327	2228	0.7
BC008_01674	2072	1.9	BC008_03995	25353	-5.6	BC008_06328	169202	-1.6
BC008_01675	1020	-2.5	BC008_03996	251	2.8	BC008_06329	210140	-1.7
BC008_01676	10272	-2.8	BC008_03997	751	-0.5	BC008_06330	134096	-2.7
BC008_01677	2281	0.7	BC008_03998	4235	1.6	BC008_06331	35330	-6.1
BC008_01678	346	-0.5	BC008_03999	1519	2.4	BC008_06332	1431	-0.1
BC008_01679	406	-0.2	BC008_04000	339	7.0	BC008_06333	610	2.5
BC008_01680	1270	-1.4	BC008_04001	432	7.3	BC008_06334	1980	-0.4
BC008_01682	2464	-1.2	BC008_04002	13195	3.0	BC008_06335	457	-0.5
BC008_01683	698	1.8	BC008_04003	587	0.1	BC008_06336	374	2.4
BC008_01684	626	0.2	BC008_04004	87781	-4.6	BC008_06337	908	1.4
BC008_01685	741	-0.9	BC008_04005	2134	1.1	BC008_06338	79	-0.9
BC008_01686	3233	-1.8	BC008_04006	1372	0.9	BC008_06339	813	-1.4
BC008_01687	4865	-1.3	BC008_04007	94	0.2	BC008_06340	1721	0.1

BC008_01688	4639	-2.9	BC008_04008	519	-1.1	BC008_06341	494	0.6
BC008_01689	1669	-4.2	BC008_04009	19923	-2.8	BC008_06342	4322	-3.8
BC008_01690	5199	-4.3	BC008_04010	22291	-1.9	BC008_06343	10486	-3.3
BC008_01691	356	-0.5	BC008_04011	628	-2.6	BC008_06344	1008	0.6
BC008_01692	1635	-1.3	BC008_04012	418	3.1	BC008_06345	1805	-1.9
BC008_01693	2535	0.0	BC008_04013	175	0.2	BC008_06346	854	-0.6
BC008_01694	1003	-2.9	BC008_04014	240	0.1	BC008_06347	2299	-0.5
BC008_01695	328	-0.8	BC008_04015	148	0.6	BC008_06348	1516	-1.4
BC008_01696	3618	-1.1	BC008_04016	310	1.2	BC008_06349	355	0.5
BC008_01697	2391	-0.5	BC008_04017	1621	-0.2	BC008_06350	1045	-1.0
BC008_01698	2256	0.3	BC008_04018	531	-1.5	BC008_06351	414	0.8
BC008_01699	2438	-2.8	BC008_04019	301	2.0	BC008_06352	3956	-3.4
BC008_01700	14891	-2.4	BC008_04020	925	-2.0	BC008_06353	2290	-2.1
BC008_01701	1198	-2.8	BC008_04021	2862	-0.8	BC008_06354	4958	-3.6
BC008_01702	2591	-0.9	BC008_04022	5446	-3.5	BC008_06355	8801	-3.2
BC008_01703	589	-1.3	BC008_04023	409	1.3	BC008_06356	141	1.2
BC008_01704	1041	0.4	BC008_04024	24	1.4	BC008_06357	948	-1.4
BC008_01705	572	-0.8	BC008_04025	1755	2.8	BC008_06358	741	0.0
BC008_01706	2698	4.5	BC008_04026	573	0.4	BC008_06359	243	-0.2
BC008_01707	749	-0.3	BC008_04027	15107	-4.3	BC008_06360	341	-1.4
BC008_01708	2241	-1.7	BC008_04028	898	0.1	BC008_06361	217	4.1
BC008_01709	63	0.7	BC008_04029	495	-0.2	BC008_06362	123	3.5
BC008_01710	1378	4.1	BC008_04030	378	0.6	BC008_06363	454	-1.0
BC008_01711	1414	-1.0	BC008_04031	175	2.4	BC008_06364	29	4.7
BC008_01712	3312	0.4	BC008_04032	3735	4.5	BC008_06365	25	2.8
BC008_01713	2020	-2.2	BC008_04033	948	2.9	BC008_06366	797	-0.3
BC008_01714	2590	-3.7	BC008_04034	512	2.4	BC008_06367	341	-1.6
BC008_01715	974	-2.6	BC008_04035	223	-0.4	BC008_06368	1702	2.2
BC008_01716	1417	-3.0	BC008_04036	369	-1.3	BC008_06369	696	-2.8
BC008_01717	2259	-1.0	BC008_04037	840	2.5	BC008_06370	196	1.3
BC008_01718	2005	-2.0	BC008_04038	62	1.9	BC008_06371	121	2.4
BC008_01719	3747	0.4	BC008_04039	36	1.8	BC008_06372	115	0.6
BC008_01720	2290	1.0	BC008_04040	177	0.1	BC008_06373	42	2.6
BC008_01721	818	0.3	BC008_04041	464	-2.3	BC008_06374	814	3.0
BC008_01722	1085	2.2	BC008_04042	396	-2.7	BC008_06375	1221	1.0
BC008_01723	63	0.0	BC008_04043	753	-2.3	BC008_06376	1348	2.3
BC008_01724	972	-1.1	BC008_04044	59	0.3	BC008_06377	612	-0.9
BC008_01725	215	0.2	BC008_04045	282	-1.7	BC008_06378	6442	-4.8
BC008_01726	354	1.8	BC008_04046	156	0.8	BC008_06379	5882	-4.8

BC008_01727	97	1.2	BC008_04047	353	2.4	BC008_06380	996	-1.6
BC008_01728	795	2.2	BC008_04048	151	1.2	BC008_06381	815	0.0
BC008_01729	67	0.9	BC008_04049	295	0.7	BC008_06382	858	1.1
BC008_01730	295	0.1	BC008_04050	1753	-0.9	BC008_06383	647	0.2
BC008_01731	200	0.8	BC008_04051	1026	-0.4	BC008_06384	2012	2.1
BC008_01732	1954	-1.3	BC008_04052	1199	1.1	BC008_06385	1236	1.9
BC008_01733	11702	-2.6	BC008_04053	5929	0.6	BC008_06386	803	0.7
BC008_01734	10572	-2.5	BC008_04054	3890	-1.5	BC008_06387	380	0.0
BC008_01735	1090	1.8	BC008_04055	349	4.3	BC008_06388	406	0.2
BC008_01736	518	3.1	BC008_04056	130	1.9	BC008_06389	1103	-0.7
BC008_01737	207	0.4	BC008_04057	295	1.5	BC008_06390	1798	-2.4
BC008_01738	6376	-4.1	BC008_04058	316	-0.7	BC008_06391	1327	-2.4
BC008_01739	1109	-1.6	BC008_04059	769	-0.1	BC008_06392	1725	-0.2
BC008_01740	116	-0.2	BC008_04060	599	0.8	BC008_06393	1246	-2.5
BC008_01741	761	0.7	BC008_04061	285	-0.8	BC008_06394	10167	-5.8
BC008_01742	139	-0.7	BC008_04062	799	-0.6	BC008_06395	3322	-1.3
BC008_01743	947	0.8	BC008_04063	401	4.8	BC008_06396	2393	-1.8
BC008_01744	1667	-1.0	BC008_04064	377	1.7	BC008_06397	1418	-0.4
BC008_01745	2862	-1.5	BC008_04065	2693	-4.4	BC008_06398	1610	2.1
BC008_01746	976	-0.5	BC008_04066	546	-0.4	BC008_06399	7092	-3.8
BC008_01747	252	-3.1	BC008_04067	5	1.1	BC008_06400	3202	-2.9
BC008_01748	576	-2.6	BC008_04068	550	0.0	BC008_06401	1038098	-5.4
BC008_01749	187	-1.2	BC008_04069	694	0.0	BC008_06402	681978	-5.0
BC008_01750	854	-3.7	BC008_04070	1558	-2.4	BC008_06403	3478	-1.7
BC008_01751	5833	-1.5	BC008_04071	303	-1.1	BC008_06404	6547	3.7
BC008_01752	2735	-1.8	BC008_04072	1814	-1.4	BC008_06405	23155	5.6
BC008_01753	5922	-2.1	BC008_04073	361	-1.6	BC008_06406	1171	-0.2
BC008_01754	511	-0.9	BC008_04074	228	-1.7	BC008_06407	578	-0.9
BC008_01755	10006	-4.0	BC008_04075	2283	-1.9	BC008_06408	581	0.8
BC008_01756	4322	-2.4	BC008_04076	1397	-1.7	BC008_06409	191	3.5
BC008_01757	500	-2.3	BC008_04077	745	-1.5	BC008_06410	158	0.1
BC008_01758	847	2.0	BC008_04078	146	-0.1	BC008_06411	408	2.7
BC008_01759	2149	1.3	BC008_04079	55	-0.4	BC008_06412	348	-0.7
BC008_01760	540	0.2	BC008_04080	50	-0.1	BC008_06413	5631	0.9
BC008_01761	17039	-1.1	BC008_04081	5899	-2.2	BC008_06414	903	-2.3
BC008_01762	8888	-3.5	BC008_04082	89	0.1	BC008_06415	93	-2.4
BC008_01763	627	-1.0	BC008_04083	4867	-2.9	BC008_06416	623	0.3
BC008_01764	818	0.8	BC008_04084	46387	-2.2	BC008_06417	69	0.3
BC008_01765	28107	-6.1	BC008_04085	109398	-2.7	BC008_06418	173	-1.3

BC008_01766	233	1.7	BC008_04086	1799	-2.6	BC008_06419	5981	-3.0
BC008_01767	1988	0.1	BC008_04087	1032	-1.3	BC008_06420	2073	-1.0
BC008_01768	136203	-0.9	BC008_04088	213	-1.0	BC008_06421	732	-1.0
BC008_01769	1594	-1.7	BC008_04089	3372	-1.6	BC008_06422	2385	0.1
BC008_01770	494	1.0	BC008_04090	2101	-1.3	BC008_06423	3931	1.0
BC008_01771	162	-3.2	BC008_04091	5833	-2.3	BC008_06424	625	-1.6
BC008_01772	1572	-1.9	BC008_04092	46980	-2.0	BC008_06425	7094	-0.9
BC008_01773	501	0.2	BC008_04093	535	-0.9	BC008_06426	305	1.0
BC008_01774	1064	-2.0	BC008_04094	2422	1.6	BC008_06427	68	0.5
BC008_01775	2658	-2.4	BC008_04095	414	0.1	BC008_06428	752	-1.5
BC008_01777	9537	-0.7	BC008_04096	111	0.9	BC008_06429	201	-0.2
BC008_01778	5004	-2.2	BC008_04097	11083	-3.7	BC008_06430	313	3.2
BC008_01779	4929	-2.0	BC008_04098	625	-0.4	BC008_06431	1699	-0.4
BC008_01780	1065	-1.7	BC008_04099	2357	-1.3	BC008_06432	2814	-1.3
BC008_01781	6283	-3.8	BC008_04100	202	-0.7	BC008_06433	898	-1.8
BC008_01782	630	1.9	BC008_04101	762	2.0	BC008_06434	664	-0.6
BC008_01783	7809	-0.6	BC008_04102	1061	1.4	BC008_06435	113	1.4
BC008_01784	844	0.2	BC008_04104	694	-0.2	BC008_06436	514	2.6
BC008_01785	1070	-1.8	BC008_04105	1821	1.2	BC008_06437	245	3.5
BC008_01786	4593	-4.4	BC008_04106	506	1.8	BC008_06438	997	0.6
BC008_01787	1032	-1.3	BC008_04107	5260	0.8	BC008_06439	4546	-1.8
BC008_01788	42047	6.6	BC008_04108	10966	-0.3	BC008_06440	2947	-2.3
BC008_01789	1794	1.4	BC008_04109	2824	-2.6	BC008_06441	1878	2.1
BC008_01790	1396	2.0	BC008_04110	1910	1.2	BC008_06442	959	2.6
BC008_01791	406	0.9	BC008_04111	6865	0.3	BC008_06443	741	3.0
BC008_01792	89	-1.4	BC008_04112	17041	0.8	BC008_06444	4651	3.7
BC008_01793	1425	1.2	BC008_04113	1730	1.0	BC008_06445	100	3.9
BC008_01794	1269	-2.1	BC008_04114	2365	1.6	BC008_06446	1157	4.3
BC008_01795	1011	1.7	BC008_04115	404	-0.9	BC008_06447	489	1.3
BC008_01796	224	-0.5	BC008_04116	1579	-0.5	BC008_06448	668	4.1
BC008_01797	529	1.4	BC008_04117	431	-2.1	BC008_06449	328	0.8
BC008_01798	748	0.5	BC008_04118	1604	2.7	BC008_06450	249	-0.2
BC008_01799	1271	-2.0	BC008_04119	804	4.8	BC008_06451	428	-1.3
BC008_01800	2354	-2.8	BC008_04120	298	3.1	BC008_06452	3457	-1.8
BC008_01801	367	1.9	BC008_04121	3156	0.8	BC008_06453	2403	-1.0
BC008_01802	672	-0.2	BC008_04122	98	1.9	BC008_06454	1337	-2.6
BC008_01803	4513	0.8	BC008_04123	948	-0.3	BC008_06455	1130	-0.1
BC008_01804	3487	0.2	BC008_04124	2056	-0.1	BC008_06456	990	-1.8
BC008_01805	2081	-2.0	BC008_04125	4934	1.0	BC008_06457	801	-0.2

BC008_01806	1500	-0.5	BC008_04126	13822	-3.0	BC008_06458	241	-1.0
BC008_01807	2528	2.7	BC008_04127	2359	-0.4	BC008_06459	951	-1.3
BC008_01808	3544	2.2	BC008_04128	1594	-0.1	BC008_06460	3182	-3.0
BC008_01809	377	2.7	BC008_04129	264	0.0	BC008_06461	1258	0.3
BC008_01810	1918	2.7	BC008_04130	1298	-1.0	BC008_06462	3402	0.2
BC008_01811	1785	2.0	BC008_04131	1297	-1.1	BC008_06463	198	6.8
BC008_01812	95	1.7	BC008_04132	2368	-0.1	BC008_06464	4112	-2.9
BC008_01813	687	-1.2	BC008_04133	2829	-1.0	BC008_06465	1647	-1.4
BC008_01814	3439	-2.3	BC008_04134	1370	1.4	BC008_06466	304	1.3
BC008_01815	2064	0.9	BC008_04135	335	2.2	BC008_06467	1254	4.3
BC008_01816	20988	-2.2	BC008_04136	361	2.5	BC008_06468	390	5.8
BC008_01817	176	1.2	BC008_04137	618	2.1	BC008_06469	28	2.1
BC008_01818	615	-0.1	BC008_04138	526	0.2	BC008_06470	546	-2.0
BC008_01819	1163	-1.4	BC008_04139	1037	4.2	BC008_06471	486	-1.4
BC008_01820	55663	-3.2	BC008_04140	626	-2.2	BC008_06472	229	-0.1
BC008_01821	1447	-0.2	BC008_04141	685	2.9	BC008_06473	539	0.4
BC008_01822	15950	-3.5	BC008_04142	996	-2.0	BC008_06474	764	-2.1
BC008_01823	490	-0.7	BC008_04143	125	1.7	BC008_06475	696	-0.8
BC008_01824	356	-1.5	BC008_04144	318	1.3	BC008_06476	831	-0.8
BC008_01825	477	0.1	BC008_04145	1140	4.3	BC008_06477	577	3.8
BC008_01826	6930	-2.7	BC008_04146	413	-0.2	BC008_06478	233	2.6
BC008_01827	9625	-1.6	BC008_04147	3418	2.1	BC008_06479	2458	3.2
BC008_01828	261	0.3	BC008_04148	7039	-0.3	BC008_06480	938	-2.7
BC008_01829	4265	2.8	BC008_04149	4104	-2.2	BC008_06481	1119	1.1
BC008_01830	18230	-6.1	BC008_04150	290	-0.8	BC008_06482	3427	-2.4
BC008_01831	47475	-5.3	BC008_04151	392	1.7	BC008_06483	1341	-3.1
BC008_01832	164	-0.2	BC008_04152	431	-0.6	BC008_06484	114	0.3
BC008_01833	465	2.9	BC008_04153	10912	-3.7	BC008_06485	2344	-0.3
BC008_01834	659	0.5	BC008_04154	355	0.7	BC008_06486	1848	1.0
BC008_01835	1924	0.3	BC008_04155	32087	-2.1	BC008_06487	2231	4.0
BC008_01836	1261	-1.7	BC008_04156	136	0.5	BC008_06488	507	-0.2
BC008_01837	732	1.3	BC008_04157	223	1.6	BC008_06489	153	2.5
BC008_01838	117	-0.5	BC008_04158	7284	5.1	BC008_06490	364	-2.7
BC008_01839	609	2.6	BC008_04159	615	5.5	BC008_06491	492	-0.4
BC008_01840	612	-1.1	BC008_04160	17959	2.2	BC008_06492	1895	1.5
BC008_01841	2241	-2.7	BC008_04161	332	0.9	BC008_06493	1436	0.7
BC008_01842	805	-0.1	BC008_04162	119	0.3	BC008_06494	1515	-2.4
BC008_01843	280	-1.5	BC008_04163	76	0.4	BC008_06495	764	-2.8
BC008_01844	1807	-1.1	BC008_04164	174	2.2	BC008_06496	1675	-2.8

BC008_01845	4154	-1.1	BC008_04165	219	0.4	BC008_06497	509	-0.6
BC008_01846	638	1.1	BC008_04166	2334	-0.5	BC008_06498	310	-2.1
BC008_01847	476	2.2	BC008_04167	2295	0.5	BC008_06499	1371	-0.5
BC008_01848	381	-0.6	BC008_04168	233	-0.4	BC008_06500	1800	-1.6
BC008_01849	123	2.4	BC008_04169	290	-1.1	BC008_06501	1781	-0.1
BC008_01850	199	3.0	BC008_04170	383	0.9	BC008_06502	389	0.8
BC008_01851	1958	-0.9	BC008_04171	1067	3.4	BC008_06503	655	-1.5
BC008_01852	7408	-0.6	BC008_04172	4861	0.1	BC008_06504	724	0.7
BC008_01853	1706	-0.6	BC008_04173	5840	-0.8	BC008_06505	2019	-3.0
BC008_01854	83729	4.5	BC008_04174	8591	-1.6	BC008_06506	2967	-0.8
BC008_01855	929	1.2	BC008_04175	191	1.9	BC008_06507	2546	-2.5
BC008_01856	758	-1.6	BC008_04176	749	3.5	BC008_06508	723	-1.4
BC008_01857	462	1.4	BC008_04177	2478	-2.1	BC008_06509	1018	-1.7
BC008_01858	489	-0.7	BC008_04178	69	0.3	BC008_06510	1110	1.5
BC008_01859	358	-1.0	BC008_04179	442	0.4	BC008_06511	1353	1.9
BC008_01861	3606	0.4	BC008_04180	55840	7.9	BC008_06512	14482	-4.8
BC008_01862	4882	-0.9	BC008_04181	432	1.5	BC008_06513	627	2.3
BC008_01863	3162	-1.3	BC008_04182	404	3.7	BC008_06514	536	2.9
BC008_01864	325	1.0	BC008_04183	1278	2.4	BC008_06515	151	4.2
BC008_01865	86	1.6	BC008_04184	173	3.6	BC008_06516	161	2.2
BC008_01866	34	1.0	BC008_04185	237	5.2	BC008_06517	50	1.6
BC008_01867	446	-1.0	BC008_04186	154	-1.5	BC008_06518	68	0.5
BC008_01868	162	-0.1	BC008_04187	1089	0.7	BC008_06519	92	-0.1
BC008_01869	297	2.0	BC008_04188	129	0.1	BC008_06520	5520	3.4
BC008_01870	197	2.0	BC008_04189	1688	-0.7	BC008_06521	429	0.9
BC008_01871	134	0.8	BC008_04190	11684	0.8	BC008_06522	145	0.7
BC008_01872	157	0.1	BC008_04191	390	3.4	BC008_06523	674	-1.5
BC008_01873	711	3.4	BC008_04192	103	3.9	BC008_06524	506	0.2
BC008_01874	354	1.5	BC008_04193	796	0.6	BC008_06525	245	2.9
BC008_01875	11886	3.9	BC008_04194	164	3.2	BC008_06526	1864	-1.2
BC008_01876	618	4.4	BC008_04195	203	4.9	BC008_06527	1139	-0.7
BC008_01877	75	0.7	BC008_04196	326	3.5	BC008_06528	1438	0.7
BC008_01878	484	6.3	BC008_04197	282	4.1	BC008_06529	6836	-1.0
BC008_01879	790	-1.9	BC008_04198	302	4.0	BC008_06530	2478	-1.6
BC008_01880	3836	-2.9	BC008_04199	285	4.8	BC008_06531	7712	1.5
BC008_01881	2105	0.3	BC008_04200	1215	3.5	BC008_06532	2265	1.0
BC008_01882	34	2.5	BC008_04201	623	6.0	BC008_06533	2018	-1.8
BC008_01883	228	3.3	BC008_04202	621	2.1	BC008_06534	860	0.1
BC008_01884	516	4.4	BC008_04203	433	1.2	BC008_06535	5955	-2.8

BC008_01885	816	2.7	BC008_04204	90	2.5	BC008_06536	1634	-2.2
BC008_01886	539	-1.3	BC008_04205	299	4.8	BC008_06541	545	2.0
BC008_01887	332	2.3	BC008_04206	102	4.3	BC008_06546	500	-0.1
BC008_01888	316	2.0	BC008_04207	334	1.1	BC008_06547	1824	-2.4
BC008_01889	350	1.5	BC008_04208	146	0.9	BC008_06548	328	1.6
BC008_01890	47	1.5	BC008_04209	642	-0.1	BC008_06549	901	1.2
BC008_01891	37	1.8	BC008_04210	263	3.2	BC008_06550	1061	-2.4
BC008_01892	556	4.0	BC008_04211	911	-2.1	BC008_06551	2133	-0.7
BC008_01893	368	5.4	BC008_04212	4135	-1.4	BC008_06552	207	6.6
BC008_01894	329	4.9	BC008_04213	212	3.6	BC008_06553	201	2.3
BC008_01895	490	2.5	BC008_04214	373	0.6	BC008_06554	250	1.2
BC008_01896	211	1.1	BC008_04215	48	3.8	BC008_06555	641	2.7
BC008_01897	5831	5.1	BC008_04216	405	7.1	BC008_06556	480	-0.2
BC008_01898	421	0.6	BC008_04217	89	7.0	BC008_06557	28369	-3.0
BC008_01899	798	-0.2	BC008_04218	18294	8.0	BC008_06558	1288	3.4
BC008_01900	2979	0.6	BC008_04219	516	0.2	BC008_06559	2057	1.5
BC008_01901	23630	-1.3	BC008_04220	234	3.2	BC008_06560	1203	0.7
BC008_01902	367	-2.0	BC008_04221	9630	-0.6	BC008_06561	441	-0.9
BC008_01903	255643	-5.0	BC008_04222	4424	-1.2	BC008_06562	316	2.4
BC008_01904	2146	0.6	BC008_04223	406	-0.3	BC008_06563	997	-2.3
BC008_01905	13576	-1.2	BC008_04224	580	0.3	BC008_06564	1904	-3.6
BC008_01906	9206	-2.0	BC008_04225	746	0.7	BC008_06565	856	-0.6
BC008_01907	912	-0.2	BC008_04226	1223	-2.3	BC008_06566	462	-0.4
BC008_01908	363	-1.8	BC008_04227	449	-2.0	BC008_06567	4977	4.8
BC008_01909	227	0.3	BC008_04228	48	1.2	BC008_06568	674	0.4
BC008_01910	226	0.7	BC008_04229	1566	-0.5	BC008_06569	4979	-4.2
BC008_01911	3870	0.8	BC008_04230	53	0.4	BC008_06570	655	-2.0
BC008_01912	1976	2.3	BC008_04231	137	2.8	BC008_06571	130	-2.2
BC008_01913	1400	0.8	BC008_04232	265	0.4	BC008_06572	905	-1.8
BC008_01914	3946	0.4	BC008_04233	356	-0.4	BC008_06573	853	-2.3
BC008_01915	2068	1.6	BC008_04234	2817	0.1	BC008_06574	928	-1.7
BC008_01916	104	2.0	BC008_04235	1373	0.7	BC008_06575	5783	-2.8
BC008_01917	2718	0.6	BC008_04236	552	2.3	BC008_06576	666	3.5
BC008_01918	514	4.1	BC008_04237	226	-3.0	BC008_06577	1645	-0.1
BC008_01919	79	2.0	BC008_04238	896	3.0	BC008_06578	405	0.7
BC008_01920	671	1.8	BC008_04239	26	3.3	BC008_06579	817	0.6
BC008_01921	756	-0.6	BC008_04240	457	0.1	BC008_06580	329	0.8
BC008_01922	1625	2.8	BC008_04241	2800	-2.6	BC008_06581	56	-0.4
BC008_01923	1024	-0.4	BC008_04242	991	-2.1	BC008_06582	1557	-2.5

BC008_01924	3483	2.6	BC008_04243	312	4.8	BC008_06583	736	0.1
BC008_01925	3892	-0.8	BC008_04244	781	2.4	BC008_06584	500	0.0
BC008_01926	1772	-1.4	BC008_04245	1611	-0.1	BC008_06585	8	1.6
BC008_01927	5603	-0.4	BC008_04246	13671	-2.6	BC008_06586	559	-0.4
BC008_01928	7180	-1.9	BC008_04247	8583	-4.3	BC008_06587	2693	-4.3
BC008_01929	967	0.4	BC008_04248	93	1.7	BC008_06588	414	1.7
BC008_01930	1054	4.8	BC008_04249	653	-3.3	BC008_06589	398	4.7
BC008_01931	116	1.2	BC008_04250	2360	-2.0	BC008_06590	790	-0.6
BC008_01932	551	6.9	BC008_04251	422	2.3	BC008_06591	289	-0.8
BC008_01933	243	1.6	BC008_04252	300	1.2	BC008_06592	622	0.7
BC008_01934	304	2.3	BC008_04253	270	2.9	BC008_06593	771	0.1
BC008_01935	1203	1.5	BC008_04254	1744	0.6	BC008_06594	337	-0.4
BC008_01936	1924	-2.3	BC008_04255	8479	-0.1	BC008_06595	289	1.7
BC008_01937	1070	0.0	BC008_04256	3789	4.1	BC008_06596	131	2.0
BC008_01938	288	1.0	BC008_04257	8677	2.0	BC008_06597	336	4.2
BC008_01939	500	0.1	BC008_04258	882	0.9	BC008_06598	3503	-1.7
BC008_01940	840	3.3	BC008_04259	263	2.5	BC008_06599	7809	-3.3
BC008_01941	672	-1.1	BC008_04260	131	0.8	BC008_06600	460	2.8
BC008_01942	78	0.1	BC008_04261	64	-1.2	BC008_06601	30	2.9
BC008_01943	1079	1.2	BC008_04262	232	1.7	BC008_06602	248	4.8
BC008_01944	855	1.2	BC008_04263	3049	-3.0	BC008_06603	210	0.7
BC008_01945	323	0.8	BC008_04264	645	-2.0	BC008_06604	221	1.8
BC008_01946	1064	-0.9	BC008_04265	5913	-2.6	BC008_06605	162	5.9
BC008_01947	90	3.6	BC008_04266	1395	2.6	BC008_06606	354	5.1
BC008_01948	294	3.1	BC008_04267	762	-1.6	BC008_06607	1038	1.0
BC008_01949	1466	1.0	BC008_04268	398	-1.5	BC008_06608	1057	1.7
BC008_01950	2829	0.3	BC008_04269	1225	0.3	BC008_06609	2249	-1.2
BC008_01951	284	2.8	BC008_04270	84	1.5	BC008_06610	31644	-4.6
BC008_01952	728	1.2	BC008_04271	2683	-2.0	BC008_06611	3742	-0.7
BC008_01953	2187	1.3	BC008_04272	773	-0.9	BC008_06612	380	1.4
BC008_01954	79	0.0	BC008_04273	7026	4.0	BC008_06613	317	1.7
BC008_01955	790	-3.6	BC008_04274	365	-1.0	BC008_06614	2634	-1.5
BC008_01956	1817	-4.0	BC008_04275	1381	0.6	BC008_06615	8230	3.6
BC008_01957	2070	-1.5	BC008_04276	5294	0.0	BC008_06616	731	-0.4
BC008_01958	1838	0.0	BC008_04277	2482	-1.7	BC008_06617	439	1.6
BC008_01959	8133	3.8	BC008_04278	18747	-0.7	BC008_06618	280	5.2
BC008_01960	3430	2.3	BC008_04279	2255	-0.7	BC008_06619	1095	4.0
BC008_01961	1279	0.5	BC008_04280	10097	-4.2	BC008_06620	325	3.1
BC008_01962	997	-1.5	BC008_04281	1008	0.2	BC008_06621	171	1.1

BC008_01963	534	2.5	BC008_04282	674	-0.6	BC008_06622	338	0.6
BC008_01964	5483	1.3	BC008_04283	876	0.9	BC008_06623	65	-0.2
BC008_01965	155	0.4	BC008_04284	6449	1.5	BC008_06624	21134	1.9
BC008_01966	198	1.6	BC008_04285	991	-2.6	BC008_06625	2612	-0.7
BC008_01967	1226	4.0	BC008_04286	2220	-2.2	BC008_06626	8471	-1.9
BC008_01968	3508	2.0	BC008_04287	5133	-2.5	BC008_06627	4614	2.2
BC008_01969	374	-0.3	BC008_04288	8157	0.1	BC008_06628	611	1.9
BC008_01970	345	-1.6	BC008_04289	7155	1.0	BC008_06629	2359	4.5
BC008_01971	1708	-0.3	BC008_04290	5346	6.7	BC008_06630	1688	2.6
BC008_01972	325	4.2	BC008_04291	1685	2.5	BC008_06631	63	1.9
BC008_01973	168	3.3	BC008_04292	1260	-1.2	BC008_06632	102	3.2
BC008_01974	330	2.0	BC008_04293	2052	-3.0	BC008_06633	145	2.7
BC008_01975	906	-2.0	BC008_04294	4628	-5.4	BC008_06634	1074	-1.3
BC008_01976	8379	-1.1	BC008_04295	932	-4.5	BC008_06635	337	1.2
BC008_01977	205	-1.8	BC008_04296	72815	-6.1	BC008_06636	310	-2.0
BC008_01978	220	-0.1	BC008_04297	34117	-6.8	BC008_06637	1605	0.7
BC008_01979	4482	1.2	BC008_04298	5382	-3.9	BC008_06638	284	2.8
BC008_01980	3319	0.4	BC008_04299	8045	-2.3	BC008_06639	562	0.6
BC008_01981	1023	0.5	BC008_04300	14404	-2.1	BC008_06640	524	2.2
BC008_01982	5731	-0.9	BC008_04301	1934	-2.4	BC008_06641	315	3.1
BC008_01983	3816	-1.9	BC008_04302	1329	-0.9	BC008_06642	4810	1.1
BC008_01984	444	0.0	BC008_04303	2352	0.1	BC008_06643	43035	-6.9
BC008_01985	7189	-2.1	BC008_04304	21730	-0.4	BC008_06644	178	-0.6
BC008_01986	2447	-1.9	BC008_04305	387	0.2	BC008_06645	836	-0.7
BC008_01987	348	-1.3	BC008_04306	647	-1.8	BC008_06646	5248	0.3
BC008_01988	7	1.4	BC008_04307	1029	-3.4	BC008_06647	45	5.5
BC008_01989	969	1.4	BC008_04308	181	1.7	BC008_06648	523	0.0
BC008_01991	4319	-0.3	BC008_04309	388	2.7	BC008_06649	712	2.1
BC008_01992	638	-0.6	BC008_04310	572	-0.6	BC008_06650	70	2.2
BC008_01993	14872	2.8	BC008_04311	1261	-1.9	BC008_06651	9094	0.0
BC008_01994	834	1.3	BC008_04312	1324	1.6	BC008_06652	1359	-0.5
BC008_01995	2692	-0.1	BC008_04313	19030	2.7	BC008_06653	1387	-0.7
BC008_01996	660	2.0	BC008_04314	3028	-1.1	BC008_06654	943	1.4
BC008_01997	510	5.3	BC008_04315	1360	0.4	BC008_06655	695	-1.6
BC008_01998	682	1.0	BC008_04316	5234	-4.2	BC008_06656	5996	-1.4
BC008_01999	1120	0.2	BC008_04317	1535	0.2	BC008_06657	11982	-2.2
BC008_02000	2032	0.4	BC008_04318	815	-0.1	BC008_06658	2045	-1.4
BC008_02001	2488	2.4	BC008_04319	115	1.9	BC008_06659	1454	-1.6
BC008_02002	645	0.7	BC008_04320	30935	-4.6	BC008_06660	1568	3.3

BC008_02003	408	0.4	BC008_04321	4329	-1.6	BC008_06661	691	-1.9
BC008_02004	1794	1.9	BC008_04322	778	1.2	BC008_06662	1622	0.9
BC008_02005	250	3.2	BC008_04323	1044	0.3	BC008_06663	1709	1.9
BC008_02006	50	1.4	BC008_04324	4363	-2.3	BC008_06664	777	1.3
BC008_02007	427	0.1	BC008_04325	372	-1.2	BC008_06665	1144	1.9
BC008_02008	695	1.3	BC008_04327	166	1.2	BC008_06666	423	-1.4
BC008_02009	5533	-1.9	BC008_04328	2618	-1.7	BC008_06667	1968	-1.3
BC008_02010	259	1.4	BC008_04329	252	3.4	BC008_06668	1070	-4.1
BC008_02011	1034	2.4	BC008_04330	720	2.3	BC008_06669	1139	-2.1
BC008_02012	256	0.3	BC008_04331	2055	0.3	BC008_06670	2097	-2.7
BC008_02013	808	-0.7	BC008_04332	1847	-2.0	BC008_06671	244	-2.2
BC008_02014	72	0.6	BC008_04333	689	-2.5	BC008_06672	76	-2.8
BC008_02015	1478	0.4	BC008_04334	2135	0.8	BC008_06673	2514	4.3
BC008_02016	528	0.6	BC008_04335	681	4.3	BC008_06674	664	5.5
BC008_02017	1453	0.7	BC008_04336	84	3.0	BC008_06675	149	-0.2
BC008_02018	434	0.7	BC008_04337	1205	-2.2	BC008_06676	28441	-4.1
BC008_02019	828	-3.3	BC008_04338	25921	-1.9	BC008_06677	922	2.2
BC008_02020	5523	-2.3	BC008_04339	237	-0.2	BC008_06678	282	1.6
BC008_02021	27481	-0.4	BC008_04340	183	-1.5	BC008_06679	1064	-2.0
BC008_02022	29063	-4.9	BC008_04341	372	-0.5	BC008_06680	6536	-2.0
BC008_02023	470	-0.9	BC008_04342	2604	-0.3	BC008_06681	2989	-2.4
BC008_02024	1113	-1.5	BC008_04343	30	4.8	BC008_06682	1259	-1.7
BC008_02025	1000	-0.6	BC008_04344	435	7.7	BC008_06683	48416	-2.1
BC008_02026	6304	-3.5	BC008_04345	570	0.8	BC008_06684	748	-1.1
BC008_02027	426	0.2	BC008_04346	160	0.6	BC008_06685	3302	-1.7
BC008_02028	561	-1.4	BC008_04347	422	2.6	BC008_06686	3431	-2.0
BC008_02029	908	-0.6	BC008_04348	1763	1.3	BC008_06687	4333	-2.6
BC008_02030	298	-1.4	BC008_04349	2341	0.3	BC008_06688	17707	-2.6
BC008_02031	1374	-1.5	BC008_04350	95	2.9	BC008_06689	21929	-3.1
BC008_02032	5293	0.7	BC008_04351	940	2.6	BC008_06690	31406	-3.6
BC008_02033	2117	-0.4	BC008_04352	1251	-1.5	BC008_06691	20221	-1.9
BC008_02034	3752	-2.8	BC008_04353	262	-0.4	BC008_06692	1889	-1.9
BC008_02035	2883	-0.9	BC008_04354	1430	5.1	BC008_06693	1492	-2.0
BC008_02036	943	-1.5	BC008_04355	1527	0.4	BC008_06694	16292	-2.7
BC008_02037	1191	1.2	BC008_04356	307	3.6	BC008_06695	22968	-2.7
BC008_02038	3810	-3.3	BC008_04357	7886	-2.5	BC008_06696	3308	-2.2
BC008_02039	786	-2.9	BC008_04358	866	3.7	BC008_06697	66448	-2.7
BC008_02040	3258	-3.9	BC008_04359	788	5.3	BC008_06698	47763	-3.3
BC008_02041	7318	-3.3	BC008_04360	122	1.0	BC008_06699	2883	-2.1

BC008_02042	23725	-1.5	BC008_04361	3891	5.3	BC008_06700	373	1.9
BC008_02043	5777	-1.0	BC008_04362	5308	6.8	BC008_06701	676	2.3
BC008_02044	2817	-0.2	BC008_04363	923	2.7	BC008_06702	123	-0.7
BC008_02045	2380	1.0	BC008_04364	246	3.9	BC008_06703	657	-0.7
BC008_02046	2991	-1.5	BC008_04365	3356	0.0	BC008_06704	1129	2.7
BC008_02047	304	3.1	BC008_04366	1694	-3.8	BC008_06705	576	0.1
BC008_02048	905	-1.9	BC008_04367	1645	-1.9	BC008_06706	874	1.5
BC008_02049	5360	-3.4	BC008_04368	5768	-3.2	BC008_06707	902	0.9
BC008_02050	5329	-2.1	BC008_04369	1504	-0.2	BC008_06708	476	0.9
BC008_02051	1372	1.1	BC008_04370	548	-1.3	BC008_06709	130	0.5
BC008_02052	2625	0.5	BC008_04371	146	-1.4	BC008_06710	265	5.1
BC008_02053	267	1.0	BC008_04372	668	5.1	BC008_06711	1402	3.5
BC008_02054	157	2.7	BC008_04373	599	-1.3	BC008_06712	112	1.8
BC008_02055	5788	3.7	BC008_04374	575	-0.1	BC008_06713	3050	3.6
BC008_02056	424	-3.2	BC008_04375	709	0.3	BC008_06714	1345	0.5
BC008_02057	1753	-0.6	BC008_04376	101	0.6	BC008_06715	183	1.1
BC008_02058	4355	1.6	BC008_04377	3791	2.1	BC008_06716	580	0.0
BC008_02059	138	-0.3	BC008_04378	4477	-2.0	BC008_06717	2082	-2.6
BC008_02060	291	1.5	BC008_04379	173	4.0	BC008_06718	2243	-1.2
BC008_02061	316	-1.7	BC008_04380	675	1.6	BC008_06719	3040	0.2
BC008_02062	1841	0.1	BC008_04381	427	2.7	BC008_06720	255	1.5
BC008_02063	1019	3.6	BC008_04382	591	-1.6	BC008_06721	2117	0.1
BC008_02064	656	1.6	BC008_04383	5296	-1.7	BC008_06722	104	2.9
BC008_02065	138	0.5	BC008_04384	23267	-4.7	BC008_06723	1566	4.2
BC008_02066	307	2.1	BC008_04385	1589	-0.8	BC008_06724	104	1.5
BC008_02067	883	3.5	BC008_04386	691	0.2	BC008_06725	367	-0.5
BC008_02068	479	-0.9	BC008_04387	2092	4.5	BC008_06726	662	1.2
BC008_02069	436	1.6	BC008_04388	5818	3.4	BC008_06727	224	1.6
BC008_02070	1289	-0.5	BC008_04389	264	0.4	BC008_06728	1452	5.4
BC008_02071	1622	1.8	BC008_04390	1111	-1.5	BC008_06729	3111	-3.3
BC008_02072	2102	-0.4	BC008_04391	11539	-0.7	BC008_06730	229	1.0
BC008_02073	463	-0.3	BC008_04392	730	-1.3	BC008_06731	1835	-1.7
BC008_02074	1396	-2.0	BC008_04393	3515	-1.4	BC008_06732	203	-0.8
BC008_02075	752	-1.9	BC008_04394	17	0.9	BC008_06733	3073	-1.4
BC008_02076	10348	1.3	BC008_04395	126	3.4	BC008_06734	1426	-0.2
BC008_02077	10269	2.2	BC008_04396	3466	-2.5	BC008_06735	51	-1.4
BC008_02078	1279	-3.9	BC008_04397	1212	-1.5	BC008_06736	49167	-1.3
BC008_02079	139	-0.4	BC008_04398	2489	-0.3	BC008_06737	107242	-1.7
BC008_02080	1314	0.9	BC008_04399	14073	6.7	BC008_06738	137769	-1.6

BC008_02081	12168	-3.8	BC008_04400	12009	0.1	BC008_06739	114769	-2.4
BC008_02082	17316	-1.6	BC008_04401	432	1.5	BC008_06740	126914	-2.7
BC008_02083	22366	-3.4	BC008_04402	65	5.3	BC008_06741	36491	-1.6
BC008_02084	1317	-2.8	BC008_04403	2078	-0.1	BC008_06742	20131	-3.2
BC008_02085	15477	-3.9	BC008_04404	12295	-3.5	BC008_06743	13242	-2.2
BC008_02086	1102	-0.3	BC008_04405	2761	0.4	BC008_06744	16962	-1.9
BC008_02087	2133	1.0	BC008_04406	1641	-1.6	BC008_06745	52169	-6.3
BC008_02088	427	-1.0	BC008_04407	1801	0.3	BC008_06746	1372	0.3
BC008_02089	1686	-1.3	BC008_04408	35	5.8	BC008_06747	4381	-1.1
BC008_02090	6411	-2.2	BC008_04409	5169	-2.0	BC008_06748	1464	-1.0
BC008_02091	3196	-1.4	BC008_04410	148	-1.2	BC008_06749	2996	-1.9
BC008_02092	2027	-4.8	BC008_04411	396	-0.8	BC008_06750	7989	-2.5
BC008_02093	315	0.4	BC008_04412	5752	-4.4	BC008_06751	2415	2.4
BC008_02094	594	-2.3	BC008_04413	1986	-0.6	BC008_06752	1722	3.2
BC008_02095	641	-1.2	BC008_04414	956	0.9	BC008_06753	330	3.2
BC008_02096	1277	1.2	BC008_04415	144	-1.7	BC008_06754	972	-2.2
BC008_02097	1490	2.8	BC008_04416	202	-3.0	BC008_06755	1849	2.1
BC008_02098	461	1.0	BC008_04417	1810	-0.2	BC008_06756	1753	1.5
BC008_02099	1752	-0.5	BC008_04418	1117	-0.3	BC008_06757	24550	-3.5
BC008_02100	5508	-1.5	BC008_04419	5718	-1.6	BC008_06758	3567	0.5
BC008_02101	1145	4.3	BC008_04420	1296	-0.3	BC008_06759	109	0.5
BC008_02102	2087	2.2	BC008_04421	1021	2.4	BC008_06760	2756	-2.7
BC008_02103	984	2.6	BC008_04422	367	0.3	BC008_06761	1737	-1.9
BC008_02104	6522	-1.7	BC008_04423	3229	-1.8	BC008_06762	63	1.8
BC008_02105	603	-1.0	BC008_04424	3364	-2.9	BC008_06763	45	0.6
BC008_02106	742	3.0	BC008_04425	711	-0.2	BC008_06764	497	-0.3
BC008_02107	2804	1.0	BC008_04426	1012	-0.1	BC008_06766	1695	2.3
BC008_02108	2395	-0.3	BC008_04427	1462	1.9	BC008_06767	64	7.3
BC008_02109	650	-0.8	BC008_04428	2114	-2.1	BC008_06768	12154	-4.4
BC008_02110	60	0.4	BC008_04429	450	-1.1	BC008_06769	179709	-5.9
BC008_02111	16349	-3.6	BC008_04430	955	-2.2	BC008_06770	187	4.1
BC008_02112	270	-0.2	BC008_04431	813	-1.4	BC008_06771	2797	0.0
BC008_02113	321	-2.6	BC008_04432	3029	2.8	BC008_06772	139	1.0
BC008_02114	1907	0.2	BC008_04433	14605	-4.0	BC008_06773	1172	1.7
BC008_02115	210	2.0	BC008_04434	93	0.8	BC008_06774	1285	1.9
BC008_02116	8341	-4.2	BC008_04435	6857	-2.6	BC008_06775	668	-0.5
BC008_02117	603	3.2	BC008_04436	870	1.5	BC008_06776	1320	0.3
BC008_02118	2211	-1.5	BC008_04437	3118	-1.6	BC008_06777	269	2.6
BC008_02119	3943	-0.3	BC008_04438	1593	-2.7	BC008_06778	1274	1.2

BC008_02120	487	-0.3	BC008_04439	8120	5.7	BC008_06779	34	0.9
BC008_02121	556	-1.0	BC008_04440	1576	3.3	BC008_06780	402	0.7
BC008_02122	225	-2.5	BC008_04441	2420	2.0	BC008_06781	880	0.6
BC008_02123	5958	-3.8	BC008_04442	977	2.5	BC008_06782	527	2.1
BC008_02124	2745	-0.8	BC008_04443	1392	0.9	BC008_06783	424	4.9
BC008_02125	5420	0.9	BC008_04444	5578	1.0	BC008_06784	304	2.9
BC008_02126	541	-0.1	BC008_04445	3571	-2.0	BC008_06785	316	2.1
BC008_02127	4562	0.7	BC008_04446	14858	-4.6	BC008_06786	794	1.1
BC008_02128	205	-1.6	BC008_04447	1854	4.2	BC008_06787	658	2.6
BC008_02129	854	-1.0	BC008_04448	1712	0.9	BC008_06788	738	5.1
BC008_02130	1323	1.6	BC008_04449	1764	0.0	BC008_06789	91	-0.6
BC008_02131	495	-0.7	BC008_04450	139	4.2	BC008_06790	685	2.0
BC008_02132	810	0.4	BC008_04451	5379	3.0	BC008_06791	928	0.8
BC008_02133	18942	-3.6	BC008_04452	617	0.8	BC008_06792	619	0.6
BC008_02134	2080	-3.3	BC008_04453	3260	1.8	BC008_06793	209	4.5
BC008_02135	74291	-1.3	BC008_04454	190	-1.8	BC008_06794	467	-2.1
BC008_02137	1358	1.1	BC008_04455	3802	2.6	BC008_06795	199	1.4
BC008_02138	182047	-6.4	BC008_04456	2213	-0.2	BC008_06796	662	-2.0
BC008_02139	599	-0.7	BC008_04457	9106	-1.5	BC008_06797	1258	-1.2
BC008_02140	794	-3.4	BC008_04458	627	-0.9	BC008_06798	3259	-3.4
BC008_02141	124	-0.2	BC008_04459	10020	-4.1	BC008_06799	5168	-1.4
BC008_02142	1121	0.4	BC008_04460	57466	-5.5	BC008_06800	881	-0.8
BC008_02143	2742	-1.9	BC008_04461	3484	-3.8	BC008_06801	2253	-1.2
BC008_02144	753	1.7	BC008_04462	1231	0.1	BC008_06802	1406	-2.6
BC008_02145	24444	3.8	BC008_04463	3110	4.6	BC008_06803	2040	-2.0
BC008_02146	38829	-1.6	BC008_04464	646	-0.5	BC008_06804	299	2.1
BC008_02147	2102	-0.7	BC008_04465	4215	-2.1	BC008_06805	437	2.6
BC008_02148	23346	-3.4	BC008_04466	1237	-0.4	BC008_06806	990	1.4
BC008_02149	2896	-1.7	BC008_04467	3331	-2.7	BC008_06807	153	1.5
BC008_02150	2461	-2.8	BC008_04468	920	-0.8	BC008_06808	1556	3.2
BC008_02151	6189	-2.0	BC008_04469	602	1.3	BC008_06809	285	2.5
BC008_02152	2199	-4.2	BC008_04470	1556	-1.4	BC008_06810	345	0.2
BC008_02153	960	-2.7	BC008_04471	5741	2.2	BC008_06811	777	-0.1
BC008_02154	25722	-1.4	BC008_04472	39	0.6	BC008_06812	1302	-1.7
BC008_02155	1869	-1.2	BC008_04473	714	-2.4	BC008_06813	408	1.0
BC008_02156	887	-1.5	BC008_04474	4676	-2.6	BC008_06814	2063	6.0
BC008_02157	421	-0.5	BC008_04475	1647	-1.2	BC008_06815	2168	-0.4
BC008_02158	1547	2.6	BC008_04476	322	-1.3	BC008_06816	342	0.4
BC008_02159	834	-1.1	BC008_04478	1753	-3.6	BC008_06817	96	0.0

BC008_02160	347	3.0	BC008_04479	500	-4.0	BC008_06818	477	4.0
BC008_02161	397	0.9	BC008_04480	623	0.0	BC008_06819	881	-1.1
BC008_02162	54	-0.4	BC008_04481	3187	-0.7	BC008_06820	421	0.7
BC008_02163	817	6.0	BC008_04482	596	-2.8	BC008_06821	11894	2.1
BC008_02164	683	5.2	BC008_04483	135	1.3	BC008_06822	6963	5.6
BC008_02165	366	0.9	BC008_04484	497	2.8	BC008_06823	20895	10.1
BC008_02166	328	1.2	BC008_04485	34354	-2.0	BC008_06824	1662	-2.0
BC008_02167	197	1.8	BC008_04486	6260	-3.2	BC008_06825	2117	-0.2
BC008_02168	3817	2.9	BC008_04487	536	2.4	BC008_06826	2248	3.6
BC008_02169	5692	0.5	BC008_04488	351	2.2	BC008_06827	2857	-1.3
BC008_02170	3059	-1.1	BC008_04489	1801	-1.3	BC008_06828	1062	-1.8
BC008_02171	277	-1.7	BC008_04490	860	-1.3	BC008_06829	181733	-6.4
BC008_02172	13803	-2.3	BC008_04491	428	-0.8	BC008_06830	34102	-5.0
BC008_02173	2864	2.8	BC008_04492	982	-1.0	BC008_06831	3207	-1.2
BC008_02174	3457	4.2	BC008_04493	2976	0.8	BC008_06832	269	-0.5
BC008_02175	507	-1.8	BC008_04494	49	2.8	BC008_06833	564	2.8
BC008_02176	2894	-0.4	BC008_04495	1013	3.6	BC008_06834	180	1.9
BC008_02177	597	1.4	BC008_04496	87	5.0	BC008_06835	1199	-1.2
BC008_02178	10434	-5.1	BC008_04497	326	-1.0	BC008_06836	783	0.9
BC008_02179	150	-0.4	BC008_04498	31115	0.8	BC008_06837	939	3.0
BC008_02180	877	-2.5	BC008_04499	1714	-0.5	BC008_06838	161	-0.8
BC008_02181	234	2.2	BC008_04500	12241	2.0	BC008_06839	35	1.1
BC008_02182	61	1.7	BC008_04501	2901	1.8	BC008_06840	646	2.5
BC008_02183	1022	2.5	BC008_04502	2541	-0.5	BC008_06841	110	1.9
BC008_02184	503	0.0	BC008_04503	60	0.0	BC008_06842	833	5.9
BC008_02185	840	0.4	BC008_04504	1954	-1.4	BC008_06843	307	-0.2
BC008_02186	340	-1.1	BC008_04505	5617	-4.7	BC008_06844	360	-0.3
BC008_02187	3319	-3.7	BC008_04506	3446	-2.2	BC008_06845	264	6.4
BC008_02188	1472	-3.5	BC008_04507	393	-1.7	BC008_06846	305	1.9
BC008_02189	481	3.0	BC008_04508	684	0.4	BC008_06847	190	3.5
BC008_02190	975	1.8	BC008_04509	4061	-1.6	BC008_06848	548	2.7
BC008_02191	774	-1.9	BC008_04510	11802	5.3	BC008_06849	1809	1.5
BC008_02192	2208	-2.4	BC008_04511	8066	-0.8	BC008_06850	40	0.1
BC008_02193	2288	3.0	BC008_04512	15462	-3.7	BC008_06851	375	1.9
BC008_02194	275	3.6	BC008_04513	4960	-3.1	BC008_06852	488	0.3
BC008_02195	394	3.8	BC008_04514	3385	2.3	BC008_06853	962	3.7
BC008_02196	273	1.9	BC008_04515	736	-1.1	BC008_06854	297	2.5
BC008_02197	879	-3.0	BC008_04516	191	1.7	BC008_06855	178	4.8
BC008_02198	261	-3.7	BC008_04517	1073	0.6	BC008_06856	1869	-1.5

BC008_02199	788	-0.7	BC008_04518	305	0.0	BC008_06857	464	3.6
BC008_02200	662	0.8	BC008_04519	539	0.3	BC008_06858	88	1.3
BC008_02201	426	3.1	BC008_04520	354	3.5	BC008_06859	666	-1.1
BC008_02202	1155	0.5	BC008_04521	1833	3.4	BC008_06860	1332	-1.1
BC008_02203	287	0.6	BC008_04522	261	-1.2	BC008_06861	4280	-2.4
BC008_02204	6955	-0.6	BC008_04523	4950	-1.0	BC008_06862	258	0.3
BC008_02205	12338	-3.7	BC008_04524	58052	-2.1	BC008_06863	2359	0.0
BC008_02206	731	-0.1	BC008_04525	419	0.4	BC008_06864	49	-0.1
BC008_02207	11173	2.0	BC008_04526	488	1.2	BC008_06865	223	0.9
BC008_02208	4786	-2.0	BC008_04527	311	1.6	BC008_06866	948	3.0
BC008_02209	755	-2.1	BC008_04528	3238	0.2	BC008_06867	712	-0.7
BC008_02210	1418	-1.4	BC008_04529	2957	1.1	BC008_06868	144	3.7
BC008_02211	7610	-2.2	BC008_04530	826	1.2	BC008_06869	418	2.2
BC008_02212	3352	-0.7	BC008_04531	570	0.0	BC008_06870	2968	3.5
BC008_02213	9819	-3.2	BC008_04532	2612	-1.2	BC008_06871	20	1.3
BC008_02214	2630	-2.1	BC008_04533	560	-0.2	BC008_06872	19	0.4
BC008_02215	58	1.6	BC008_04534	2308	-0.2	BC008_06873	85	-0.2
BC008_02216	286	0.1	BC008_04535	7729	0.6	BC008_06874	176	-0.9
BC008_02217	1535	5.1	BC008_04536	277	-0.4	BC008_06875	103	-0.4
BC008_02218	272	1.1	BC008_04538	386	2.5	BC008_06876	386	0.4
BC008_02219	1650	1.3	BC008_04539	1370	-0.1	BC008_06877	368	-0.6
BC008_02220	1122	1.2	BC008_04540	288	0.5	BC008_06878	1257	-1.0
BC008_02221	150035	-4.8	BC008_04541	20866	-4.5	BC008_06879	3711	3.4
BC008_02222	1308	-2.8	BC008_04542	244	2.1	BC008_06880	446	1.3
BC008_02223	1141	-0.6	BC008_04543	5997	8.7	BC008_06881	83	1.2
BC008_02224	594	-2.1	BC008_04544	1235	-1.1	BC008_06882	19	0.4
BC008_02225	168	-2.0	BC008_04545	514	-0.4	BC008_06883	77	0.2
BC008_02226	1204	-1.9	BC008_04546	535	-0.3	BC008_06884	84	2.1
BC008_02227	245	0.4	BC008_04547	1630	1.0	BC008_06885	222	0.4
BC008_02228	1627	-1.3	BC008_04548	359	4.4	BC008_06886	812	-1.6
BC008_02230	363	-0.7	BC008_04549	4084	1.2	BC008_06887	639	0.1
BC008_02231	68	-1.5	BC008_04550	160	2.6	BC008_06888	3484	0.9
BC008_02232	974	-3.5	BC008_04551	553	0.3	BC008_06889	1843	-0.7
BC008_02233	1777	-3.4	BC008_04552	1543	-2.8	BC008_06890	2172	-1.3
BC008_02234	6855	-3.7	BC008_04553	748	-1.6	BC008_06891	52	2.4
BC008_02235	1984	-2.8	BC008_04554	1937	-2.9	BC008_06892	275	2.4
BC008_02236	1376	-0.9	BC008_04555	1438	-0.7	BC008_06893	538	3.6
BC008_02237	7432	1.0	BC008_04556	1426	0.4	BC008_06894	1243	3.5
BC008_02238	3905	-2.2	BC008_04557	1472	-2.2	BC008_06895	939	3.6

BC008_02239	1475	-3.0	BC008_04558	1500	2.3	BC008_06896	534	1.6
BC008_02240	11952	3.2	BC008_04559	2479	-0.7	BC008_06897	135	3.2
BC008_02241	8610	2.2	BC008_04560	1995	-2.3	BC008_06898	2465	-0.5
BC008_02242	9187	2.1	BC008_04561	50	0.3	BC008_06899	4379	0.5
BC008_02243	177	1.5	BC008_04562	2496	-0.9	BC008_06900	2075	-1.1
BC008_02244	570	-1.3	BC008_04563	260	2.9	BC008_06901	34	0.6
BC008_02245	1971	-0.7	BC008_04564	583	4.6	BC008_06902	397	0.5
BC008_02246	706	-0.3	BC008_04565	2633	4.1	BC008_06903	210	-1.3
BC008_02247	508	-0.7	BC008_04566	44530	-3.6	BC008_06904	1516	-1.5
BC008_02249	1754	-4.2	BC008_04567	11108	-1.4	BC008_06905	362	-1.8
BC008_02250	378	0.5	BC008_04568	4208	0.0	BC008_06906	228	-1.7
BC008_02251	46	0.8	BC008_04569	23690	-3.5	BC008_06907	2278	-2.1
BC008_02252	18941	-4.9	BC008_04570	13571	-5.1	BC008_06908	1367	-1.8
BC008_02253	8518	-3.2	BC008_04571	2113	-2.6	BC008_06909	741	-1.5
BC008_02254	474	-1.4	BC008_04572	1753	-3.9	BC008_06910	148	-0.3
BC008_02255	186	-2.1	BC008_04573	46058	-5.2	BC008_06911	49	-0.5
BC008_02256	1592	-2.1	BC008_04574	53052	-5.8	BC008_06912	46	-0.3
BC008_02257	662	-2.2	BC008_04575	6500	-3.1	BC008_06913	5896	-2.2
BC008_02258	2071	-1.6	BC008_04576	7608	-4.3	BC008_06914	416	0.1
BC008_02259	942	0.0	BC008_04577	102	3.0	BC008_06915	151	6.0
BC008_02260	3854	-4.2	BC008_04578	274	-1.1	BC008_06916	59	4.9
BC008_02261	680	-1.9	BC008_04579	5124	-3.7	BC008_06917	169	0.6
BC008_02262	562	-1.9	BC008_04580	2065	-1.0	BC008_06918	25	3.0
BC008_02263	3066	-1.6	BC008_04581	285	1.3	BC008_06919	56	3.8
BC008_02264	242	1.9	BC008_04583	308	0.4	BC008_06920	134	9.2
BC008_02265	1187	-2.0	BC008_04585	58	3.6	BC008_06921	128	4.0
BC008_02266	5855	-2.9	BC008_04586	1453	1.1	BC008_06922	444	0.1
BC008_02267	1406	-1.2	BC008_04587	324	0.9	BC008_06923	36	1.7
BC008_02268	192	0.1	BC008_04588	1000	2.0	BC008_06924	443	3.4
BC008_02269	398	2.0	BC008_04589	295	-0.4	BC008_06925	325	1.2
BC008_02270	128	1.1	BC008_04590	2322	0.4	BC008_06926	4300	-2.3
BC008_02271	6295	-3.2	BC008_04591	1736	-1.4	BC008_06927	216	-1.1
BC008_02272	2283	-1.0	BC008_04592	1763	-3.0	BC008_06929	401	0.4
BC008_02273	1105	-1.0	BC008_04593	1324	-1.8	BC008_06930	1129	1.6
BC008_02274	253	2.4	BC008_04594	479	-0.9	BC008_06931	368	1.9
BC008_02275	1215	0.6	BC008_04595	587	0.7	BC008_06932	391	-0.8
BC008_02276	2543	0.5	BC008_04596	570	-1.4	BC008_06933	416	2.5
BC008_02277	1236	6.7	BC008_04597	786	-0.2	BC008_06934	1673	1.0
BC008_02278	201	-0.9	BC008_04598	578	2.0	BC008_06935	1673	-1.4

BC008_02279	7491	-1.1	BC008_04599	514	-0.3	BC008_06936	1101	-0.1
BC008_02280	1385	-0.4	BC008_04600	568	0.8	BC008_06937	1819	-3.5
BC008_02281	599	1.3	BC008_04601	2045	-0.2	BC008_06938	9781	0.3
BC008_02282	5122	-0.7	BC008_04602	899	0.4	BC008_06939	4946	0.6
BC008_02283	4511	-0.5	BC008_04603	1362	1.0	BC008_06940	2451	-0.2
BC008_02284	431	0.5	BC008_04604	570	0.2	BC008_06941	1988	1.6
BC008_02285	793	2.8	BC008_04605	2337	0.7	BC008_06942	1839	-0.1
BC008_02286	2871	4.7	BC008_04606	313	-2.7	BC008_06943	93	3.8
BC008_02287	11380	8.8	BC008_04607	101	-1.3	BC008_06944	458	2.1
BC008_02288	1315	4.2	BC008_04608	101	-0.3	BC008_06945	494	2.7
BC008_02289	1521	4.4	BC008_04609	81	0.7	BC008_06946	82	-0.5
BC008_02290	**525**	**6.7**	BC008_04610	685	1.9	BC008_06947	979	0.3
BC008_02291	**395**	**5.2**	BC008_04611	2391	-3.2	BC008_06948	7832	8.6
BC008_02292	**324**	**4.0**	BC008_04612	642	-2.2	BC008_06949	45	4.2
BC008_02293	**59**	**1.3**	BC008_04613	21636	0.3	BC008_06950	102	-1.1
BC008_02294	**76**	**3.7**	BC008_04614	978	-1.9	BC008_06951	988	3.5
BC008_02295	**410**	**5.0**	BC008_04615	619	-1.0	BC008_06952	163	1.5
BC008_02296	48	2.5	BC008_04616	822	3.1	BC008_06953	451	1.6
BC008_02297	**391**	**6.5**	BC008_04617	5418	-1.0	BC008_06954	741	0.9
BC008_02298	812	9.7	BC008_04618	1755	-0.3	BC008_06955	2374	-0.8
BC008_02299	**219**	**5.0**	BC008_04619	576	-1.1	BC008_06956	26925	-3.2
BC008_02300	294	-1.3	BC008_04620	2237	-1.8	BC008_06958	1371	-2.7
BC008_02301	377	1.4	BC008_04621	1272	-1.2	BC008_06959	335	-0.4
BC008_02302	313	-0.6	BC008_04622	4055	0.8	BC008_06960	2968	-3.9
BC008_02303	3197	-2.7	BC008_04623	688	-0.9	BC008_06961	225	0.5
BC008_02304	11119	0.4	BC008_04624	220	-1.0	BC008_06962	626	1.5
BC008_02305	474	-1.0	BC008_04625	4837	-2.2	BC008_06963	458	-0.5
BC008_02306	771	-2.2	BC008_04626	2567	-1.0	BC008_06964	84	3.1
BC008_02307	3626	0.4	BC008_04627	1024	1.0	BC008_06965	252	0.2
BC008_02308	2065	2.4	BC008_04628	948	4.5	BC008_06966	64	1.1
BC008_02309	836	1.4	BC008_04629	683	0.1	BC008_06967	198	2.0
BC008_02310	50	2.7	BC008_04630	34	2.5	BC008_06968	195	0.7
BC008_02311	2598	1.6	BC008_04631	913	6.0	BC008_06969	541	4.0
BC008_02312	3765	2.5	BC008_04632	769	1.6	BC008_06970	178	3.8
BC008_02313	587	-1.6	BC008_04633	2560	1.8	BC008_06971	589	4.4
BC008_02314	2572	-1.0	BC008_04634	200	1.3	BC008_06972	79	1.5
BC008_02315	1751	0.4	BC008_04635	1412	2.4	BC008_06973	1341	0.7
BC008_02316	778	-1.6	BC008_04636	4369	2.8	BC008_06974	434	-0.4
BC008_02317	1473	-1.3	BC008_04637	1263	2.2	BC008_06975	262	1.0

BC008_02318	128	-0.2	BC008_04638	159	0.1	BC008_06976	5378	-3.4
BC008_02319	413	-1.5	BC008_04639	6635	0.1	BC008_06977	7	3.9
BC008_02320	8016	-1.3	BC008_04640	1969	4.0	BC008_06978	17	5.7
BC008_02321	1602	-0.8	BC008_04641	5335	5.6	BC008_06979	4	2.2
BC008_02322	1276	-2.2	BC008_04642	850	1.4	BC008_06980	9	4.2
BC008_02323	1152	-1.9	BC008_04643	1251	4.4	BC008_06981	27	3.8
BC008_02324	328	-1.2	BC008_04644	135	3.8			
BC008_02325	7029	3.8	BC008_04645	184	5.4			